Close Homolog of L1 (CHL1) Mediates Guidance of Thalamocortical Axons Through Extracellular and Intracellular Interactions

Amanda Gates Wright

A dissertation submitted to the faculty of the University of North Carolina at Chapel Hill in partial fulfillment of the requirements for the degree of Doctor of Philosophy in the Department of Biochemistry and Biophysics.

Chapel Hill
2007

Approved by:

Patricia Maness, PhD

Eva Anton, PhD

Steve Crews, PhD

Nikolay Dokholyan, PhD

Carol Otey, PhD

Franck Polleux, PhD

Abstract

Amanda Gates Wright: Close Homolog of L1 (CHL1) Mediates Guidance of Thalamocortical Axons Through Extracellular and Intracellular Interactions (Under the direction of Patricia F. Maness, PhD)

Close Homolog of L1 (CHL1), an L1 cell adhesion molecule expressed on thalamocortical and corticofugal axons, is identified as a regulator of thalamocortical axon guidance via extracellular interactions with Neuropilin1 (Npn1) and integrins and intracellular interactions with the actin cytoskeleton. CHL1 deletion in mice disrupted the topographic projection of somatosensory thalamic axons, causing them to inappropriately target the visual cortex. This shift was first observed in the ventral telencephalon (VTe), an intermediate target with graded Sema3A expression, where axons from the ventral basal complex (VB) of the dorsal thalamus were shifted caudally. Caudal thalamic axons were also dependent upon CHL1 for preferential guidance through high Sema3A territories. A similar pattern of aberrant guidance was observed in $Npn1^{Sema-/-}$ mutant embryos, in which axons are nonresponsive to Sema3A. CHL1 associated with Npn1 through a sequence in the extracellular domain of CHL1, which was required for Sema3A-induced growth cone collapse. Deletion of both L1 and CHL1 further disrupted thalamocortical topography, resulting in aberrant targeting of somatosensory and motor thalamic axons to the visual cortex. For the first time, these results demonstrate a role for Sema3A, Npn1, and CHL1 in regulating the topography of thalamocortical axons in

the VTe. CHL1 linkage to the cytoskeleton through ezrin, radixin, and moesin (ERM) proteins and ankyrin is critical for axon growth and guidance and cell migration. CHL1 associated with ERM proteins through a conserved sequence in the intracellular domain of CHL1, important for cell migration, neurite outgrowth and branching, and for Sema3A-mediated growth cone collapse. The cytoskeletal adaptor protein, ankyrin, was also recruited to the plasma membrane though a sequence in the CHL1 cytoplasmic domain containing a conserved tyrosine residue (Phe-Ile-Gly-Ala-Try), which was required for promoting integrin-dependent migration. CHL1 potentiated cell migration to extracellular matrix proteins by functionally interacting with β_1 integrins, mediated by c-Src, phosphatidylinositol 3-kinase, and ERK MAP (mitogen-activated protein) kinase.

In summary, a novel role for CHL1 has been demonstrated in mediating the cellular responses of Sema3A and Npn1, important for thalamic axon guidance. In addition, the mechanism by which CHL1 associates with Npn1 and couples to the actin cytoskeleton has been defined.

To my wonderful husband, Greg

my parents, Gordon and Teresa Gates

and

my brother and sister-in-law, Matt and Lori Gates

Your constant support and encouragement have been invaluable.

Acknowledgements

This work would not have been possible without the network of great people surrounding me throughout my career here at the University of North Carolina. I am indebted to many people to whom I would like to express my deepest thanks. First, I must express my sincerest gratitude to my advisor, Dr. Patricia Maness, who has provided constant support, both intellectually and personally, throughout this process. She has been extremely patient with me, and working under her supervision has not only improved my skills as a neuroscientist, but also made me a better scientist in general. Dr. Maness' kindness and graciousness have made my five years here very enjoyable.

I am forever grateful to my husband Greg, whose unwavering support, unconditional love, and continuous encouragement sustains and drives me to be a better person. Without him by my side, the daily struggles would seem unbearable. This work would not have been possible without his emotional support, technical expertise, and immense understanding. I am constantly amazed by his devotion and will be forever in his debt. I would also like to thank my parents, Gordon and Teresa Gates, for all of their encouragement, advice, and late night phone calls. Thank you for giving me the opportunity for education. I consider this our accomplishment. I am also indebted to my brother and sister-in-law, Matt and Lori Gates, whose love and support motivated me to persevere and arrive at my

dream of being a Tar Heel. Furthermore, the encouragement and comforting words from my extended family, Dr. Dave and Marsha Warthen and Rick and Anne Wright, have been instrumental in completing this goal. I would also like to extend my heartfelt appreciation to the many people with whom I have interacted and formed friendships during my time here. First, I am deeply grateful to Dr. Franck Polleux and Ashton Powell for their assistance with this project and for many enlightening discussions. I would also like to thank the other members of my committee, Drs. Carol Otey, Steve Crews, Eva Anton, and Nikolay Dokholyan, for their encouragement, kind words, and guidance. I am additionally grateful to past and present members of the Maness laboratory for enjoyable scientific discussions and teaching me so much about neuroscience, but more importantly, their friendships. Special thanks to Mona Buhusi, Galina Demyanenko, Anitha Panicker, Neeta Pilliar-Nair, Leann Brennamen, and Monika Schlatter. These extraordinary women have been invaluable to my work and I will always treasure the bond we share.

Last, I would be remiss if I did not mention the woman who introduced me to the world of science and instilled in me a love and excitement for research, Mrs. Ashley (Hoffman) Guess, my high school chemistry teacher. Her genuine enthusiasm for science and endless quest for answers made me realize where my own passions lie. She is an inspiration and I owe her many thanks.

I whole-heartedly acknowledge that a work of this magnitude is a collaborative effort and this would not have been possible without the influence of all of you.

“Any developmental neuroscientist with a tendency to masochism is encouraged to contemplate the development of thalamocortical projections”

(Molnar and Blakemore, 1995)

“The Will of God will never take you where the Grace of God will not protect you”

Unknown

Table of Contents

List of Figures xi

List of Abbreviations xiv

Chapters

1. Introduction 1

    1.1. Summary 2

    1.2. Establishment of Thalamocortical Connections 3

    1.3. The Ventral Telencephalon: An Intermediate Target in the Topographic Mapping of Thalamocortical Axons 8

    1.4. L1 Neural Cell Adhesion Molecules 17

    1.5. Goals of Thesis 23

    1.6. References 25

2. Close Homolog of L1 (CHL1) and Neuropilin1 Mediate Guidance of Thalamocortical Axons at the Ventral Telencephalon 38

    2.1. Abstract 40

    2.2. Introduction 40

    2.3. Results 44

    2.4. Discussion 57

    2.5. Methods 62

    2.6. References 68

3. Area-Specific Targeting of Thalamocortical Axons Through Interaction With EphA-EphrinA 107

3.1. Abstract 108

3.2. Introduction 108

3.3. Results 111

3.4. Discussion 113

3.5. Methods 115

3.6. References 117

4. Interaction of Close Homolog of L1 (CHL1) With ERM Proteins Promotes Neurite Elaboration and Sema3A-Induced Growth Cone Collapse 128

4.1. Abstract 130

4.2. Introduction 130

4.3. Results 134

4.4. Discussion 143

4.5. Methods 148

4.6. References 158

5. Close Homolog of L1 (CHL1) is an Enhancer of Integrin-Mediated Cell Migration 179

5.1. Abstract 181

5.2. Introduction 182

5.3. Results 185

5.4. Discussion 193

5.5. Methods 198

5.6. References 204

6. Discussion 228

6.1. CHL1-Neuropilin1 Interaction as a Regulator of Thalamocortical Axon Guidance 229

6.2. Sema3A-Neuropilin1 Interactions in Thalamocortical Axon Development 230

6.3. CHL1 in Corticofugal Axon Development 233

6.4. Redundant Functions of CHL1 and L1 in Thalamocortical Development 234

6.5. Repulsive Axon Guidance: Economic Molecular Mechanisms 236

6.6. Conclusions 239

6.7. References 240

List of Figures

Figure 1.1: Embryonic and Adult Thalamocortical Topography 35

Figure 1.2: Structure and Interactions of Close Homolog of L1 (CHL1) 37

Figure 2.1: CHL1 is Expressed in the Developing Thalamocortical Pathway 77

Figure 2.2: Projection of Somatosensory Thalamic Axons is Caudally Shifted to the Visual Cortex in CHL1-Minus Mice 80

Figure 2.3: CHL1 is Required for Guidance of Caudal Thalamic Axons in the Ventral Telencephalon at E15.5 84

Figure 2.4: CHL1 is Required for Guidance of Ventral Basal Thalamic Axons in the Telencephalon at E15.5 87

Figure 2.5: Segregation and Fasciculation of Thalamic and Cortical Axons Within the Ventral Telencephalon is Not Altered in CHL1-minus Embryos (E16.5) 89

Figure 2.6: Expression of CHL1, Neuropilin1, and Sema3A in the Embryonic Dorsal Thalamus and Telencephalon 92

Figure 2.7: Neuropilin1 Binding to Sema3A is Required for Guidance of Caudal Thalamic Axons Within the Ventral Telencephalon 96

Figure 2.8: Neuropilin1-Sema Interactions are Required for Guidance of Ventral Basal Thalamic Axons 98

Figure 2.9: Neuropilin1 and CHL1 Form a Stable Complex 101

Figure 2.10: CHL1 is Required for the Growth Cone Collapsing Effects of Sema3A in Cultures of Thalamic Neurons (E14.5) 104

Figure 2.11: CHL1 and Neuropilin1 Mediate Guidance of Thalamocortical Axons at the Ventral Telencephalon 106

Figure 3.1: CHL1 is Required for EphrinA5-Induced Growth Cone Collapse 123

Figure 3.2: L1 and EphA4 Form a Stable Complex 125

Figure 3.3: CHL1 and L1 Cooperate to Regulate Thalamocortical Axon Targeting 127

Figure 4.1: Schematic Representation of CHL1 and L1 Cytoplasmic Domains 165

Figure 4.2: CHL1 Recruits Ezrin to the Cell Membrane Through the Membrane Proximal RGGKYSV Sequence 167

Figure 4.3: Intracellular Interaction with ERM Proteins is Essential for CHL1-Mediated Adhesion to Fibronectin 169

Figure 4.4: CHL1/ERM Interaction is Essential for Potentiated Haptotactic Migration of HEK293 Cells 171

Figure 4.5: CHL1-Stimulated Neurite Outgrowth and Branching is Dependent on Intracellular ERM Protein Binding 174

Figure 4.6: The ERM Binding Domain of CHL1 is Required for Sema3A-Induced Growth Cone Collapse in Embryonic Cortical Neurons 176

Figure 4.7: Semaphorin3A Inhibits CHL1wt-Mediated Neurite Outgrowth and Branching 178

Figure 5.1: CHL1 Potentiates Haptotactic Migration of HEK293 Cells to Extracellular Matrix Proteins 214

Figure 5.2: CHL1 Potentiates Migration of HEK293 Cells Through β_1 Integrins 216

Figure 5.3: CHL1 Mutations in Extracellular Ig6 (DGEA) and Cytoplasmic (FIGAY) Domains Suppress CHL1-Potentiated Migration to Collagen 218

Figure 5.4: c-Src, PI3 Kinase, and MAP Kinase are Required for CHL1-Potentiated Migration of HEK293 Cells 220

Figure 5.5: β_1 Integrin and CHL1 Co-cap on the Surface of CHL1-Expressing HEK293 Cells 222

Figure 5.6: CHL1 is Able to Recruit Ankyrin to the Cell Membrane Through the FIGAY Sequence 225

Figure 5.7: Hypothetical Model of the Molecular Interactions Involved in CHL1-Potentiated Migration Through β_1 Integrins 227

Abbreviations

5-HT	serotonin
AC	anterior commissure
AGEV	Ala-Gly-Glu-Val
AIS	axon initial segment
AP	alkaline phosphatase
BSA	bovine serum albumin
CHL1	Close Homolog of L1
CP	cortical plate
CRASH	corpus callosum agenesis, mental retardation, adducted thumbs, spasticity, and hydrocephalus
Cx	cerebral cortex
DCC	deleted in colorectal cancer
DGEA	Asp-Gly-Glu-Ala
DiA	4-4-dihexadecyl aminostyryl N-methyl-pyridinium iodide
DIC	differential interference contrast
DiI	1,1',dioctadecyl-3,3,3',3'-tetramethylindocarbocyanine perchlorate
DMEM	Dulbecco's modified Eagle's medium
DT	dorsal thalamus
DTC	caudal dorsal thalamus
DTe	dorsal telencephalon
DTR	rostral dorsal thalamus
E14.5	embryonic day 14.5

ECM	extracellular matrix
EGFP	enhanced green fluorescent protein
ERM	ezrin, radixin, moesin
FBS	fetal bovine serum
Fgf8	Fibroblast Growth Factor 8
FIGQY	Phe-Ile-Gly-Gln-Tyr
FN	fibronectin
GEF	guanine nucleotide exchange factor
GPI	glycosylphosphatidyl inositol
HBSS	Hank's Balanced Salt Solution
HC	hippocampus
IACUC	Institutional Animal Care and Use Committee
IC	internal capsule
Ig	immunoglobulin
IZ	intermediate zone
kDA	kiloDaltons
KGE	Lys-Gly-Glu
L1-CAMs	L1 cell adhesion molecules
LGE	lateral ganglionic eminence
LGN	lateral geniculate nucleus
MAP kinase	mitogen-activated protein kinase
MGE	medial ganglionic eminence
MZ	marginal zone

Ngn2	Neurogenin2
NO	nitric oxide
Npn1	Neuropilin1
Npn2	Neuropilin2
Nrg1	neuregulin1
P5	postnatal day 5
PBS	phosphate-buffered saline
PFA	paraformaldehyde
PI3 kinase	phosphatidylinositol 3-kinase
PIP2	phosphatidylinositol *bis* phosphate
PKG	cGMP-dependent protein kinase
RGC	retinal ganglion cell
RGD	Arg-Gly-Asp
RT	room temperature
S1	primary somatosensory cortex
SC	superior colliculus
SEM	standard error of the mean
Sema3A	Semaphorin3A
Sema3C	Semaphorin3C
SGC	soluble guanylate cyclase
V1	primary visual cortex
VA	ventroanterior
VB	ventrobasal

VL	ventrolateral
VPL	ventro-posterolateral
VPM	ventro-posteromedial
VTe	ventral telencephalon
WT	wild type

Chapter 1

Introduction

1.1 Summary

During development of the nervous system, sophisticated mechanisms control the connectivity between the thalamus and the cerebral cortex, the most highly organized information processing center in the brain. The cerebral cortex is divided into different areas, the functions of which are determined by sensory inputs from the thalamus. Most thalamic nuclei project axons to distinct cortical areas in a topographic manner organized along both rostrocaudal and mediolateral axes. Rostral cortical areas receive input from rostromedial thalamic nuclei, and caudal cortical regions are targeted by caudolateral thalamic nuclei (Figure 1.1). Despite decades of research, the mechanisms that control the precise connections between the thalamus and the cerebral cortex are only partly understood. Along with several other guidance molecules, new roles are emerging for L1 neural cell adhesion molecules (L1-CAMs) as regulators of axon guidance. Close Homolog of L1 (CHL1), a member of the L1-CAM family, was examined in Chapter 2 for a novel, functional role in the development of thalamocortical axon topography controlled by interaction of the CHL1 extracellular region with Neuropilin1, a Semaphorin3A receptor. A potential cooperation between L1 and CHL1 in controlling thalamocortical topography by mediating axon responses to EphA/ephrinA guidance cues was investigated in Chapter 3. Chapters 4 and 5 describe associations of the intracellular domain of CHL1 with ERM (ezrin, radixin, moesin) proteins and ankyrin, which couple to the actin cytoskeleton. Taken together these results demonstrate, for the first time, a requirement for CHL1 in establishing contacts necessary for axon growth, guidance, and targeting.

1.2 Establishment of Thalamocortical Connections

Timing and Early Patterning of Thalamic Axon Outgrowth

Proper topographic mapping of thalamic axons to distinct targets in the neocortex requires a series of guidance decisions at both subcortical (diencephalic-telencephalic boundary) and cortical (pallial-subpallial boundary) levels. Developing thalamic axons initially project ventrally from the dorsal thalamus, turn dorsolaterally to enter the internal capsule (IC) of the ventral telencephalon (VTe), an intermediate target, and eventually target specific neocortical areas (Figure 1.1 A). Similarly, neurons from cortical layer VI extend axons that travel through the IC to specific targets in the thalamus (Lopez-Bendito and Molnar, 2003). The molecular determinants regulating these events, and developmental mechanisms underlying the complex topography of thalamocortical projections, remains unclear. Transcription factors with graded expression in the thalamus (Neurogenin2 (Seibt et al., 2003) and Gbx2 (Hevner et al., 2002)) are important determinants of early thalamocortical topography, contributing to guidance decisions at the diencephalic-telencephalic boundary. Neurogenin2 (Ngn2), which is expressed in a high-rostral to low-caudal gradient in the dorsal thalamus, specifies the projection of rostral thalamic axons to frontal cortical areas by mediating the responsiveness of axons to cues within the VTe (Seibt et al., 2003). Mice deficient in Gbx2, a homeobox gene expressed at early stages in the dorsal thalamus, display defects in both thalamocortical and corticothalamic development (Hevner et al., 2002). Thalamic axons are reduced in number and do not enter the cortex, while cortical axons (which do not express Gbx2) suspend growth in the IC, or misproject to the cerebral

peduncle, without entering the thalamus. This finding suggests that thalamocortical and corticothalamic axons might depend on each other for axon guidance (Hevner et al., 2002). While cues within the dorsal thalamus are sufficient to initiate the topography of thalamocortical projections, there is evidence that cues within the cortex also play a role in patterning the specificity of thalamic axons (Zhou et al., 1999; Mallamaci et al., 2000; Bishop et al., 2002; Shimogori and Grove, 2005).

Thalamocortical Topography and Cortical Arealization

Although thalamic axons reach the neocortex around E16 in the mouse, only lower cortical layers are formed at this time and the cortical plate is not yet permissive to axonal growth. In fact, the target cells of most thalamic axons (layer IV) are not in place until after birth (Lund and Mustari, 1977). For this reason, thalamic fibers remain in the intermediate zone and subplate until E17 before invading the cortical plate. This waiting period has been shown to be critical in the topographic targeting of thalamocortical axons (Ghosh and Shatz, 1992). While thalamic axons accumulate in the subplate, they engage in activity-dependent interactions through side branch formation that leads to their realignment and proper targeting (Catalano and Shatz, 1998). Thus, the initial phase of target selection by thalamocortical axons may depend on dynamic interactions of growing thalamic axons within the subplate.

Significant cortical invasion of thalamic axons commences just before birth (E18-E19 in the mouse), when axons detach from the subplate and grow into the cortical plate. Axons make a dorsal turn from their path in the intermediate zone, and the vast majority of fibers grow radially into the cortex (Agmon et al., 1993). The

initial topography established during early thalamic axon outgrowth is continued during invasion of the cortex, with individual thalamic nuclei targeting specific cortical regions (inter-areal topography). Axons from the rostrally located ventroanterior (VA) or ventrolateral (VL) nuclei project to the motor cortex; axons from the ventrobasal complex (VB) project to the somatosensory cortex; and axons from the lateral geniculate nucleus (LGN), located in the caudal thalamus, target the visual cortex (Caviness and Frost, 1980; Dufour et al., 2003; Lopez-Bendito and Molnar, 2003) (Figure 1.1 B). Within each neocortical area, a second level of organization is established where thalamocortical projections form a physical map of the sensory information (intra-areal topography). Intra-areal topography emerges later in development and is refined during the first postnatal week by activity dependent and independent mechanisms (Antonini and Stryker, 1993; Feldheim et al., 1998; Lopez-Bendito and Molnar, 2003).

Recent experiments have shown that the neocortex is regionalized early in development, prior to invasion of thalamocortical axons (Nakagawa et al., 1999). Cues such as Emx2, COUP-TFI, and Fibroblast Growth Factor 8 (Fgf8), with distinct expression patterns in the cortex, have been implicated in the positioning of cortical areas (Zhou et al., 1999; Bishop et al., 2000; Fukuchi-Shimogori and Grove, 2001; Zhou et al., 2001), targeting of limbic thalamic axons (Mann et al., 1998; Uziel et al., 2002), and intra-areal topography of thalamocortical axons (Vanderhaeghen et al., 2000). Therefore, it is plausible that such cues could also control inter-areal topographic mapping and targeting of thalamocortical axons. This idea is supported by the analysis of Emx2 and COUP-TFI mutant mice, where the entire neocortex is

shifted caudally and thalamocortical axons demonstrate a corresponding caudal shift in the targeting of cortical areas (Zhou et al., 1999; Bishop et al., 2000; Mallamaci et al., 2000). Furthermore, thalamic axons respond to shifts in cortical boundaries due to ectopic Fgf8 expression resulting in altered thalamocortical targeting (Shimogori and Grove, 2005).

An alternative mechanism to explain thalamocortical topography was proposed by Molnar and colleagues (Molnar and Blakemore, 1991; Molnar et al., 1998; Lopez-Bendito and Molnar, 2003), suggesting that thalamic axons may be instructed to target specific cortical areas by interacting with apposing cortical axons originating from that area. This idea, the "handshake hypothesis," is supported by the finding that thalamic axons and axons from the subplate and the telencephalon meet in the lateral region of the IC at E15 in the rat and grow in close contact through the VTe, (Lopez-Bendito and Molnar, 2003). Though this theory remains controversial, it is supported by several mutant mouse models. For example, analysis of corticothalamic and thalamocortical connections in mice with mutations in transcription factors, Tbr1 (expressed in the cortex), Gbx2 (expressed in dorsal thalamus), and Pax6 (expressed in both), demonstrate that the reciprocal connections may not form independently. Defects in corticothalamic or thalamocortical pathfinding lead to guidance errors in the reciprocal population of axons in all mutants (Hevner et al., 2002). One interpretation of these results is that fasciculation between thalamic and cortical axons is required for the establishment of connections between the thalamus and neocortex.

On the other hand, *in vitro* experiments using cortical and thalamic rat explants reveal that axon fasciculation does not occur between cortical and thalamic axons. Regional specificity for axonal connections was examined *in vitro* by co-culturing slices of visual cortex with explants from LGN. Cortical and thalamic fibers do not form heterotypic fascicles, and in most cases growth cones retract when approaching axons of the opposite type (Bagnard et al., 2001). Conversely, homotypic axon fasciculation is prominent. Thalamic growth cones extend along the surface of other thalamic axons and cortical growth cones form fascicles with other cortical axons. These results suggest that cortical and thalamic fibers may express different collapse factors that prevent them from directly interacting.

Although the cortex is clearly a source of cues important for instructive guidance of thalamocortical axons, mechanisms controlling topographic guidance and area-specific targeting within the neocortex are unclear. There is a growing body of evidence which suggests that molecular events outside the neocortex are responsible for the initial sorting and guidance of thalamocortical axons (Metin and Godement, 1996; Tuttle et al., 1999; Braisted et al., 2000; Garel et al., 2002; Dufour et al., 2003; Seibt et al., 2003). The VTe has emerged as a key intermediate target for thalamic axon sorting to cortical areas along the rostrocaudal axis (Dufour et al., 2003; Seibt et al., 2003; Lopez-Bendito et al., 2006; Bonnin et al., 2007); however, the guidance cues within this region and mechanisms controlling this level of organization are just beginning to be revealed.

1.3 The Ventral Telencephalon: An Intermediate Target in the Topographic Mapping of Thalamocortical Axons

As thalamic axons leave the thalamus, they turn dorsolaterally at the diencephalic-telencephalic border and enter the IC of the VTe by E13 in the mouse. The VTe constitutes the region below the DTe extending to the lateral ventricle, including the medial, lateral, and caudal ganglionic eminences, as well as more ventral structures, the caudate putamen, globus pallidus, and amygdala. Chemoattractant signals within the VTe, along with a chemorepellent signal in the hypothalamus, are responsible for the dorsolateral turn of thalamic axons into the IC (Metin and Godement, 1996; Braisted et al., 1999; Braisted et al., 2000). At the thalamic eminence, the border between the thalamus and VTe, thalamocortical fibers form distinct fascicles which open up in a fan-shaped fashion in the IC (Garel et al., 2002; Dufour et al., 2003). Spatial positioning of thalamic axons within the VTe determines the rostrocaudal level of neocortex that the axons will subsequently target. Support for a role of the VTe in thalamocortical axon sorting is three-fold. First, contact-mediated interactions between thalamic axons and ventral telencephalic neurons play a role in thalamocortical axon guidance. Second, regionalization of the VTe due to expression of regulatory genes affects proper guidance of thalamic axons through the intermediate target. Lastly, attractive and repulsive guidance cues expressed within the VTe influence thalamic axon growth.

Contact-Mediated Interactions

There is clear evidence that transient axonal projections from cell groups within the VTe guide the early outgrowth of thalamocortical axons through the IC

(Metin and Godement, 1996; Molnar et al., 1998). Mash1, a basic helix-loop-helix transcription factor, is expressed in the lateral, medial, and caudal ganglionic eminences of the VTe. A subset of ventral telencephalic cells and their projections are absent in Mash1 knockout mice. As a result, thalamocortical pathfinding is misrouted and fewer axons project out of the thalamus. Those that do fail to enter the VTe or innervate the cortex, despite normal cortical regionalization and proper corticothalamic axon development (Tuttle et al., 1999). Mice deficient in Pax6 demonstrate misrouted ventral telencephalic axons at the diencephalic-telencephalic border, causing a subset of thalamocortical axons to be misguided in a similar manner (Stoykova and Gruss, 1994; Hevner et al., 2002; Jones et al., 2002). Both instances suggest that thalamic axons require interaction with projections from ventral telencephalic cells for guidance through the VTe. A recent study further supports this hypothesis by demonstrating a role for the tangentially migrating cells of the VTe (Lopez-Bendito et al., 2006). Specifically, the early migration of neuregulin1 (Nrg1)-expressing GABAergic cells from the lateral ganglionic eminence forms a permissive corridor for thalamic axon navigation through the VTe. In the absence of corridor cells, thalamic axons fail to enter the telencephalon, suggesting that interaction of thalamic axons with this cellular group is essential for the development of topographic thalamocortical projections. The molecular basis for this guidance mechanism depends upon two different isoforms of the Nrg1 gene and their receptor, ErbB4, which is expressed by thalamic neurons at the time they begin extending axons toward the telencephalon (Lopez-Bendito et al., 2006). However,

topography persists in Nrg1 and ErbB4 mutant embryos, suggesting the necessity for other mechanisms to control thalamocortical axon guidance through the VTe.

Regionalization of the VTe and Effects on Thalamic Axon Guidance

Several transcription factors, including Ebf1 and Dlx1/2, are expressed in the VTe, and are important initial determinants of thalamocortical sorting at this site. Ebf1 encodes a helix-loop-helix transcription factor that is expressed in the VTe, the cortical marginal zone, and the dorsal thalamus (Garel et al., 1999). Targeted inactivation of Ebf1 results in alteration of the molecular identity of cells within the VTe, resulting in the expression of an abnormal combination of genes in the intermediate target. This mutant phenotype leads to defects in the size and properties of the VTe (Garel et al., 1999), without disrupting regionalization of the dorsal thalamus or the neocortex (Garel et al., 2002). Consequently, thalamic axons from the LGN display an altered trajectory within the VTe of Ebf1 mutant mice. These axons fail to turn dorsolaterally within the intermediate target, and instead misproject toward the amygdala. Axons from the VB complex are shifted to more caudal regions of the IC and subsequently invade more caudal territories of the neocortex (Garel et al., 2002).

Dlx1 and Dlx2 encode homeodomain transcription factors that control differentiation of GABAergic neurons (Anderson et al., 1997), which constitutes the large majority of ventral telencephalic cells. Dlx1/2 is expressed in the VTe and the ventral thalamus, but not the dorsal thalamus (Garel et al., 2002). Inactivation of Dlx1/2 also disrupts ventral telencephalic development, demonstrated by expansion of the subventricular zone due to abnormal localization of cells within the lateral

ganglionic eminence of the VTe (Anderson et al., 1997). This defect leads to disorganization of axons within the IC. In Dlx1/2 mutant embryos, thalamic axons from the LGN are misrouted in the VTe and fail to reach the cortex. The topography of the remaining axons (including those from the VB nucleus) is shifted caudally in the IC and the neocortex, similar to the defects observed in Ebf1 mutant mice (Garel et al., 2002). These results suggest that topography of thalamocortical axons is regulated non-autonomously by the spatial positioning and molecular identity of cells within the VTe, which is governed by the expression of regulatory genes located in this region. Transcription factors may also have a role in controlling thalamocortical topography in a cell-autonomous manner by specifying axon responsiveness to guidance cues, such as ephrins, netrin1, and semaphorins.

Guidance Cues in the Thalamocortical Pathway

Recent studies have demonstrated that the VTe contains cues that regulate the topographic patterning of thalamocortical projections (Dufour et al., 2003; Seibt et al., 2003; Bonnin et al., 2007) by eliciting attractive and repulsive responses from thalamic axons to direct their outgrowth to appropriate cortical regions. Several molecules that control the pathfinding of thalamocortical axons within the intermediate target have been identified.

Ephrins and Eph Receptors. Ephrins are a widely studied family of axon guidance ligands with receptors known as Eph receptor tyrosine kinases. Members of the EphA-receptor and ephrinA gene families play key roles in retinal axon guidance to the superior colliculus and the LGN in the thalamus (reviewed in Flanagan, 2006). EphrinA2, A3, and A5 triple knockout mice display severe defects

in visual area map formation (Cang et al., 2005). The primary visual cortex is shifted medially, rotated, and compressed and the internal organization is degraded. Intra-areal topographic projections within the visual cortex are also disrupted due to loss of the three ephrin ligands (Cang et al., 2005). Furthermore, complementary gradients of ephrinA5 in the somatosensory cortex (high medial, low lateral) and EphA4 in the VB nucleus of the thalamus (high lateral, low medial) direct the intra-areal topographic mapping of thalamic afferents within the primary somatosensory cortex (S1). Loss of ephrinA5 disrupts the formation of the barrel field in S1 (Vanderhaeghen et al., 2000). EphrinA/EphA gradients also regulate the precision and reciprocity of thalamocortical and corticothalamic projections between neocortical areas (inter-areal topography) (Vanderhaeghen et al., 2000; Dufour et al., 2003; Torii and Levitt, 2005). Analysis of ephrinA5/EphA4 double mutant mice reveals that gradients of ephrinA5 within the VTe and EphA4 on thalamic axons are important for early axon sorting within the intermediate target (Dufour et al., 2003). In mice lacking the receptor-ligand pair, some axons from the ventrolateral thalamic nucleus, which normally project to the rostrally located motor cortex, are shifted posteriorly to target the more caudal somatosensory cortex. This shift in thalamocortical topography is first detected in the VTe, suggesting that ephrinAs and EphAs control the pathfinding of rostral thalamic axons within this region (Dufour et al., 2003). Nevertheless, somatosensory and visual thalamic axons maintain topography in ephrinA5/EphA4 double knock out mice, indicating a role for other axon guidance cues in mediating the topographic guidance of thalamocortical axons in the VTe. Chapter 3 further defines the mechanism for ephrinA5 in controlling

thalamic axon guidance, suggesting cooperation with adhesion molecules, L1 and CHL1.

Netrin1. Netrin1 is a bifunctional molecule triggering attraction or repulsion of growing axons, depending on the nature of the molecular interactions encountered (Burgess et al., 2006). Netrin1 is expressed in medial dorsal thalamic nuclei, and in a high rostral to low caudal gradient in the VTe, during the time of thalamocortical navigation through the IC (Metin and Godement, 1996; Braisted et al., 2000; Bonnin et al., 2007). One factor that determines the response of axons to netrin1 is the composition of netrin receptors available on the surface of growth cones. Deleted in colorectal cancer (DCC) and a DCC paralog, neogenin, are responsible for the attractant effects of netrin1 and are expressed by thalamic axons. Chemorepulsion by netrin1 is dependent upon expression of an UNC5 homolog (UNC5A-D) and, in some instances, co-expression of DCC (Stein et al., 2001). Analysis of netrin1 knockout mice reveals that thalamic axons are disorganized within the VTe and are restricted to dorsomedial areas. Although fewer thalamic axons reach the cortex in netrin1 mutant mice, those that do display normal area-specific targeting. These results suggest that netrin1 is an axon guidance cue within the VTe, but it most likely works in combination with other guidance molecules to control thalamocortical pathfinding. Recent studies have shown that serotonin (5-HT) modulates the response of thalamocortical axons to netrin1 (Bonnin et al., 2007). *In vitro*, axons from the posterior dorsal thalamus grow toward a source of netrin1 while anterior dorsal thalamic axons grow away from netrin1. Activation of 5-HT receptors switches the response of posterior thalamic axons to netrin1 from attraction to

repulsion by decreasing intracellular cAMP levels. Electroporation experiments further demonstrate a role for 5-HT in thalamocortical axon sorting within the IC. Overexpression of serotonin receptors in the dorsal thalamus elicits a repulsive response of axons that are normally attracted to netrin1, causing them to follow a more dorsally restricted path in the IC. In addition, this change in receptor expression results in decreased intracellular levels of cAMP. On the other hand, reducing expression of the same two receptors, which likely leads to increased cAMP levels, causes thalamic axons to spread into more ventrolateral regions of the IC due to attractive responses to netrin1 (Bonnin et al., 2007). Thus, sorting of thalamocortical axons within the VTe is, in part, dependent upon axonal responses to netrin1, which are modulated by serotonergic signaling to control cAMP levels.

Semaphorins and Neuropilins. Another important family of guidance molecules is the semaphorins, which include transmembrane and secreted proteins, and their receptors, neuropilin1/2 (Raper, 2000). Semaphorins have been shown to control many aspects of axonal development, including growth cone collapse, axon repulsion, inhibition of terminal arbor formation, suppression of branching, and homotypic fasciculation (Yazdani and Terman, 2006). Studies have demonstrated that semaphorins can act as both repulsive and attractive guidance cues. *In vitro* assays reveal that Semaphorin3A (Sema3A) has repulsive effects on cortical axons and prevents branching (Bagnard et al., 1998; Bagnard et al., 2001; Dent et al., 2004). However, Semaphorin3C (Sema3C) attracts cortical axons when encountered in an increasing gradient. Growth cones are very sensitive to the direction of semaphorin gradients and respond strongly to increasing concentrations,

but are unaffected when they encounter decreasing or uniform concentrations (Bagnard et al., 2000). *In situ* hybridization experiments demonstrate that Sema3A and Sema3C are expressed in the cortex and receptors for Sema3A/3C (Neuropilin1/2) are expressed on cortical axons during early embryonic stages (Bagnard et al., 1998). Sema3A mRNA is predominantly detected in the cortical ventricular and subventricular zones, while Sema3C is restricted to the subventricular zone. Attractant signals, in combination with repulsive molecules, may be required to direct early corticofugal axon outgrowth. In particular, cortical efferent axons may be attracted to the deep intermediate zone by the gradient of Sema3C until they encounter the repulsive Sema3A, which prevents them from entering the subventricular and ventricular zones (Bagnard et al., 1998).

Sema3A also has chemoattractive roles in the developing cortex. Dendrites of pyramidal neurons are attracted toward the pial surface by a diffusible source of Sema3A near the marginal zone, while axons are repelled toward the white matter (Polleux et al., 2000). The differential response of axons and dendrites to Sema3A is mediated by preferential localization of soluble guanylate cyclase (SGC) to the apical dendrite. The chemoattractive effect of Sema3A toward apical dendrites is dependent upon SGC signaling through the downstream effector, cGMP-dependent protein kinase (PKG), as treatment with a PKG specific inhibitor blocked the oriented growth of dendrites toward the pial surface (Polleux et al., 2000).

Recent tracing experiments have implicated Semaphorin6A in thalamic axon guidance (Leighton et al., 2001). Caudal thalamic axons of Sema6A knockout mice fail to enter the IC and instead project downwards toward the amygdala (Leighton et

al., 2001). Moreover, sema3A, which is expressed in the IC during times of axonal growth (Skaliora et al., 1998; Tamamaki et al., 2003), is involved in maintaining homotypic segregation via growth cone collapse and axon retraction (Bagnard et al., 2001); however, its role in thalamocortical guidance is unclear. The cell adhesion molecule L1 has been implicated in Sema3A signaling. L1 and Npn1 interaction through their extracellular domains to mediate axonal responses to Sema3A, important for normal pyramidal decussation of corticospinal tract axons (Castellani et al., 2000). Sema3A is secreted from the ventral spinal cord, repelling pyramidal tract fibers and forcing them to enter the contralateral dorsal spinal column. L1-deficient cortical axons lose their responsiveness to Sema3A resulting in altered pyramidal decussation. Upon binding of Sema3A to Npn1, L1 and Npn1 are co-internalized, leading to growth cone collapse and axon retraction (Castellani et al., 2004). Soluble L1 binding to Npn1 in *trans* switches Sema3A-induced repulsion to attraction and leads to activation of the nitric oxide (NO) synthase/cGMP pathway (Castellani et al., 2002). The studies presented in Chapter 2 investigate a role for Sema3A and Npn1 in controlling guidance of thalamic axons in the VTe in cooperation with CHL1.

Taken together, these studies provide compelling evidence that the VTe is a key environment for complex intermolecular interactions needed to sort thalamocortical axons to discrete neocortical areas along the rostrocaudal axis. It is vitally important to identify and understand the molecular mechanisms underlying the topographic guidance and targeting of thalamocortical axons in the VTe enabling their projection to distinct neocortical regions. The molecular interactions of Sema3A and ephrinA5 are shown here, for the first time, to cooperate with CHL1.

These interactions are necessary for topographic guidance and targeting of thalamocortical axons.

1.4 L1 Neural Cell Adhesion Molecules

L1 neural cell adhesion molecules (L1-CAMs) are immunoglobulin-class recognition molecules that promote axon growth and neuronal migration in the developing nervous system (Maness, 2007). The vertebrate L1 family consists of four structurally related transmembrane proteins: L1, Close Homolog of L1 (CHL1), NrCAM, and neurofascin. The importance of L1-CAMs is exemplified by abnormalities observed in mutant mice and humans deficient in these molecules. L1 mutations are present in X-linked mental retardation (Kenwrick et al., 2000), and the human homolog of CHL1, CALL, is implicated in a syndrome associated with low IQ and developmental delays (Frints et al., 2003). Polymorphisms in the NrCAM gene have recently been linked to autism, and those in CHL1 and L1 have been associated with schizophrenia in some populations (Kurumaji et al., 2001; Sakurai et al., 2002; Bonora et al., 2005). The extracellular regions of L1-CAMs interact homophilically or heterophilically with multiple partners to activate intracellular signaling pathways important for neuronal migration and survival, synaptic plasticity, and axon growth and fasciculation.

Close Homolog of L1 (CHL1)

The newest member of the L1 family, CHL1, is a transmembrane protein comprised of six immunoglobulin (Ig)-like domains and five fibronectin type III domains, followed by a conserved cytoplasmic region of approximately 110 residues

(Figure 1.2). The amino acid sequence of CHL1 is approximately 60% homologous with L1 in the extracellular region and approximately 40% in the cytoplasmic domain (Holm et al., 1996). CHL1 is a strong promoter of neurite outgrowth (Hillenbrand et al., 1999), dendrite projection (Demyanenko et al., 2004), and controls axon guidance (Montag-Sallaz et al., 2002). The laminar positioning of deep layer pyramidal neurons and neuronal process orientation within posterior cortical regions (somatosensory and visual cortex) is regulated by CHL1 (Demyanenko et al., 2004). CHL1 exhibits graded cortical area-specific expression in embryonic cortical neurons in a high caudal to low rostral gradient from E14 until birth (Hillenbrand et al., 1999; Liu et al., 2000; Demyanenko et al., 2004). The early differential expression of CHL1 is established prior to thalamocortical axon invasion, and is most prominently expressed in the lower half of the intermediate zone, the location of corticofugal axons from the subplate. Because CHL1 is also expressed in the thalamus during axonal projection to the VTe (Liu et al., 2000), we reasoned that CHL1 might participate in axon guidance at the intermediate target, perhaps in conjunction with other ventral telencephalic cues. The hypothesis that CHL1 controls the topographic guidance of different subsets of thalamocortical axons will be investigated in Chapters 2 and 3.

L1-CAMs in Axon Pathfinding and Fasciculation

The prototypical CAM, L1, mediates axon guidance in different regions of the nervous system. Topographic mapping of retinal ganglion cell (RGC) axons to targets in the superior colliculus (SC) is dependent upon L1 (Demyanenko and Maness, 2003). Temporal axons of L1 mutant mice fail to arborize in appropriate

anterior-medial sites, and instead overshoot their targets to form termination zones in the posterior-lateral SC. The topographic mapping of RGC axons, along both anteroposterior and mediolateral axes of the SC, is dependent upon complementary gradients of ephrin ligands and Eph receptors (Feldheim et al., 1998; Feldheim et al., 2000; Wilkinson, 2001). Thus, L1 and Eph repellent guidance receptors may work together to regulate formation of the retinotopic map.

In thalamocortical mapping, L1 regulates fasciculation of thalamocortical axons, but a clear-cut role in topographic mapping remains to be determined. In mice lacking L1, thalamocortical axons are hyperfasciculated and a subset of caudal thalamic axons are misrouted in the VTe, making a sharp posterior turn toward the ventricular wall instead of projecting to the cortex (Ohyama et al., 2004; Wiencken-Barger et al., 2004). Loss of L1 also disrupts thalamic growth cone morphology within the subplate. In this region, mutant growth cones are longer and more complex than normal, suggesting that L1 may alter the cell adhesion machinery of migrating growth cones (Wiencken-Barger et al., 2004). The distribution of L1-minus thalamocortical axons within the cortex is more diffuse compared to wild type. Instead of following a confined path through the subplate, thalamic axons of L1-mutant mice spread to enter the intermediate zone and the subventricular zone (Ohyama et al., 2004). Despite these defects, area-specific targeting of thalamocortical axons was reported to occur normally in L1 mutant mice (Wiencken-Barger et al., 2004).

Corticothalamic axons are also hyperfasciculated in the IC of L1 mutant mice (Ohyama et al., 2004). In contrast to thalamocortical axons, corticothalamic axons

are significantly reduced and fail to reach their targets in the dorsal thalamus. Thus, L1 could function in the thalamocortical pathway by binding heterophically to the substrate to maintain segregation between axonal bundles within the IC. Abnormal fasciculation of thalamocortical axons due to loss of L1 may directly or indirectly influence fasciculation and pathfinding of corticothalamic axons.

NrCAM is expressed on developing fiber tracts and engages in multiple interactions regulating neurite outgrowth and fasciculation (Grumet, 1997; Fitzli et al., 2000). During anterior commissure (AC) development, deletion of NrCAM induces defasciculation and aberrant guidance of AC fibers (Falk et al., 2005). Interestingly, the molecular basis for this mechanism requires two secreted semaphorins (Sema3B and Sema3F) and their receptor, Neuropilin2 (Npn2). NrCAM associates with Npn2 to mediate the attractive and repulsive responses of Sema3B and Sema3F, which are required for proper AC axon development (Falk et al., 2005). NrCAM also regulates midline guidance of retinal axons (Williams et al., 2006) and spinal commissural axons (Zou et al., 2000).

CHL1 also functions in axon guidance, as its deletion in mice alters the trajectories of hippocampal mossy fibers and olfactory axons (Montag-Sallaz et al., 2002). In CHL1-deficient mice, mossy fibers inappropriately invade the CA3 pyramidal cell layer of the hippocampus. Also, the mossy fiber synaptic bouton lamination pattern is altered in CHL1 mutant mice, with terminals distributed throughout the CA3 pyramidal cell body layer, as well as in the suprapyramidal and infrapyramidal bundles. In wild type mice, olfactory neurons terminate exclusively in the olfactory bulb glomeruli with one axon contacting one glomerulus. In the

olfactory bulb of CHL1-deficient mice, axons instead project to multiple glomeruli, or pass through the glomerular layer and terminate in the external plexiform layer (Montag-Sallaz et al., 2002). This thesis investigates a requirement for CHL1 in controlling the topographic mapping of thalamocortical axons and the mechanisms underlying the establishment of this topography.

Intracellular and Extracellular Interactions of L1-CAMs

L1 is coupled to the actin cytoskeleton by reversibly binding to the spectrin adaptor protein, ankyrin, via a conserved sequence (FIGQY) in the cytoplasmic domain. Evidence supports the view that ankyrin binding to L1-CAMs stabilizes cell or axonal contacts. For example, interactions between ankyrin and neurofascin are necessary for the formation and stabilization of GABAergic basket cell synapses with the axon initial segment (AIS) of Purkinje cells (Ango et al., 2004). CHL1 is the only family member with an altered sequence in the presumed ankyrin-binding domain (FIGAY; Figure 1.2). Thus, it was unclear whether CHL1 can interact with the cytoskeleton through ankyrin binding. The ability of CHL1 to bind ankyrin and a role for this potential interaction in neural development is addressed in Chapter 5.

L1 has also been shown to engage the cytoskeleton though the interaction with ERM (ezrin-radixin-moesin) proteins. Two different motifs in the L1 intracellular domain mediate direct binding to ERM proteins: (1) a membrane-proximal sequence SKGGKY (Cheng et al., 2005) and (2) YRSLE motif, which is not present in CHL1, but is conserved in NrCAM and neurofascin (Kayyem et al., 1992; Volkmer et al., 1992; Dickson et al., 2002; Cheng et al., 2005). Due to structural differences in the cytoplasmic domain of CHL1, it is not known whether CHL1 can link to the

cytoskeleton through ERM protein binding. CHL1 has the potential to interact with ERM proteins though a conserved membrane-proximal sequence, RGGKYSV in the CHL1 intracellular domain (Figure 1.2). By coupling to the actin cytoskeleton through ERM protein binding, CHL1 may contribute to adhesive functions necessary for neurite outgrowth, branching, and axon guidance. The capability of CHL1 to interact with ERM proteins and the cellular and neuronal consequences of this interaction are addressed in Chapter 4.

CHL1 Interactions with Integrins

We showed that CHL1 functionally interacts with β_1 integrins to potentiate cell migration (Buhusi et al., 2003). The sixth Ig domain of CHL1 contains a potential integrin binding site, Asp-Gly-Glu-Ala (DGEA; Figure 1.2), which mediates integrin-collagen interactions in platelets (Staatz et al., 1991). A physical association between CHL1 and β_1 integrins was established by antibody-induced co-capping experiments. The molecular basis for the involvement of CHL1 in integrin-mediated cellular migration is addressed in Chapter 5.

Recent evidence indicates that Semaphorins can also interact with integrins to regulate cell adhesion and migration. Sema7A, which promotes axon growth from olfactory bulb neurons, contains an RGD sequence and can associate with β_1 integrins. Mutation of the integrin binding motif or treatment with integrin binding RGD peptides blocks Sema7A-mediated axon growth, supporting a direct role for integrins (Pasterkamp et al., 2003). Although class 3 Semaphorins have no RGD sequence, Sema3A inhibits the adhesion of endothelial cells to the extracellular matrix and slows their directional motility by antagonizing integrin activity (Serini et

al., 2003). In addition, dominant-negative forms of neuropilin1 and plexinA1, a co-receptor for Sema3A, enhance attachment and migration of endothelial cells via a mechanism involving $\alpha_5\beta_1$ and $\alpha_v\beta_1$ integrins. Thus, Sema3A can regulate integrin activation through signals from its receptors, neuropilin1 and plexinA1. A molecular connection between Sema3A and integrins to regulate axonal development or cellular migration in the nervous system is unclear; however, CHL1 may provide a scaffold to facilitate integrin-dependent signaling.

1.5 Goals of Thesis

Here I have addressed the following research topics to provide insight into understanding the molecular interactions of CHL1 to control axon growth and guidance:

(1) The role of CHL1 in regulating the topographic guidance and targeting of thalamocortical axons to posterior neocortical areas;

(2) A specific interaction between CHL1 and the Sema3A receptor, Neuropilin1, in mediating responses of thalamic axons to ventral telencephalic cues;

(3) Cooperation between L1 and CHL1 to control thalamocortical targeting by mediating axonal responses to ephrinA5/EphA4 repellent guidance cues;

(3) Linkage of CHL1 to the cytoskeleton through ERM proteins and the cellular and molecular consequences of this interaction, specifically on growth cone collapse due to Sema3A;

(4) The association of CHL1 with β_1 integrins and ankyrin and the neuronal responses controlled by these interactions.

1.6 References

Agmon, A., Yang, L. T., O'Dowd, D. K., and Jones, E. G. (1993). Organized growth of thalamocortical axons from the deep tier of terminations into layer IV of developing mouse barrel cortex. J Neurosci *13*, 5365-5382.

Anderson, S. A., Qiu, M., Bulfone, A., Eisenstat, D. D., Meneses, J., Pedersen, R., and Rubenstein, J. L. (1997). Mutations of the homeobox genes Dlx-1 and Dlx-2 disrupt the striatal subventricular zone and differentiation of late born striatal neurons. Neuron *19*, 27-37.

Ango, F., di Cristo, G., Higashiyama, H., Bennett, V., Wu, P., and Huang, Z. J. (2004). Ankyrin-based subcellular gradient of neurofascin, an immunoglobulin family protein, directs GABAergic innervation at purkinje axon initial segment. Cell *119*, 257-272.

Antonini, A., and Stryker, M. P. (1993). Rapid remodeling of axonal arbors in the visual cortex. Science *260*, 1819-1821.

Bagnard, D., Chounlamountri, N., Puschel, A. W., and Bolz, J. (2001). Axonal surface molecules act in combination with semaphorin 3A during the establishment of corticothalamic projections. Cereb Cortex *11*, 278-285.

Bagnard, D., Lohrum, M., Uziel, D., Puschel, A. W., and Bolz, J. (1998). Semaphorins act as attractive and repulsive guidance signals during the development of cortical projections. Development *125*, 5043-5053.

Bagnard, D., Thomasset, N., Lohrum, M., Puschel, A. W., and Bolz, J. (2000). Spatial distributions of guidance molecules regulate chemorepulsion and chemoattraction of growth cones. J Neurosci *20*, 1030-1035.

Bishop, K. M., Goudreau, G., and O'Leary, D. D. (2000). Regulation of area identity in the mammalian neocortex by Emx2 and Pax6. Science *288*, 344-349.

Bishop, K. M., Rubenstein, J. L., and O'Leary, D. D. (2002). Distinct actions of Emx1, Emx2, and Pax6 in regulating the specification of areas in the developing neocortex. J Neurosci *22*, 7627-7638.

Bonnin, A., Torii, M., Wang, L., Rakic, P., and Levitt, P. (2007). Serotonin modulates the response of embryonic thalamocortical axons to netrin-1. Nat Neurosci *10*, 588-597.

Bonora, E., Lamb, J. A., Barnby, G., Sykes, N., Moberly, T., Beyer, K. S., Klauck, S. M., Poustka, F., Bacchelli, E., Blasi, F.*, et al.* (2005). Mutation screening and association analysis of six candidate genes for autism on chromosome 7q. Eur J Hum Genet *13*, 198-207.

Braisted, J. E., Catalano, S. M., Stimac, R., Kennedy, T. E., Tessier-Lavigne, M., Shatz, C. J., and O'Leary, D. D. (2000). Netrin-1 promotes thalamic axon growth and is required for proper development of the thalamocortical projection. J Neurosci *20*, 5792-5801.

Braisted, J. E., Tuttle, R., and O'Leary D, D. (1999). Thalamocortical axons are influenced by chemorepellent and chemoattractant activities localized to decision points along their path. Dev Biol *208*, 430-440.

Buhusi, M., Midkiff, B. R., Gates, A. M., Richter, M., Schachner, M., and Maness, P. F. (2003). Close homolog of L1 is an enhancer of integrin-mediated cell migration. J Biol Chem *278*, 25024-25031.

Burgess, R. W., Jucius, T. J., and Ackerman, S. L. (2006). Motor axon guidance of the mammalian trochlear and phrenic nerves: dependence on the netrin receptor Unc5c and modifier loci. J Neurosci *26*, 5756-5766.

Cang, J., Kaneko, M., Yamada, J., Woods, G., Stryker, M. P., and Feldheim, D. A. (2005). Ephrin-As guide the formation of functional maps in the visual cortex. Neuron *48*, 577-589.

Castellani, V., Chedotal, A., Schachner, M., Faivre-Sarrailh, C., and Rougon, G. (2000). Analysis of the L1-deficient mouse phenotype reveals cross-talk between Sema3A and L1 signaling pathways in axonal guidance. Neuron *27*, 237-249.

Castellani, V., De Angelis, E., Kenwrick, S., and Rougon, G. (2002). Cis and trans interactions of L1 with neuropilin-1 control axonal responses to semaphorin 3A. EMBO J *21*, 6348-6357.

Castellani, V., Falk, J., and Rougon, G. (2004). Semaphorin3A-induced receptor endocytosis during axon guidance responses is mediated by L1 CAM. Mol Cell Neurosci *26*, 89-100.

Catalano, S. M., and Shatz, C. J. (1998). Activity-dependent cortical target selection by thalamic axons. Science *281*, 559-562.

Caviness, V. S., Jr., and Frost, D. O. (1980). Tangential organization of thalamic projections to the neocortex in the mouse. J Comp Neurol *194*, 335-367.

Cheng, L., Itoh, K., and Lemmon, V. (2005). L1-mediated branching is regulated by two ezrin-radixin-moesin (ERM)-binding sites, the RSLE region and a novel juxtamembrane ERM-binding region. J Neurosci *25*, 395-403.

Demyanenko, G. P., and Maness, P. F. (2003). The L1 cell adhesion molecule is essential for topographic mapping of retinal axons. J Neurosci *23*, 530-538.

Demyanenko, G. P., Schachner, M., Anton, E., Schmid, R., Feng, G., Sanes, J., and Maness, P. F. (2004). Close homolog of L1 modulates area-specific neuronal positioning and dendrite orientation in the cerebral cortex. Neuron *44*, 423-437.

Dent, E. W., Barnes, A. M., Tang, F., and Kalil, K. (2004). Netrin-1 and semaphorin 3A promote or inhibit cortical axon branching, respectively, by reorganization of the cytoskeleton. J Neurosci *24*, 3002-3012.

Dickson, T. C., Mintz, C. D., Benson, D. L., and Salton, S. R. (2002). Functional binding interaction identified between the axonal CAM L1 and members of the ERM family. J Cell Biol *157*, 1105-1112.

Dufour, A., Seibt, J., Passante, L., Depaepe, V., Ciossek, T., Frisen, J., Kullander, K., Flanagan, J. G., Polleux, F., and Vanderhaeghen, P. (2003). Area specificity and topography of thalamocortical projections are controlled by ephrin/Eph genes. Neuron *39*, 453-465.

Falk, J., Bechara, A., Fiore, R., Nawabi, H., Zhou, H., Hoyo-Becerra, C., Bozon, M., Rougon, G., Grumet, M., Puschel, A. W.*, et al.* (2005). Dual functional activity of semaphorin 3B is required for positioning the anterior commissure. Neuron *48*, 63-75.

Feldheim, D. A., Kim, Y. I., Bergemann, A. D., Frisen, J., Barbacid, M., and Flanagan, J. G. (2000). Genetic analysis of ephrin-A2 and ephrin-A5 shows their requirement in multiple aspects of retinocollicular mapping. Neuron *25*, 563-574.

Feldheim, D. A., Vanderhaeghen, P., Hansen, M. J., Frisen, J., Lu, Q., Barbacid, M., and Flanagan, J. G. (1998). Topographic guidance labels in a sensory projection to the forebrain. Neuron *21*, 1303-1313.

Fitzli, D., Stoeckli, E. T., Kunz, S., Siribour, K., Rader, C., Kunz, B., Kozlov, S. V., Buchstaller, A., Lane, R. P., Suter, D. M.*, et al.* (2000). A direct interaction of axonin-1 with NgCAM-related cell adhesion molecule (NrCAM) results in guidance, but not growth of commissural axons. J Cell Biol *149*, 951-968.

Flanagan, J. G. (2006). Neural map specification by gradients. Curr Opin Neurobiol *16*, 59-66.

Frints, S. G. M., Marynen, P., Hartmann, D., Fryns, J. P., Steyaert, J., Schachner, M., Rolf, B., Craessaerts, K., Snellinx, A., Hollanders, K.*, et al.* (2003). CALL interrupted in a patient with nonspecific mental retardation: gene dosage-dependent alteration of murine brain development and behavior. Hum Mol Genet *12*, 1463-1474.

Fukuchi-Shimogori, T., and Grove, E. A. (2001). Neocortex patterning by the secreted signaling molecule FGF8. Science *294*, 1071-1074.

Garel, S., Marin, F., Grosschedl, R., and Charnay, P. (1999). Ebf1 controls early cell differentiation in the embryonic striatum. Development *126*, 5285-5294.

Garel, S., Yun, K., Grosschedl, R., and Rubenstein, J. L. (2002). The early topography of thalamocortical projections is shifted in Ebf1 and Dlx1/2 mutant mice. Development *129*, 5621-5634.

Ghosh, A., and Shatz, C. J. (1992). Pathfinding and target selection by developing geniculocortical axons. J Neurosci *12*, 39-55.

Grumet, M. (1997). Nr-CAM: a cell adhesion molecule with ligand and receptor functions. Cell Tissue Res *290*, 423-428.

Hevner, R. F., Miyashita-Lin, E., and Rubenstein, J. L. (2002). Cortical and thalamic axon pathfinding defects in Tbr1, Gbx2, and Pax6 mutant mice: evidence that cortical and thalamic axons interact and guide each other. J Comp Neurol *447*, 8-17.

Hillenbrand, R., Molthagen, M., Montag, D., and Schachner, M. (1999). The close homologue of the neural adhesion molecule L1 (CHL1): patterns of expression and promotion of neurite outgrowth by heterophilic interactions. Eur J Neurosci *11*, 813-826.

Holm, J., Hillenbrand, R., Steuber, V., Bartsch, U., Moos, M., Lubbert, H., Montag, D., and Schachner, M. (1996). Structural features of a close homologue of L1 (CHL1) in the mouse: a new member of the L1 family of neural recognition molecules. Eur J Neurosci *8*, 1613-1629.

Jones, L., Lopez-Bendito, G., Gruss, P., Stoykova, A., and Molnar, Z. (2002). Pax6 is required for the normal development of the forebrain axonal connections. Development *129*, 5041-5052.

Kayyem, J. F., Roman, J. M., de la Rosa, E. J., Schwarz, U., and Dreyer, W. J. (1992). Bravo/Nr-CAM is closely related to the cell adhesion molecules L1 and Ng-CAM and has a similar heterodimer structure. J Cell Biol *118*, 1259-1270.

Kenwrick, S., Watkins, A., and Angelis, E. D. (2000). Neural cell recognition molecule L1: relating biological complexity to human disease mutations. Hum Mol Genet *9*, 879-886.

Kurumaji, A., Nomoto, H., Okano, T., and Toru, M. (2001). An association study between polymorphism of L1CAM gene and schizophrenia in a Japanese sample. Am J Med Genet *105*, 99-104.

Leighton, P. A., Mitchell, K. J., Goodrich, L. V., Lu, X., Pinson, K., Scherz, P., Skarnes, W. C., and Tessier-Lavigne, M. (2001). Defining brain wiring patterns and mechanisms through gene trapping in mice. Nature *410*, 174-179.

Liu, Q., Dwyer, N. D., and O'Leary, D. D. (2000). Differential expression of COUP-TFI, CHL1, and two novel genes in developing neocortex identified by differential display PCR. J Neurosci *20*, 7682-7690.

Lopez-Bendito, G., Cautinat, A., Sanchez, J. A., Bielle, F., Flames, N., Garratt, A. N., Talmage, D. A., Role, L. W., Charnay, P., Marin, O., and Garel, S. (2006). Tangential neuronal migration controls axon guidance: a role for neuregulin-1 in thalamocortical axon navigation. Cell *125*, 127-142.

Lopez-Bendito, G., and Molnar, Z. (2003). Thalamocortical Development: How Are We Going To Get There? Nature Reviews Neuroscience *4*, 276-289.

Lund, R. D., and Mustari, M. J. (1977). Development of the geniculocortical pathway in rats. J Comp Neurol *173*, 289-306.

Mallamaci, A., Muzio, L., Chan, C. H., Parnavelas, J., and Boncinelli, E. (2000). Area identity shifts in the early cerebral cortex of Emx2-/- mutant mice. Nat Neurosci *3*, 679-686.

Maness, P. F. and Schachner, M. (2007). Neural recognition molecules of the immunoglobulin superfamily: signal transducers of axons guidance and neuronal migration. Nat Neurosci *10*, 19-26.

Mann, F., Zhukareva, V., Pimenta, A., Levitt, P., and Bolz, J. (1998). Membrane-associated molecules guide limbic and nonlimbic thalamocortical projections. J Neurosci *18*, 9409-9419.

Metin, C., and Godement, P. (1996). The ganglionic eminence may be an intermediate target for corticofugal and thalamocortical axons. J Neurosci *16*, 3219-3235.

Molnar, Z., Adams, R., and Blakemore, C. (1998). Mechanisms underlying the early establishment of thalamocortical connections in the rat. J Neurosci *18*, 5723-5745.

Molnar, Z., and Blakemore, C. (1991). Lack of regional specificity for connections formed between thalamus and cortex in coculture. Nature *351*, 475-477.

Montag-Sallaz, M., Schachner, M., and Montag, D. (2002). Misguided axonal projections, neural cell adhesion molecule 180 mRNA upregulation, and altered behavior in mice deficient for the close homolog of L1. Mol Cell Biol *22*, 7967-7981.

Nakagawa, Y., Johnson, J. E., and O'Leary, D. D. (1999). Graded and areal expression patterns of regulatory genes and cadherins in embryonic neocortex independent of thalamocortical input. J Neurosci *19*, 10877-10885.

Ohyama, K., Tan-Takeuchi, K., Kutsche, M., Schachner, M., Uyemura, K., and Kawamura, K. (2004). Neural cell adhesion molecule L1 is required for fasciculation and routing of thalamocortical fibres and corticothalamic fibres. Neurosci Res *48*, 471-475.

Pasterkamp, R. J., Peschon, J. J., Spriggs, M. K., and Kolodkin, A. L. (2003). Semaphorin 7A promotes axon outgrowth through integrins and MAPKs. Nature *424*, 398-405.

Polleux, F., Morrow, T., and Ghosh, A. (2000). Semaphorin 3A is a chemoattractant for cortical apical dendrites. Nature *404*, 567-573.

Raper, J. A. (2000). Semaphorins and their receptors in vertebrates and invertebrates. Curr Opin Neurobiol *10*, 88-94.

Sakurai, K., Migita, O., Toru, M., and Arinami, T. (2002). An association between a missense polymorphism in the close homologue of L1 (CHL1, CALL) gene and schizophrenia. Mol Psychiatry *7*, 412-415.

Seibt, J., Schuurmans, C., Gradwhol, G., Dehay, C., Vanderhaeghen, P., Guillemot, F., and Polleux, F. (2003). Neurogenin2 specifies the connectivity of thalamic neurons by controlling axon responsiveness to intermediate target cues. Neuron *39*, 439-452.

Serini, G., Valdembri, D., Zanivan, S., Morterra, G., Burkhardt, C., Caccavari, F., Zammataro, L., Primo, L., Tamagnone, L., Logan, M.*, et al.* (2003). Class 3 semaphorins control vascular morphogenesis by inhibiting integrin function. Nature *424*, 391-397.

Shimogori, T., and Grove, E. A. (2005). Fibroblast growth factor 8 regulates neocortical guidance of area-specific thalamic innervation. J Neurosci *25*, 6550-6560.

Skaliora, I., Singer, W., Betz, H., and Puschel, A. W. (1998). Differential patterns of semaphorin expression in the developing rat brain. Eur J Neurosci *10*, 1215-1229.

Staatz, W. D., Fok, K. F., Zutter, M. M., Adams, S. P., Rodriguez, B. A., and Santoro, S. A. (1991). Identification of a tetrapeptide recognition sequence for the alpha 2 beta 1 integrin in collagen. J Biol Chem *266*, 7363-7367.

Stein, E., Zou, Y., Poo, M., and Tessier-Lavigne, M. (2001). Binding of DCC by netrin-1 to mediate axon guidance independent of adenosine A2B receptor activation. Science *291*, 1976-1982.

Stoykova, A., and Gruss, P. (1994). Roles of Pax-genes in developing and adult brain as suggested by expression patterns. J Neurosci *14*, 1395-1412.

Tamamaki, N., Fujimori, K., Nojyo, Y., Kaneko, T., and Takauji, R. (2003). Evidence that Sema3A and Sema3F regulate the migration of GABAergic neurons in the developing neocortex. J Comp Neurol *455*, 238-248.

Torii, M., and Levitt, P. (2005). Dissociation of corticothalamic and thalamocortical axon targeting by an EphA7-mediated mechanism. Neuron *48*, 563-575.

Tuttle, R., Nakagawa, Y., Johnson, J. E., and O'Leary, D. D. (1999). Defects in thalamocortical axon pathfinding correlate with altered cell domains in Mash-1-deficient mice. Development *126*, 1903-1916.

Uziel, D., Muhlfriedel, S., Zarbalis, K., Wurst, W., Levitt, P., and Bolz, J. (2002). Miswiring of limbic thalamocortical projections in the absence of ephrin-A5. J Neurosci *22*, 9352-9357.

Vanderhaeghen, P., Lu, Q., Prakash, N., Frisen, J., Walsh, C. A., Frostig, R. D., and Flanagan, J. G. (2000). A mapping label required for normal scale of body representation in the cortex. Nat Neurosci *3*, 358-365.

Volkmer, H., Hassel, B., Wolff, J. M., and Rathjen, F. G. (1992). Structure of the axonal surface recognition molecule neurofascin and its relationship to a neural subgroup of the immunoglobulin superfamily. J Cell Biol *118*, 149-161.

Wiencken-Barger, A. E., Mavity-Hudson, J., Bartsch, U., Schachner, M., and Casagrande, V. A. (2004). The role of L1 in axon pathfinding and fasciculation. Cereb Cortex *14*, 121-131.

Wilkinson, D. G. (2001). Multiple roles of EPH receptors and ephrins in neural development. Nat Rev Neurosci *2*, 155-164.

Williams, S. E., Grumet, M., Colman, D. R., Henkemeyer, M., Mason, C. A., and Sakurai, T. (2006). A Role for Nr-CAM in the Patterning of Binocular Visual Pathways. Neuron *50*, 535-547.

Yazdani, U., and Terman, J. R. (2006). The semaphorins. Genome Biol *7*, 211.

Zhou, C., Qiu, Y., Pereira, F. A., Crair, M. C., Tsai, S. Y., and Tsai, M. J. (1999). The nuclear orphan receptor COUP-TFI is required for differentiation of subplate neurons and guidance of thalamocortical axons. Neuron *24*, 847-859.

Zhou, C., Tsai, S. Y., and Tsai, M. J. (2001). COUP-TFI: an intrinsic factor for early regionalization of the neocortex. Genes Dev *15*, 2054-2059.

Zou, Y., Stoeckli, E., Chen, H., and Tessier-Lavigne, M. (2000). Squeezing axons out of the gray matter: a role for slit and semaphorin proteins from midline and ventral spinal cord. Cell *102*, 363-375.

Figure 1.1: **Embryonic and Adult Thalamocortical Topography**

(A) Scheme depicting a coronal section of embryonic mouse brain (E14) illustrating the pathway taken by thalamocortical axons (red line). Thalamic axons grow ventrally out of the dorsal thalamus (DT) into the ventral thalamus (VT). They turn dorsolaterally at the diencephalic-telencephalic border to enter the ventral telencephalon (VTe) and finally target the neocortex (NCx).

(B) Scheme illustrating a horizontal section of the adult mouse brain thalamocortical projection patterns. Axons from the rostrally located ventroanterior (VA) or ventrolateral (VL) nuclei project to the motor cortex. The ventral basal (VB) complex projects to the primary somatosensory (S1) cortex. Axons from the lateral geniculate nucleus (LGN), located in the caudal dorsal thalamus, project to the primary visual cortex (V1).

Figure 1.1

A

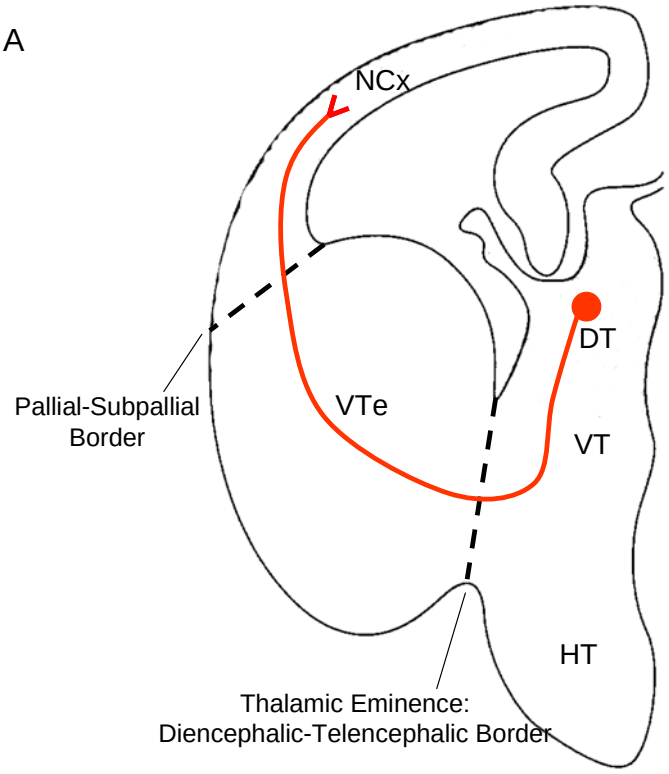
NCx
DT
Pallial-Subpallial
Border
VTe
VT
HT
Thalamic Eminence:
Diencephalic-Telencephalic Border

B

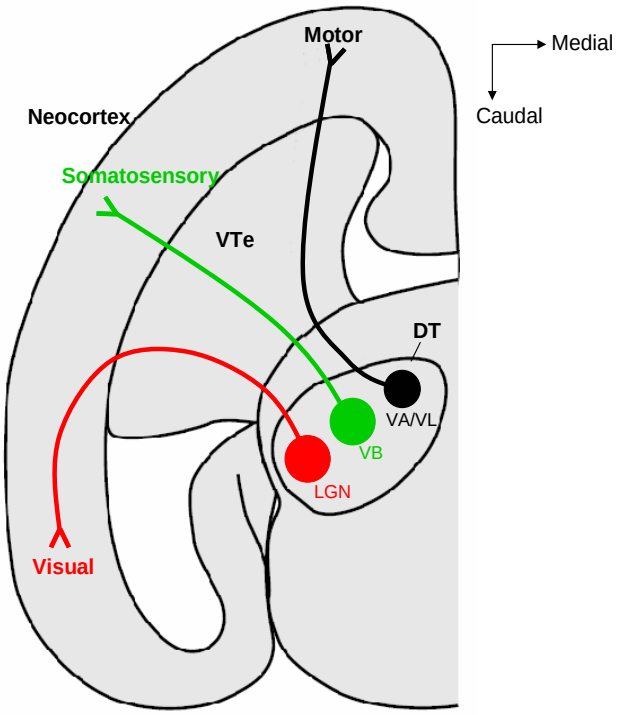
Motor
Medial
Caudal
Neocortex
Somatosensory
VTe
DT
VA/VL
VB
LGN
Visual

Figure 1.2: **Structure and Interactions of CHL1**

Structure of Close Homolog of L1 (CHL1) indicating the position of extracellular and intracellular binding sites. A potential integrin binding site is located in the sixth Ig domain (Ig6) (DGEA). A potential Npn1 binding site is located in Ig1 (FASNRL), linking CHL1 to Sema3A. A binding site for ezrin, radixin, moesin (ERM) proteins, RGGKYSV, is located in a membrane proximal region of the cytoplasmic tail. ERM proteins interact directly with F-actin. The ankyrin binding domain, FIGAY, is also located in the cytoplasmic tail. Ankyrin has two binding sites for cell adhesion molecules, and therefore may form linear arrays of dimeric complexes on the cell membrane. The complex is further immobilized by binding the spectrin tetramer, which associates with the actin cytoskeleton.

Figure 1.2

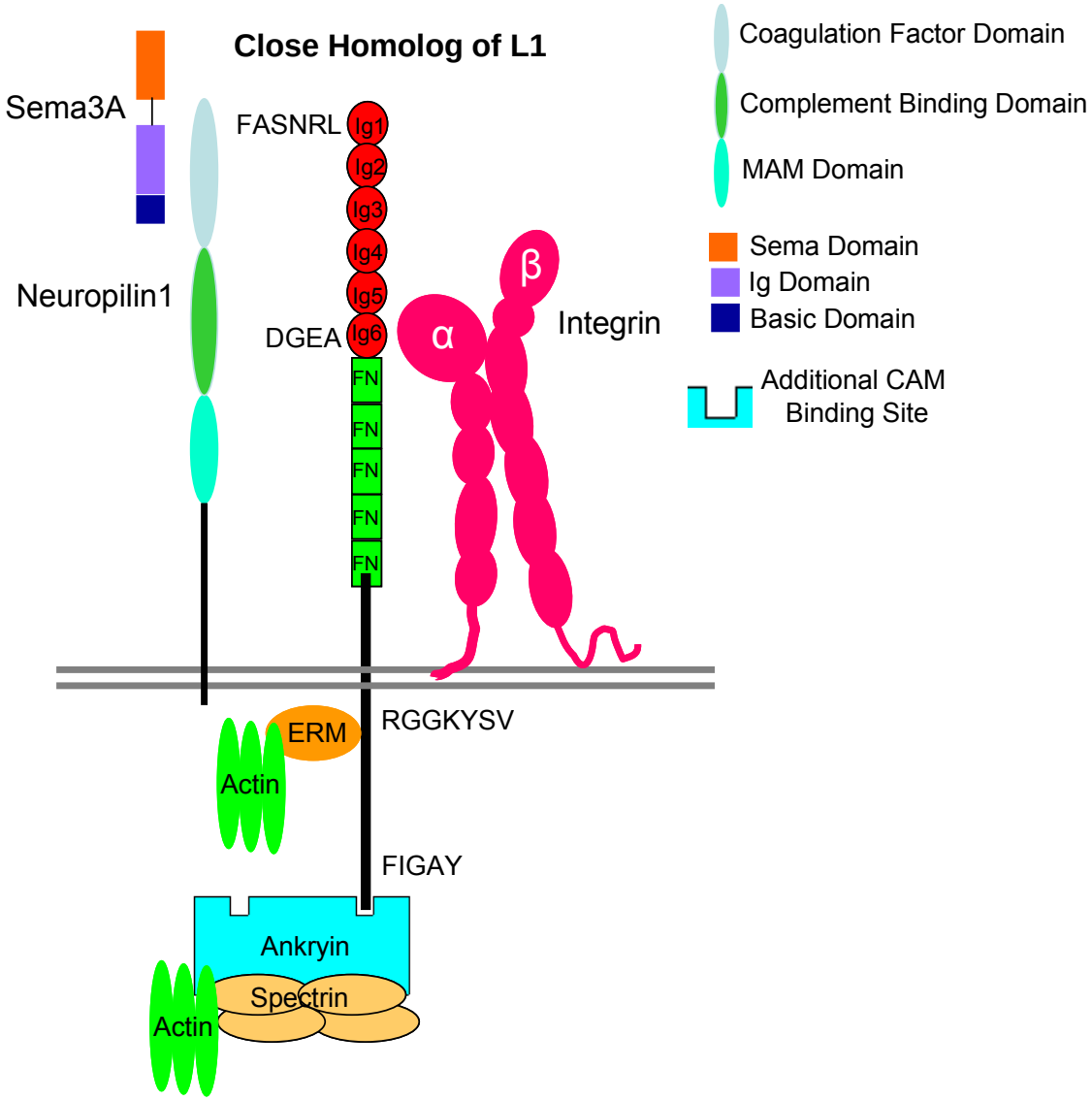
Close Homolog of L1
Sema3A
FASNRL
Ig1
Ig2
Ig3
Ig4
Ig5
Ig6
Neuropilin1
DGEA
FN
FN
FN
FN
FN
β
α
Integrin
ERM
Actin
RGGKYSV
FIGAY
Ankryin
Spectrin
Actin
Coagulation Factor Domain
Complement Binding Domain
MAM Domain
Sema Domain
Ig Domain
Basic Domain
Additional CAM
Binding Site

Chapter 2

Close Homolog of L1 (CHL1) and Neuropilin1 Mediate Guidance of Thalamocortical Axons at the Ventral Telencephalon

Manuscript submitted to Journal of Neuroscience

Amanda G. Wright, Galina P. Demyanenko, Ashton Powell, Melitta Schachner, Lilian Enriquez-Barreto, Tracy S. Tran, Franck Polleux, and Patricia F. Maness

Modifications have been made for the purpose of this dissertation

This was a collaborative effort. I performed most experiments with the exception of the following: Whole mount preparations were performed by Ashton Powell and Dr. Franck Polleux and Figure 12 was modified from an original image from Ashton Powell for the purposes of this dissertation; *In situ* hybridizations were performed by the UNC Confocal and Hybridization Core Facility; Cytochrome oxidase and Nissl staining, as well as segregation experiments were preformed by Lilian Enriquez-Baretto.

2.1 Abstract

We report a cooperation between the neural adhesion molecule, Close Homolog of L1 (CHL1) and the semaphorin3A (Sema3A) receptor, neuropilin1 (Npn1), important for the establishment of topography of area-specific thalamocortical projections. CHL1 deletion in mice selectively disrupted the topographic projection of somatosensory thalamic axons, causing them to shift caudally in the ventral telencephalon (VTe), an intermediate target with graded Sema3A expression, and ultimately target the visual cortex. CHL1 was also required for caudal thalamic axon guidance in the VTe. A similar pattern of aberrant guidance was observed in $Npn1^{Sema-/-}$ mutants, in which axons are nonresponsive to Sema3A. CHL1 co-localized with Npn1 on thalamic axons, and associated with Npn1 through a sequence in the CHL1 Ig1 domain that was required for Sema3A-induced growth cone collapse. Soluble CHL1, acting as an additional binding partner for CHL1-Npn1 complexes, silenced the Sema3A-induced collapse response, supporting a model whereby CHL1 on corticofugal axons directs caudal thalamic axon growth through the VTe. These results identify a novel function for CHL1 in thalamic axon responsiveness to ventral telencephalic as well as cortical cues, and demonstrate a role for CHL1 and Npn1 in establishment of proper topography of thalamocortical projections.

2.2 Introduction

L1 neural cell adhesion molecules (L1-CAMs) are immunoglobulin-class recognition proteins that promote axon growth and migration in developing neurons

(Maness, 2007). The mammalian L1 family consists of L1, Close Homolog of L1 (CHL1), NrCAM, and neurofascin, whose importance in development of cortical connectivity is underscored by association of their mutation with neuropsychiatric disorders, such as mental retardation, schizophrenia, and autism (Kurumaji et al., 2001; Sakurai et al., 2002; Frints et al., 2003; Bonora et al., 2005). CHL1 is unique among L1-CAMs in exhibiting cortical area-specific expression in a high caudal to low rostral gradient (Hillenbrand et al., 1999; Liu et al., 2000; Demyanenko et al., 2004). In posterior cortical areas (primary somatosensory and visual cortex), CHL1 is required for correct laminar positioning and dendritic projection of pyramidal neurons (Buhusi et al., 2003; Demyanenko et al., 2004). CHL1 is also expressed in subpopulations of developing neurons in the dorsal thalamus, hippocampus, and olfactory tract (Liu et al., 2000; Montag-Sallaz et al., 2002). Molecules such as CHL1 with graded or restricted expression patterns are candidates for axon guidance determinants regulating topographic projections to targets in the central nervous system.

Proper topographic mapping of thalamic axons to area-specific targets in the neocortex requires a series of guidance decisions at both cortical and subcortical levels. Thalamocortical mapping is initially specified by transcription factors and morphogens exhibiting graded expression in the thalamus (neurogenin-2 (Seibt et al., 2003), Gbx2 (Hevner et al., 2002)) and dorsal telencephalon (DTe) (FGF8(Shimogori and Grove, 2005), Emx2 (Hamasaki et al., 2004), CoupTFI (Liu et al., 2000)). The ventral telencephalon (VTe) has emerged as a key intermediate target where thalamic axons are sorted to cortical areas along the rostrocaudal axis

(Dufour et al., 2003). Transcription factors Dlx1/2, Ebf1, and Mash1 in the VTe are important primary determinants of thalamocortical axon targeting (Tuttle et al., 1999; Garel et al., 2002), and may direct the expression of axon guidance molecules. During initial stages of projection (Embryonic day 13 (E13)-E14 in mouse), thalamic axons are attracted to the VTe by neuregulin1 (Lopez-Bendito et al., 2006), where rostral thalamic axons are sorted toward the motor cortex based on complementary gradients of ephrinA ligands and EphA receptors (Dufour et al., 2003).

At E15-16, thalamic axons reach the cortical subplate and wait (Ghosh et al., 1990) until other cortical cues, such as neurotrophin-3 (Ma et al., 2002), induce axons to invade the cortex. EphrinA/EphA gradients influence the precise targeting of thalamocortical axons within adjacent cortical areas (Cang et al., 2005; Torii and Levitt, 2005), and the initially diffuse projection of axons within each cortical area is further refined to layer IV by activity-dependent and independent mechanisms (Katz and Crowley, 2002).

Although ephrinA/EphA gradients influence sorting of rostral thalamic axons in the VTe (Dufour et al., 2003), guidance molecules that direct the targeting of somatosensory and visual axons to more posterior neocortical areas remain to be elucidated. CHL1 might participate in topographic guidance of these axons at the VTe, as it is expressed in the embryonic thalamus and posterior neocortex during thalamocortical projection (Liu et al., 2000; Demyanenko et al., 2004). Moreover, its close structural relative, L1, has a guidance function in topographic mapping of retinal axons to the superior colliculus (Demyanenko and Maness, 2003). The secreted semaphorin, Sema3A, is also a candidate thalamocortical axon guidance

cue, as it is expressed along the pathway of projecting thalamocortical axons (Skaliora et al., 1998; Tamamaki et al., 2003), and induces collapse of thalamic growth cones to promote homotypic axon interaction *in vitro* (Bagnard et al., 2001). A link between CHL1 and the Sema3A receptor, neuropilin1 (Npn1), is plausible, based on the association of L1 and NrCAM with neuropilins, important for development of the corticospinal tract and anterior commissure, respectively (Castellani et al., 2000; Falk et al., 2005).

The juxtaposition of corticothalamic and thalamocortical axons in the VTe is also important for thalamocortical development, according to the "handshake hypothesis," which states that thalamic axons are instructed *en route* to the cortex by following the path established by closely apposed cortical efferents (McConnell et al., 1989; Molnar et al., 1998). This theory is supported by studies of mice with mutations in transcription factor genes expressed in the cortex (Tbr1), the thalamus (Gbx2), or both (Pax6) (Storykova 1998; Hevner; Jones 2002), in which thalamic and cortical connections are aberrant and do not reach their final targets. An outstanding question is to what degree molecular determinants with graded expression on cortical axons instruct the patterning of thalamocortical projections.

Here I investigated whether CHL1 participates in topographic mapping of thalamocortical projections to posterior cortical areas by mediating axon guidance at the VTe. Axon tracing in postnatal CHL1-minus mice (P5) showed that loss of CHL1 caused a contingent of somatosensory thalamic axons to misproject to the visual cortex. Guidance of thalamic axons in CHL1-minus embryos (E15.5) was selectively impaired along the rostrocaudal axis of the VTe, with ventrobasal (VB) and caudal,

but not rostral, axons displaying aberrant topography. Axonal tracing in Npn1$^{Sema-/-}$ mice, which express a mutant form of Npn1 that is incapable of Sema3A binding (Gu et al., 2003), showed that Sema3A-nonresponsive thalamic axons misprojected similarly to CHL1-minus axons within the VTe. Furthermore, CHL1 colocalized with the Sema3A receptor (Npn1) during the thalamocortical projection, associated with Npn1 through a sequence in the CHL1 IgI domain, and was required for Sema3A-induced collapse of thalamic growth cones. Thus, the studies presented here reveal a novel cooperation between CHL1 and Npn1, important for the establishment of the topography of thalamocortical projections.

2.3 Results

CHL1 is Expressed in the Thalamocortical Pathway

Expression of CHL1 was analyzed in mouse embryos at E14.5, during projection of thalamic axons across the VTe, and at E16.5, when thalamic axons have reached the DTe (Seibt et al., 2003) by immunofluorescence staining. At E14.5, CHL1 immunoreactivity was robust within the dorsal thalamus (DT) and internal capsule (IC) of the VTe, as well as in the cortical intermediate zone (IZ), cortical plate (CP) and marginal zone (MZ) as shown in a coronal section midway along the rostrocaudal axis (Fig 2.1A). A similar pattern of CHL1 expression was observed at E16.5 in the DT, IC, and neocortex (Fig 2.1B,C). No staining was observed with nonimmune IgG (Fig 2.1C). *In situ* hybridization showed expression of CHL1 mRNA within the DT at E14.5. Examination of serial horizontal sections through the DT indicated that CHL1 was expressed in a high ventral to low dorsal

gradient, corresponding to the approximate location of VB axons (Altman, 1995) (Fig 2.1D). CHL1 transcripts were also evident in the CP and IZ, most likely corresponding to migrating neurons, but not in the lateral or medial ganglionic eminence (LGE,MGE) (Fig 2.1E). To better define the localization of CHL1 protein to thalamocortical and/or corticofugal axons, explants from the DT were isolated from transgenic mouse embryos (E14.5) expressing enhanced green fluorescent protein (EGFP) from the chicken β-actin promoter (Okabe et al., 1997), and co-cultured with a wholemount of isochronic telencephalic vesicle from unlabeled embryos (Dufour et al., 2003; Seibt et al., 2003). CHL1 immunofluorescence was evident on EGFP-expressing thalamic axons, where it localized to growth cones and axon shafts (Fig 2.1F,G). CHL1 staining was also apparent on non-EGFP-expressing axons derived from the telencephalon (red fibers, Fig 2.1F). These results indicated that CHL1 was localized on both embryonic thalamocortical and corticofugal axons during thalamocortical projection.

CHL1 is Required for Topographic Mapping of Thalamocortical Projections to the Somatosensory Cortex

Retrograde axon tracing of thalamocortical projections was carried out in wild type (WT) and homozygous CHL1 mutant mice at postnatal day 5 (P5), when thalamocortical targeting is established (Agmon et al., 1995). WT and CHL1-minus littermates were dually injected with DiI into the primary visual cortex (V1) and DiA into the primary somatosensory cortex (S1) (Fig 2.2A). The accuracy of all injections was monitored for correct rostral-caudal and dorsal-ventral positioning by

epifluorescence microscopy. *In vivo,* DiI is almost exclusively taken up by thalamic axons and transported retrogradely via active transport, labeling cell bodies in the thalamus (see Fig 2.2E, inset). In all WT mice, DiI injection (red) into V1 retrogradely labeled the lateral geniculate nucleus (LGN) of the dorsal thalamus, and DiA injection (green) into S1 retrogradely labeled the ventro-posterolateral (VPL) and ventro-posteromedial (VPM) nuclei of the ventrobasal complex (VB) (Fig 2.2B,C,G). In CHL1-minus mice, injection of DiI into V1 resulted in unexpected labeling (red) of neuronal cell bodies in VB nuclei, in addition to expected labeling of the LGN (Fig 2.2D,E). Injection of DiA into S1 resulted in appropriate labeling of the VPL and VPM nuclei in all CHL1 mutants. Mistargeting of VB axons to the visual cortex was almost fully penetrant (16 of 18 mutant hemispheres), whereas none of the 13 WT hemispheres analyzed displayed these defects. Chi-square analysis showed that this defect was significant for CHL1-mutants ($X^2_{0.005}$=13.72).

Previous studies have shown that for proper cortical targeting, thalamic axons must encounter appropriate subplate and cortical plate layers, within which axons interact with positional cues necessary for proper guidance and targeting (Ghosh and Shatz, 1993; Shimogori and Grove, 2005). CHL1 is expressed in subplate neurons (Liu et al., 2000), however CHL1 deficiency did not affect the generation or laminar positioning of these cells, as determined either by staining for Tbr1, a marker of subplate/layer VI neurons at P0 (not shown) or by BrdU labeling of these cells at E11.5 followed by analysis at P0 (Demyanenko et al., 2004). Mistargeting of somatosensory thalamic axons in CHL1-minus mice did not obviously affect the number or positioning of barrels in the somatosensory cortex seen by Nissl (Fig

2.2J,K) or cytochrome oxidase staining (Fig 2.2L,M), although subtle alterations in barrel positioning may not have been detected.

To determine if thalamic axons projected aberrantly to the primary motor cortex (M1), DiI was injected into the M1 area of WT and CHL1-minus littermates at P5. In all WT (n=8) and CHL1-minus (n=6) mice, DiI (red) injections resulted in appropriate labeling of the ventrolateral nucleus, a motor thalamic nucleus (Fig 2.2F,H). This result indicated that motor thalamic axons were not dependent upon CHL1 for correct topographic mapping to M1, and that axons from non-motor thalamic nuclei do not target the motor cortex.

In summary, axon tracing experiments revealed that a contingent of thalamic axons from VB nuclei projected inappropriately to targets in the visual cortex in CHL1-minus mice, whereas motor and visual thalamic axons targeted correct cortical areas (Fig 2.2I).

CHL1 is Required for Guidance of Thalamic Axons within the Telencephalon

To determine whether CHL1 influences guidance of thalamic axons in the VTe, anterograde axon tracing was carried out in WT and CHL1-minus embryos at E15.5, when thalamic axons have migrated across the VTe and reached the DTe. At this stage axons from the rostral dorsal thalamus (DTR) preferentially grow through the rostral domain of the VTe, while caudal dorsal thalamic axons grow through caudal territories (Seibt et al., 2003). DiI was injected into the rostral third and DiA into the caudal third of the DT, and thalamic axon projections were analyzed (Fig 2.3A). DTR axons of CHL1 mutants projected normally across the VTe and

were visible at the same level within WT and CHL1-minus embryos (Fig 2.3B,C). Analysis of DTR axons throughout the rostrocaudal extent of the VTe confirmed a similar distribution for WT and CHL1 mutant populations (Fig 2.3D), and approximately equal mean distances from the rostral-most axon in the VTe to the thalamic eminence (Fig 2.3E).

In contrast, axons from the caudal dorsal thalamus (DTC) of CHL1-minus embryos were shifted rostrally within the VTe. For example, DTR (red) and DTC (green) axons were visible within the same section of WT VTe (Fig 2.3F), whereas only DTR axons were visible in the CHL1 mutant VTe at the same level (Fig 2.3G). At a more rostral level, both DTR (red) and DTC (green) axons were visible in CHL1 mutant VTe (Fig 2.3H). Analysis of the distribution of labeled DTC axons in the VTe confirmed that axons were shifted rostrally (Fig 2.3I) and that the mean distance from the caudal-most axon to the thalamic eminence was lower in CHL1 mutants compared to WT (Fig 2.3J). These results support a role for CHL1 in guidance of caudal thalamic axons through the intermediate target.

To determine if CHL1 was required for guidance of somatosensory axons, DiI was injected deep in the central third of the DT of WT and CHL1-minus littermates (E15.5) (Fig 2.4A). Axons from the VB nuclei of CHL1-minus embryos were shifted caudally within the VTe. No labeled axons were visible in WT VTe in sections approximately 400 μm caudal to the thalamic eminence (Fig 2.4B), whereas DiI labeled fibers were consistently observed in the VTe of CHL1-minus mice at an equivalent level (Fig 2.4C). DiI labeled fibers from the VB were observed in more rostral levels of the WT VTe (Fig 2.4D). Analysis of the distribution of labeled VB

axons in the VTe confirmed that CHL1-minus axons were shifted caudally (Fig 2.4E) and that the mean distance of the caudal-most axon from the thalamic eminence was significantly greater in CHL1 mutants compared to WT (Fig 2.4F). These results point to a requirement for CHL1 for proper guidance of medial thalamic axons in the IC. Thus, guidance of caudal and medial, but not rostral, thalamic axons through the IC of the VTe are dependent upon CHL1.

To investigate the fate of VB axons that were misguided in the VTe, the localization of these axons within the DTe was examined. Axons from the VB nuclei of CHL1-minus embryos were also shifted caudally within the DTe. In sections approximately 800 μm caudal to the thalamic eminence, no labeled axons were visible in WT DTe (Fig 2.4G). However, DiI labeled fibers were observed in the DTe of CHL1-minus mice at an equivalent level (Fig 2.4H). Analysis of the distribution of labeled VB axons in the DTe confirmed a caudal shift of CHL1-minus axons (Fig 2.4I). These results suggest that a subset of the caudally shifted somatosensory axons in the VTe project to more posterior areas of the DTe.

In vitro studies have indicated a role for Sema3A in homotypic fasciculation of thalamic and cortical axons that may be important for maintaining their segregation during projection to the neocortex (Bagnard et al., 2001). To determine if CHL1 was required for fasciculation within the VTe, DiI was injected into the cortex and DiA into the DT of WT and CHL1-minus embryos (E16.5). No defects in fasciculation or segregation of thalamic and cortical axons within the VTe were observed (Fig 2.5). Segregation within the cortex could not be visualized due to intense labeling of DiI.

CHL1 Colocalizes with the Sema3A Receptor Neuropilin-1

To investigate whether CHL1 participates in thalamic axon responses to Sema3A, co-expression of CHL1 and Npn1 was investigated by immunofluorescence staining during thalamocortical outgrowth (E14.5), cortical targeting (E16.5), and after the establishment of thalamocortical projections (P5). At both embryonic stages, Npn1 was expressed in the DT and VTe and colocalized extensively with CHL1 on fibers (Fig 2.6A,B,D). Coronal sections through ventral regions of the dorsal thalamus, where CHL1 is prominently expressed, are shown here. In the E14.5 cortex, Npn1 was present in the IZ and CP, and colocalized with CHL1 on axons within the IZ (Fig 2.6C). At E16.5, thalamocortical axons enter the neocortex and travel within the upper IZ, segregated from corticothalamic axons in the lower IZ(Bagnard et al., 1998). At this stage, Npn1 and CHL1 colocalized in both the upper and lower IZ, suggesting that they may reside on both axonal subsets (Fig 2.6E). Npn1 exhibited a non-graded pattern of expression at both stages along the rostrocaudal cortical axis. Npn1 also co-localized with CHL1-positive fibers in the DT at P5 (Fig 2.6F), specifically in the VB complex (Fig 2.6F') suggesting that the receptor for Sema3A may play a role in guiding these axons to their final targets.

In situ hybridization for Sema3A transcripts at E14.5 showed robust expression within the VTe but not in the DT. Throughout serial horizontal sections, a high-caudal to low-rostral gradient of Sema3A expression was observed in the intermediate zone of the ganglionic eminence within the VTe (Fig 2.6G,H). The control sense probe did not generate signals above background levels (data not shown). The gradient of Sema3A expression was quantified by measuring pixel

densities along the rostrocaudal axis of the VTe and normalizing these values to background levels. The average pixel density in the caudal VTe was significantly greater than in rostral regions and the data fit a linear regression (Fig 2.6I). Thus, Sema3A forms a spatial gradient (high caudal to low rostral) of gene expression in the VTe at E14.5. Sema3A mRNA was also seen in the VZ and to a lesser extent in the CP of the neocortex at E14.5 (Fig 2.6J), in accord with previous studies (Bagnard et al., 1998; Skaliora et al., 1998; Tamamaki et al., 2003).

Npn1 Binding to Sema3A is Required for Guidance of Thalamic Axons within the Ventral Telencephalon

To establish a role for Npn1 and Sema3A in thalamocortical axon guidance *in vivo*, thalamic axons were traced in $Npn1^{Sema-/-}$ mutant mice at E16.5. $Npn1^{Sema-/-}$ mice express normal levels of Npn1 protein and retain VEGF-Npn1 signaling, but Sema-Npn1 signaling is abolished and neurons are completely unresponsive to Sema3A (Gu et al., 2003). Because Npn1 null mice die midway though gestation (~E10.5-E12.5) (Kitsukawa et al., 1997; Kawasaki et al., 1999), $Npn1^{Sema-/-}$ mice were chosen to study the role of Npn1-Sema signaling on thalamocortical axon guidance. DiI was injected into the rostral third (DTR) and DiA into the caudal third (DTC) of the dorsal thalamus of WT and $Npn1^{Sema-/-}$ littermates and thalamic axon distribution was analyzed (Fig 2.7A). DTR axons from $Npn1^{Sema-/-}$ mutants projected normally across the VTe and were visible at the same level as observed in WT (Fig 2.7B,C). Analysis of the distribution of DTR axons across the rostrocaudal extent of the VTe revealed a similar pattern for WT and $Npn1^{Sema-/-}$ mutant populations (Fig

2.7D), and approximately equal mean distances from the rostral-most axon in the VTe to the thalamic eminence (Fig 2.7E).

In contrast, caudal thalamic axons were shifted rostrally within the VTe. For example, both DTR (red) and DTC (green) axons were observed in a section of WT VTe 500 μm caudal to the thalamic eminence (Fig 2.7F), whereas only DTR axons were visible in the Npn1$^{Sema-/-}$ mutant at an equivalent level (Fig 2.7G). However, at a more rostral level, where only DTR (red) axons were visible in WT VTe (Fig 2.7H), both DTR (red) and DTC (green) axons were visible in the Npn1$^{Sema-/-}$ VTe (Fig 2.7I). Analysis of DTC axons throughout the VTe confirmed that these axons were shifted rostrally and the mean distance from the caudal-most axon to the thalamic eminence was significantly less in Npn1$^{Sema-/-}$ mutants compared to WT (Fig 2.7J,K). Thus, while DTR axons migrated normally across the Npn1$^{Sema-/-}$ VTe, DTC axons were altered in the VTe of Npn1$^{Sema-/-}$ mutant mice, supporting a role for Npn1 in the guidance of this population of thalamic axons.

To further explore the role of Npn1 in thalamocortical axon guidance, axons originating from VB nuclei of Npn1$^{Sema-/-}$ mutants were analyzed in the intermediate target. Somatosensory thalamic axons were shifted caudally in the VTe. In these experiments, DiI was injected deep into the central third of the DT of WT and Npn1$^{Sema-/-}$ littermates (Fig 2.8A). In sections approximately 400 μm caudal to the thalamic eminence, no labeled axons were visible in WT VTe (Fig 2.8B), whereas DiI labeled fibers were consistently observed in the VTe of Npn1$^{Sema-/-}$ mice at an equivalent level (Fig 2.8C). DiI labeled fibers from VB nuclei were observed at more rostral levels of the WT VTe (Fig 2.8D). Analysis of the distribution of labeled VB

axons in the VTe confirmed that somatosensory axons from Npn1$^{Sema-/-}$ embryos were shifted caudally (Fig 2.8E) and that the mean distance from the caudal-most axon to the thalamic eminence was significantly greater in Npn1$^{Sema-/-}$ mutants compared to WT (Fig 2.8F). Therefore, axons from the VB complex are dependent upon Npn1 and its ability to bind Sema3A for guidance through the intermediate target. Furthermore, the aberrant guidance of somatosensory and caudal thalamic axons in Npn1$^{Sema-/-}$ mutants phenocopied the shifts observed in CHL1-minus mice, providing *in vivo* evidence that CHL1 and Npn1 may cooperate to control the topographic mapping of subpopulations of thalamocortical axons.

CHL1 Associates with the Semaphorin3A Receptor Neuropilin1

I next investigated whether CHL1 could form a complex with Npn1 by antibody-induced co-capping within the plasma membrane. CHL1 and Npn1 were transiently expressed in COS-7 cells, and then Npn1 was clustered on the cell surface by cross-linking with anti-Npn1 antibody. After fixation, Npn1 caps were detected on the cell surface by labeling with FITC-secondary antibodies, and co-capping of CHL1 was observed by indirect immunofluorescence with anti-CHL1 and TRITC-secondary antibodies (Fig 2.9A). Co-capping of CHL1 and Npn1 was observed on 82% of CHL1-expressing cells. In reverse co-capping experiments, CHL1 clustering induced co-capping of Npn1 in 75% of cells (Fig 2.9B). Cells treated with non-immune rabbit IgG did not induce capping of Npn1 or clustering of CHL1 (Fig 2.9C). These results suggest that CHL1 interacts in *cis* with Npn1, either directly or indirectly.

L1 associates with Npn1 through a sequence (FASNKL) in the first L1 Ig domain, within which a missense mutation (L120V) disrupts L1-Npn1, but not L1-L1 binding (Castellani et al., 2002). This conservative mutation within the FG loop of L1 results in a change in the size and shape of a surface hydrophobic residue (L120) (Bateman et al., 1996). Furthermore, the mutation of L120V in human L1 resulted in severe L1 mental retardation syndrome with hydrocephalus, indicating its functional importance (De Angelis et al., 1999). Because the sequence is conserved in the Ig1 domain of CHL1 (FASNRL), we investigated whether the equivalent mutation (L115V) would prevent CHL1 interaction with Npn1 in COS-7 cells. Very little co-capping was observed (17% of cells) between Npn1 and the $CHL1_{L115V}$ mutant protein, shown by the uniform distribution of $CHL1_{L115V}$ mutant protein in the plasma membrane (Fig 2.9D). These results suggest that the conserved sequence, FASNRL, in Ig1 of CHL1 is necessary for Npn1 association.

The association between CHL1 and Npn1 was further explored by co-immunoprecipitation experiments. CHL1 or $CHL1_{L115V}$ were transiently co-transfected with myc-tagged Npn1 in COS-7 cells. After 2 days, cell lysates were immunoprecipitated with mouse anti-myc antibody (Gift from Dr. Henrick Dohlman). Precipitates were evaluated by gel electrophoresis, and the presence of CHL1 was analyzed by immunoblotting with anti-CHL1 goat polyclonal antibody. CHL1 protein, expressed as a doublet of 180 and 165 kiloDaltons (kDa), was detected in the immunoprecipitates of cells transfected with CHL1wt and Npn1, supporting the interaction between the two proteins (Fig 2.9E). The two isoforms of CHL1 (185 and 165 kDa) most likely correspond to two glycosylation variants (Hillenbrand et al.,

1999). An additional explanation for the two isoforms involves protein processing within the cell. The higher molecular weight isoform could be non-processed, intracellular CHL1 (containing the signal peptide) while the lower molecular weight isoform is processed CHL1 on the cell surface. Consistent with this observation, only the lower molecular weight isoform is detected in crude membrane fractions from mouse embryos under physiological buffer conditions (Hillenbrand et al., 1999). The association between CHL1 and Npn1 was shown to be dependent upon the critical leucine residue in the Ig1 extracellular domain of CHL1, as $CHL1_{L115V}$ was not immunoprecipitated with Npn1 (Fig 2.9E). CHL1 also co-immunoprecipitated with Npn1 in whole brain extracts from E16.5 WT embryos (Fig 2.9E). Western blots for Npn1 demonstrated the specificity of the immunoprecipitation, with protein present at 130 kDa (Fig 2.9E).

CHL1 is Required for Sema3A-Induced Growth Cone Collapse of Thalamic Axons

To investigate whether CHL1 is required for growth cone collapse of thalamic axons in response to Sema3A, genetic rescue experiments were performed in which cultures of dissociated thalamic neurons from CHL1-minus embryos (E14.5) were transfected with plasmids encoding CHL1wt, mutant $CHL1_{L115V}$, defective in Npn1 binding, or empty vector, together with a GFP expression plasmid. After 3 days, cells were treated with Sema3A protein fused to alkaline phosphatase (Sema3A-AP) or control Fc protein fused to alkaline phosphatase (Fc-AP). Cellular actin was stained with phalloidin and GFP-expressing cells were scored for growth cone collapse by phalloidin fluorescence. Co-transfection was efficient, as the percentage of GFP-

positive neurons expressing CHL1 or $CHL1_{L115V}$ was 84% and 81%, respectively. CHL1-minus neurons transfected with vector alone showed a small but significant growth cone collapse response to Sema3A-AP compared to Fc-AP control (Fig 2.10A,B,G). The percent of collapsed growth cones in CHL1-minus cultures did not change when Fc-AP was added (not shown). In CHL1-minus thalamic neurons transfected with CHL1wt cDNA, the growth cone collapse response to Sema3A-AP significantly increased over control Fc-AP (Fig 2.10C,D,G). Strikingly, transfection of CHL1-minus neurons with the $CHL1_{L115V}$-expressing plasmid did not increase the growth cone collapse response to Sema3A (Fig 2.10E,F). The smaller Sema3A collapse response that remained in CHL1-minus and $CHL1_{L115V}$ -expressing cultures compared to treatment with Fc-AP (Fig 2.10G) was not significantly different in CHL1-minus and mutant-expressing neurons, and might represent an L1/Npn1-dependent mechanism.

L1 interaction with Npn1 mediates Sema3A-induced growth cone collapse in neonatal cortical and sensory neurons (Castellani et al., 2002), and L1 acting in *trans* as a ligand for L1-Npn1 complexes converts Sema3A-mediated repulsion to attraction (Castellani et al., 2000). To test whether soluble CHL1 was capable of modifying the response of thalamic axons to Sema3A, recombinant CHL1 protein was added to cultures of dissociated thalamic neurons 15 min prior to addition of Sema3A-AP. While CHL1 protein had little effect on neurons expressing no CHL1 or mutant $CHL1_{L115V}$, soluble CHL1 significantly decreased the percent of CHL1wt-expressing growth cones that collapsed in response to Sema3A-AP (Fig 2.10G),

suggesting that CHL1 as a ligand could reverse, or silence, much of the collapse response to Sema3A.

In explant cultures containing nondissociated neurons from embryonic thalamus (E14.5), Sema3A-AP similarly induced robust growth cone collapse of thalamic axons from WT embryos, but was much less effective at collapsing CHL1-minus thalamic axons (Fig 2.10H).

These results indicate that CHL1 is responsible for a majority of the Sema3A-induced growth cone collapse in embryonic thalamic axons at this stage, and that a single point mutation within the Npn1 binding site in CHL1 Ig1 domain is critical for rescuing the response in CHL1-minus thalamic neurons. In addition, CHL1 acting as a ligand for CHL1-Npn1 complexes can silence Sema3A-induced collapse. These data support a mechanism in which CHL1 associates with Npn1 through the CHL1 Ig1 domain to form a receptor complex for Sema3A, important for growth cone collapse of thalamic axons that could regulate guidance in the VTe.

2.4 Discussion

Here we identify CHL1 as a new molecular determinant of thalamocortical axon projection to specific neocortical areas, acting within an intermediate target, the VTe. CHL1 deletion disrupted the final thalamocortical map by causing a contingent of axons from somatosensory thalamic nuclei to incorrectly target the visual cortex. CHL1 colocalized Npn1 on thalamic axons, and axonal tracing demonstrated that thalamic axons from VB nuclei of CHL1-minus and Sema3A-nonresponsive $Npn1^{Sema-/-}$ mutants misprojected caudally within the VTe, consistent with loss of

repellent axon guidance to the high-caudal to low-rostral Sema3A gradient (Fig 2.11). This mechanism is supported by genetic rescue experiments in CHL1-minus thalamic neurons, which demonstrated that a single point mutation (L115V) in the CHL1 Ig1 domain was critical for both Sema3A-induced growth cone collapse and association of CHL1 with Npn1. In addition, caudal thalamic axons were shifted rostrally in the VTe of CHL1-minus and Npn1$^{Sema-/-}$ mutant embryos, consistent with impaired permissive axon guidance through high Sema3A caudal territories of the VTe, possibly due to loss of CHL1-Npn1 signaling (Fig 2.11). Our results reveal a novel cooperation between CHL1 and Npn1 for axon guidance responsible for topographic sorting of specific thalamocortical projections at the VTe in response to Sema3A.

The aberrant caudal shift of VB axons in the VTe of CHL1-minus and Npn1$^{Sema-/-}$ mice is consistent with a cooperative function for CHL1 and Npn1 in mediating axon repulsion from the descending caudal gradient of Sema3A in the VTe. The caudal shift of VB thalamic axons in the CHL1-minus telencephalon culminates in misrouting of these axons to the posterior visual cortex. A number of mutant axons misguided in the telencephalon may be lost during later stages of development, prior to barrel formation, as a substantial portion of VB axons correctly targeted the somatosensory cortex. This could potentially account for the relatively normal barrel field in CHL1-minus mice. Mice deficient in Sema3A (Ulupinar et al., 1999) and PlexinA4, a Npn1 co-receptor (Suto et al., 2005), display relatively normal barrels as well. CHL1 probably does not factor in the tangential migration of cells that form a permissive corridor for thalamocortical axon navigation into the

telencephalon (Lopez-Bendito et al., 2006), as CHL1 transcripts were not detected in the ganglionic eminence. The ability of CHL1 to promote Sema3A-induced growth cone collapse in thalamic neurons mediated by an identified Npn1 binding site in the CHL Ig1 domain supports the interpretation that VB thalamic axons are repelled from the increasing Sema3A gradient along the rostrocaudal axis of the VTe.

The high ventral to low dorsal gradient of CHL1 in the dorsal thalamus is consistent with preferential expression of CHL1 in somatosensory nuclei. In addition, plexinA4, a component of the Sema3A signaling complex, is preferentially expressed in the VPM/VPL nuclei (Suto et al., 2005). These expression patterns may explain the differential response of posterior thalamic axons due to loss of CHL1/Npn1 signaling.

Since CHL1 is expressed on corticofugal axons in a high caudal to low rostral gradient (Demyanenko 2004; Liu 2000), some aspects of thalamocortical misrouting might be secondary due to cell non-autonomous functions of CHL1 on caudal corticothalamic axons. The rostral shift of caudal axons is also observed in $Npn1^{Sema-/-}$ embryos, consistent with cooperation between CHL1 and Npn1 to control navigation of caudal thalamic axons through the VTe. CHL1 on caudal corticofugal axon subpopulations within the VTe could act as a binding ligand for CHL1-Npn1 complexes on caudal thalamic axons, abrogating growth cone collapse to Sema3A, as shown in growth cone collapse assays. This silencing may enable caudal thalamic axons to migrate preferentially within caudal territories of the VTe *en route* to the cortex. In the absence of CHL1 or Npn1-Sema3A signaling, an unidentified repellent guidance mechanism may predominate, resulting in the rostral shift of

caudal thalamic axons. Netrin1 has recently been implicated in guidance of thalamocortical axons through the VTe. A recent study demonstrated that activation of serotonin (5-HT) converts netrin1-mediated attraction of caudal thalamic axons to repulsion (Bonnin et al., 2007), which could provide a possible mechanism for the rostral shift of caudal thalamic axons observed in CHL1 and Npn1$^{Sema-/-}$ mutant mice. Thus, CHL1/Npn1 complexes may cooperate with netrin1 responses to control topographic mapping of caudal thalamocortical axons, although the molecular basis for such an interaction remains unclear.

Co-capping and co-immunoprecipitation studies demonstrated that CHL1 and Npn1 constitutively associate through a critical leucine residue within a motif (FASNRL^{115}) in the CHL1 Ig1 domain. This motif is homologous to the Npn1 binding site of L1 (FASNKL), which is required for Sema3A-induced growth cone collapse in neonatal cortical and sensory neurons (Castellani et al., 2000). The residual Sema3A-dependent growth cone collapse, observed in CHL1-minus or CHL1$_{L115V}$-expressing thalamic neurons, is likely due to Npn1 signaling through L1, which is also expressed on developing thalamic axons (Fukuda et al., 1997). Despite their similar roles in mediating Sema3A-induced growth cone collapse, genetic deletion of CHL1 or L1 causes different thalamocortical phenotypes *in vivo*. Thalamocortical axons in L1-minus mice are hyperfasciculated but normally target the motor, somatosensory, and visual cortex (Ohyama et al., 2004; Wiencken-Barger et al., 2004), whereas thalamocortical axons of CHL1-minus mice are not altered in fasciculation at the VTe or cortex but do show misrouting of somatosensory projections. Differential expression of CHL1 and L1 in thalamic neuron

subpopulations, or interaction with different homophilic and heterophilic partners along the thalamocortical pathway, might account for these differences. It is also possible that L1 might functionally compensate for loss of CHL1 in certain subpopulations of thalamic neurons.

EphrinA5 is an important axon guidance cue identified previously to influence thalamocortical axon sorting at the VTe (Dufour et al., 2003). The high caudal gradient of ephrinA5 in the VTe preferentially regulates sorting of rostral thalamic axons, ensuring targeting to the motor cortex. We demonstrate that CHL1 and Npn1 mediate sorting of caudal and VB, but not rostral thalamic axons. The rostrocaudal expression levels of Sema3A, ephrinA5, and their receptors may render CHL1/Npn1 the predominant guidance system for sorting of posterior thalamic axons at the VTe. Differential expression of plexinAs (Yaron et al., 2005), MICALs (Pasterkamp et al., 2006), or RanBPM (Togashi et al., 2006), which bind Npn1, might also influence CHL1 interaction with Npn1 and downstream signaling.

Semaphorins and Npns are regulators of repulsive axon guidance through the nervous system, where they are important for pathfinding and fasciculation of olfactory, spinal and cranial axons, and other major tracts (Kitsukawa et al., 1997; Giger et al., 2000; Cloutier et al., 2002; Gu et al., 2003) Our study extends the role of Sema3A and Npn1 to the thalamocortical pathway, one of the main topographic projections in the brain. The results further reveal a prominent new role for CHL1 as a coreceptor for Npn1, mediating axon guidance to Sema3A in the VTe, vital for establishment of the topography of specific thalamocortical projections.

2.5 Methods

Mice

CHL1 heterozygous mutant mice on a C57Bl/6 background (Montag-Sallaz et al., 2002) were intercrossed to obtain CHL1 homozygous null mutants and WT littermates. Embryonic day 0.5 was defined as the plug date and postnatal day 0 (P0) as day of birth. Animal care and treatment were in accordance with guidelines provided by the UNC Institutional Animal Care and Use Committee (IACUC).

Immunostaining and Histology

CHL1 rabbit polyclonal antibody 12146 was raised against recombinant CHL1 fused to the Fc portion of human IgG, and affinity purified, as described (Chen et al., 1999). The antibody was specific for CHL1, shown by Western blotting in the mouse forebrain from E13-P15 and adult (Hillenbrand et al., 1999). In addition, commercially available CHL1 antibody was used (R&D systems, 1:200) with similar results. Other antibodies used were rabbit polyclonal anti-green fluorescent protein (GFP) (Molecular Probes; 1:1000) and rabbit polyclonal anti-Npn1 (Gift from Dr. David Ginty or Calbiochem; 1:70). Whole mounts were permeabilized at 4^{o}C overnight using 5% normal goat serum, 3% bovine serum albumin, and 0.3% Triton X-100 in 0.1 M PBS. The sections were then incubated in primary antibody at room temperature during the day and at 4^{o}C overnight. After 24 hours of washing with 0.1 M PBS, the sections were incubated all day at room temperature and overnight at 4^{o}C in FITC or TRITC-conjugated secondary antibodies. For histology experiments, WT and CHL1-minus littermates were anesthetized and perfused and brains were

processed for cytochrome oxidase (Boyd and Matsubara, 1996) or Nissl (Demyanenko et al., 1999).

In Situ Hybridization

cDNA encoding the extracellular region of mouse CHL1 was subcloned into psBluescript KS(-) and sense and antisense probes were generated by restriction digest (amino acids 1-1083 from Accession Number NM_007697), as previously described (Villegas and Tufro, 2002). Brains from WT embryos (E14.5) were immersion fixed in 4% PFA overnight and cryoprotected in sucrose prior to sectioning (horizontally or sagittally). *In situ* hybridization was performed as described using DIG-labeled probes (Colbert et al., 1995).

In vivo Axon Tracing

Retrograde axon tracing was performed by focal injection of 1,1',dioctadecyl-3,3,3'3'-tetramethylindocarbocyanine perchlorate (DiI) and 4-4-dihexadecyl aminostyryl N-methyl-pyridinium iodide (DiA) (Molecular Probes) solutions (5% in ethanol) in two distinct cortical areas of living mice anesthetized by hypothermia. Injections were made with capillary micropipettes connected to a Picospritzer II. Mice were sacrificed two days later and fixed by transcardial perfusion. Forebrains were vibratome sectioned in the coronal plane (100 μm). Injection sites were monitored microscopically, and only those injections restricted to the neocortex without entering the white matter were further analyzed. The exact locations and positions of the injection sites and the position of thalamic nuclei were identified using bisbenzimide nuclear staining and comparison to atlas coordinates.

For anterograde tracing, WT, CHL1-minus, and $Npn1^{Sema-/-}$ embryonic brains were fixed in 4% PFA overnight at 4°C. Following hemidissection, DiA or DiI crystals were inserted into the dorsal thalamus. After diffusion for 2-4 weeks at room temperature, the brains were coronally vibratome sectioned (100 µm). Sections were mounted in gel mount containing anti-fading agents (Biomedia) and imaged using epifluorescence microscopy. The size and position of the crystals with respect to the thalamic eminence reference point were verified microscopically. Acceptable injections were within 300 µm of the thalamic eminence (for rostral or caudal labeling) or 100 µm (for VB labeling).

Co-capping Assay

COS-7 cells were co-transfected with pCos-BMN-Npn1 and pcDNA3-CHL1 or pcDNA3-$CHL1_{L115V}$ mutant. The cells were then dissociated with 5mM EDTA in Hank's Balanced Salt Solution (HBSS), washed with 10% fetal bovine serum in DMEM, and resuspended in ice cold DMEM. To cap surface Npn1, the cells (30,000 cells/100 µl) were incubated with anti-Npn1 rabbit polyclonal antibody (40 µg/ml) at 4°C for 20 min. To cap surface CHL1, cells were incubated with anti-CHL1 goat polyclonal antibody (40 µg/ml). The cells were washed in ice cold DMEM, resuspended in DMEM containing 10 µg/ml of mouse anti-rabbit IgG to cluster Npn1 or mouse anti-goat IgG to cluster CHL1, and incubated for 20 min on ice. After washing with ice cold DMEM, cells were resuspended in 10% fetal bovine serum in DMEM and plated onto fibronectin coated MatTek dishes (MatTek Corp). Cells were incubated for 1 hr at 37°C and then fixed with 4% PFA for 15 min. After washing, cells were blocked in 10% donkey serum for 1 hr at room temperature. To label

CHL1, the cells were incubated with anti-CHL1 antibody (20 µg/ml in blocking buffer) for 2 hr at room temperature and washed with PBS. To label Npn1, cells were incubated with anti-Npn1 (20 µg/ml). Npn1 and CHL1 were detected by incubating the cells with FITC- and TRITC-conjugated secondary antibodies (diluted 1:100 in blocking buffer) for 1 hr at room temperature. Finally, the cells were washed, mounted in Vectashield, and imaged using an Olympus FV500 laser confocal microscope.

Co-immunoprecipitation

COS-7 cells were co-transfected with CHL1 or $CHL1_{L115V}$ and myc-tagged Npn1 using Lipofectamine 2000. After 2 days, cells were lysed on ice with immunoprecipitation buffer (20mM Tris HCl, 150mM NaCl, 5mM Na^+EDTA, 2mM Na^+EGTA, 10mM sodium fluoride, 1mM sodium pervanadate, 1mM phenlymethylsulfonyl fluoride, 1% Triton X-100) including protease inhibitors. Whole brains were isolated from E16.5 WT embryos and lysed in complete RIPA buffer (20mM Tris HCl, 0.15M NaCl, 5mM Na+EDTA, 1mM Na+EGTA, 1% NP-40, 1% Na-deoxycholate, 0.1% SDS, 0.2mM sodium orthovadandate, 10mM sodium fluoride) including protease inhibitors. The lysates were incubated for 10 min at 4^{o}C and clarified by centrifugation for 10 min. After preclearing with mouse or rabbit IgG for 30 min at 4^{o}C, samples were immunoprecipitated with mouse anti-myc (10 µg) or rabbit anit-Npn1 (1µg/ml, Chemicon) antibodies for 1 hour at 4^{o}C. The beads were then washed and the precipitates were analyzed by immunoblotting with anti-CHL1 goat polyclonal antibody (1:1000) and an HRP-conjugated bovine anti-goat IgG antibody using enhanced chemiluminescent detection (Pierce).

Growth Cone Collapse Assay

CHL1-minus thalamic embryonic (E14.5) neurons were obtained by isolating the thalamus and dissociating the cells in 3 ml of ice-cold HBSS. Cells were further dissociated by trituration with a 10 ml pipette, followed by a wide bore Pasteur pipette, and immediately co-transfected with pMax-GFP and pcDNA3-CHL1wt, pcDNA3-CHL1$_{L115V}$, or empty pcDNA by electroporation using an Amaxa Nucleofector Device and Mouse Neuron Nucleofector Kit (Amaxa Corp). Briefly, 5 x 10^6 cells were resuspended in transfection buffer and program O-05 was used to electroporate the DNA into the cells. Cells were allowed to recover in RPMI medium (Gibco) for 5 minutes, and then plated on fibronectin-coated MatTek dishes in 10% fetal bovine serum and DMEM. The day after plating, the media was changed to Neurobasal media containing B27 supplement and glutamate (25uM) to select for neurons. After 48 hours of incubation, cells were treated with either FC-AP or Sema3A-AP fusion proteins (30 nM) for 30 min. In some experiments, cells were treated with 3 µg/ml of recombinant extracellular CHL1 (R&D Systems) protein for 15 minutes prior to the addition of Sema3A-AP or FC-AP. FC-AP and Sema3A-AP were prepared by transfecting HEK293T cells using Lipofectamine 2000. After two days, media was collected and the concentration was determined as described in (Flanagan and Leder, 1990), with slight modifications. Cells were then fixed with 4% PFA and permeabilized with 0.2% TritonX-100 for 5 min. After washing, cells were treated with rhodamine-conjugated phalloidin (Molecular Probes; 1:40) for 30 min at room temperature to visualize actin within the growth cone. Only cells expressing

GFP were included in the analysis. Cells were mounted in Vectashield, and growth cone morphology was observed using confocal microscopy.

For explant studies, WT and CHL1-minus embryonic (E14.5) brains were vibratome sectioned (300 μm) and thalamic regions were obtained by microdissection in ice cold HBSS. Explants were plated on fibronectin-coated Mat-Tek dishes using a plasma clot (20 μl bovine thrombin with 20 μl chicken plasma; Sigma) to ensure adherence of the explant. The explants were cultured and growth cone morphology was analyzed as described above.

2.6 References

Agmon, A., Yang, L. T., Jones, E. G., and O'Dowd, D. K. (1995). Topological precision in the thalamic projection to neonatal mouse barrel cortex. J Neurosci *15*, 549-561.

Altman, J. a. B., S.A. (1995). Atlas of prenatal rat brain development (Boca Raton, Ann Arbor, London, Tokyo, CRC Press).

Bagnard, D., Chounlamountri, N., Puschel, A. W., and Bolz, J. (2001). Axonal surface molecules act in combination with semaphorin 3a during the establishment of corticothalamic projections. Cereb Cortex *11*, 278-285.

Bagnard, D., Lohrum, M., Uziel, D., Puschel, A. W., and Bolz, J. (1998). Semaphorins act as attractive and repulsive guidance signals during the development of cortical projections. Development *125*, 5043-5053.

Bateman, A., Jouet, M., MacFarlane, J., Du, J. S., Kenwrick, S., and Chothia, C. (1996). Outline structure of the human L1 cell adhesion molecule and the sites where mutations cause neurological disorders. EMBO J *15*, 6050-6059.

Bonnin, A., Torii, M., Wang, L., Rakic, P., and Levitt, P. (2007). Serotonin modulates the response of embryonic thalamocortical axons to netrin-1. Nat Neurosci *10*, 588-597.

Bonora, E., Lamb, J. A., Barnby, G., Sykes, N., Moberly, T., Beyer, K. S., Klauck, S. M., Poustka, F., Bacchelli, E., Blasi, F.*, et al.* (2005). Mutation screening and association analysis of six candidate genes for autism on chromosome 7q. Eur J Hum Genet *13*, 198-207.

Boyd, J. D., and Matsubara, J. A. (1996). Laminar and columnar patterns of geniculocortical projections in the cat: relationship to cytochrome oxidase. J Comp Neurol *365*, 659-682.

Buhusi, M., Midkiff, B. R., Gates, A. M., Richter, M., Schachner, M., and Maness, P. F. (2003). Close homolog of L1 is an enhancer of integrin-mediated cell migration. J Biol Chem *278*, 25024-25031.

Cang, J., Kaneko, M., Yamada, J., Woods, G., Stryker, M. P., and Feldheim, D. A. (2005). Ephrin-as guide the formation of functional maps in the visual cortex. Neuron *48*, 577-589.

Castellani, V., Chedotal, A., Schachner, M., Faivre-Sarrailh, C., and Rougon, G. (2000). Analysis of the L1-deficient mouse phenotype reveals cross-talk between Sema3A and L1 signaling pathways in axonal guidance [see comments]. Neuron *27*, 237-249.

Castellani, V., De Angelis, E., Kenwrick, S., and Rougon, G. (2002). Cis and trans interactions of L1 with neuropilin-1 control axonal responses to semaphorin 3A. EMBO J *21*, 6348-6357.

Chen, S., Mantei, N., Dong, L., and Schachner, M. (1999). Prevention of neuronal cell death by neural adhesion molecules L1 and CHL1. J Neurobiol *38*, 428-439.

Cloutier, J. F., Giger, R. J., Koentges, G., Dulac, C., Kolodkin, A. L., and Ginty, D. D. (2002). Neuropilin-2 mediates axonal fasciculation, zonal segregation, but not axonal convergence, of primary accessory olfactory neurons. Neuron *33*, 877-892.

Colbert, M. C., Rubin, W. W., Linney, E., and LaMantia, A. S. (1995). Retinoid signaling and the generation of regional and cellular diversity in the embryonic mouse spinal cord. Dev Dyn *204*, 1-12.

De Angelis, E., MacFarlane, J., Du, J. S., Yeo, G., Hicks, R., Rathjen, F. G., Kenwrick, S., and Brummendorf, T. (1999). Pathological missense mutations of neural cell adhesion molecule L1 affect homophilic and heterophilic binding activities. EMBO J *18*, 4744-4753.

Demyanenko, G., Tsai, A., and Maness, P. F. (1999). Abnormalities in neuronal process extension, hippocampal development, and the ventricular system of L1 knockout mice. J Neurosci *19*, 4907-4920.

Demyanenko, G. P., and Maness, P. F. (2003). The L1 cell adhesion molecule is essential for topographic mapping of retinal axons. J Neurosci *23*, 530-538.

Demyanenko, G. P., Schachner, M., Anton, E., Schmid, R., Feng, G., Sanes, J., and Maness, P. F. (2004). Close homolog of L1 modulates area-specific neuronal positioning and dendrite orientation in the cerebral cortex. Neuron *44*, 423-437.

Dufour, A., Seibt, J., Passante, L., Depaepe, V., Ciossek, T., Frisen, J., Kullander, K., Flanagan, J. G., Polleux, F., and Vanderhaeghen, P. (2003). Area specificity and topography of thalamocortical projections are controlled by ephrin/Eph genes. Neuron *39*, 453-465.

Falk, J., Bechara, A., Fiore, R., Nawabi, H., Zhou, H., Hoyo-Becerra, C., Bozon, M., Rougon, G., Grumet, M., Puschel, A. W.*, et al.* (2005). Dual functional activity of semaphorin 3B is required for positioning the anterior commissure. Neuron *48*, 63-75.

Flanagan, J. G., and Leder, P. (1990). The kit ligand: a cell surface molecule altered in steel mutant fibroblasts. Cell *63*, 185-194.

Frints, S. G. M., Marynen, P., Hartmann, D., Fryns, J. P., Steyaert, J., Schachner, M., Rolf, B., Craessaerts, K., Snellinx, A., Hollanders, K.*, et al.* (2003). CALL interrupted in a patient with nonspecific mental retardation: gene dosage-dependent alteration of murine brain development and behavior. Hum Mol Genet *12*, 1463-1474.

Fukuda, T., Kawano, H., Ohyama, K., Li, H. P., Takeda, Y., Oohira, A., and Kawamura, K. (1997). Immunohistochemical localization of neurocan and L1 in the formation of thalamocortical pathway of developing rats. J Comp Neurol *382*, 141-152.

Garel, S., Yun, K., Grosschedl, R., and Rubenstein, J. L. (2002). The early topography of thalamocortical projections is shifted in Ebf1 and Dlx1/2 mutant mice. Development *129*, 5621-5634.

Ghosh, A., Antonini, A., McConnell, S. K., and Shatz, C. J. (1990). Requirement for subplate neurons in the formation of thalamocortical connections. Nature *347*, 179-181.

Ghosh, A., and Shatz, C. J. (1993). A role for subplate neurons in the patterning of connections from thalamus to neocortex. Development *117*, 1031-1047.

Giger, R. J., Cloutier, J. F., Sahay, A., Prinjha, R. K., Levengood, D. V., Moore, S. E., Pickering, S., Simmons, D., Rastan, S., Walsh, F. S.*, et al.* (2000). Neuropilin-2 is required in vivo for selective axon guidance responses to secreted semaphorins. Neuron *25*, 29-41.

Gu, C., Rodriguez, E. R., Reimert, D. V., Shu, T., Fritzsch, B., Richards, L. J., Kolodkin, A. L., and Ginty, D. D. (2003). Neuropilin-1 conveys semaphorin and VEGF signaling during neural and cardiovascular development. Dev Cell *5*, 45-57.

Hamasaki, T., Leingartner, A., Ringstedt, T., and O'Leary, D. D. (2004). EMX2 regulates sizes and positioning of the primary sensory and motor areas in neocortex by direct specification of cortical progenitors. Neuron *43*, 359-372.

Hevner, R. F., Miyashita-Lin, E., and Rubenstein, J. L. (2002). Cortical and thalamic axon pathfinding defects in Tbr1, Gbx2, and Pax6 mutant mice: evidence that cortical and thalamic axons interact and guide each other. J Comp Neurol *447*, 8-17.

Hillenbrand, R., Molthagen, M., Montag, D., and Schachner, M. (1999). The close homologue of the neural adhesion molecule L1 (CHL1): patterns of expression and promotion of neurite outgrowth by heterophilic interactions. Eur J Neurosci *11*, 813-826.

Katz, L. C., and Crowley, J. C. (2002). Development of cortical circuits: lessons from ocular dominance columns. Nat Rev Neurosci *3*, 34-42.

Kawasaki, T., Kitsukawa, T., Bekku, Y., Matsuda, Y., Sanbo, M., Yagi, T., and Fujisawa, H. (1999). A requirement for neuropilin-1 in embryonic vessel formation. Development *126*, 4895-4902.

Kitsukawa, T., Shimizu, M., Sanbo, M., Hirata, T., Taniguchi, M., Bekku, Y., Yagi, T., and Fujisawa, H. (1997). Neuropilin-semaphorin III/D-mediated chemorepulsive signals play a crucial role in peripheral nerve projection in mice. Neuron *19*, 995-1005.

Kurumaji, A., Nomoto, H., Okano, T., and Toru, M. (2001). An association study between polymorphism of L1CAM gene and schizophrenia in a Japanese sample. Am J Med Genet *105*, 99-104.

Liu, Q., Dwyer, N. D., and O'Leary, D. D. (2000). Differential expression of COUP-TFI, CHL1, and two novel genes in developing neocortex identified by differential display PCR. J Neurosci *20*, 7682-7690.

Lopez-Bendito, G., Cautinat, A., Sanchez, J. A., Bielle, F., Flames, N., Garratt, A. N., Talmage, D. A., Role, L. W., Charnay, P., Marin, O., and Garel, S. (2006).

Tangential neuronal migration controls axon guidance: a role for neuregulin-1 in thalamocortical axon navigation. Cell *125*, 127-142.

Ma, L., Harada, T., Harada, C., Romero, M., Hebert, J. M., McConnell, S. K., and Parada, L. F. (2002). Neurotrophin-3 is required for appropriate establishment of thalamocortical connections. Neuron *36*, 623-634.

Maness, P. F. and Schachner, M. (2007). Neural recognition molecules of the immunoglobulin superfamily: signal transducers of axons guidance and neuronal migration. Nat Neurosci *10*, 19-26.

McConnell, S. K., Ghosh, A., and Shatz, C. J. (1989). Subplate neurons pioneer the first axon pathway from the cerebral cortex. Science *245*, 978-982.

Molnar, Z., Adams, R., and Blakemore, C. (1998). Mechanisms underlying the early establishment of thalamocortical connections in the rat. J Neurosci *18*, 5723-5745.

Montag-Sallaz, M., Schachner, M., and Montag, D. (2002). Misguided axonal projections, neural cell adhesion molecule 180 mRNA upregulation, and altered behavior in mice deficient for the close homolog of L1. Mol Cell Biol *22*, 7967-7981.

Ohyama, K., Tan-Takeuchi, K., Kutsche, M., Schachner, M., Uyemura, K., and Kawamura, K. (2004). Neural cell adhesion molecule L1 is required for fasciculation and routing of thalamocortical fibres and corticothalamic fibres. Neurosci Res *48*, 471-475.

Okabe, M., Ikawa, M., Kominami, K., Nakanishi, T., and Nishimune, Y. (1997). 'Green mice' as a source of ubiquitous green cells. FEBS Lett *407*, 313-319.

Pasterkamp, R. J., Dai, H. N., Terman, J. R., Wahlin, K. J., Kim, B., Bregman, B. S., Popovich, P. G., and Kolodkin, A. L. (2006). MICAL flavoprotein monooxygenases: expression during neural development and following spinal cord injuries in the rat. Mol Cell Neurosci *31*, 52-69.

Sakurai, K., Migita, O., Toru, M., and Arinami, T. (2002). An association between a missense polymorphism in the close homologue of L1 (CHL1, CALL) gene and schizophrenia. Mol Psychiatry *7*, 412-415.

Seibt, J., Schuurmans, C., Gradwhol, G., Dehay, C., Vanderhaeghen, P., Guillemot, F., and Polleux, F. (2003). Neurogenin2 specifies the connectivity of thalamic neurons by controlling axon responsiveness to intermediate target cues. Neuron *39*, 439-452.

Shimogori, T., and Grove, E. A. (2005). Fibroblast growth factor 8 regulates neocortical guidance of area-specific thalamic innervation. J Neurosci *25*, 6550-6560.

Skaliora, I., Singer, W., Betz, H., and Puschel, A. W. (1998). Differential patterns of semaphorin expression in the developing rat brain. Eur J Neurosci *10*, 1215-1229.

Suto, F., Ito, K., Uemura, M., Shimizu, M., Shinkawa, Y., Sanbo, M., Shinoda, T., Tsuboi, M., Takashima, S., Yagi, T., and Fujisawa, H. (2005). Plexin-a4 mediates axon-repulsive activities of both secreted and transmembrane semaphorins and plays roles in nerve fiber guidance. J Neurosci *25*, 3628-3637.

Tamamaki, N., Fujimori, K., Nojyo, Y., Kaneko, T., and Takauji, R. (2003). Evidence that Sema3A and Sema3F regulate the migration of GABAergic neurons in the developing neocortex. J Comp Neurol *455*, 238-248.

Togashi, H., Schmidt, E. F., and Strittmatter, S. M. (2006). RanBPM contributes to Semaphorin3A signaling through plexin-A receptors. J Neurosci *26*, 4961-4969.

Torii, M., and Levitt, P. (2005). Dissociation of corticothalamic and thalamocortical axon targeting by an EphA7-mediated mechanism. Neuron *48*, 563-575.

Tuttle, R., Nakagawa, Y., Johnson, J. E., and O'Leary, D. D. (1999). Defects in thalamocortical axon pathfinding correlate with altered cell domains in Mash-1-deficient mice. Development *126*, 1903-1916.

Ulupinar, E., Datwani, A., Behar, O., Fujisawa, H., and Erzurumlu, R. (1999). Role of semaphorin III in the developing rodent trigeminal system. Mol Cell Neurosci *13*, 281-292.

Villegas, G., and Tufro, A. (2002). Ontogeny of semaphorins 3A and 3F and their receptors neuropilins 1 and 2 in the kidney. Mech Dev *119 Suppl 1*, S149-153.

Wiencken-Barger, A. E., Mavity-Hudson, J., Bartsch, U., Schachner, M., and Casagrande, V. A. (2004). The role of L1 in axon pathfinding and fasciculation. Cereb Cortex *14*, 121-131.

Yaron, A., Huang, P. H., Cheng, H. J., and Tessier-Lavigne, M. (2005). Differential requirement for Plexin-A3 and -A4 in mediating responses of sensory and sympathetic neurons to distinct class 3 Semaphorins. Neuron *45*, 513-523.

Figure 2.1: CHL1 is Expressed in the Developing Thalamocortical Pathway

A. Immunofluorescence staining for CHL1 in a mid-coronal section (to best observe the entire thalamocortical pathway) of WT brain during projection of thalamic axons to the neocortex at E14.5, visualized by confocal microscopy. CHL1 protein is evident within the dorsal thalamus (DT), internal capsule (IC), intermediate zone (IZ), marginal zone (MZ), and cortical plate (CP). No staining was observed with nonimmuge IgG.

B. Immunofluorescence staining for CHL1 in a mid-coronal section of E16.5 WT brain visualized by confocal microscopy. CHL1 protein is prominent in the DT and IC, and is also present in the hippocampus (HC).

C. CHL1 localization in the caudal cortex of E16.5 WT brain visualized by confocal microscopy. CHL1 is most prominent in the IZ and MZ, and to a lesser extent in the CP. No staining was observed with nonimmune IgG.

D-E. (D) *In situ* hybridization for CHL1 mRNA in WT embryos (E14.5) in serial horizontal sections (to best observe the dorsal thalamus). CHL1 was expressed in a low dorsal to high ventral gradient throughout the dorsal thalamus. (E) CHL1 transcripts were also evident in the pretectal area and the cortical IZ and CP, but not the lateral or medial ganglionic eminence (LGE, MGE).

F-G. EGFP-labeled WT thalamic explants were co-cultured with unlabeled WT telencephalic whole mounts (E14.5) and immunostained for CHL1 (red) and GFP (green). (F), Thalamocortical axons (green) show localization with CHL1 (yellow in merge). Corticofugal axons also show CHL1 localization (red in merge). Scale bar=100 μm (G), Single TC axon expressing CHL1 shown by localization of EGFP (green) with CHL1 (red) along the axon shaft and within the growth cone (yellow in merge). Scale bar=50 μm

Figure 2.1

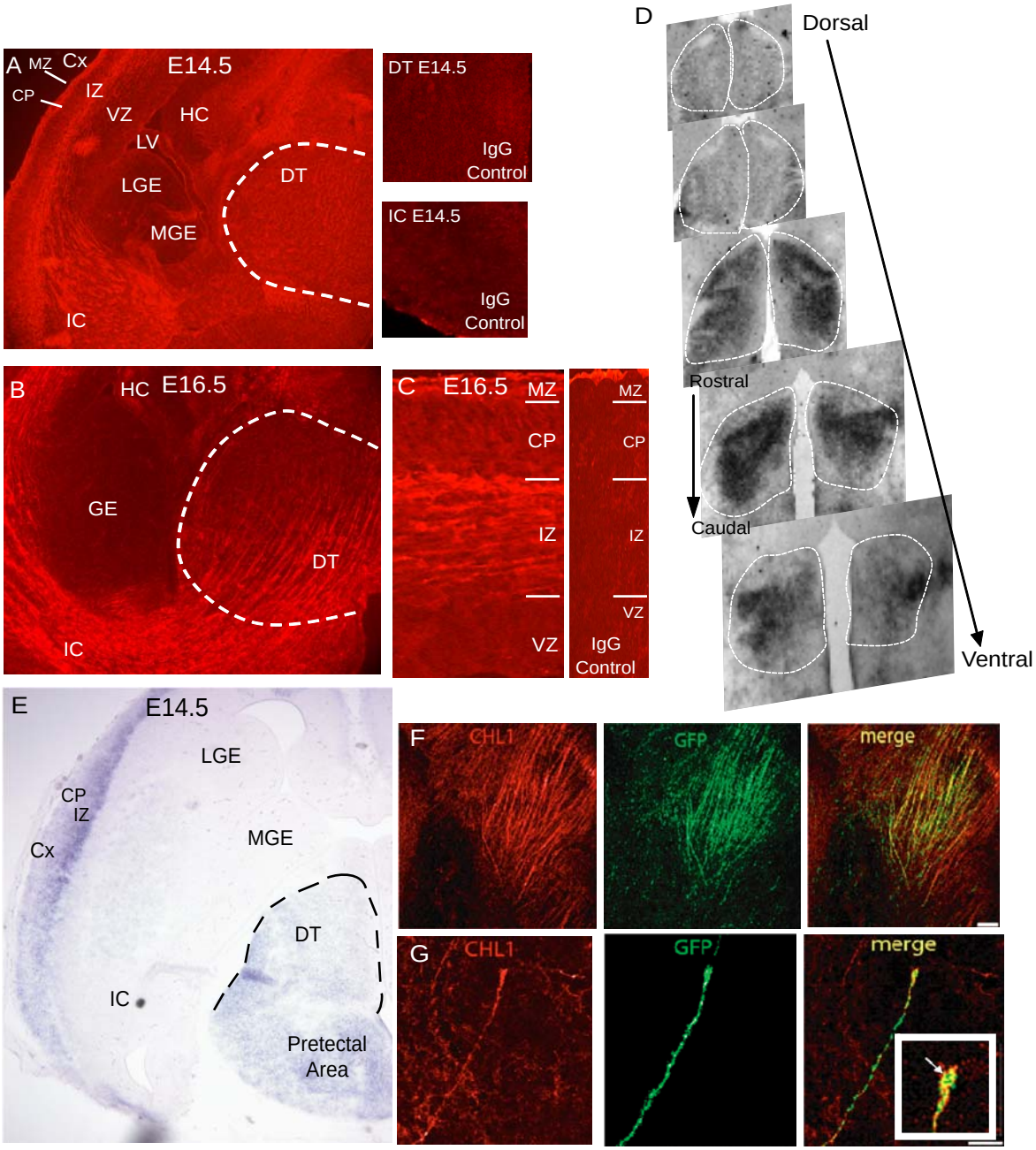
A
MZ
Cx
CP
IZ
VZ
HC
LV
LGE
E14.5
DT
MGE
IC
DT E14.5
IgG
Control
IC E14.5
IgG
Control
B
HC
E16.5
GE
DT
IC
C
E16.5
MZ
CP
IZ
VZ
MZ
CP
IZ
VZ
IgG
Control
D
Dorsal
Rostral
Caudal
Ventral
E
E14.5
LGE
CP
IZ
Cx
MGE
DT
IC
Pretectal
Area
F
CHL1
GFP
merge
G
CHL1
GFP
merge

Figure 2.2: Projection of Somatosensory Thalamic Axons is Caudally Shifted to the Visual Cortex in CHL1-Minus Mice

A. Scheme illustrating location of injections of DiI (visual cortex) and DiA (somatosensory cortex) of P5 mice. Appropriate location and position of injections were confirmed using fluorescent microscopy.

B-C. Retrograde labeling of thalamocortical axons of WT mice (B, n=13, scale bar=100 μm; C, scale bar=50 μm). Expected projection patterns of DiI labeling (red) in the LGN and DiA labeling (green) in the VB (VPM and VPL) are shown.

D-E. Retrograde labeling of thalamocortical axons in CHL1-minus mice (D, n=18, scale bar=100 μm; E, scale bar=50 μm). Appropriate DiA labeling (green) in the VPL and VPM was evident. Expected DiI labeling (red) in the LGN, as well as unexpected labeling of the VPL and VPM was observed. INSET: High magnification image of cell bodies in the dorsal thalamus retrogradely labeled by DiI.

F. Retrograde labeling of thalamocortical axons of WT mice (n=8) injected with DiI in the motor cortex at P5. DiI labeling (red) is present only in the appropriate location of the ventrolateral nucleus. Scale bar=100 μm.

G. Scheme illustrating the thalamocortical projection pathway of WT mice. Normal TC axons from the LGN project to the visual cortex; axons from the VB complex

project to the somatosensory cortex; and axons from the VA/VL project to the motor cortex.

H. Retrograde labeling with DiI injected in the motor cortex of CHL1-minus mice (n=6) at P5. DiI labeling (red) is present only in the ventrolateral nucleus. Scale bar=100 μm.

I. Scheme illustrating the altered thalamocortical topography in CHL1-minus mice. TC axons from the LGN project appropriately to the visual cortex, while axons from the VB complex project appropriately to the SS cortex and inappropriately to the primary visual cortex (dashed red line). Axons from the VA/VL project appropriately to the motor cortex

J-K. Nissl staining of WT and CHL1-minus adult mice demonstrate the positioning of barrels in layer IV of S1. No differences were observed.

L-M. Cytochrome oxidase staining of WT and CHL1-minus littermates at P5 to observe the barrels in layer IV of S1. Number and positioning of barrels was not affected by loss of CHL1.

LGN-lateral geniculate nucleus, VB-ventral basal complex, VA-ventroanterior nucleus, VL-ventrolateral nucleus, VPL-ventroposterior lateral nucleus, VPM-ventroposterior medial nucleus

Figure 2.2

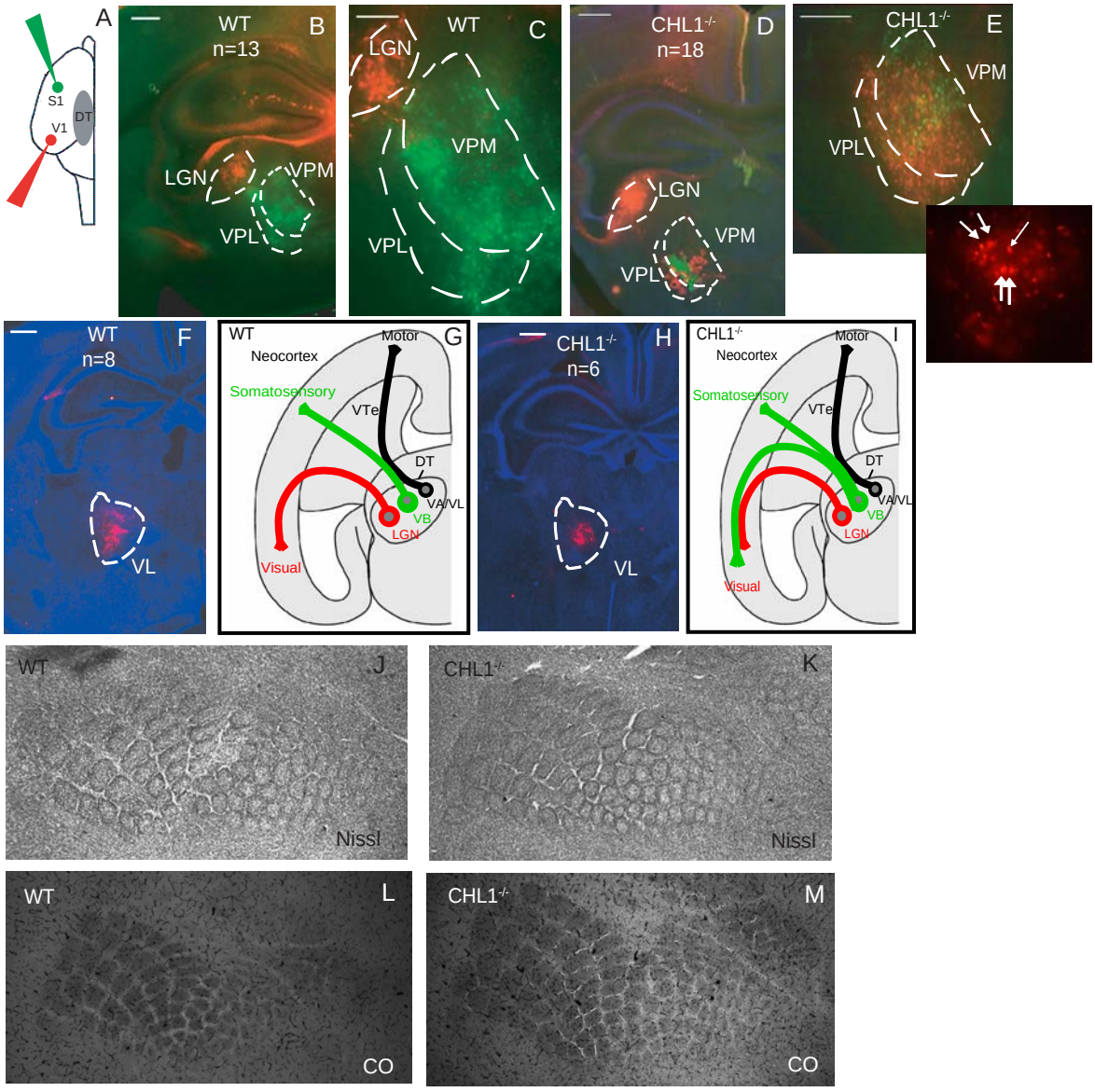
A
S1
V1
DT
WT
n=13
B
LGN
VPM
VPL
WT
C
LGN
VPM
VPL
CHL1-/-
n=18
D
LGN
VPM
VPL
CHL1-/-
E
VPM
VPL
WT
n=8
F
VL
WT
G
Neocortex
Motor
Somatosensory
VTe
DT
VA/VL
VB
LGN
Visual
CHL1-/-
n=6
H
VL
CHL1-/-
I
Neocortex
Motor
Somatosensory
VTe
DT
VA/VL
VB
LGN
Visual
WT
J
Nissl
CHL1-/-
K
Nissl
WT
L
CO
CHL1-/-
M
CO

Figure 2.3: CHL1 is Required for Guidance of Caudal Thalamic Axons in the Ventral Telencephalon at E15.5

A. Scheme illustrating placement of DiI crystal in rostral dorsal thalamus and DiA crystal in caudal dorsal thalamus of mouse embryos. Line indicates level of sections at 400 μm rostral of the thalamic eminence

B-C. Anterograde tracing of (B) WT (n=9) and (C) CHL1-minus (n=8) embryos with only rostral (red) axons present in the VTe. Seven of eight mutant hemispheres displayed normal topography. Scale bar=50 μm

D. Quantification of the rostrocaudal distribution of rostral thalamic axons within the VTe of WT and CHL1-minus embryos. The reference point (0) corresponds to the first section of the thalamic eminence, where axons leave the diencephalon and enter the VTe. The normalized frequency of labeled hemispheres (expressed as a proportion of total number of hemispheres examined) where rostral axons were found was plotted versus the normalized section number along the rostrocaudal axis for both WT (blue curve) and CHL1-minus (red curve) mice. There is no difference in the distributions.

E. Quantification of the distance from the rostral-most rostral thalamic axons to the thalamic eminence in WT (1.2 ± 0.14 mm) and CHL1-minus embryos (1.17 ± 0.18 mm). The y-axis represents the mean distance measured between the first section

where rostral axons are visible and the thalamic eminence. (Mann-Whitney, two-tailed, M=58.5, α=0.05).

Scheme illustrating the placement of DiI and DiA crystals in the rostral and caudal dorsal thalamus of embryos at E15.5. Line indicates levels of sections at 100 μm caudal to the thalamic eminence (F,G) and 300 μm rostral of the thalamic eminence (H).

F-H. Images of the VTe from coronal sections located 100 μm caudal to the thalamic eminence show the presence of both rostral (red) and caudal (green) thalamic axons in WT (F) compared to CHL1-minus (G) where only rostral thalamic axons were present. (H) At 300 μm rostral of the thalamic eminence in the CHL1-minus VTe both rostral (red) and caudal (green) thalamic axons were present, indicating a rostral shift of the caudal axons (5 of 8 mutant hemispheres displayed aberrant topography). Scale bar=50 μm

I. Quantification of the rostrocaudal distribution of caudal thalamic axons within the VTe of WT (n=8) and CHL1-minus (n=8) embryos (E15.5). Normalized frequency of labeled hemispheres was plotted, as described above, for WT (blue) and CHL1-minus (red) mice. A rostral shift of caudal axons is indicated.

J. Quantification of the rostral shift of caudal thalamic axons of CHL1-minus embryos (0.31 ± 0.07 mm) compared to WT (0.75 ± 0.15 mm). The y-axis

represents the mean distance measured between the thalamic eminence (0 reference point) and the last section where caudal axons are visible. Asterisk indicates significant difference (Mann-Whitney, two-tailed, M=50.5, α=0.1). Error bars represent standard error to the mean.

Figure 2.3

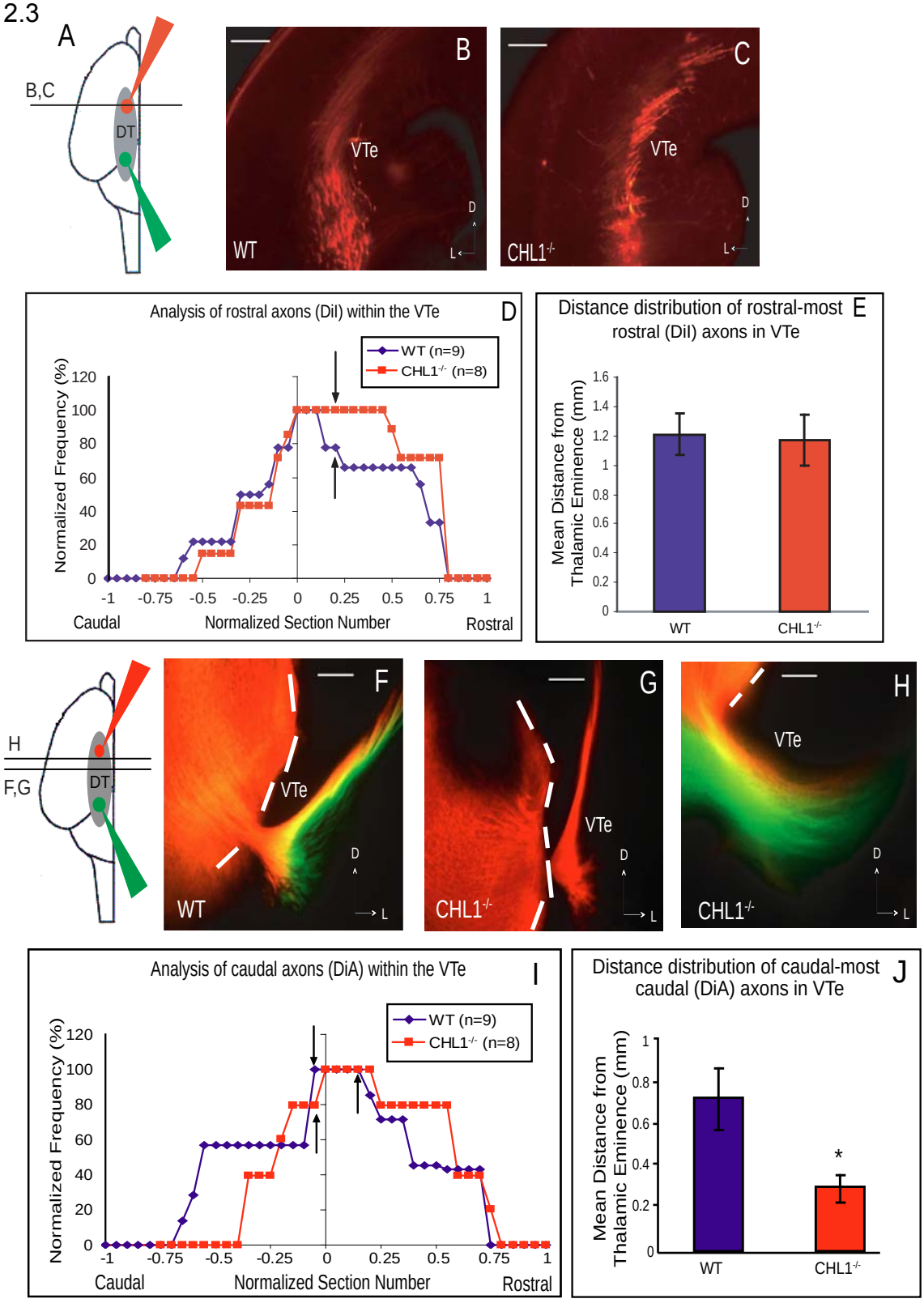
A
B,C
DT
B
VTe
WT
C
VTe
CHL1-/-
Analysis of rostral axons (DiI) within the VTe
D
WT (n=9)
CHL1-/- (n=8)
Normalized Frequency (%)
120
100
80
60
40
20
0
-1
-0.75
-0.5
-0.25
0
0.25
0.5
0.75
1
Caudal
Normalized Section Number
Rostral
Distance distribution of rostral-most rostral (DiI) axons in VTe
E
Mean Distance from Thalamic Eminence (mm)
1.6
1.4
1.2
1
0.8
0.6
0.4
0.2
0
WT
CHL1-/-
H
F,G
DT
F
VTe
WT
G
VTe
CHL1-/-
H
VTe
CHL1-/-
D
L
Analysis of caudal axons (DiA) within the VTe
I
WT (n=9)
CHL1-/- (n=8)
Normalized Frequency (%)
Caudal
Normalized Section Number
Rostral
Distance distribution of caudal-most caudal (DiA) axons in VTe
J
Mean Distance from Thalamic Eminence (mm)
*
WT
CHL1-/-

Figure 2.4: CHL1 is Required for Guidance of Ventral Basal Thalamic Axons in the Telencephalon at E15.5

A. Scheme illustrating placement of DiI crystal in the central third of the dorsal thalamus of mouse embryos. Lines indicate level of sections at 400 μm caudal of the thalamic eminence (B,C) and 500 μm rostral to the same reference point (D).

B-D. Images of the VTe located 400 μm caudal to the thalamic eminence show no labeled axons in WT (B) compared to CHL1-minus (C) where DiI-labeled thalamic axons were present. (D) At 500 μm rostral of the thalamic eminence in WT VTe rostral (red) thalamic axons were present. 10 of 12 mutant hemispheres displayed aberrant topography.

E. Quantification of the rostrocaudal distribution of VB thalamic axons within the VTe of WT (n=8) and CHL1-minus (n=12) embryos. The reference point (0) represents the first section of the thalamic eminence, and normalized frequency of labeled hemispheres was plotted as described above for both WT (blue) and CHL1-minus (red) mice. A caudal shift of VB axons within CHL1-minus VTe is evident.

F. Quantification of the caudal shift of VB thalamic axons of CHL1-minus embryos (0.49 ± 0.08 mm) compared to WT (0.150 ± 0.05 mm). The y-axis represents the mean distance measured between the thalamic eminence (0 reference point) and the last section where VB axons are visible. Asterisk indicates significant difference

(Mann-Whitney, two-tailed, M=50.5, α=0.1). Error bars represent standard error to the mean.

G-H. Images of the DTe located 800 μm caudal to the thalamic eminence show no labeled axons in WT (G) compared to CHL1-minus (H) where DiI-labeled thalamic axons were present. 10 of 12 mutant hemispheres displayed aberrant topography.

I. Quantification of the rostrocaudal distribution of VB thalamic axons within the DTe of WT (n=9) and CHL1-minus (n=12) embryos. The reference point (0) represents the first section of the thalamic eminence, and normalized frequency of labeled hemispheres was plotted as described above for both WT (blue) and CHL1-minus (red) mice. A caudal shift of VB axons within CHL1-minus DTe is evident. Asterisks indicate significance between WT and CHL1-minus at individual points (p-value<0.05; F-test).

Figure 2.4

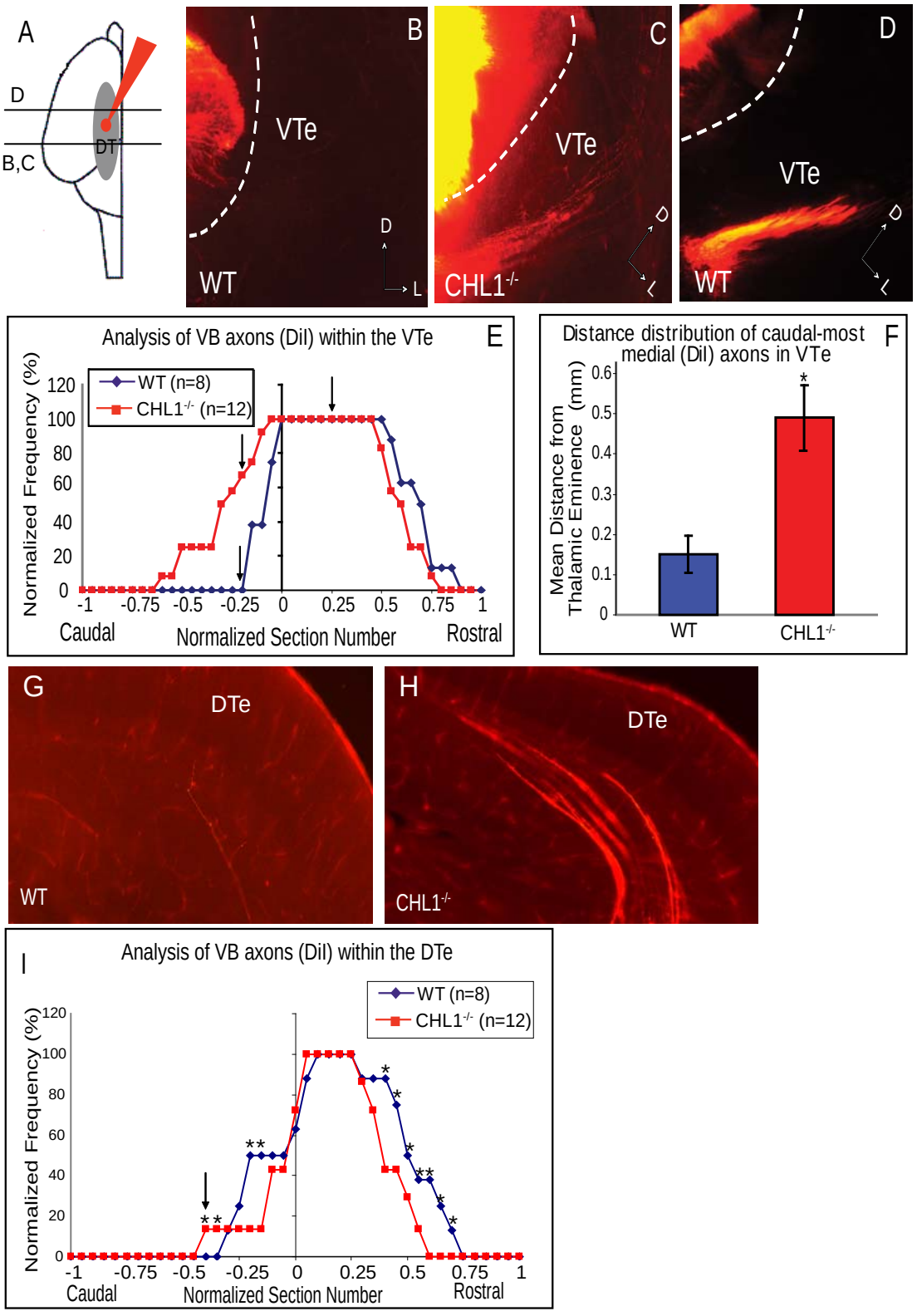
A
D
DT
B,C
B
VTe
D
L
WT
C
VTe
D
L
CHL1-/-
D
VTe
D
L
WT
E
Analysis of VB axons (DiI) within the VTe
WT (n=8)
CHL1-/- (n=12)
Normalized Frequency (%)
120
100
80
60
40
20
0
-1
-0.75
-0.5
-0.25
0
0.25
0.5
0.75
1
Caudal
Normalized Section Number
Rostral
F
Distance distribution of caudal-most medial (DiI) axons in VTe
Mean Distance from Thalamic Eminence (mm)
0.6
0.5
0.4
0.3
0.2
0.1
0
*
WT
CHL1-/-
G
DTe
WT
H
DTe
CHL1-/-
I
Analysis of VB axons (DiI) within the DTe
WT (n=8)
CHL1-/- (n=12)
Normalized Frequency (%)
120
100
80
60
40
20
0
**
**
*
*
**
*
*
-1
-0.75
-0.5
-0.25
0
0.25
0.5
0.75
1
Caudal
Normalized Section Number
Rostral

Figure 2.5: Segregation and Fasciculation of Thalamic and Cortical Axons Within the Ventral Telencephalon is Not Altered in CHL1-minus Embryos (E16.5)

A, D. DiA was injected in the dorsal thalamus of WT (A) and CHL1-minus (D) embryos at E16.5. There was no difference in overall fasciculation of thalamic axons due to loss of CHL1.

B, E. In the same embryos (E16.5), DiI was injected in the cortex to label corticofugal axons. Loss of CHL1 did not affect the overall fasciculation of cortical axons in the VTe.

C, F. Merged images of thalamic and cortical axons from WT (C) and CHL1-minus (F) embryos at the VTe indicate that CHL1 loss did not alter segregation between the two axonal populations.

Figure 2.5

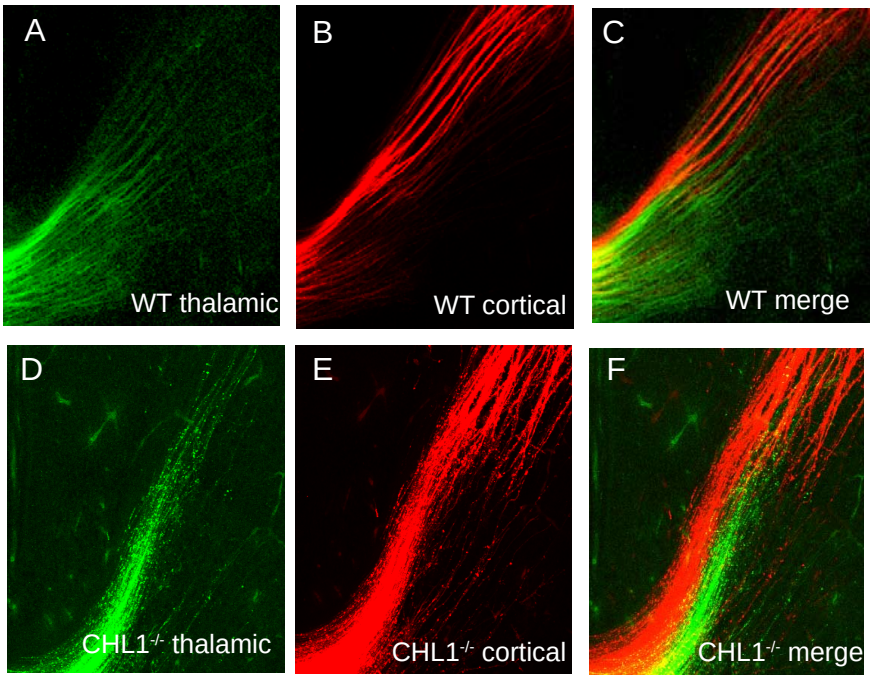
A
WT thalamic
B
WT cortical
C
WT merge
D
CHL1-/- thalamic
E
CHL1-/- cortical
F
CHL1-/- merge

Figure 2.6: Expression of CHL1, Neuropilin1, and Sema3A in the Embryonic Dorsal Thalamus and Telencephalon

A-C. Immunofluorescence staining for Npn1 (green) and CHL1 (red) in coronal sections of WT brain at E14.5 through the DT (A), the VTe (B), and the cortex (Cx) (C). CHL1 colocalized with Npn1 in fibers of the upper intermediate zone (IZ) (C) and in axons of the DT and VTe, consistent with the location of thalamocortical fibers. Scale bar= 20 μm (B); 100 μm (A, C).

D-E. Npn1 (green) and CHL1 (red) colocalization was observed by immunofluorescence staining at E16.5 in coronal sections through the DT (D) and Cx (E). Fibers in the DT and the upper and lower IZ express both CHL1 and Npn1. The location of these fibers is consistent with the positioning of thalamocortical and corticofugal axons. Scale bar=20 μm (D); 100 μm (E)

F-F'. Immunofluorescence staining for Npn1 (green) and CHL1 (red) in coronal sections at P5 though the DT. The merged image shows colocalization of Npn1 and CHL1 within the DT. (F') High magnification of fibers within the VB complex of the DT, indicating colocalization of Npn1 and CHL1.

G-H. *In situ* hybridization for Sema3A mRNA in WT embryos at E14.5 in horizontal sections. Sema3A mRNA was evident within the IZ of the ganglionic eminence (GE) in a high-caudal to low-rostral gradient. No expression was observed in the DT (G). Scale bar=50 μm (G); 20 μm (H)

I. Pixel densities were measured along the rostrocaudal axis of the VTe from serial sections of three embryos using ImageJ Software and normalized to background levels. These data fit a linear regression with an R^2 value equal to 0.78.

J. *In situ* hybridization for Sema3A in a sagittal section through the neocortex. Sema3A transcripts were robustly expressed in the ventricular zone and marginal zone with little in the IZ. Scale bar=100 μm

Figure 2.6

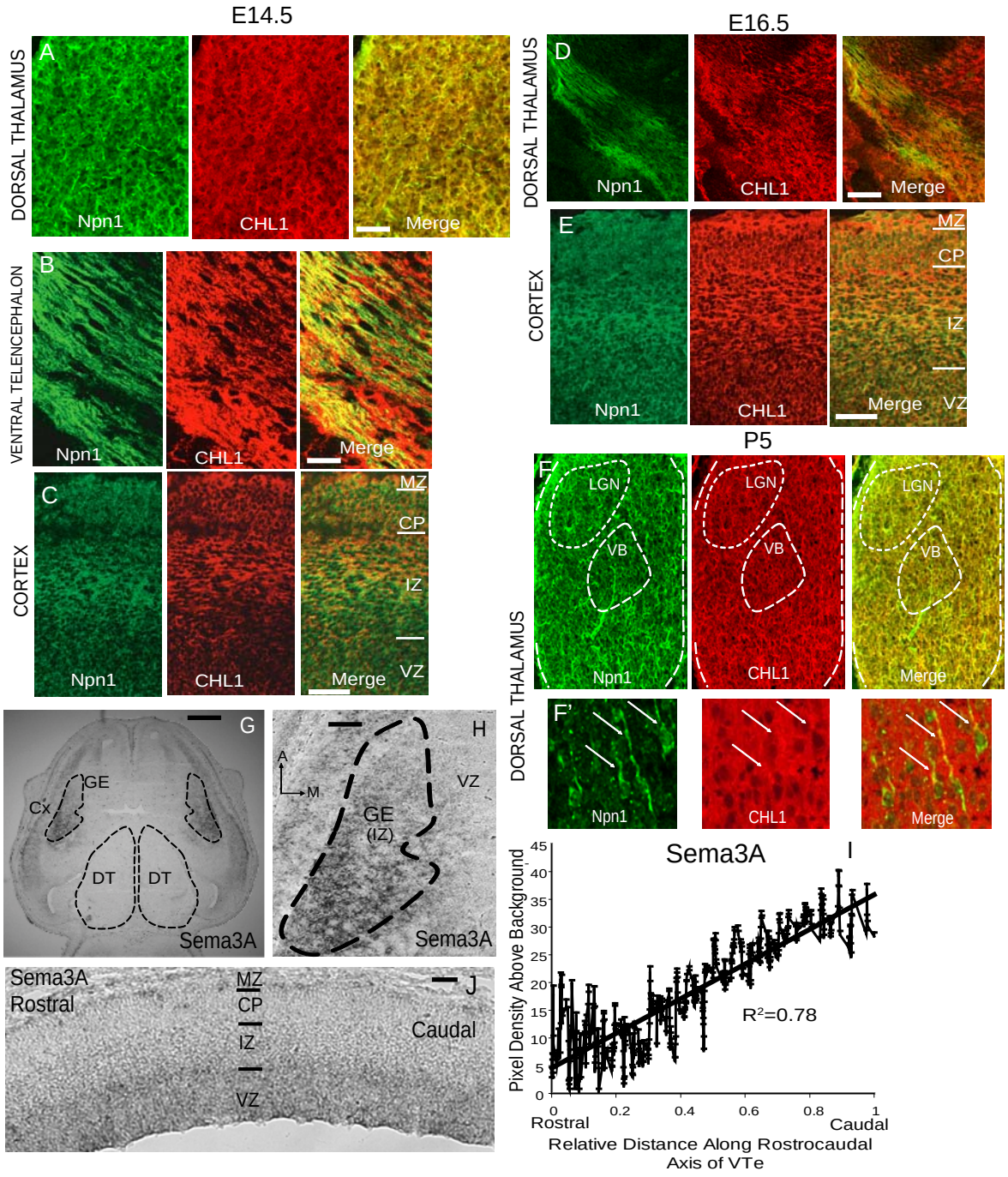
E14.5
E16.5
P5
DORSAL THALAMUS
VENTRAL TELENCEPHALON
CORTEX
A
B
C
D
E
F
F'
Npn1
CHL1
Merge
MZ
CP
IZ
VZ
LGN
VB
G
H
GE
Cx
DT
Sema3A
A
M
(IZ)
Sema3A
Rostral
Caudal
J
I
Pixel Density Above Background
R²=0.78
Rostral
Caudal
Relative Distance Along Rostrocaudal Axis of VTe

Figure 2.7: Neuropilin1 Binding to Sema3A is Required for Guidance of Caudal Thalamic Axons Within the Ventral Telencephalon

A. Scheme illustrating placement of DiI crystal in rostral dorsal thalamus and DiA crystal in the caudal dorsal thalamus of mouse embryos at E16.5. Line indicates level of sections at 600 μm rostral of the thalamic eminence.

B-C. Images of the VTe located 600 μm rostral to the thalamic eminence show the presence of rostral axons only in WT (B) and $Npn1^{Sema-/-}$ (C). Scale bar=50 μm

D. Quantification of the rostrocaudal distribution of rostral thalamic axons within the VTe of WT and $Npn1^{Sema-/-}$ embryos. The reference point (0) corresponds to the first section of the thalamic eminence, where axons leave the diencephalon and enter the VTe. The normalized frequency of labeled hemispheres (expressed as a proportion of total number of hemispheres examined) where rostral axons were found was plotted versus the normalized section number along the rostrocaudal axis for both WT (blue) and $Npn1^{Sema-/-}$ (red) mice. There are no significant differences in the distribution.

E. Quantification of the distance from the rostral-most rostral thalamic axons to the thalamic eminence in WT (0.82 ± 0.08 mm) compared to $Npn1^{Sema-/-}$ (0.78 ± 0.05 mm). The y-axis represents the mean distance measured between the thalamic eminence (0 reference point) and the last section where rostral axons are visible. Error bars represent standard error to the mean.

Scheme illustrating placement of DiI crystal in rostral dorsal thalamus and DiA crystal in caudal dorsal thalamus of mouse embryos at E15.5. Lines indicate level of sections at 500 μm caudal of the thalamic eminence (F,G) and 900 μm rostral to the same reference point (H,I).

F-I. Images of the VTe from coronal sections located 500 μm caudal to the thalamic eminence show the presence of both rostral (red) and caudal (green) thalamic axons in WT (F) compared to Npn1$^{Sema-/-}$ (G) where only rostral thalamic axons were present. At 900 μm rostral of the thalamic eminence in the WT VTe (H) only rostral (red) thalamic axons were present. However at an equivalent level in Npn1$^{Sema-/-}$ (I), both rostral (red) and caudal (green) axons were visible, indicating a rostral shift of the caudal axons (5 of 5 mutant hemispheres displayed aberrant topography). Scale bar=50 μm

J. Quantification of the rostrocaudal distribution of caudal thalamic axons within the VTe of WT (n=5) and Npn1$^{Sema-/-}$ (n=5) embryos (E15.5). The reference point (0) represents the first section of the thalamic eminence and normalized frequency of labeled hemispheres was plotted as described above for both WT (blue) and Npn1$^{Sema-/-}$ (red) mice. A rostral shift of caudal axons within the Npn1$^{Sema-/-}$ VTe is evident.

K. Quantification of the rostral shift of caudal thalamic axons of Npn1$^{Sema-/-}$ embryos (0.46 ± 0.06 mm) compared to WT (1.2 ± 0.1 mm). The y-axis represents the mean

distance measured between the thalamic eminence (0 reference point) and the last section where caudal axons are visible. Asterisk indicates significant difference (Mann-Whitney, two-tailed, M=50.5, α=0.1). Error bars represent standard error to the mean.

Figure 2.7

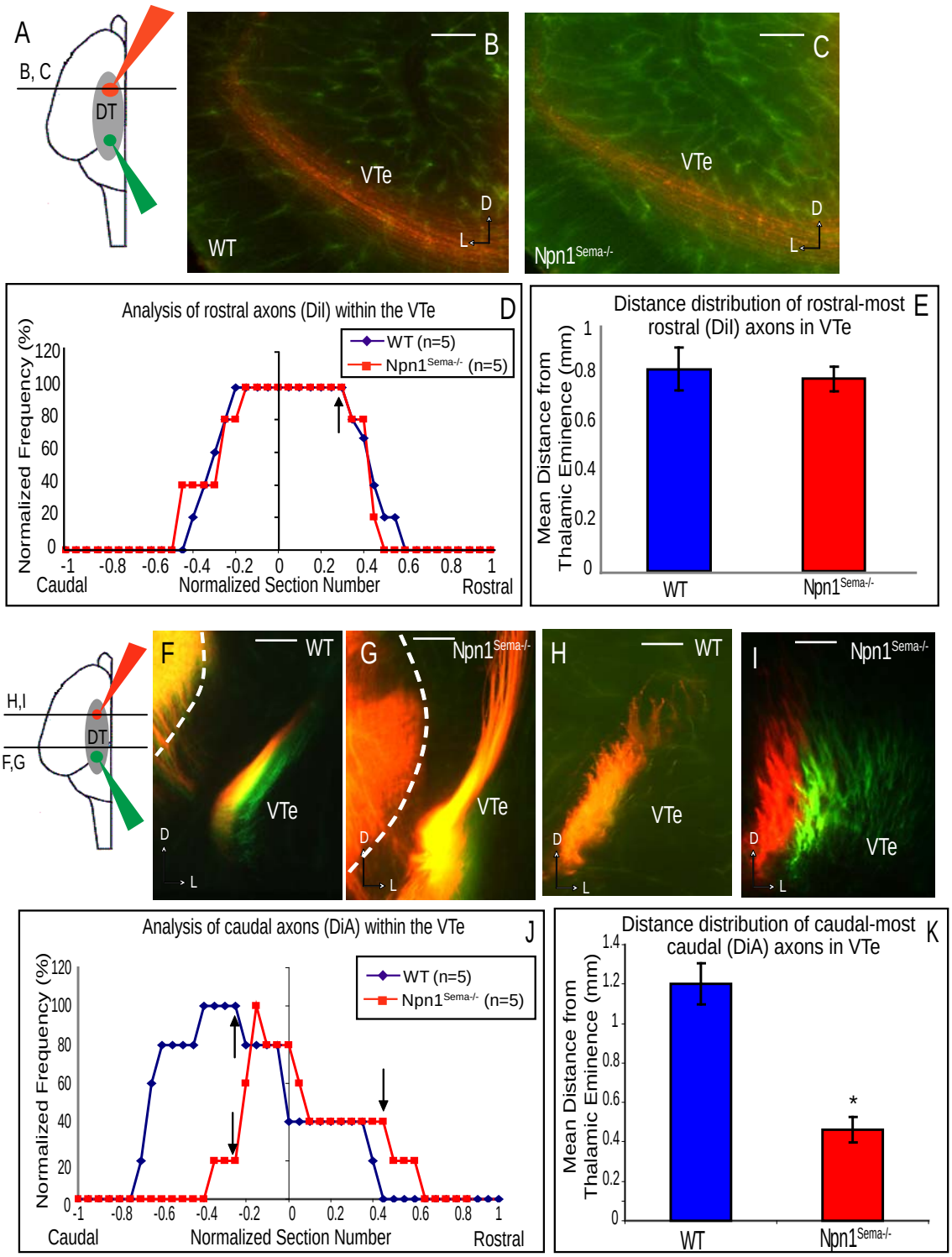
A
B, C
DT
B
VTe
WT
D
L
C
VTe
Npn1Sema-/-
D
L
Analysis of rostral axons (DiI) within the VTe
D
WT (n=5)
Npn1Sema-/- (n=5)
Normalized Frequency (%)
120
100
80
60
40
20
0
-1 -0.8 -0.6 -0.4 -0.2 0 0.2 0.4 0.6 0.8 1
Caudal
Normalized Section Number
Rostral
Distance distribution of rostral-most rostral (DiI) axons in VTe
E
Mean Distance from Thalamic Eminence (mm)
1
0.8
0.6
0.4
0.2
0
WT
Npn1Sema-/-
H,I
DT
F,G
F
WT
VTe
D
L
G
Npn1Sema-/-
VTe
D
L
H
WT
VTe
D
L
I
Npn1Sema-/-
VTe
D
L
Analysis of caudal axons (DiA) within the VTe
J
WT (n=5)
Npn1Sema-/- (n=5)
Normalized Frequency (%)
120
100
80
60
40
20
0
-1 -0.8 -0.6 -0.4 -0.2 0 0.2 0.4 0.6 0.8 1
Caudal
Normalized Section Number
Rostral
Distance distribution of caudal-most caudal (DiA) axons in VTe
K
Mean Distance from Thalamic Eminence (mm)
1.4
1.2
1
0.8
0.6
0.4
0.2
0
*
WT
Npn1Sema-/-

Figure 2.8: Neuropilin1-Sema Interactions are Required for Guidance of Ventral Basal Thalamic Axons

A. Scheme illustrating placement of DiI crystal in the central third of the dorsal thalamus of mouse embryos. Lines indicate level of sections at 400 μm caudal of the thalamic eminence (B,C) and 700 μm rostral to the same reference point (D).

B-D. Images of the VTe located 400 μm caudal to the thalamic eminence show no labeled axons in WT (B) compared to $Npn1^{Sema-/-}$ (C) where DiI-labeled thalamic axons were present. (D) At 700 μm rostral of the thalamic eminence in WT VTe, rostral (red) thalamic axons were present. 4 of 5 mutant hemispheres displayed aberrant topography. Scale bar=50 μm

E. Quantification of the rostrocaudal distribution of VB thalamic axons within the VTe of WT (n=10) and $Npn1^{Sema-/-}$ (n=5) embryos. The reference point (0) represents the thalamic eminence, and normalized frequency of labeled hemispheres was plotted as described above for both WT (blue) and $Npn1^{Sema-/-}$ (red) mice. A caudal shift of VB axons within $Npn1^{Sema-/-}$ VTe is evident.

F. Quantification of the caudal shift of VB thalamic axons of $Npn1^{Sema-/-}$ embryos (0.65 ± 0.06 mm) compared to WT (0.17 ± 0.04 mm). The y-axis represents the mean distance measured between the thalamic eminence and the last section where VB axons are visible. Asterisk indicates significant difference (Mann-Whitney, two-tailed, M=50.5, α=0.1). Error bars represent standard error to the mean.

Figure 2.8

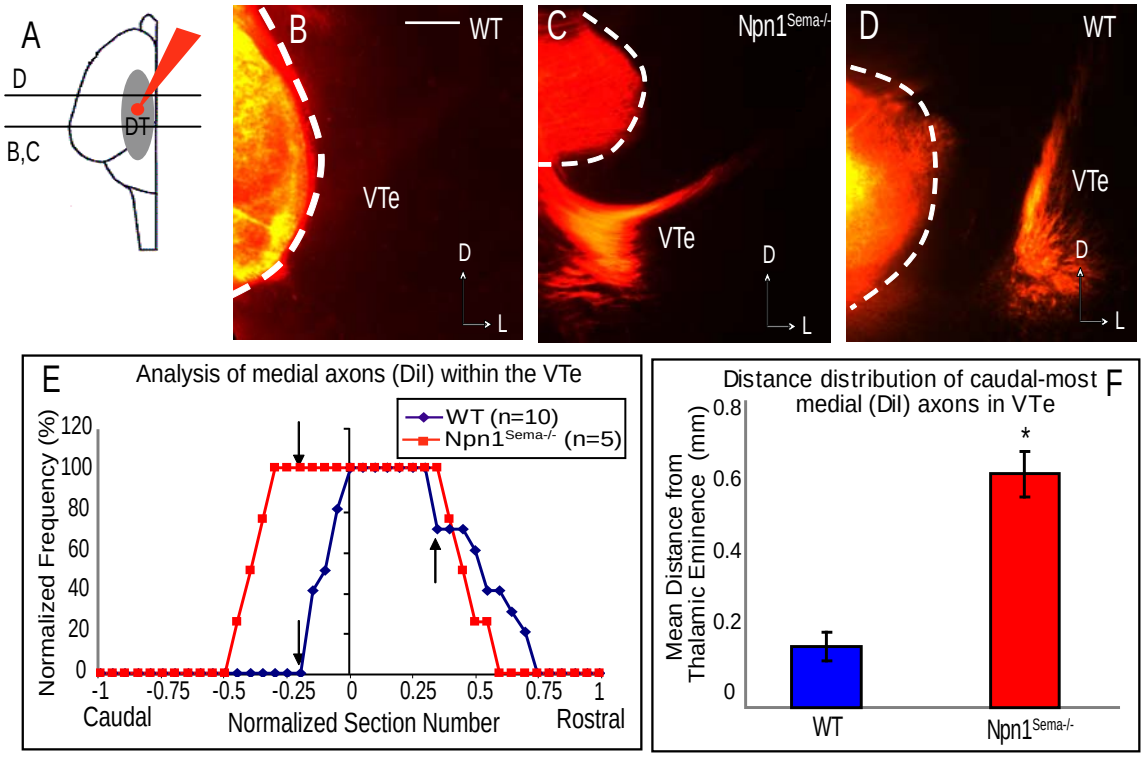
A
D
DT
B,C
B
WT
VTe
D
L
C
Npn1Sema-/-
VTe
D
L
D
WT
VTe
D
L
E
Analysis of medial axons (DiI) within the VTe
WT (n=10)
Npn1Sema-/- (n=5)
Normalized Frequency (%)
120
100
80
60
40
20
0
-1
-0.75
-0.5
-0.25
0
0.25
0.5
0.75
1
Caudal
Normalized Section Number
Rostral
F
Distance distribution of caudal-most medial (DiI) axons in VTe
Mean Distance from Thalamic Eminence (mm)
0.8
0.6
0.4
0.2
0
*
WT
Npn1Sema-/-

Figure 2.9: Neuropilin1 and CHL1 Form a Stable Complex

A. Npn1 capping (green) was induced by cross-linking with Npn1 antibody and detected with a FITC-labeled secondary antibody. CHL1wt protein (red) labeled with CHL1 antibody and a TRITC-labeled secondary antibody was recruited to Npn1 caps. Merged images show co-localization of CHL1 and Npn1 (yellow). Co-capping was observed in 82% of cells expressing both CHL1wt and Npn1. The last panel illustrates the differential interference contrast (DIC) of each cell.

B. In reverse experiments, CHL1wt (green) was clustered on the cell membrane with CHL1-polyclonal antibody and detected with a FITC-labeled secondary antibody. Npn1 (red) was recruited to the CHL1wt cap shown in the merged image by colocalization of the two proteins (yellow). Co-capping was observed in 75% of cells expressing CHL1wt and Npn1.

C. Non-immune rabbit IgG did not induce capping of Npn1 (green), nor was CHL1wt protein (red) clustered in response to non-immune rabbit IgG. No colocalization was observed in the merged image.

D. Npn1 capping (green) was induced as described above. $CHL1_{L115V}$ mutant protein (red), detected by CHL1 polyclonal antibody and TRITC-labeled secondary antibody, was not recruited to Npn1 caps, indicated by little co-localization in the merge image. Instead, $CHL1_{L115V}$ was evenly distributed around the plasma membrane. Co-capping was detected in only 17% of cells expressing both

$CHL1_{L115V}$ and Npn1, significantly reduced from CHl1wt-expressing cells (p-value>0.05).

E. COS7 cells were transiently transfected with CHL1wt or $CHL1_{L115V}$ and myc-tagged Npn1. Lysates were immunoprecipitated with anti-myc antibody, and proteins were analyzed using gel electrophoresis. The presence of CHL1 was detected using anti-CHL1 goat polyclonal antibody. In cells transfected with CHL1wt and Npn1, a doublet was detected at 185 and 165 kDa, corresponding to CHL1. No band was detected in lysates from cells transfected with Npn1 and the mutant form of CHL1. Lysates from E16.5 WT whole brain extract were immunoprecipitated with anti-Npn1 antibody (Calbiochem) and the presence of CHL1 was detected as described above. WT E16.5 lysates were used as positive control for CHL1. Western blots for Npn1 demonstrated the specificity of the immunoprecipitation, with protein present at 130 kDa, corresponding to Npn1.

Figure 2.9

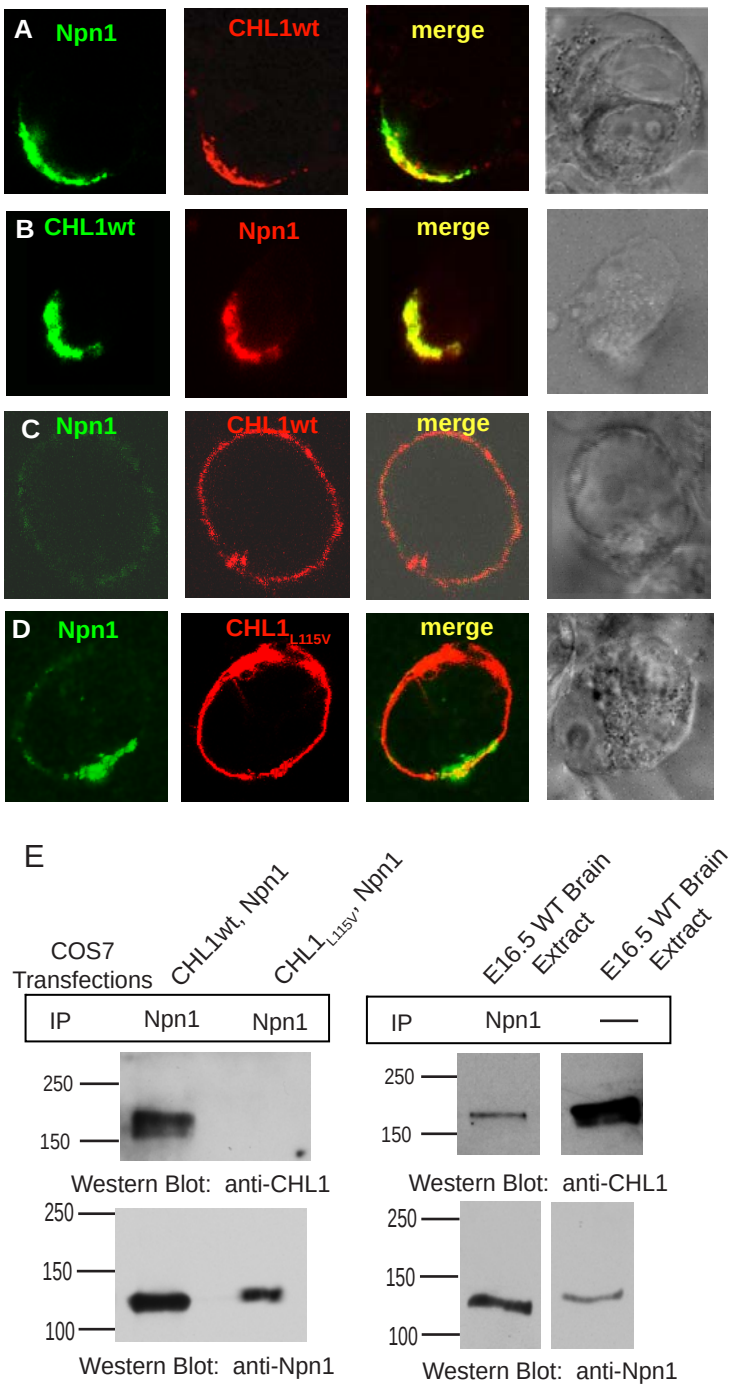
A Npn1
CHL1wt
merge
B CHL1wt
Npn1
merge
C Npn1
CHL1wt
merge
D Npn1
CHL1L115V
merge
E
COS7 Transfections
CHL1wt, Npn1
CHL1L115V, Npn1
E16.5 WT Brain Extract
E16.5 WT Brain Extract
IP
Npn1
Npn1
IP
Npn1
—
250
150
Western Blot: anti-CHL1
250
150
Western Blot: anti-CHL1
250
150
100
Western Blot: anti-Npn1
250
150
100
Western Blot: anti-Npn1

Figure 2.10: CHL1 is Required for the Growth Cone Collapsing Effects of Sema3A in Cultures of Thalamic Neurons (E14.5)

A,C,E. Growth cones of dissociated thalamic neurons from CHL1-minus embryos (E14.5) transfected with empty vector (A), CHL1wt (C), or $CHL1_{L115V}$ mutant (E) were not collapsed in response to FC-AP fusion protein. Non-collapsed growth cones are indicated with white arrows.

B, D, F. Sema3A had little effect on the growth cones of neurons expressing no CHL1 (B) and or the mutant form, $CHL1_{L115V}$ (F) and most growth cones are not collapsed (white arrows). However, growth cones of CHL1-minus thalamic neurons transfected with CHL1wt (D) were collapsed upon treatment with 30nM Sema3A-AP fusion protein (white arrows).

G. Quantification of percent growth cones collapsed from thalamic neurons in response to Sema3A. Sema3A significantly increased the percentage of collapsed CHL1wt-expressing growth cones compared to Fc-AP (asterisk indicates significance, p=0.005). While Sema3A had a significantly reduced effect on growth cones expressing no CHL1 or $CHL1_{L115V}$, Sema3A did significantly increase growth cone collapse compared to control (asterisk indicates significance; $CHL1^{-/-}$ p=0.035; $CHL1_{L115V}$ p=0.04). Soluble CHL1 silenced the growth cone collapse induced by Sema3A in CHL1wt-expressing cells (~50% reduction in collapse), but had no effect on growth cones expressing no CHL1 or $CHL1_{L115V}$.

H. Sema3A significantly increased the percentage of collapsed growth cones in WT explants isolated from the caudal half of the dorsal thalamus (n=57 growth cones). Sema3A had only marginal effects on growth cone collapse of CHL1-minus caudal explants (n=48); however it did significantly increase growth cone collapse compared to control. No differences were observed in the percentage of collapsed growth cones treated with control FC-AP. Asterisk indicates significance at two-tailed T-test ($p<0.05$).

Figure 2.10

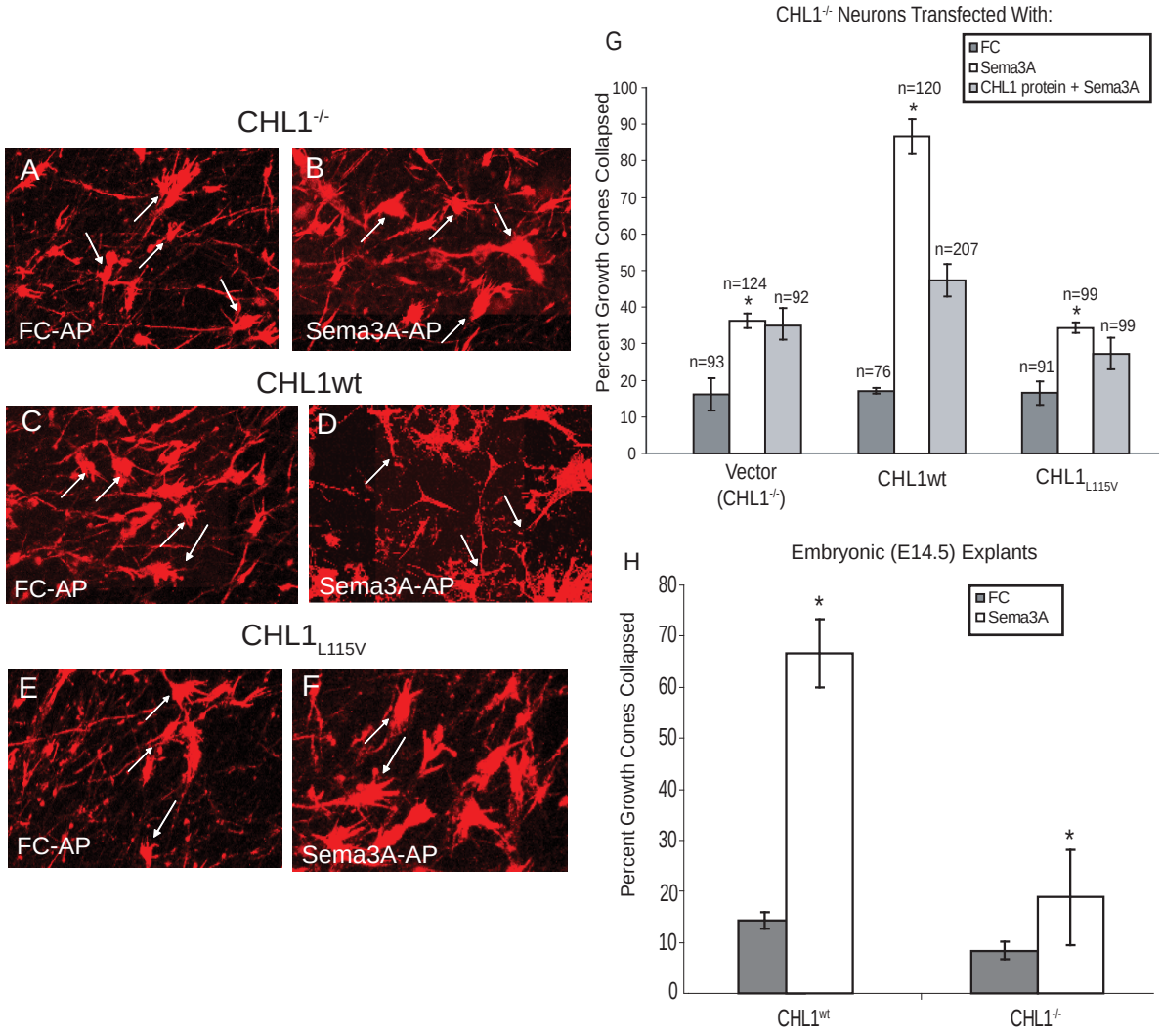
CHL1-/-
A
FC-AP
B
Sema3A-AP
CHL1wt
C
FC-AP
D
Sema3A-AP
CHL1L115V
E
FC-AP
F
Sema3A-AP
G
CHL1-/- Neurons Transfected With:
FC
Sema3A
CHL1 protein + Sema3A
Percent Growth Cones Collapsed
n=93
n=124
n=92
n=76
n=120
n=207
n=91
n=99
n=99
Vector (CHL1-/-)
CHL1wt
CHL1L115V
H
Embryonic (E14.5) Explants
FC
Sema3A
Percent Growth Cones Collapsed
CHL1wt
CHL1-/-

Figure 2.11: CHL1 and Neuropilin1 Mediate Guidance of Thalamocortical Axons at the Ventral Telencephalon

Model for mapping and final targeting of thalamocortical axons in WT and CHL1$^{-/-}$ mice. WT and CHL1-minus axons from the motor thalamic nuclei (VA/VL) project to the motor cortex (blue lines). WT axons from the ventral basal complex (VB) project to the somatosensory cortex (solid red line). Deletion of CHL1 causes a contingent of these axons to shift caudally in the VTe due to lack of repulsion by the high concentration of Sema3A in this region. These misguided axons inappropriately target the visual cortex (red dashed line, red arrow). WT Axons from the lateral geniculate nucleus (LGN) target the visual cortex (green lines). Loss of CHL1 causes a subset of these axons to shift rostrally in the VTe due to impaired CHL1-Npn1 signaling; however, these axons do not reach the cortex (green dashed line, green arrow).

Figure 2.11

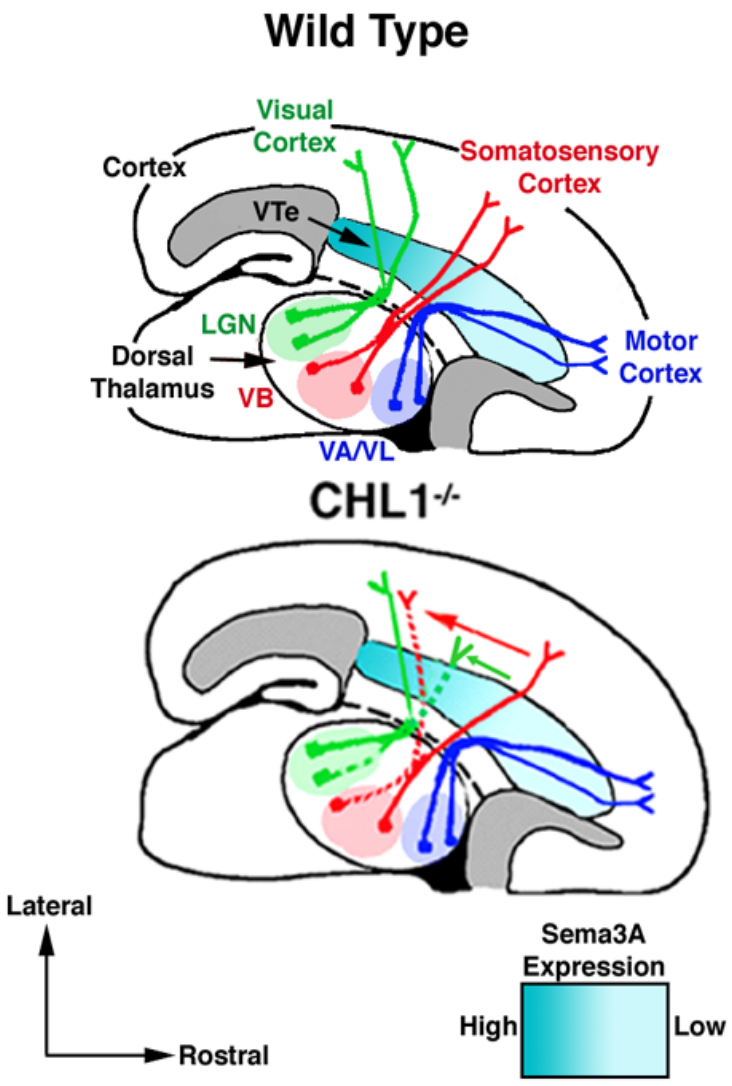
Wild Type
Visual Cortex
Somatosensory Cortex
Cortex
VTe
LGN
Dorsal Thalamus
VB
Motor Cortex
VA/VL
CHL1-/-
Lateral
Rostral
Sema3A Expression
High
Low

Chapter 3

L1 and Close Homolog of L1 (CHL1) Regulate Area-Specific Targeting of Thalamocortical Axons Through Interaction with EphA-EphrinA Guidance Cues

3.1 Abstract

Eph receptors and ephrin ligands regulate guidance of several major axonal pathways within the nervous system, including retinocollicular maps and thalamocortical topography, via repellent guidance mediated by growth cone collapse. Here, I demonstrate a requirement for CHL1 in ephrinA5-mediated growth cone collapse of thalamic axons. L1 was shown to interact with EphA4, an ephrinA5 receptor, through co-immunoprecipitation studies. In addition, deletion of L1 and CHL1 in mice severely disrupted thalamocortical targeting, with motor and somatosensory thalamic axons misprojecting to the visual cortex. These results suggest that L1 and CHL1 may work in concert to specify thalamocortical targeting by mediating repellent responses to EphA-ephrinA guidance cues.

3.2 Introduction

Ephrin ligands and their receptors, Eph tyrosine kinases, are important axon guidance cues during neuronal development. Ephrin ligands are divided into two subclasses: (1) EphrinAs, which are linked to the membrane through a glycosylphosphatidyl inositol (GPI) anchor, and (2) EphrinBs, which are transmembrane proteins. Eph-receptors are characterized by sequence similarity and ligand affinity. While there are some exceptions (notably EphA4), EphA receptors typically bind ephrinA ligands and EphB receptors bind ephrinB ligands (Wilkinson, 2001; Knoll and Drescher, 2002). Because Eph receptors and ephrins are both membrane bound, activation and signaling of Ephs and ephrins requires cell-cell interactions. Eph receptors autophosphorylate upon binding to their ligands

(forward signaling) and subsequently activate downstream signaling cascades, modulating the actin cytoskeleton through activation of guanine nucleotide exchange factors (GEFs), such as Ephexin, Vav2, and Tiam1 (Shamah et al., 2001; Noren and Pasquale, 2004; Tanaka et al., 2004; Cowan et al., 2005; Hunter et al., 2006). In addition to GEFs, Eph receptors associate with p120-RasGAP (Dail et al., 2006), an interaction that is important for growth cone collapse and axon repulsion. An interesting feature of the ephrin system is that signaling can also occur via the ligands (reverse signaling), typically leading to attractive responses of ephrins. Studies have shown that forward and reverse modes of Eph-ephrin signaling are critical for axon guidance in the retinocollicular projection (Feldheim et al., 1998; Birgbauer et al., 2000; Mann et al., 2002; Hansen et al., 2004), anterior commissure development (Henkemeyer et al., 1996; Kullander et al., 2001; Cowan et al., 2004), the vomeronasal tract (Knoll et al., 2001), and thalamocortical mapping (Vanderhaeghen et al., 2000; Mann et al., 2002; Dufour et al., 2003).

In the retinocollicular system, topographic connections between retinal ganglion cell (RGC) axons and their targets in the superior colliculus (SC) depend upon complementary gradients of ephrinA ligands and EphA receptors, including ephrinA2 and ephrinA5 (Frisen et al., 1998; Brown et al., 2000; Feldheim et al., 2000). Topographic mapping of RGC axons to the SC is also dependent upon expression of the cell adhesion molecule, L1 (Demyanenko and Maness, 2003). Defects observed in retinocollicular targeting in L1 mutant mice suggest an altered responsiveness of RGC axons to ephrin gradients in the SC. Thus, L1 and Eph guidance receptors may work together to regulate formation of the retinotopic map.

The ephrin family of axon guidance molecules is also important for development of thalamocortical mapping. Analysis of knockout mice reveals that interactions between ephrinA5 and EphA4 are required for the topographic mapping of thalamic axons to the primary motor cortex (Dufour et al., 2003). Ephrins have also been implicated in the cortical targeting of limbic thalamic axons (Gao et al., 1998; Mann et al., 2002; Uziel et al., 2002), intra-areal topographic mapping within somatosensory (Vanderhaeghen et al., 2000; Dufour et al., 2003) and visual (Cang et al., 2005) cortical areas, and reciprocal corticothalamic axon guidance (Torii and Levitt, 2005).

Recently, the importance of L1 family molecules, L1 and Close Homolog of L1 (CHL1), in regulating thalamocortical mapping has been described. L1 is essential for maintaining segregation between thalamic and cortical axons *en route* to the cortex, while CHL1 is critical for targeting of VB thalamic axons to the somatosensory cortex (Ohyama et al., 2004; Wiencken-Barger et al., 2004) (Chapter 2). Here, we expanded the roles of L1 and CHL1 to include mapping to motor thalamic axons. Analysis of $CHL1^{-/-}/L1^{-/y}$ double mutant mice reveals severe defects in the topographic targeting of thalamocortical axons, with axons from motor and somatosensory thalamic nuclei misprojecting to visual cortical areas. CHL1 was required for ephrinA5-induced growth cone collapse, and L1 directly interacted with EphA4. Thus, these results suggest compensatory roles for L1 and CHL1 in specifying cortical targeting, possibly through interactions with EphA/ephrinA repellent guidance cues.

3.3 Results

CHL1 and L1 Cooperate to Regulate Thalamocortical Axon Targeting

Mice deficient in CHL1 and L1 displayed severe defects in overall development and were 55-60% smaller than CHL1-minus mice (Fig 3.1A). The contribution of L1 and CHL1 to thalamocortical axon targeting was analyzed by retrograde axon tracing of $CHL1^{-/-}/L1^{-/y}$ double mutant mice at postnatal day 5. DiI was injected into the visual cortex, and thalamocortical axon targeting was examined (Fig 3.1B). In all cases, appropriate labeling of cell bodies in the lateral geniculate nucleus (LGN) was apparent in $CHL1^{-/-}/L1^{-/y}$ double mutant mice (Fig 3.1C). However, inappropriate labeling of VB nuclei (somatosensory), as well as motor thalamic nuclei (ventroanterior (VA) and ventrolateral (VL)), was also observed (Fig 3.1C,D,G). Mistargeting of somatosensory and motor thalamic axons was fully penetrant (7 of 7 hemispheres displayed aberrant topography), whereas all of the 13 WT hemispheres analyzed displayed expected topography (Fig 3.1F). Chi-square analysis demonstrated these defects were significant for $CHL1^{-/-}/L1^{-/y}$ mutants (X^2=20.30). To isolate the contribution of L1 to thalamocortical axon topography, retrograde tracings were performed in L1-minus mice. Injections of DiI into the visual cortex of L1-minus mice revealed expected labeling in the LGN only (Fig 3.1E,H). Previous studies demonstrated that somatosensory thalamic axons projected aberrantly to the visual cortex in CHL1-minus mice, but motor thalamic axon targeting was normal (Chapter 2, Fig 3.1I). In summary, targeting of motor thalamic axons is dependent upon compensatory contributions of CHL1 and L1.

Based on complementary gradients of ephrinA5/EphA4 guidance cues, it is possible that CHL1 and L1 mediate responses of ephrinA5 in thalamocortical mapping.

CHL1 is Required for EphrinA5-Induced Growth Cone Collapse

To investigate whether CHL1 is required for growth cone collapse of thalamic axons in response to ephrinA5 during axon guidance, WT and CHL1-minus thalamic explants were cultured for 3 days *in vitro* followed by treatment with 30 nM ephrinA5 protein fused to alkaline phosphatase (ephrinA5-AP), or control Fc protein fused to alkaline phosphatase (Fc-AP). Cellular actin was stained with phalloidin and axons were scored for growth cone collapse. EphrinA5-AP induced robust growth cone collapse of thalamic axons from WT embryos (Fig 3.2B,E) compared to control (Fig 3.2A,E). However, ephrinA5-AP was much less effective at collapsing CHL1-minus thalamic axons (Fig 3.2C,D,E). The growth cone collapse response to Fc-AP was not different from untreated explants (not shown), and the response due to Fc-AP treatment was not different in WT and CHL1-minus cultures. Thus, CHL1 was required for ephrinA5-induced growth cone collapse of thalamic axons.

L1 Forms a Stable Complex with EphA4

The role of CHL1 and L1 in mediating responses to ephrinA5 was further explored by co-immunoprecipitation experiments with EphA4, an ephrinA5 receptor. CHL1 or L1 were transiently co-transfected with EphA4 in HEK293 cells. After 2 days, cell lysates were immunoprecipitated with mouse anti-EphA4 antibody. Precipitates were evaluated by gel electrophoresis, and the presence of CHL1 or L1

was analyzed by immunoblotting with anti-CHL1 goat polyclonal antibody or anti-L1 mouse monoclonal antibody. L1 protein was detected at a molecular weight of approximately 250 kiloDaltons (kDa) in the immunoprecipitates of cells transfected with L1 and EphA4, supporting a constitutive interaction between the two proteins (Fig 3.3). An association between CHL1 and EphA4 was not detected by these methods. However, this interaction could be transient or require stimulation with ephrinA5 or other signaling molecules, such as integrins.

3.4 Discussion

Here, we identify a cooperative role for CHL1 and L1 in mediating guidance of motor thalamic axons. Analysis of $CHL1^{-/-}/L1^{-/y}$ double mutant mice showed that deletion of CHL1 and L1 severely disrupted the final thalamocortical map, causing a contingent of motor and somatosensory thalamic axons to inappropriately target the visual cortex. CHL1 was required for ephrinA5-mediated growth cone collapse of thalamic axons, and L1interacted with EphA4 to form a stable complex. Thus, CHL1 and L1 may mediate ephrinA5-induced repulsion of motor thalamic axons from posterior cortical areas.

Gradients of EphA receptors (EphA4, EphA7) in the dorsal thalamus and ephrinA5 in the VTe are critical for targeting of thalamic axons to the primary motor cortex (Dufour et al., 2003). The requirement for CHL1 in ephrinA5-induced growth cone collapse of thalamic axons and the association of L1 with EphA4 supports the interpretation that CHL1and L1 may functionally cooperate with EphA4/ephrinA5

complexes to prevent motor thalamic axons from entering posterior cortical regions. The lack of aberrant motor thalamic axon targeting in CHL1-minus or L1-minus mice supports a compensatory role for these L1 family adhesion molecules. EphrinA5/EphA4 signaling may not be entirely compromised by loss of either CHL1 of L1, whereas loss of both adhesion molecules might completely interrupt the receptor complex, leading to defective growth cone collapse.

The aberrant caudal shift of somatosensory thalamic axons in $CHL1^{-/-}/L1^{-/y}$ double mutant mice is consistent with previous results from CHL1-minus single mutant mice reported in Chapter 2. This mistargeting is the result of impaired CHL1-Npn1 interaction that mediates axon repulsion from the descending caudal gradient of Sema3A in the VTe. A corresponding shift was not observed in L1-minus mutant mice, suggesting that L1 is most likely not involved in the final targeting of VB axons to the primary somatosensory cortex (S1).

Despite the role shown here for CHL1 in mediating ephrinA5-induced growth cone collapse, the molecular mechanisms controlling this functional response are unclear, as direct interaction between CHL1 and EphA4 receptor was not detected. L1 did associate with EphA4, therefore a CHL1/L1/EphA4 receptor complex is conceivable. As L1 and CHL1 both functionally interact with β_1 integrins (Buhusi et al., 2003; Panicker et al., 2006), an intriguing hypothesis involves regulation of growth cone dynamics through crosstalk with integrins. Activation of EphA receptors induces a conformational change of integrins to an inactive state, leading to reduced cell adhesion, axonal retraction, and growth cone collapse (Miao et al., 2000). Thus,

it will be interesting to further explore the interactions of CHL1/L1/EphA4 complexes with β_1 integrins to regulate ephrinA5-mediated growth cone collapse.

Taken together, these results demonstrate that CHL1 and L1 may act cooperatively to regulate motor thalamic axon topography by mediating ephrinA5-induced growth cone collapse.

3.5 Methods

Growth Cone Collapse Assay

WT and CHL1-minus embryonic (E14.5) brains were vibratome sectioned (300 µm) and thalamic regions were obtained by microdissection in ice cold HBSS. Explants were plated on fibronectin-coated inserts using a plasma clot (20 µl bovine thrombin with 20 µl chicken plasma; Sigma) to ensure adherence of the explant. The day after plating, the media was changed to Neurobasal media containing B27 supplement and glutamate (25µM) to select for neurons. After 48 hours of incubation, cells were treated with either Fc-AP or EphrinA5-AP fusion proteins (30 nM) for 30 min. Fc-AP and EphrinA5-AP were prepared by transfecting HEK293T cells using Lipofectamine 2000, as described in Chapter 2. Explants were then fixed with 4% paraformaldehyde (PFA) and permeabilized with 0.2% TritonX-100 for 5 min. After washing, explants were treated with rhodamine-conjugated phalloidin (Molecular Probes; 1:40) for 30 min at room temperature to visualize actin within the growth cone. Explants were mounted in Vectashield and growth cone morphology was observed using confocal microscopy.

Co-immunoprecipitation

HEK293 cells were co-transfected with CHL1 or L1 and EphA4 using Lipofectamine 2000. Cells were lysed and proteins immunoprecipitated, as described in Chapter 2. Lysates were treated with mouse anti-EphA4 antibody (10 µg, Chemicon) for 1 hour at 4^{o}C. The beads were then washed and the precipitates were analyzed by immunoblotting with anti-CHL1 goat polyclonal antibody (1:1000) or anti-L1 mouse monoclonal antibody (Abcam, 1:200) and chemiuminescent detection.

In vivo Axon Tracing

Retrograde axon tracing was performed by focal injection of 1,1',di-octadecyl-3,3,3'3'-tetramethylindocarbocyanine perchlorate (DiI) (Molecular Probes) solution (5% in ethanol) into the visual cortex of living mice anesthetized by hypothermia, as described in Chapter 2.

3.6 References

Birgbauer, E., Cowan, C. A., Sretavan, D. W., and Henkemeyer, M. (2000). Kinase independent function of EphB receptors in retinal axon pathfinding to the optic disc from dorsal but not ventral retina. Development *127*, 1231-1241.

Brown, A., Yates, P. A., Burrola, P., Ortuno, D., Vaidya, A., Jessell, T. M., Pfaff, S. L., O'Leary, D. D., and Lemke, G. (2000). Topographic mapping from the retina to the midbrain is controlled by relative but not absolute levels of EphA receptor signaling. Cell *102*, 77-88.

Buhusi, M., Midkiff, B. R., Gates, A. M., Richter, M., Schachner, M., and Maness, P. F. (2003). Close homolog of L1 is an enhancer of integrin-mediated cell migration. J Biol Chem *278*, 25024-25031.

Cang, J., Kaneko, M., Yamada, J., Woods, G., Stryker, M. P., and Feldheim, D. A. (2005). Ephrin-as guide the formation of functional maps in the visual cortex. Neuron *48*, 577-589.

Cowan, C. A., Yokoyama, N., Saxena, A., Chumley, M. J., Silvany, R. E., Baker, L. A., Srivastava, D., and Henkemeyer, M. (2004). Ephrin-B2 reverse signaling is required for axon pathfinding and cardiac valve formation but not early vascular development. Dev Biol *271*, 263-271.

Cowan, C. W., Shao, Y. R., Sahin, M., Shamah, S. M., Lin, M. Z., Greer, P. L., Gao, S., Griffith, E. C., Brugge, J. S., and Greenberg, M. E. (2005). Vav family GEFs link activated Ephs to endocytosis and axon guidance. Neuron *46*, 205-217.

Dail, M., Richter, M., Godement, P., and Pasquale, E. B. (2006). Eph receptors inactivate R-Ras through different mechanisms to achieve cell repulsion. J Cell Sci *119*, 1244-1254.

Demyanenko, G. P., and Maness, P. F. (2003). The L1 cell adhesion molecule is essential for topographic mapping of retinal axons. J Neurosci *23*, 530-538.

Dufour, A., Seibt, J., Passante, L., Depaepe, V., Ciossek, T., Frisen, J., Kullander, K., Flanagan, J. G., Polleux, F., and Vanderhaeghen, P. (2003). Area specificity and topography of thalamocortical projections are controlled by ephrin/Eph genes. Neuron *39*, 453-465.

Feldheim, D. A., Kim, Y. I., Bergemann, A. D., Frisen, J., Barbacid, M., and Flanagan, J. G. (2000). Genetic analysis of ephrin-A2 and ephrin-A5 shows their requirement in multiple aspects of retinocollicular mapping [see comments]. Neuron *25*, 563-574.

Feldheim, D. A., Vanderhaeghen, P., Hansen, M. J., Frisen, J., Lu, Q., Barbacid, M., and Flanagan, J. G. (1998). Topographic guidance labels in a sensory projection to the forebrain. Neuron *21*, 1303-1313.

Frisen, J., Yates, P. A., McLaughlin, T., Friedman, G. C., O'Leary, D. D., and Barbacid, M. (1998). Ephrin-A5 (AL-1/RAGS) is essential for proper retinal axon guidance and topographic mapping in the mammalian visual system. Neuron *20*, 235-243.

Gao, P. P., Yue, Y., Zhang, J. H., Cerretti, D. P., Levitt, P., and Zhou, R. (1998). Regulation of thalamic neurite outgrowth by the Eph ligand ephrin-A5: implications in the development of thalamocortical projections. Proc Natl Acad Sci U S A *95*, 5329-5334.

Hansen, M. J., Dallal, G. E., and Flanagan, J. G. (2004). Retinal axon response to ephrin-as shows a graded, concentration-dependent transition from growth promotion to inhibition. Neuron *42*, 717-730.

Henkemeyer, M., Orioli, D., Henderson, J. T., Saxton, T. M., Roder, J., Pawson, T., and Klein, R. (1996). Nuk controls pathfinding of commissural axons in the mammalian central nervous system. Cell *86*, 35-46.

Hunter, S. G., Zhuang, G., Brantley-Sieders, D., Swat, W., Cowan, C. W., and Chen, J. (2006). Essential role of Vav family guanine nucleotide exchange factors in EphA receptor-mediated angiogenesis. Mol Cell Biol *26*, 4830-4842.

Knoll, B., and Drescher, U. (2002). Ephrin-As as receptors in topographic projections. Trends Neurosci *25*, 145-149.

Knoll, B., Zarbalis, K., Wurst, W., and Drescher, U. (2001). A role for the EphA family in the topographic targeting of vomeronasal axons. Development *128*, 895-906.

Kullander, K., Croll, S. D., Zimmer, M., Pan, L., McClain, J., Hughes, V., Zabski, S., DeChiara, T. M., Klein, R., Yancopoulos, G. D., and Gale, N. W. (2001). Ephrin-B3 is the midline barrier that prevents corticospinal tract axons from recrossing, allowing for unilateral motor control. Genes Dev *15*, 877-888.

Mann, F., Peuckert, C., Dehner, F., Zhou, R., and Bolz, J. (2002). Ephrins regulate the formation of terminal axonal arbors during the development of thalamocortical projections. Development *129*, 3945-3955.

Miao, H., Burnett, E., Kinch, M., Simon, E., and Wang, B. (2000). Activation of EphA2 kinase suppresses integrin function and causes focal-adhesion-kinase dephosphorylation. Nat Cell Biol *2*, 62-69.

Noren, N. K., and Pasquale, E. B. (2004). Eph receptor-ephrin bidirectional signals that target Ras and Rho proteins. Cell Signal *16*, 655-666.

Ohyama, K., Tan-Takeuchi, K., Kutsche, M., Schachner, M., Uyemura, K., and Kawamura, K. (2004). Neural cell adhesion molecule L1 is required for fasciculation and routing of thalamocortical fibres and corticothalamic fibres. Neurosci Res *48*, 471-475.

Panicker, A. K., Buhusi, M., Erickson, A., and Maness, P. F. (2006). Endocytosis of beta1 integrins is an early event in migration promoted by the cell adhesion molecule L1. Exp Cell Res *312*, 299-307.

Shamah, S. M., Lin, M. Z., Goldberg, J. L., Estrach, S., Sahin, M., Hu, L., Bazalakova, M., Neve, R. L., Corfas, G., Debant, A., and Greenberg, M. E. (2001). EphA receptors regulate growth cone dynamics through the novel guanine nucleotide exchange factor ephexin. Cell *105*, 233-244.

Tanaka, M., Ohashi, R., Nakamura, R., Shinmura, K., Kamo, T., Sakai, R., and Sugimura, H. (2004). Tiam1 mediates neurite outgrowth induced by ephrin-B1 and EphA2. Embo J *23*, 1075-1088.

Torii, M., and Levitt, P. (2005). Dissociation of corticothalamic and thalamocortical axon targeting by an EphA7-mediated mechanism. Neuron *48*, 563-575.

Uziel, D., Muhlfriedel, S., Zarbalis, K., Wurst, W., Levitt, P., and Bolz, J. (2002). Miswiring of limbic thalamocortical projections in the absence of ephrin-A5. J Neurosci *22*, 9352-9357.

Vanderhaeghen, P., Lu, Q., Prakash, N., Frisen, J., Walsh, C. A., Frostig, R. D., and Flanagan, J. G. (2000). A mapping label required for normal scale of body representation in the cortex. Nat Neurosci *3*, 358-365.

Wiencken-Barger, A. E., Mavity-Hudson, J., Bartsch, U., Schachner, M., and Casagrande, V. A. (2004). The role of L1 in axon pathfinding and fasciculation. Cereb Cortex *14*, 121-131.

Wilkinson, D. G. (2001). Multiple roles of EPH receptors and ephrins in neural development. Nat Rev Neurosci *2*, 155-164.

Figure 3.1: CHL1 and L1 Cooperate to Regulate Thalamocortical Axon Targeting

A. $CHL1^{-/-}/L1^{-/y}$ double mutant mice display several development defects, including overall reduction in size. Double mutant mice are approximately half the size of CHL1-minus single mutants.

B. Scheme illustrating location of injection of DiI into the visual cortex of P5 mice. Appropriate location and position of injections were confirmed using fluorescent microscopy.

C-D. Retrograde labeling of thalamocortical axons of $CHL1^{-/-}/L1^{-/y}$ double mutant mice (n=7). Projection patterns of appropriate DiI labeling (red) in the LGN (C) and inappropriate labeling of the VB complex and VA/VL nuclei (D) are shown.

E. Retrograde labeling from the visual cortex of L1-minus mutant mice. Expected labeling of the LGN is observed (n=3).

F. Scheme illustrating expected projection patterns of WT thalamocortical axons. LGN axons project to the visual cortex, VB axons project to the somatosensory cortex, and VA/VL axons project to the motor cortex.

G. Scheme illustrating the altered thalamocortical topography in $CHL1^{-/-}/L1^{-/y}$ double mutant mice. TC axons from the LGN project appropriately to the visual cortex,

while axons from the VB complex and VA/VL nuclei misproject to the primary visual cortex.

H-I. Scheme illustrating the normal projection of LGN axons to the primary visual cortex of L1 mutant mice (H). Scheme illustrating the altered thalamocortical topography in CHL1-minus mice (I). TC axons from the LGN project appropriately to the visual cortex, while axons from the VB complex project both to the SS cortex and inappropriately to the primary visual cortex. Axons from the VA/VL project appropriately to the motor cortex

Figure 3.1

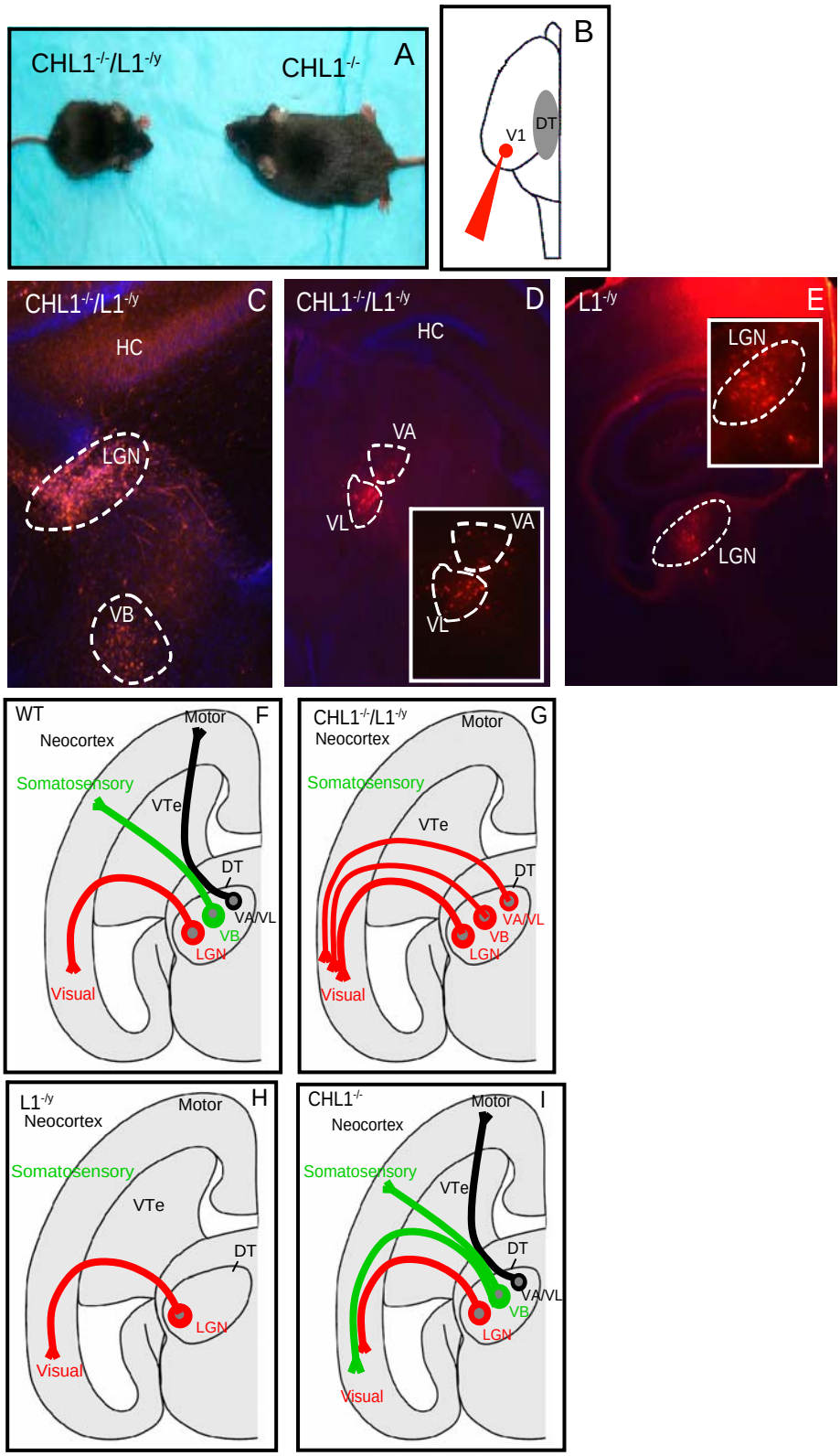
A
CHL1-/-/L1-/y
CHL1-/-
B
V1
DT
C
CHL1-/-/L1-/y
HC
LGN
VB
D
CHL1-/-/L1-/y
HC
VA
VL
VA
VL
E
L1-/y
LGN
LGN
F
WT
Neocortex
Motor
Somatosensory
VTe
DT
VA/VL
VB
LGN
Visual
G
CHL1-/-/L1-/y
Neocortex
Motor
Somatosensory
VTe
DT
VA/VL
VB
LGN
Visual
H
L1-/y
Neocortex
Motor
Somatosensory
VTe
DT
LGN
Visual
I
CHL1-/-
Neocortex
Motor
Somatosensory
VTe
DT
VA/VL
VB
LGN
Visual

Figure 3.2: CHL1 is Required for EphrinA5-Induced Growth Cone Collapse

A,B. Growth cones from WT thalamic explants were not collapsed in response to Fc-AP (n=67). However, ephrinA5 significantly increased the percentage of collapsed growth cones compared to control (n=83).

C,D. EphrinA5 had no significant effect on growth cone collapse of CHL1-minus thalamic explants (n=102) compared to Fc-AP control (n=84 growth cones). Representative non-collapsed growth cones are shown.

E. Quantification of percent growth cones collapsed from thalamic neurons in response to EphrinA5. While ephrinA5 had no effect on growth cone collapse of CHL1-minus explants, the percentage of collapsed growth cones from WT explants was significantly increased following treatment with ephrinA5, compared to control (asterisk indicates significance, t-test, p=0.005).

Figure 3.2

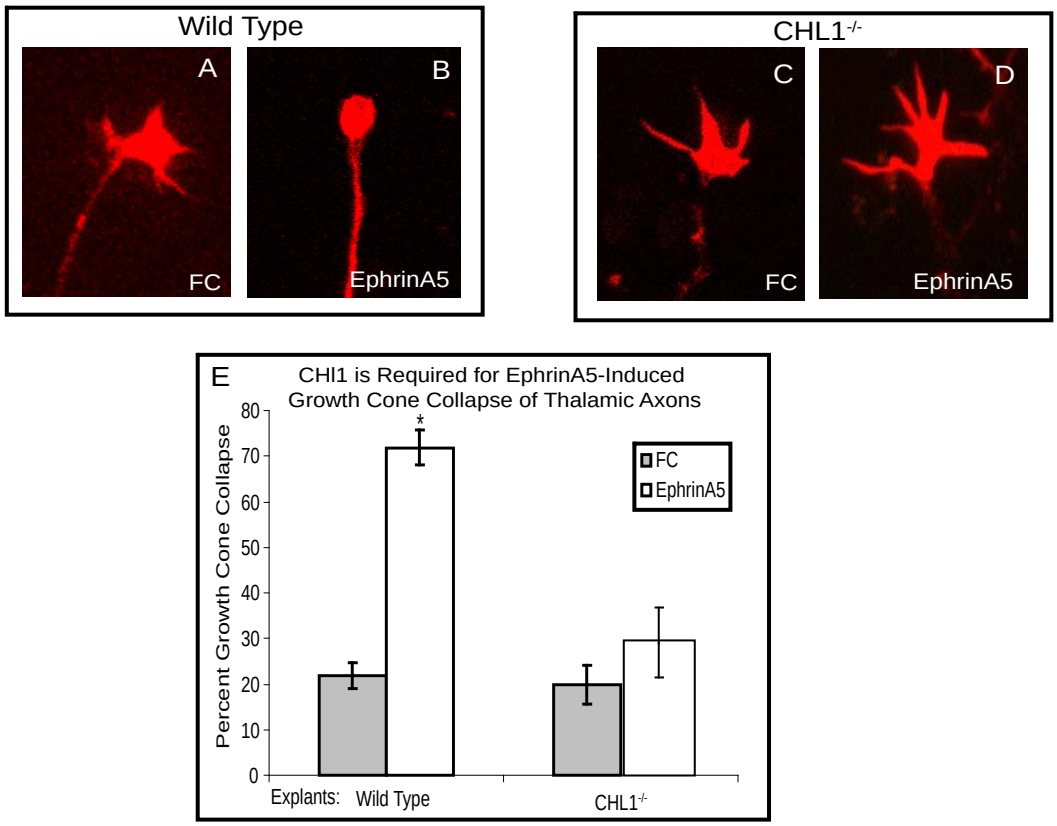
Wild Type
A
FC
B
EphrinA5
CHL1-/-
C
FC
D
EphrinA5
E
CHI1 is Required for EphrinA5-Induced
Growth Cone Collapse of Thalamic Axons
Percent Growth Cone Collapse
80
70
60
50
40
30
20
10
0
*
FC
EphrinA5
Explants:
Wild Type
CHL1-/-

Figure 3.3: L1 and EphA4 Form a Stable Complex

HEK293 cells were transiently transfected with CHL1 or L1 and EphA4. Lysates were immunoprecipitated with mouse anti-EphA4 antibody and proteins were analyzed using gel electrophesis. The presence of L1 was detected using anti-L1 mouse monoclonal antibody and an HRP-conjugated donkey anti-mouse secondary antibody. In cells transfected with L1 and EphA4, protein was detected at 250 kDa, corresponding to L1. CHL1 was detected using anti-CHL1 goat polyclonal and HRP-conjugated bovine anti-goat antibodies. No band was detected in lysates from cells transfected with CHL1 and EphA5. Western blots of E14.5 cortical extracts were used as a positive control for the detection of L1.

Figure 3.3

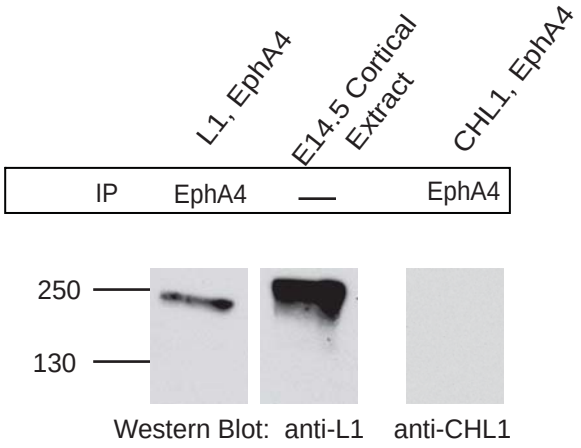
L1, EphA4
E14.5 Cortical Extract
CHL1, EphA4
IP
EphA4
—
EphA4
250
130
Western Blot: anti-L1
anti-CHL1

Chapter 4

Interaction of Close Homolog of L1 (CHL1) with ERM Proteins Promotes Neurite Elaboration and Sema3A-induced Growth Cone Collapse

Manuscript submitted to Journal of Neurochemistry

Monika C. Schlatter, Mona Buhusi, Amanda G. Wright, and Patricia F. Maness

This was a collaborative effort. I performed growth cone collapse assays to demonstrate the requirement for CHL1-ERM protein interactions in Sema3A-induced growth cone collapse.

4.1 Abstract

Close Homolog of L1 (CHL1) is a member of the L1 family of cell adhesion molecules that functions in axon guidance and cortical neuron positioning during development, and mutations of which are associated with neuropsychiatric disorders. Here it is shown that the cytoplasmic domain of CHL1 interacts with ezrin, a member of the ezrin-radixin-moesin (ERM) family of F-actin binding proteins, at the membrane-proximal RGGKYSV sequence. This interaction is demonstrated to promote outgrowth and branching of mouse embryonic cortical neurons, haptotactic cell migration, and cellular adhesion to fibronectin. Moreover, CHL1/ERM interaction mediates growth cone collapse of cortical embryonic neurons induced by Sema3A. These findings reveal important functions for the interaction between CHL1 and ERM proteins in fundamental processes relevant to axon guidance in neuronal development.

4.2 Introduction

CHL1 is a transmembrane adhesion receptor of the L1 family of cell adhesion molecules (L1-CAMs). L1 family members, including CHL1, L1, Nr-CAM and neurofascin, are widely expressed in the developing nervous system, where they modulate diverse aspects of axonal guidance and cell migration (Maness and Schachner, 2007).

Studies in CHL1 knock-out mice indicate a vital role for CHL1 in the development of neuronal connectivity. CHL1 null mutants display defects in axon guidance of hippocampal and olfactory neurons (Montag-Sallaz et al., 2002), and

behavioral deficits consistent with altered cortical connectivity (Montag-Sallaz et al., 2003; Pratte et al., 2003; Frints et al., 2003). In the developing neocortex loss of CHL1 delays radial migration of cortical neurons, resulting in laminar displacement, and misorientation of apical dendrites (Demyanenko et al., 2004). This effect might be due to an altered response to Sema3A, since apical dendrites of cortical neurons are attracted to the pial surface by a Sema3A gradient (Polleux et al., 2000). Indeed, CHL1 mediates Sema3A-induced collapse of thalamic and cortical growth cones important for thalamocortical axon guidance (Wright et al., submitted). The critical role of CHL1 in human neural development is underscored by the association of mutations in the human ortholog of CHL1 with mental retardation (Frints et al., 2003) and schizophrenia (Chen et al., 2005; Sakurai et al., 2002).

CHL1 consists of six (Ig)-like domains followed by five fibronectin type III repeats, a short transmembrane sequence, and a cytoplasmic domain that is highly conserved among L1 family members (Holm et al., 1996). CHL1 interacts with β_1 integrins through a sequence in the Ig6 domain (DGEA) that is important for potentiating cell migration to extracellular matrix proteins (Buhusi et al., 2003). CHL1 associates with the subcortical actin cytoskeleton through a conserved motif in the cytoplasmic domain (S^{1181}FIGAY) (Buhusi et al., 2003), which binds the spectrin adaptor protein ankyrin (Bennett et al., 1985). Ankyrin-mediated cytoskeletal linkage is necessary for CHL1 (Buhusi et al., 2003), as well as L1 (Thelen et al., 2002), to potentiate haptotactic cell migration toward extracellular matrix proteins in an integrin-dependent mechanism.

L1 also engages the cytoskeleton by interaction with ERM (ezrin-radixin-moesin) proteins (Cheng et al., 2005; Dickson et al., 2002). ERM proteins bind to diverse cell adhesion molecules, including L1, ICAMs, VCAMs, L-Selectin, and CD44, through their N-terminal FERM (Band 4.1, ERM) domain, while their C-terminal domain interacts with filamentous (F)-actin (Barreiro et al., 2002; Bretscher et al., 2002; Hamada et al., 2003; Ramesh et al., 2004). ERM proteins are subject to regulation by intracellular signaling at the plasma membrane. They are activated for actin binding by binding phosphatidylinositol *bis* phosphate (PIP2) and by phosphorylation on a conserved threonine residue catalyzed by PKCα, PKCθ, or Rho kinase (Barret et al., 2000, Fievert et al., 2004; Ramesh et al., 2004). ERM protein binding to the L1 cytoplasmic domain occurs at two different motifs (Figure 4.1): the membrane-proximal SKGGKY$_{1151}$ sequence (Cheng et al., 2005) and the Y$_{1176}$RSLE motif, which is specific to the neuronal L1 isoform (Cheng et al., 2005; Dickson et al., 2002). Mutation of Y$_{1151}$ or Y$_{1176}$ or deletion of RSLE leads to loss of ezrin binding, indicating that both sequences are essential for proper L1/ezrin interaction (Cheng et al., 2005; Dickson et al., 2002). In cerebellar neuron cultures, L1/ERM binding promotes neurite outgrowth and branching on an L1 substrate (Cheng et al., 2005), suggesting that their linkage enhances axonal growth and complexity. Moreover, L1 and phosphorylated ezrin were found to co-distribute *in vivo* in the intermediate zone of the developing rat cortex (Mintz et al., 2003), indicating that interaction of ERM proteins with cell adhesion molecules may provide flexible adhesions necessary during early axon outgrowth.

By coupling to the actin cytoskeleton through ERM proteins, CHL1 could provide such dynamic adhesive functions necessary for neurite outgrowth, migration, and Sema3A responses. However, due to structural differences in the cytoplasmic domains of CHL1 and L1, it is not known if CHL1 is capable of binding ERM proteins. CHL1 lacks a motif similar to YRSLE, but contains a membrane-proximal RGGKYSV sequence homologous to the KGGKYSV sequence in L1 (Figure 4.1). The consequences of such an interaction might be different for CHL1, because CHL1 and L1 have dissimilar cortical functions and expression patterns, bind distinct integrin subclasses at different Ig domains, and are associated with clinically variant human retardation syndromes (Maness and Schachner, 2007).

In this study, we sought to determine whether CHL1 was capable of ERM protein binding, and if so to elucidate the cellular and neuronal consequences of this interaction in cortical neurons. We found that ezrin-GFP is recruited to the cell membrane by expression of CHL1, and that this recruitment is mediated by the membrane-proximal RGGKYSV sequence of the CHL1 cytoplasmic domain. The CHL1/ERM protein interaction is required for CHL1-stimulated neurite outgrowth and branching of embryonic cortical neurons, haptotactic cell migration, and adhesion to fibronectin. Moreover, we show that Sema3A induces growth cone collapse and reduces neuronal outgrowth via CHL1/ERM interactions. We therefore provide the first evidence of an interaction between ERM proteins and CHL1, and show that ERM proteins are required for cellular functions of CHL1 in fundamental processes, such as neurite outgrowth and growth cone collapse relevant for axon guidance.

4.3 Results

A Membrane-Proximal Sequence in the CHL1 Cytoplasmic Domain is Required for Ezrin Recruitment

To investigate whether the CHL1 cytoplasmic domain was able to interact with ERM proteins, we evaluated the ability of CHL1 to recruit C-terminal GFP-tagged ezrin to CHL1 in the plasma membrane using a modified cytofluorescence assay, which has been used to demonstrate recruitment of ankyrin to the cytoplasmic domains of CHL1 and L1 (Buhusi et al., 2003; Needham et al., 2001). Co-transfection of HEK293 cells, which have some endogenous ERM protein expression (Figure 4.2 and 4.3, insert) but do not express L1 family members, with plasmids encoding ezrin-GFP and CHL1wt or L1wt ensures similar expression levels of the proteins. Moreover, endogenous ERM proteins in untransfected HEK293 cells are already partially recruited to the cell membrane (Figure 4.2, insert, panERM), hindering the visualization of membrane recruitment events.

Recruitment of cytosolic ezrin-GFP to the plasma membrane of transfected HEK293 cells was detected by confocal microscopy. In cells transfected with empty vector, ezrin-GFP was abundant throughout the cytosol and absent from the nucleus (Figure 4.2B). Some fluorescence at the plasma membrane may represent binding to PIP_2 or other endogenous receptors (Barret et al., 2000). In cells expressing CHL1wt, ezrin-GFP became prominently recruited to the cell membrane, where CHL1 was localized (Figure 4.2F). Expression of L1wt similarly induced recruitment of ezrin-GFP to the plasma membrane (Figure 4.2N). These results indicate that CHL1 is able to recruit ezrin to the cell membrane. However, CHL1/ezrin interactions

may be transient or of low affinity as co-immunoprecipitation experiments of CHL1 with ezrin-GFP did not reveal positive results (data not shown).

To localize sites of activated ezrin, immunofluorescence staining was carried out with an antibody recognizing the phosphorylated Thr567 residue in ezrin, as well as Thr564 and Thr558 in radixin and moesin, respectively. In cells transfected with empty vector together with ezrin-GFP, phospho-ERM staining was evident at the membrane in a dispersed, punctate distribution, with no staining in the cytoplasm (Figure 4.2C), similar to untransfected cells (Figure 4.2, insert, pERM). However, phospho-ERM immunoreactivity became more prominent and uniformly distributed within the plasma membrane in cells expressing ezrin-GFP together with either CHL1wt or L1wt (Figure 4.2G,O). Merged images showed the correspondence of ezrin-GFP and phospho-ERM immunofluorescence with CHL1wt or L1wt at the plasma membrane (Figure 4.2H,P). These findings suggested that ezrin became phosphorylated on Thr567 when recruited to the cytoplasmic domain of CHL1wt or L1wt at the plasma membrane.

To determine if ERM protein interact with the CHL1 cytoplasmic domain at the juxtamembrane RGGKYSV sequence, we mutated 3 residues within this sequence (R1108, Y1112, V1114) to alanine ($CHL1_{AAA}$) (Figure 4.1). When HEK293 cells were transfected with the $CHL1_{AAA}$ mutant together with ezrin-GFP, more ezrin-GFP could be found in the cytosol compared to cells expressing CHL1wt (Figure 4.2J). Residual ezrin-GFP at the membrane of $CHL1_{AAA}$-expressing cells may have represented interaction with endogenous receptors, as seen in cells transfected with the empty vector (Figure 4.2B) or in untransfected cells (Figure 4.2, insert,

panERM). In accord with the cytosolic re-distribution of ezrin-GFP in cells expressing $CHL1_{AAA}$, only low levels of phosphorylated ERM proteins were detected in these cells (Figure 4.2K).

Taken together, these experiments showed that CHL1 was able to recruit ezrin to the cell membrane where it was phosphorylated on Thr567, and that the membrane-proximal RGGKYSV sequence in the CHL1 cytoplasmic domain was mediating the interaction with ezrin.

Interactions of CHL1 and L1 with ERM Proteins Regulate Cellular Adhesion and Migration

ERM protein binding to cell surface molecules provides a link between the extracellular matrix and the cytoskeleton necessary for cell adhesion and migration. We therefore addressed whether deletion of ERM protein interaction with CHL1 altered its ability to promote cell adhesion to fibronectin. For these experiments we turned to rat B35 neuroblastoma cells, a homogeneous CNS-derived cell line, which exhibits higher adhesion rates than HEK293 cells after 1 hr of incubation (data not shown) and in which intracellular signaling and cell migration induced by CHL1 and L1 have been extensively characterized (Otey et al., 2003; Thelen et al., 2002). B35 neuroblastoma cells, which express endogenous ezrin (Figure 4.3, insert), were co-transfected with CHL1wt, $CHL1_{AAA}$, L1wt, or pcDNA3 as control, together with a plasmid encoding GFP. 24 h after transfection, cells were assayed for the ability to adhere to fibronectin-coated dishes within 1 hr, after which the wells were rinsed to remove non-adherent cells and the number of adherent GFP-expressing cells was

scored. Expression of CHL1wt enhanced cell adhesion to fibronectin by 70% ($p<0.001$) compared to control B35 cells (Figure 4.3). In contrast, cells expressing $CHL1_{AAA}$ mutant protein showed no significant increase in cell adhesion compared to control B35 cells. L1wt expression also significantly stimulated cell adhesion compared to control B35 cells. These results indicated that cell adhesion to fibronectin, stimulated by CHL1, is dependent on interaction with ERM proteins.

To support the finding that altered CHL1/ERM protein interaction is responsible for the observed defects, adhesion of B35 cells co-transfected with plasmids encoding CHL1wt and ezrin-GFP or a GFP-tagged dominant negative ezrin mutant (ezrin DN with the mutation T567A, Gautreau et al., 2000) was analyzed. This mutant form of ezrin is not able to be phosphorylated and thus, although associated with the membrane, cannot link to F-actin (Gautreau et al., 2000). Expression of ezrin DN significantly reduced adhesion of CHL1-expressing B35 cells compared to ezrin wt expressing cells. This indicates that deleted linkage of CHL1 to the cytoskeleton by ERM proteins is responsible for the adhesion defects seen in the $CHL1_{AAA}$ mutant.

To investigate the requirement of the CHL1/ERM interaction in potentiating migration of HEK293 cells toward extracellular matrix proteins, *in vitro* assays of haptotactic migration were performed. HEK293 cells, which endogenously express ERM proteins (Figure 4.2 and 4.3, insert), were transiently transfected with pcDNA3 plasmids encoding CHL1wt, $CHL1_{AAA}$, L1wt, and differences in cell migration of transfected cells compared to non-transfected cells on fibronectin were monitored after incubation for 3 h. This assay reflects dynamic adhesive interactions of the cell

to fibronectin mediated by β_1-integrins and the actin cytoskeleton (Buhusi et al., 2003; Panicker et al., 2006).

Nontransfected HEK293 cells displayed reduced random migration toward bovine serum albumin when compared with migration toward fibronectin (Figure 4.4). Expression of CHL1wt strongly potentiated haptotactic migration of cells to fibronectin, relative to basal migration of HEK293 cells. In contrast, $CHL1_{AAA}$ was less effective in stimulating cellular migration towards fibronectin. Nonetheless, migration of $CHL1_{AAA}$ expressing cells was significantly greater than basal migration of HEK293 cells, indicating that additional factors, such as ankyrin binding (Buhusi et al., 2003), may contribute to migration. Similarly to CHL1wt, expression of L1wt strongly enhanced migration of HEK293 cells toward fibronectin. To exclude that mutation of the CHL1 cytoplasmic domain alters CHL1/β_1 integrin interaction leading to defects in β_1 integrin mediated migration, co-capping assays (Buhusi et al., 2003) and internalization experiments (Panicker et al., 2006) were performed in transfected HEK293 cells. No difference of CHL1wt and $CHL1_{AAA}$ in co-localization with β_1 integrins on the cell surface or in the levels of co-endocytosis with β_1 integrins could be observed (data not shown). Thus, ERM protein binding to the CHL1 cytoplasmic domain is important for potentiating integrin-mediated haptotactic migration of HEK293 cells.

Regulation of Neurite Outgrowth and Branching by Intracellular Interaction of ERM Proteins to CHL1

To investigate the role of CHL1/ERM protein interaction in a neuronal context, we analyzed its effect on promoting outgrowth and branching of cortical neuronal processes on a fibronectin substrate. For this study, embryonic cortical neurons (E14.5) from CHL1-minus mice were co-transfected by electroporation with CHL1wt, $CHL1_{AAA}$, or empty vector, together with a plasmid encoding GFP, and were then cultured on fibronectin-coated dishes for 3 days. Evaluation of cell surface expression of CHL1wt and $CHL1_{AAA}$ proteins 72 h after transfection showed that mutation of the ERM binding sequence did not affect CHL1 expression levels or localization to the plasma membrane (fluorescence pixel density of $CHL1_{AAA}$ surface staining was 104% of CHL1wt staining, $p=0.7$). Expression of ERM proteins in cortical neurons was confirmed by immunostaining with a panERM antibody and was found throughout the growth cone, the axon and the soma in CHL1wt and $CHL1_{AAA}$ neurons (Figure 4.5A). To compare neuronal process outgrowth in GFP-labeled neurons, we measured two parameters: the length of the longest neurite and total neurite length. Branching of neuronal processes was compared by quantifying the total branching number, the number of primary neurites extending from the soma, and the number of secondary neurites extending from other neurites.

Expression of CHL1wt in CHL1-minus neurons significantly stimulated neurite outgrowth of embryonic cortical neurons (Figure 4.5B,C). Neurites from CHL1wt transfected neurons ($n=88$) showed an increase of 37 ± 8% ($p<0.001$) in the average length of the longest neurite, and 53 ± 9% ($p<0.001$) in the average total neurite

length compared to CHL1-minus neurons (n=78, length of longest neurite 65 μm, total neurite length 140 μm). CHL1 also significantly promoted process branching of cortical neurons (Figure 4.5B,D). CHL1wt-expressing neurons displayed an increase in branching number of 33 ± 7% ($p<0.001$) compared to CHL1-minus neurons (branching number 3.5). This increase in branching can be mainly attributed to the enhanced formation of secondary neurites (71 ± 16%, $p<0.001$) and to a minor extent to primary neurite elaboration (15 ± 5%, $p<0.02$). Whereas expression of CHL1wt increased total neurite length and branching compared to CHL1-minus neurons, neurons expressing $CHL1_{AAA}$ mutant (n=75) showed no significant differences in any parameter of neurite outgrowth or branching compared to CHL1-minus neurons (Figure 4.5B,C,D). These results showed that expression of CHL1 promoted neurite outgrowth and branch formation of cortical embryonic neurons on fibronectin, and that intracellular interaction of CHL1 with ERM proteins was important for CHL1-dependent neurite outgrowth and branching.

CHL1 Interaction with ERM Proteins is Required for Semaphorin 3A-Induced Growth Cone Collapse

Sema3A induces growth cone collapse by dynamic remodeling of actin filaments and endocytosis (Fan et al., 1993; Fournier et al., 2000; Jurney et al., 2002). To evaluate if ERM protein interaction with CHL1 mediates growth cone collapse induced by Sema3A, embryonic cortical neurons from CHL1-minus mice were transfected with CHL1wt, $CHL1_{AAA}$, or empty vector, together with a plasmid encoding GFP protein. Neurons were treated with 30 nM Sema3A-Fc fusion protein

or control Fc protein for 30 min, and the percentage of collapsed growth cones in each condition was determined by confocal microscopy (Figure 4.6).

Addition of Sema3A-AP to CHL1wt expressing neurons resulted in a striking increase in growth cone collapse compared to treatment with control Fc-AP. In contrast, addition of Sema3A-AP to CHL1-minus neurons only slightly enhanced the percentage of collapsed growth cones compared to control Fc-AP, as we have recently described (Wright et al., submitted). Similarly, when the $CHL1_{AAA}$ mutant was expressed in CHL1-minus neurons Sema3A exhibited only a small growth cone collapse response. It seems likely that the small effects of Sema3A on growth cone collapse of CHL1-minus and $CHL1_{AAA}$ neurons are mediated by L1 (Castellani et al., 2000), which is expressed at lower levels than CHL1 on embryonic cortical neurons. These results suggest that the CHL1/ERM protein interaction is required for Sema3A-induced growth cone collapse in embryonic cortical neurons.

In addition to induction of growth cone collapse, Sema3A is known to inhibit neurite outgrowth and branching in diverse neuronal systems (Bagnard et al., 1998; Bagri et al., 2003; Chaudhry et al., 2006; Dent et al., 2004; Niclou et al., 2003; Togashi et al., 2006). To determine whether CHL1 expression and CHL1/ERM protein interaction also contributed to the reduction of neurite outgrowth and branching induced by Sema3A, CHL1-minus embryonic cortical neurons (E14.5) were transfected with CHL1wt, $CHL1_{AAA}$, or empty vector, respectively, together with a plasmid encoding GFP protein. After 24 h in culture, neurons were treated with 30 nM Sema3A-AP or Fc-AP protein for 48 h, and analysis of neurite outgrowth and branching was performed as described above. Expression of CHL1wt promoted

neurite outgrowth and branching of CHL1-minus cortical neurons (Figure 7; 100% values for CHL1-minus: length of longest neurite 45 µm, total neurite length 90 µm, branching number 2.7). Importantly, addition of Sema3A to CHL1wt expressing neurons prevented the stimulatory effect of CHL1wt on neurite outgrowth and branching. CHL1-minus neurons treated with Sema3A showed a slight tendency for lower neurite outgrowth, but this effect was found to be not significant (Figure 4.7). These results demonstrated that the inhibitory effect of Sema3A on cortical neurite outgrowth and branching is dependent on CHL1 expression.

We then compared neurite process elaboration of $CHL1_{AAA}$ transfected neurons stimulated with Sema3A to Fc control treated neurons. Expression of $CHL1_{AAA}$ did not substantially rescue Sema3A response in CHL1-minus cortical neurons (Figure 4.7). Although there was a slight trend in Sema3A treated $CHL1_{AAA}$ neurons to reduced neurite outgrowth and branching compared to Fc treated neurons, this was only significant for the average longest neurite length ($P<0.05$) but not for any other examined parameter. Similar to the results obtained in the growth cone collapse assay, these smaller effects of Sema3A on CHL1-minus and $CHL1_{AAA}$ neurite outgrowth may be mediated by L1 (Chaudhry et al., 2006). These results suggested that Sema3A-induced inhibition of neurite outgrowth and branching of embryonic cortical neurons requires both CHL1 expression and intracellular interaction of CHL1 with ERM proteins.

Taken together, our results demonstrated important roles for CHL1 expression and CHL1/ERM interaction in cell adhesion, migration, neurite outgrowth and branching and in Sema3A-induced growth cone collapse. These findings

support a vital role for CHL1 and ERM proteins in neuronal process elaboration and axon guidance during embryonic cortical development.

4.4 Discussion

Here we show that interaction of the cytoskeletal linker proteins ezrin-radixin-moesin (ERM) with the cytoplasmic domain of CHL1 is important for CHL1-mediated neuronal functions. We have identified an intracellular membrane-proximal sequence in CHL1 as an interaction site for ERM proteins, and demonstrated that CHL1/ERM protein interaction is required for CHL1-stimulated neurite outgrowth and branching of embryonic cortical neurons, cell migration and adhesion. We also showed that Sema3A-induced growth cone collapse and inhibition of neurite outgrowth depend on CHL1/ERM interaction. These findings demonstrate that interaction of ERM proteins with CHL1 is required for diverse neuronal functions of CHL1.

CHL1 was found to be capable of recruiting ezrin to the plasma membrane by interaction of ezrin with the CHL1 cytoplasmic domain through three amino acids of the membrane-proximal RGGKYSV sequence (R1108, Y1112 and V1114). This sequence corresponds to a consensus ERM-binding motif, RxxTYxVxxA, which mediates interaction of ERM proteins with cell adhesion molecules such as ICAM, VCAM, and CD44 (Hamada et al., 2003), and a highly homologous sequence, KGGKYSV, in L1 mediates ERM protein binding to its cytoplasmic domain (Cheng et al., 2005). Mutation of the CHL1/ERM interaction motif involves Y1112 in CHL1, a potential phosphorylation site, and could therefore alter intracellular signaling.

Intracellular mutation of CHL1 could further alter interaction with other cytosolic binding partners, but experiments with L1 have shown that ankyrin binding is not impaired by membrane-proximal mutations (Cheng et al., 2005). A second binding site for ERM proteins in L1 is the YRSLE sequence (Cheng et al., 2005; Dickson et al., 2002), which is lacking in CHL1. Because mutation of the membrane proximal RGGKYSV sequence in the CHL1 intracellular domain did not completely inhibit ezrin recruitment to the cell membrane, there may be an additional unidentified sequence in CHL1 that promotes ERM protein association. While CHL1 effectively recruited ezrin-GFP to the cell membrane, no co-immunoprecipitation of CHL1 with ezrin-GFP from transfected HEK293 cells could be observed (data not shown). Similarly, binding of ezrin to both L1 and neurofascin was demonstrated in yeast two-hybrid assays but not by direct co-immunoprecitation (Cheng et al., 2005, Dickson et al., 2002, Gunn-Moore et al., 2006), indicating that interactions of L1 family cell adhesion molecules and ERM protein family members may be transient or of low affinity.

Expression of CHL1 markedly enhanced outgrowth and branching of embryonic cortical neurons on fibronectin. A stimulating effect of CHL1 on neurite outgrowth was demonstrated previously using substrate-coated CHL1 (Hillenbrand et al., 1999) or soluble CHL1 protein (Hillenbrand et al., 1999, Naus et al., 2004), acting in *trans* with an unidentified heterophilic receptor on neurons. Our studies instead indicate that neuronal CHL1 promotes neurite outgrowth in response to fibronectin as a substrate. This response may be due to a cooperative interaction of CHL1 in the plasma membrane with β_1 integrins, in agreement with the ability of

CHL1 to functionally interact with β_1 integrins for haptotactic cell migration (Buhusi et al., 2003). We further showed that ERM protein interaction with the CHL1 cytoplasmic domain promotes outgrowth and branching of embryonic cortical neurons on a fibronectin substrate as mutation of the ERM interaction site in CHL1 decreased neurite outgrowth and branching to basal levels of CHL1-minus neurons. This was not due to altered interaction in *cis* with β_1 integrins as co-capping and co-internalization of $CHL1_{AAA}$ and β_1 integrins were found to be normal (data not shown). Cerebellar neurons cultured on an L1 substrate also exhibited decreased neurite outgrowth and branching when ERM protein binding sites in L1 were mutated (Cheng et al., 2005), indicating that interaction with the cytoskeletal linker proteins ERM may play a general role in neural process formation promoted by L1 family adhesion molecules.

Our finding that ERM protein interaction with CHL1 is important for neurite outgrowth and branching is also in accord with studies showing that suppression of radixin and moesin in hippocampal neurons inhibits neurite outgrowth and dramatically alters growth cone morphology (Paglini et al., 1998). Moreover, a coordinated activation of radixin in the growth cone was implicated in branching of dorsal root ganglion neurons (Castelo et al., 1999). The defects in neurite outgrowth and branching seen in $CHL1_{AAA}$ neurons are likely to result from the reduced ability of CHL1 to recruit ERM proteins to the growth cone membrane, thereby altering growth cone functions that depend on actin dynamics. Alternatively, as ERM proteins bind directly to F-actin (Ramesh et al., 2004) and, beside interaction with CHL1, associate with β_1 integrins in growth cones (Wu et al., 1996), a CHL1/β_1/ERM

protein complex could connect the plasma membrane to the underlying cytoskeleton, establishing a regulated, dynamic link that mediates adhesive force necessary for neurite outgrowth and branching, as well as migration and growth cone collapse. Involvement of ERM proteins in cell adhesion and migration has been demonstrated in several different cellular systems (Elliott et al., 2005; Li et al., 2007; Rossy et al., 2007; Takeuchi et al., 1994). We show here that deletion of ERM protein binding to CHL1 significantly altered adhesive properties to the extracellular matrix protein fibronectin and inhibited integrin-dependent haptotactic migration. Inhibition of cell adhesion was due to defective linkage of CHL1 to the cytoskeleton as demonstrated by adhesion assays with a dominant-negative mutant of ezrin, which is unable to link to F-actin (Gautreau et al., 2000). Therefore, a CHL1/β_1/ERM protein complex connecting the extracellular matrix and the cytoskeleton may be necessary to establish an adhesive complex or to modulate integrin function in an inside-out manner.

We further demonstrated that Sema3A abolished the stimulating effects of CHL1 expression on outgrowth and branching of embryonic cortical neurons, but had no effect on neurons lacking CHL1 or expressing the ERM-binding deficient mutant $CHL1_{AAA}$. Embryonic neurons of the cortex (Bagnard et al., 1998; Dent et al., 2004), the hippocampus (Bagri et al., 2003) and dorsal root ganglia (DRG) (Chaudhry et al., 2006; Niclou et al., 2003; Togashi et al., 2006) react to Sema3A with decreased neurite outgrowth and/or branching. We show here that these neuronal responses in embryonic cortical neurons can be mediated through CHL1/ERM protein interaction. We recently demonstrated that CHL1 mediates

Sema3-induced growth cone collapse in cultures of embryonic cortical or thalamic neurons through its ability to bind the Sema3A receptor neuropilin-1 (Wright et al., submitted). In this regard CHL1 resembles L1, which binds neuropilin-1 and mediates Sema3A-induced growth cone collapse in postnatal cortical explants (Castellani et al., 2000, 2004). It seems likely that both CHL1 and L1 can act as a receptor for Sema3A-induced functions at different developmental stages in accordance with their different expression patterns during cortical development (Mintz et al., 2003, Demyanenko et al., 2004).

We now extend these findings to show that a CHL1 mutant lacking ERM protein interaction capability does not support Sema3A-induced growth cone collapse in cortical neurons. Modulation of neurite outgrowth and branching by Sema3A is thought to have a different underlying mechanism from Sema3A-induced growth cone collapse (Dent et al., 2004). However, we show that both processes require CHL1 expression and CHL1 interaction with ERM proteins. It is noteworthy that Sema3A triggers growth cone membrane endocytosis during collapse, which, like neurite outgrowth and branching, involves actin rearrangements (Fournier et al., 2000), and could require dynamic ERM protein binding to actin filaments.

A limitation of our studies is that the function of CHL1/ERM protein interaction has not been demonstrated in the developing cerebral cortex *in vivo*. For example, CHL1/ERM protein interactions may direct apical dendrites of cortical pyramidal cells to the pial surface (Demyanenko et al., 2004), which has been shown to involve attraction toward Sema3A in the upper cortical layers (Polleux et al., 2000). CHL1/ERM protein interaction might also promote radial migration of neuronal

precursors (Demyanenko et al., 2004), as ERM proteins are expressed in the intermediate zone at the time when these cells migrate to form the distinct layers of the cortex (Mintz et al., 2003). In addition, CHL1/ERM protein-mediated growth cone collapse to Sema3A may be required for proper axon guidance in olfactory and hippocampal pathways, which is impaired in CHL1-minus mice (Montag-Sallaz et al., 2002). Analysis of mice deleted for ERM protein expression could give insights into the function of the CHL1/ERM protein complex in neuronal development, but is hindered by the high redundancy of the three members of the family, which may mask a phenotype *in vivo* (Bretscher et al., 2002).

Taken together our results suggest that ERM protein interaction with the CHL1 cytoplasmic domain represents a crucial component in the link between the extracellular matrix and the cytoskeleton, which in cooperation with β_1 integrins, is necessary for neurite outgrowth and branching, as well as growth cone collapse in response to Sema3A.

4.5 Methods

Plasmids, Antibodies and Fusion Proteins

The following cDNAs in pcDNA3 (Stratagene, La Jolla, CA) were used: wild type mouse CHL1 (NM_007697; Holm et al., 1996; Buhusi et al., 2003), a CHL1 mutant ($CHL1_{AAA}$) in which the membrane-proximal RGGKYSV sequence was mutated to AGGKASA, and a wild type human L1 (from J. Hemperly, BD Technologies, Research Triangle Park, NC). The $CHL1_{AAA}$ mutation was introduced in the sequence corresponding to the CHL1 cytoplasmic domain subcloned in pBlueScript

through a 3-step site-directed mutagenesis (QuikChange Site-Directed Mutagenesis, Stratagene), using the following primer pairs: A_Mut_F 5'-GGTGGAAAGTATTCAGCAAAAGAAAAGGAAGATTACACCCC -3' and A_Mut_R 5'- GGGGTGTAATCTTCCTTTTCTTTTGCTGAATACTTTCCACC -3' for the V to A mutation, ASA_Mut_F 5'-GAGGAACAGAGGTGGAAAGGCTTCAGCAAAAGAAAAGGAAG -3' and ASA_Mut_R 5'- CTTCCTTTTCTTTTGCTGAAGCCTTTCCACCTCTGTTCCTC -3' for the YSV to ASA mutation and AGGKASA_FP 5'-CTTTGTGAAGAGGAACGCAGGTGGAAAGGCTTCAGC -3' and AGGKASA_RP 5'-GCTGAAGCCTTTCCACCTGCGTTCCTCTTCACAAAG -3' for the final RGGKASA to AGGKASA step. After the triple mutation was confirmed through sequencing, the mutated CHL1 cytoplasmic domain was transferred (by digestion with Eco47III and XhoI followed by ligation) to the pcDNA3 CHL1 plasmid to replace the wild-type sequence.

A plasmid encoding mouse ezrin fused to green fluorescent protein (Ezrin-GFP) was generated by cloning ezrin (IMAGE: 6826190; ATCC, Manassas, VA) into the pEGFP-N1 vector (Clontech, Mountain View, CA). Briefly, the ezrin coding sequence was amplified using the following primers: Ezrin-FP 5'-TTGCTAGCCAAGAGCCCAAGCCAATCAAC-3' and Ezrin-nostop-RP 5'-TTAAGCTTTCCTCCTCCCATGGCCTCGAACTCGTC-3', the PCR product and pEGFP-N1 were digested with NheI and HindIII and then ligated. The T567A mutation in Ezrin-GFP was generated through site-directed mutagenesis using the following primers: EzrinA-FP 5'-

GCAGGGACAAGTATAAGCCGCTGCGCCAAATCAGGCAGG-3' and EzrinA-RP 5'-CCTGCCTGATTTGGCGCAGCGCCTTATACTTGTCCCTGC-3'. The mutation was confirmed through DNA sequencing.

Goat anti-mouse CHL1 antibody was obtained from R&D Systems (Minneapolis, MN). Mouse anti-human L1 monoclonal antibody UJ127 was from Abcam Inc. (Cambridge, MA). Anti-L1 polyclonal rabbit antibody 6096 was a generous gift of John Hemperly (BD Technologies). Rabbit anti-phospho-ERM polyclonal antibody from Chemicon (Temecula, CA) recognizes phosphorylated threonine 567(ezrin), 564 (radixin), 558(moesin). Mouse IgM monoclonal antibody to members of the ERM family (panERM, clone 13H9) was a generous gift from F. Solomon (Massachusetts Institute of Technology, Cambridge, MA). Mouse anti-ezrin monoclonal antibody for Western blotting was from Chemicon. All secondary antibodies were from Jackson ImmunoResearch Laboratories Inc (West Grove, PA). All cell culture media and supplements were from Gibco (Carlsbad, CA).

To prepare Sema3A-AP and Fc-AP fusion proteins, HEK293T cells were transfected with alkaline phosphatase (AP)-tagged Sema3A or AP-tagged mouse Fc encoding cDNA using LipofectAMINE 2000 (Invitrogen) according to the manufacturers' protocol. Two days after transfection, media was collected and the concentration of Sema3A-AP or Fc-AP was determined using the colorimetric assay described in (Flanagan and Leder 1990) with the modification that media were mixed with lysis buffer (10 mM Tris pH 8, 1% Triton X-100) instead of heating.

Cell Culture and Transfection

HEK293 and rat B35 neuroblastoma cell cultures were maintained in Dulbecco's modified Eagle's medium (DMEM) with 10% heat-inactivated fetal bovine serum (FBS). For transient protein expression, cultures at 80-90% confluence in 60-mm dishes were transfected with pcDNA3 plasmids (4-5 µg) using LipofectAMINE 2000 in OptiMEM for 18- 24h at 37°C.

To generate primary cortical neurons, pregnant CHL1-minus homozygous mutant mice on a C57Bl/6 background (E14.5) (Montag-Sallaz et al., 2002) were anesthetized, embryos removed, and their cortices were dissociated in complete Hanks' balanced saline solution (HBSS) by trituration. Cells were then co-transfected with pMax-GFP and pcDNA3-CHL1wt, pcDNA3-CHL1$_{AAA}$ or empty pcDNA3 by electroporation using an Amaxa Nucleofector Device with a Mouse Neuron Nucleofector Kit (Amaxa, Gaithersburg, MD). Briefly, 5 x 10^6 cells in transfection buffer were electroporated with plasmid cDNA and allowed to recover in RPMI medium. After 5 min, cells in DMEM/10% FBS were plated on MatTek dishes coated with poly-D-lysine/fibronectin (Sigma, 5µg/ml). One day after plating, the medium was changed to Neurobasal medium containing B27 supplement and glutamate (25µM). Animal care and treatment were in accordance with guidelines provided by the UNC Institutional Animal Care and Use Committee (IACUC).

Analysis of ERM protein expression and of CHL1 cell surface expression

For analysis of ERM protein expression in B35 and HEK293 cell lines, cells were lysed in RIPA buffer (20 mM Tris pH 7.0, 0.15 M NaCl, 5 mM EDTA, 1 mM EGTA, 1% NP-40, 1% Na-deoxycholate, 0.1% SDS, 0.2 mM sodium

orthovadandate, 10 mM sodium fluoride) including protease inhibitors (Sigma), and 30 µg cell lysate was examined by gel electrophoresis followed by immunoblotting with an anti-ezrin antibody and an HRP-conjugated goat- anti mouse IgG antibody using the enhanced chemiluminescence kit from Pierce.

For analysis of neuronal ERM protein expression, transfected neurons on fibronectin-coated MatTek dishes were fixed after 72 h in culture with 4% paraformaldehyde in 0.1M phosphate buffer, pH 7.4, (PFA) for 15 min. For ERM protein staining, neurons were blocked with 10% donkey serum in phosphate-buffered saline (PBS) for 60 min at room temperature (RT) followed by permeabilization with 0.05% Triton X-100 in 10% donkey serum/PBS for 30 min at RT. Neurons were then incubated with mouse anti-panERM antibody (1:50) for 60 min at RT, followed by washes with PBS and incubation with Cy5-conjugated donkey anti-mouse antibody (1:100) for 45 min at RT. After additional washes with PBS and mounting in Gel/Mount (Biomeda, Foster City, CA), neurons were analyzed using an Olympus FV500 laser confocal microscope at the Microscopy Service Laboratory (Dept. of Pathology, University of North Carolina).

For CHL1 cell surface staining, unpermeabilized neurons were incubated with goat anti-CHL1 (1:200) and TRITC-conjugated donkey anti-goat (1:100) antibodies as described for ERM protein staining. Images were acquired using an Olympus FV 500 laser confocal microscope (60x objective) with a constant exposure time representing unsaturated conditions. Approximately 25 neurons were analyzed per experiment and condition as described in (Cheng et al., 2005). At three different locations along the longest neurite, pixel density was determined using ImageJ

software, and the average pixel density for each neuron was calculated. Values were then averaged, and $CHL1_{AAA}$ cell surface expression was expressed as percent of CHL1wt expression.

Cytofluorescence Assay for CHL1/ ERM protein recruitment

Recruitment of soluble ERM proteins to the cytoplasmic domains of CHL1 and L1 at the plasma membrane was analyzed in a cytofluorescence assay similar to that described for ankyrin recruitment to CHL1 (Buhusi et al., 2003). Briefly, HEK293 cells on PDL-coated MatTek dishes were co-transfected with ezrin-GFP (mouse ezrin in pEGFP-N1) and pcDNA3 plasmids encoding CHL1wt, $CHL1_{AAA}$ or L1wt or the empty vector as control (ratio 1:10) using LipofectAMINE 2000. After 24 h, cells were fixed with 4% PFA for 15 min, washed, and incubated in 10% donkey serum in PBS including 0.2% Triton X-100 for 30 min. To visualize CHL1, L1 or phosphorylated ERM proteins (pERM), cells were incubated for 4 h at RT with goat anti-CHL1 antibody (5 µg/ml in blocking buffer), mouse anti-L1 antibody UJ127 (5 µg/ml), and rabbit anti-pERM antibody (5 ug/ml). Cells were washed and incubated for 2 h with TRITC-conjugated donkey anti-goat IgG (for CHL1), TRITC-conjugated donkey anti-mouse IgG (for L1) and Cy5-conjugated donkey anti-rabbit IgG (for pERM), each diluted 1:100 10% donkey serum in PBS. Cells were washed and mounted in Vectashield (Vector Laboratories, Burlingame, CA). GFP/immunofluorescence images were recorded on an Olympus FV500 laser confocal microscope using the appropriate filters.

Haptotactic Migration Assay

Haptotactic migration of HEK293 cells transiently expressing CHL1, L1 or mutant proteins was assayed as previously described (Buhusi et al., 2003), using modified Boyden chambers with 8-μm pore filters (Transwells 3422, Corning Inc., Corning, NY). The bottom side of the filters was coated with fibronectin (5 μg/ml) or 2% bovine serum albumin (BSA, Sigma) in PBS at 4°C overnight and blocked with 2% BSA. Cells were detached with 5 mM EDTA in HBSS and plated at 20,000 cells/filter in serum-free DMEM. Cells were allowed to migrate for 3-4 h at 37°C and 5% CO_2 before fixation with 4% PFA, followed by incubation in blocking solution (10% goat serum, 0.2% fish skin gelatin, PBS) for either 1 h at RT or overnight at 4°C.

To visualize migrated cells, cells from the upper or lower sides of filters were removed, and cells on the opposite side were stained by indirect immunofluorescence with polyclonal CHL1 antibody (20 μg/ml) (Buhusi et al., 2003) or L1 polyclonal antibody 6096 (20 μg/ml) in blocking solution for 4 h at RT, followed by FITC-conjugated donkey anti-rabbit secondary antibody diluted 1:75 to 1:100 in blocking solution. Cells were counterstained with 10 μM bis-benzimide (Hoechst 33258, Molecular Probes, Eugene, OR). The filters were mounted with Vectashield on glass slides, and the cells were scored on both top and bottom surfaces of filters under epifluorescence illumination. Counting of cells and analysis of migration data was performed as described (Buhusi et al., 2003).

Cell Adhesion Assay

24-well plates were incubated with 100 µl of nitrocellulose solution (1 cm^2 in 100 ml MeOH) for 30 min at RT. Dried wells were washed with water and immediately incubated with 5 µg/ml fibronectin in PBS for 1 h at 37°C or at 4°C overnight. Wells were blocked with 1% BSA in PBS for 1 hr at 37°C. B35 rat neuroblastoma cells were co-transfected with cDNA encoding CHL1wt, L1wt, $CHL1_{AAA}$ mutant protein or the empty vector (control) and pMAX-GFP cDNA or cDNA encoding CHL1wt and ezrin-GFP or ezrin(T567A)-GFP respectively. Cells were detached with 5mM EDTA in HBSS and washed once in serum-free DMEM. 25,000 cells/well were incubated in DMEM, 10% FBS for 1 h at 37°C. Non-adherent cells were removed by two washes with PBS, and adherent cells were fixed with 4% PFA for 20 min. GFP-labeled cells were scored in 10 randomly selected fields per well under epifluorescence illumination using a 40x objective of a Zeiss Axiovert 200 microscope. Samples were performed in duplicates and the experiment was repeated three times. Percentage of adherent cells per field was standardized to the number of adherent control cells for each experiment. Values obtained from independent experiments were averaged, standard errors were determined, and statistical significance was examined using the t-test ($p<0.05$).

Neurite Outgrowth and Branching Analysis

Dissociated embryonic cortical neurons were transfected with the respective plasmids by electroporation and incubated for 24 h with DMEM/10% FBS. Then medium was changed to Neurobasal/B27/glutamate (25uM), supplemented with either Fc-AP or Sema3A-AP fusion proteins (30 nM). After 48 h of incubation, cells

were fixed with 4% PFA and mounted in Gel/Mount (Biomeda, Foster City, CA). Images of GFP expressing neurons were captured on a Zeiss Axiovert 200 inverted microscope using an Axiocam MRc5 digital camera, and image analysis was performed using NIH Image J. The analysis of neurite outgrowth and branching was performed as described (Cheng et al., 2005; Hinkle et al., 2006). In cortical neuronal cultures maintained in Neurobasal medium about 97% of the neurons are cortical neurons and only neurons of highly similar type were analyzed. Neurites at least 10 μm in length and not in contact with any other neuron were measured. Total neurite length was defined as the sum of the lengths of all neuritic branches from a single neuron. The longest single neurite was the longest neurite length elaborated from the soma. Branching number represented the sum of all branch points from a single neuron, including primary neurites (extending directly from the soma) and secondary neurites (extending form a neurite). Between 30 and 90 neurons were analyzed per condition in each experiment, and each condition was assayed at least twice. The values from one experiment were normalized to the mean of CHL1-minus neurons in the same experiment. Mean values were compared using the Student's *t* test to evaluate significant differences ($p < 0.05$ or 0.01).

Growth Cone Collapse Assay

Dissociated embryonic cortical neurons transfected with the indicated plasmids were incubated for 24 h with DMEM/10% FBS and then changed to Neurobasal/B27 supplement/glutamate (25uM). Cells were then treated with either Fc-AP or Sema3A-AP fusion proteins (30 nM) for 30 minutes to induce growth cone collapse. Cells were fixed with 4% PFA and permeabilized with 0.2% TritonX-100

for 5 min. After washing, cells were treated with rhodamine-conjugated phalloidin (Molecular Probes; 1:40) for 30 min at RT to visualize actin within the growth cone. Cells were mounted in Gel/Mount and GFP positive neurons were scored for growth cone collapse using confocal microscopy. Growth cones were considered collapsed if no filopodial or lamellipodial protrusions were observed, and results were reported as percentage of collapsed growth cones. Three independent experiments were performed, and between 150 and 250 growth cones were scored per condition. Results were reported as percentage of GFP-positive cells with collapsed growth cones using the means of three experiments +/- standard error of the mean (SEM). Statistical significance was determined using the one-tailed t-test ($p<0.05$). Comparison of CHL1-minus neurons treated with Fc protein with non-treated cells revealed that Fc protein did not have any effect on growth cone morphology (data not shown).

4.6 References

Bagnard D., Lohrum M., Uziel D., Puschel A. W. and Bolz J. (1998) Semaphorins act as attractive and repulsive guidance signals during the development of cortical projections. *Development* 125, 5043-5053.

Bagri A., Cheng H. J., Yaron A., Pleasure S. J. and Tessier-Lavigne M. (2003) Stereotyped pruning of long hippocampal axon branches triggered by retraction inducers of the semaphorin family. *Cell* 113, 285-299.

Barreiro O., Yanez-Mo M., Serrador J. M., Montoya M. C., Vicente-Manzanares M., Tejedor R., Furthmayr H. and Sanchez-Madrid F. (2002) Dynamic interaction of VCAM-1 and ICAM-1 with moesin and ezrin in a novel endothelial docking structure for adherent leukocytes. *J Cell Biol* 157, 1233-1245.

Barret C., Roy C., Montcourrier P., Mangeat P. and Niggli V. (2000) Mutagenesis of the phosphatidylinositol 4,5-bisphosphate (PIP(2)) binding site in the NH(2)-terminal domain of ezrin correlates with its altered cellular distribution. *J Cell Biol* 151, 1067-1080.

Bennett V., Baines A. J. and Davis J. Q. (1985) Ankyrin and synapsin: spectrin-binding proteins associated with brain membranes. *J Cell Biochem* 29, 157-169.

Bretscher A., Edwards K. and Fehon R. G. (2002) ERM proteins and merlin: integrators at the cell cortex. *Nat Rev Mol Cell Biol* 3, 586-599.

Buhusi M., Midkiff B. R., Gates A. M., Richter M., Schachner M. and Maness P. F. (2003) Close homolog of L1 is an enhancer of integrin-mediated cell migration. *J Biol Chem* 278, 25024-25031.

Castellani V., Chedotal A., Schachner M., Faivre-Sarrailh C. and Rougon G. (2000) Analysis of the L1-deficient mouse phenotype reveals cross-talk between Sema3A and L1 signaling pathways in axonal guidance. *Neuron* 27, 237-249.

Castellani V., Falk J. and Rougon G. (2004) Semaphorin3A-induced receptor endocytosis during axon guidance responses is mediated by L1 CAM. *Mol Cell Neurosci* 26, 89-100.

Castelo L. and Jay D. G. (1999) Radixin is involved in lamellipodial stability during nerve growth cone motility. *Mol Biol Cell* 10, 1511-1520.

Chaudhry N., de Silva U. and Smith G. M. (2006) Cell adhesion molecule L1 modulates nerve-growth-factor-induced CGRP-IR fiber sprouting. *Exp Neurol* 202, 238-249.

Chen Q. Y., Chen Q., Feng G. Y., Lindpaintner K., Chen Y., Sun X., Chen Z., Gao Z., Tang J. and He L. (2005) Case-control association study of the close homologue of L1 (CHL1) gene and schizophrenia in the Chinese population. *Schizophr Res* 73, 269-274.

Cheng L., Itoh K. and Lemmon V. (2005) L1-mediated branching is regulated by two ezrin-radixin-moesin (ERM)-binding sites, the RSLE region and a novel juxtamembrane ERM-binding region. *J Neurosci* 25, 395-403.

Demyanenko G. P., Schachner M., Anton E., Schmid R., Feng G., Sanes J. and Maness P. F. (2004) Close homolog of L1 modulates area-specific neuronal positioning and dendrite orientation in the cerebral cortex. *Neuron* 44, 423-437.

Dent E. W., Barnes A. M., Tang F. and Kalil K. (2004) Netrin-1 and semaphorin 3A promote or inhibit cortical axon branching, respectively, by reorganization of the cytoskeleton. *J Neurosci* 24, 3002-3012.

Dickson T. C., Mintz C. D., Benson D. L. and Salton S. R. (2002) Functional binding interaction identified between the axonal CAM L1 and members of the ERM family. *J Cell Biol* 157, 1105-1112.

Elliott B. E., Meens J. A., SenGupta S. K., Louvard D. and Arpin M. (2005) The membrane cytoskeletal crosslinker ezrin is required for metastasis of breast carcinoma cells. *Breast Cancer Res* 7, 365-373.

Fan J., Mansfield S. G., Redmond T., Gordon-Weeks P. R. and Raper J. A. (1993) The organization of F-actin and microtubules in growth cones exposed to a brain-derived collapsing factor. *J Cell Biol* 121, 867-878.

Fievet B. T., Gautreau A., Roy C., Del Maestro L., Mangeat P., Louvard D. and Arpin M. (2004) Phosphoinositide binding and phosphorylation act sequentially in the activation mechanism of ezrin. *J Cell Biol* 164, 653-659.

Flanagan J. G. and Leder P. (1990) The kit ligand: a cell surface molecule altered in steel mutant fibroblasts. *Cell* 63, 185-194.

Fournier A. E., Nakamura F., Kawamoto S., Goshima Y., Kalb R. G. and Strittmatter S. M. (2000) Semaphorin3A enhances endocytosis at sites of receptor-F-actin colocalization during growth cone collapse. *J Cell Biol* 149, 411-422.

Frints S. G., Marynen P., Hartmann D., Fryns J. P., Steyaert J., Schachner M., Rolf B., Craessaerts K., Snellinx A., Hollanders K., D'Hooge R., De Deyn P. P. and Froyen G. (2003) CALL interrupted in a patient with non-specific mental retardation: gene dosage-dependent alteration of murine brain development and behavior. *Hum Mol Genet* 12, 1463-1474.

Garver T. D., Ren Q., Tuvia S. and Bennett V. (1997) Tyrosine phosphorylation at a site highly conserved in the L1 family of cell adhesion molecules abolishes ankyrin binding and increases lateral mobility of neurofascin. *J Cell Biol* 137, 703-714.

Gautreau A., Louvard D., Arpin M. (2000) Morphogenic effects of ezrin require a phosphorylation-induced transition from oligomers to monomers at the plasma membrane. *J Cell Biol* 150, 193-204.

Gunn-Moore F.J., Hill M., Davey F., Herron L.R., Tait S., Sherman D., Brophy P.J. (2006) A functional FERM domain binding motif in neurofascin. *Mol Cell Neurosci* 33, 441-446.

Hamada K., Shimizu T., Yonemura S., Tsukita S. and Hakoshima T. (2003) Structural basis of adhesion-molecule recognition by ERM proteins revealed by the crystal structure of the radixin-ICAM-2 complex. *Embo J* 22, 502-514.

Hillenbrand R., Molthagen M., Montag D. and Schachner M. (1999) The close homologue of the neural adhesion molecule L1 (CHL1): patterns of expression and promotion of neurite outgrowth by heterophilic interactions. *Eur J Neurosci* 11, 813-826.

Hinkle C. L., Diestel S., Lieberman J. and Maness P. F. (2006) Metalloprotease-induced ectodomain shedding of neural cell adhesion molecule (NCAM). *J Neurobiol* 66, 1378-1395.

Holm J., Hillenbrand R., Steuber V., Bartsch U., Moos M., Lubbert H., Montag D. and Schachner M. (1996) Structural features of a close homologue of L1 (CHL1) in the mouse: a new member of the L1 family of neural recognition molecules. *Eur J Neurosci* 8, 1613-1629.

Jurney W. M., Gallo G., Letourneau P. C. and McLoon S. C. (2002) Rac1-mediated endocytosis during ephrin-A2- and semaphorin 3A-induced growth cone collapse. *J Neurosci* 22, 6019-6028.

Li Y., Harada T., Juang Y. T., Kyttaris V. C., Wang Y., Zidanic M., Tung K. and Tsokos G. C. (2007) Phosphorylated ERM is responsible for increased T cell polarization, adhesion, and migration in patients with systemic lupus erythematosus. *J Immunol* 178, 1938-1947.

Maness P. F. and Schachner M. (2007) Neural recognition molecules of the immunoglobulin superfamily: signaling transducers of axon guidance and neuronal migration. *Nat Neurosci* 10, 19-26.

Mintz C. D., Dickson T. C., Gripp M. L., Salton S. R. and Benson D. L. (2003) ERMs colocalize transiently with L1 during neocortical axon outgrowth. *J Comp Neurol* 464, 438-448.

Montag-Sallaz M., Baarke A. and Montag D. (2003) Aberrant neuronal connectivity in CHL1-deficient mice is associated with altered information processing-related immediate early gene expression. *J Neurobiol* 57, 67-80.

Montag-Sallaz M., Schachner M. and Montag D. (2002) Misguided axonal projections, neural cell adhesion molecule 180 mRNA upregulation, and altered behavior in mice deficient for the close homolog of L1. *Mol Cell Biol* 22, 7967-7981.

Naus S., Richter M., Wildeboer D., Moss M., Schachner M. and Bartsch J. W. (2004) Ectodomain shedding of the neural recognition molecule CHL1 by the metalloprotease-disintegrin ADAM8 promotes neurite outgrowth and suppresses neuronal cell death. *J Biol Chem* 279, 16083-16090.

Needham L. K., Thelen K. and Maness P. F. (2001) Cytoplasmic domain mutations of the L1 cell adhesion molecule reduce L1-ankyrin interactions. *J Neurosci* 21, 1490-1500.

Ng T., Parsons M., Hughes W. E., Monypenny J., Zicha D., Gautreau A., Arpin M., Gschmeissner S., Verveer P. J., Bastiaens P. I. and Parker P. J. (2001) Ezrin is a downstream effector of trafficking PKC-integrin complexes involved in the control of cell motility. *Embo J* 20, 2723-2741.

Niclou S. P., Franssen E. H., Ehlert E. M., Taniguchi M. and Verhaagen J. (2003) Meningeal cell-derived semaphorin 3A inhibits neurite outgrowth. *Mol Cell Neurosci* 24, 902-912.

Otey C. A., Boukhelifa M. and Maness P. (2003) B35 neuroblastoma cells: an easily transfected, cultured cell model of central nervous system neurons. *Methods Cell Biol* 71, 287-304.

Paglini G., Kunda P., Quiroga S., Kosik K. and Caceres A. (1998) Suppression of radixin and moesin alters growth cone morphology, motility, and process formation in primary cultured neurons. *J Cell Biol* 143, 443-455.

Panicker A. K., Buhusi M., Erickson A. and Maness P. F. (2006) Endocytosis of beta1 integrins is an early event in migration promoted by the cell adhesion molecule L1. *Exp Cell Res* 312, 299-307.

Polleux F., Morrow T. and Ghosh A. (2000) Semaphorin 3A is a chemoattractant for cortical apical dendrites. *Nature* 404, 567-573.

Pratte M., Rougon G., Schachner M. and Jamon M. (2003) Mice deficient for the close homologue of the neural adhesion cell L1 (CHL1) display alterations in emotional reactivity and motor coordination. *Behav Brain Res* 147, 31-39.

Ramesh V. (2004) Merlin and the ERM proteins in Schwann cells, neurons and growth cones. *Nat Rev Neurosci* 5, 462-470.

Rossy J., Gutjahr M. C., Blaser N., Schlicht D. and Niggli V. (2007) Ezrin/moesin in motile Walker 256 carcinosarcoma cells: signal-dependent relocalization and role in migration. *Exp Cell Res* 313, 1106-1120.

Sakurai K., Migita O., Toru M. and Arinami T. (2002) An association between a missense polymorphism in the close homologue of L1 (CHL1, CALL) gene and schizophrenia. *Mol Psychiatry* 7, 412-415.

Takeuchi K., Sato N., Kasahara H., Funayama N., Nagafuchi A., Yonemura S. and Tsukita S. (1994) Perturbation of cell adhesion and microvilli formation by antisense oligonucleotides to ERM family members. *J Cell Biol* 125, 1371-1384.

Thelen K., Kedar V., Panicker A. K., Schmid R. S., Midkiff B. R. and Maness P. F. (2002) The neural cell adhesion molecule L1 potentiates integrin-dependent cell migration to extracellular matrix proteins. *J Neurosci* 22, 4918-4931.

Togashi H., Schmidt E. F. and Strittmatter S. M. (2006) RanBPM contributes to Semaphorin3A signaling through plexin-A receptors. *J Neurosci* 26, 4961-4969.

Wu D. Y., Wang L. C., Mason C. A. and Goldberg D. J. (1996) Association of beta 1 integrin with phosphotyrosine in growth cone filopodia. *J Neurosci* 16, 1470-1478.

Figure 4.1: Schematic Representation of CHL1 and L1 Cytoplasmic Domains

CHL1wt: Structure of the cytoplasmic domain of wild-type CHL1. The membrane-proximal RGGKYSV sequence shares homology with the KGGKYSV sequence in L1. CHL1 lacks the RSLE sequence of L1 exon 27. CHL1/ankyrin interaction is mediated by FIGAY (Buhusi et al., 2003).

L1wt: Structure of the L1 cytoplasmic domain and its association with cytoskeletal linker proteins. The membrane-proximal KGGKYSV sequence is a binding site for ERM proteins, and Y1151 is crucial for this association (Cheng et al., 2005). The YRSLE sequence in exon 27 is a second interaction site for ERM proteins (Cheng et al., 2005; Dickson et al., 2002). Y1229 within the FIGQY sequence is essential for ankyrin binding (Garver et al., 1997).

$CHL1_{AAA}$: CHL1 construct where 3 amino acid residues (R1108, Y1112, V1114) were mutated to alanine.

Figure 4.1

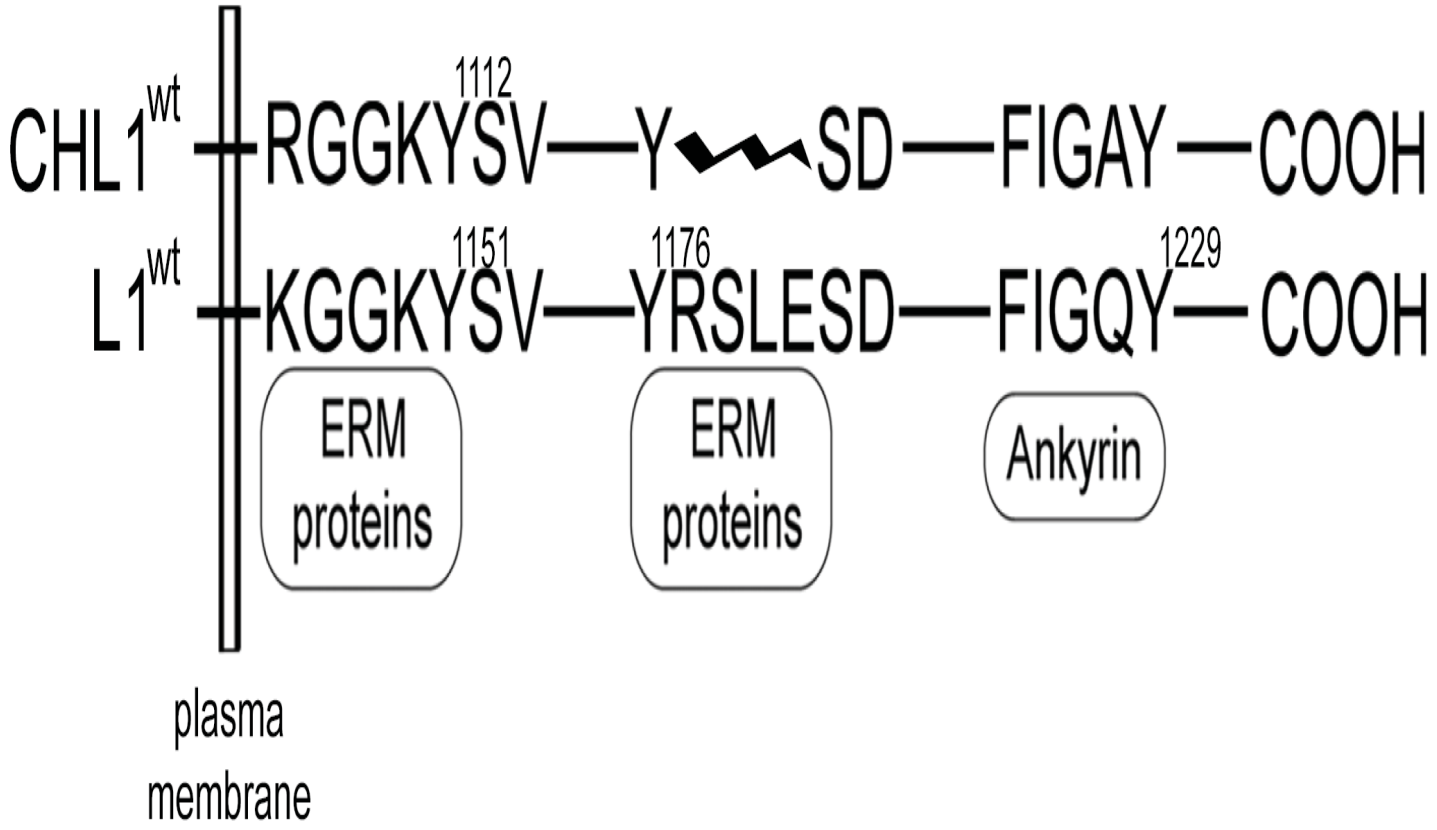

$CHL1^{AAA}$: RGGKYSV → AGGKASA

Figure 4.2: CHL1 Recruits Ezrin to the Cell Membrane Through the Membrane-Proximal RGGKYSV Sequence

HEK293 cells were co-transfected with GFP-tagged ezrin and the following expression plasmids: (B-D) pcDNA3, (E-H) CHL1wt, (I-L) $CHL1_{AAA}$, and (M-P) L1wt. After transfection (24 hr), cells were fixed and immunolabelled with antibodies against CHL1 or L1 (L1CAMs) and antibodies directed against activated, phosphorylated ERM proteins (phospho-ERM). Recruitment of ezrin-GFP to the cell membrane (B,F,J,N), CHL1/L1 expression (E,I,M) and Thr 567/564/558 phosphorylation of ERM proteins (C,G,K,O) was analyzed by confocal microscopy. Merged images are shown as an overlay in panels D,H,L, and P.
Insert shows endogenous expression of ERM proteins in untransfected HEK293 cells detected by immunolabeling with an antibody against all three ERM family members (panERM) or against phosphorylated ERM proteins (pERM).

Figure 4.2

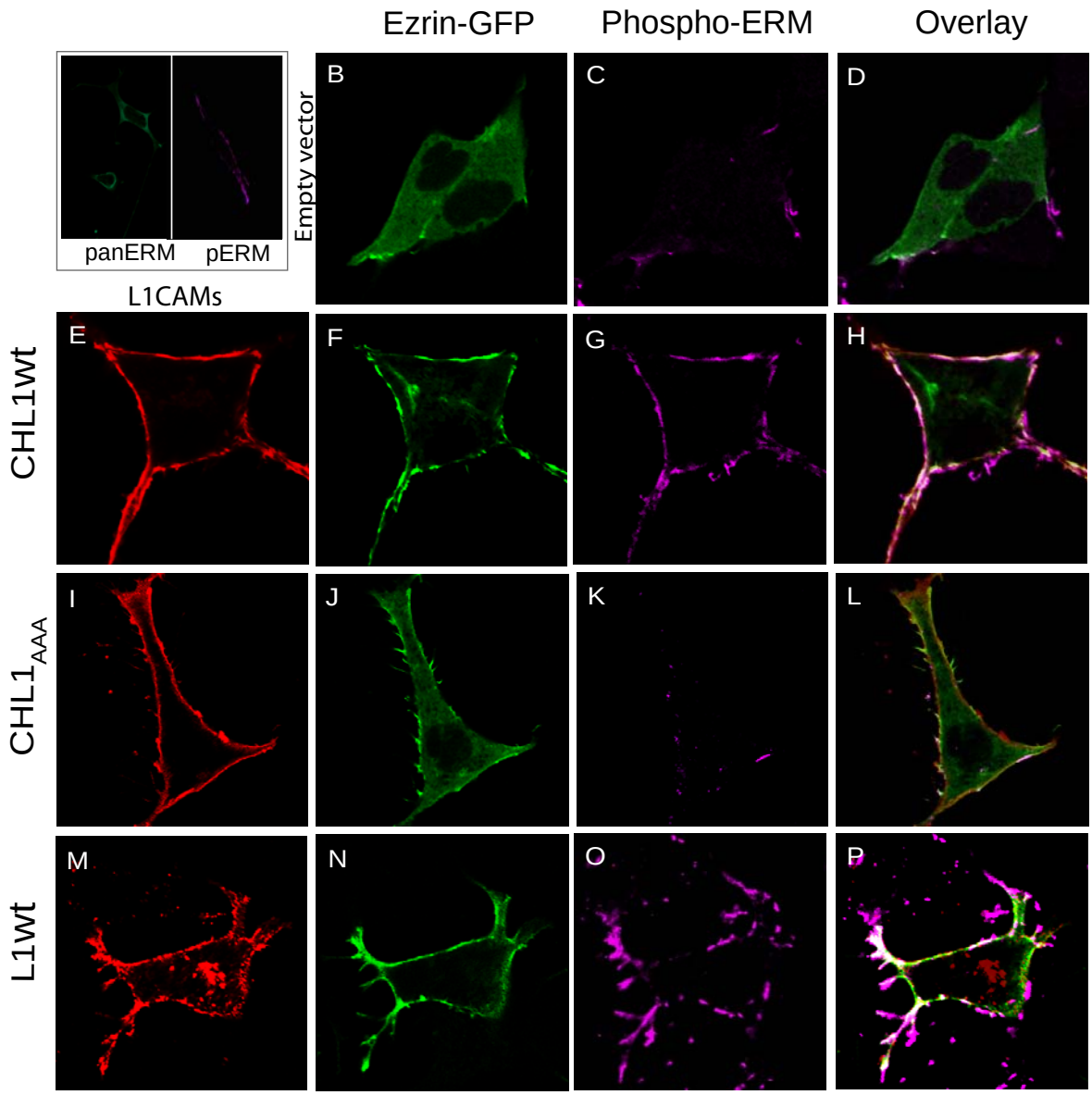
Ezrin-GFP
Phospho-ERM
Overlay
panERM
pERM
Empty vector
L1CAMs
CHL1wt
CHL1AAA
L1wt
B
C
D
E
F
G
H
I
J
K
L
M
N
O
P

Figure 4.3: Intracellular Interaction with ERM Proteins is Essential for CHL1-Mediated Adhesion to Fibronectin

Top*:* B35 neuroblastoma cells were co-transfected with expression pcDNA3 plasmids encoding CHL1wt, $CHL1_{AAA}$, or L1wt together with a GFP expression plasmid.

Bottom: B35 cells were co-transfected with pcDNA3 plasmids encoding CHL1wt and ezrin-GFP (ezrin wt) or ezrin(T567A)-GFP (ezrin DN) respectively. Cells were allowed to adhere to fibronectin-coated wells of 24-well plates for 1 h at 37°C, washed to remove non-adherent cells and fixed. Number of adherent cells was determined by counting GFP-labeled cells in 10 randomly selected fields per well. Samples were performed in duplicate, and the experiment was repeated three times. Percentage of adherent cells per field were standardized to number of adherent control cells for each experiment. Values represent means of percentage adherent cells per field of all experiments. **, statistically significant differences in means compared with control cells using the t-test (* $p<0.01$).
Insert shows Western blot analysis of ezrin expression in cell lysates from B35 and HEK293 cells.

Figure 4.3

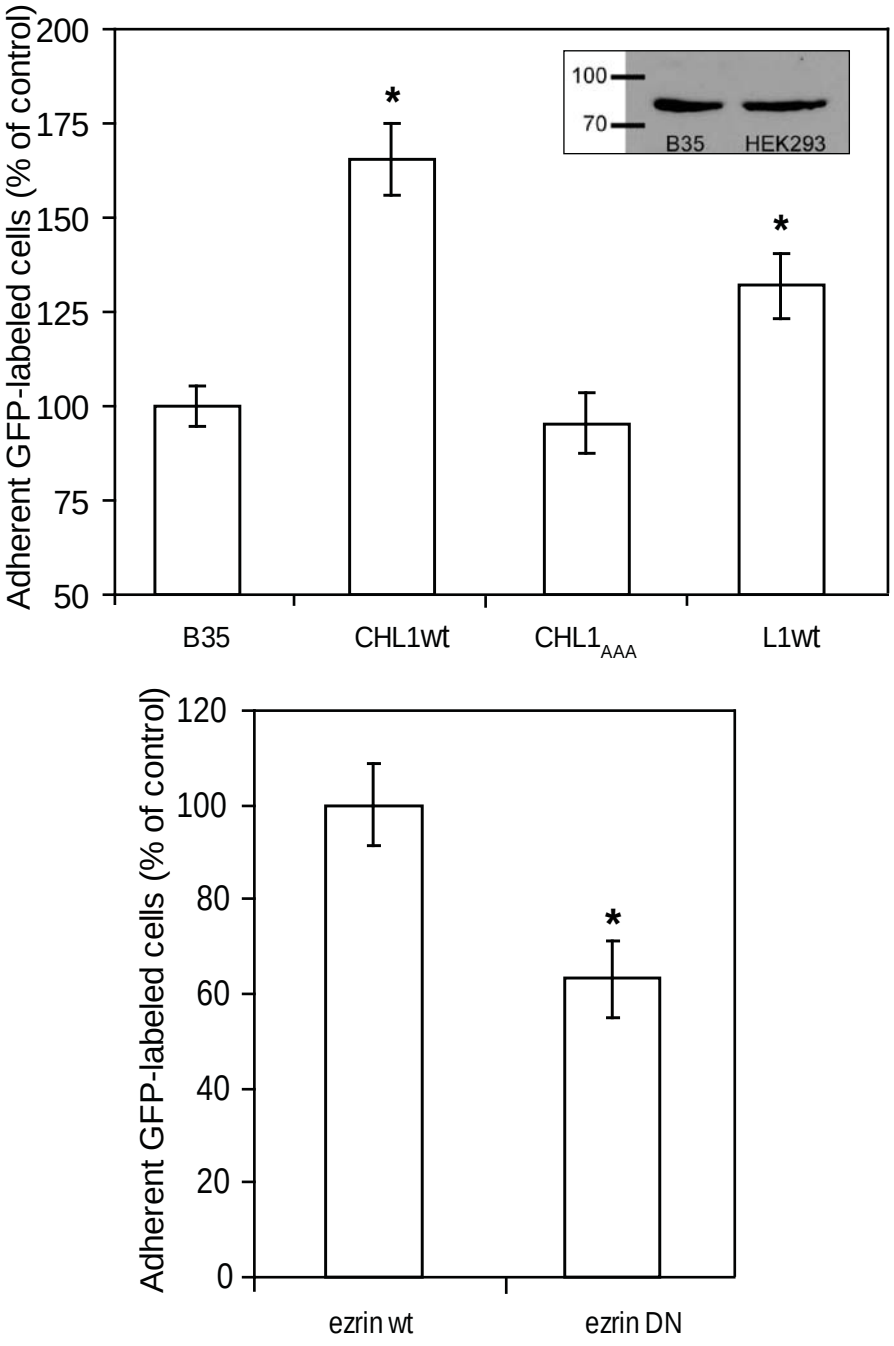
Adherent GFP-labeled cells (% of control)
200
175
150
125
100
75
50
*
*
100
70
B35
HEK293
B35
CHL1wt
CHL1AAA
L1wt
Adherent GFP-labeled cells (% of control)
120
100
80
60
40
20
0
*
ezrin wt
ezrin DN

Figure 4.4: CHL1/ERM Interaction is Essential for Potentiated Haptotactic Migration of HEK293 Cells

Cell migration of transiently transfected HEK293 cells was analyzed using Transwell chambers coated with fibronectin (FN) or BSA as a control after 3 h of incubation. Samples were assayed in triplicate, and the experiments were repeated at least twice with similar results. Statistically significant differences in means of nontransfected cells on BSA, or transfected cells expressing CHL1wt, $CHL1_{AAA}$ or L1wt on fibronectin *versus* nontransfected cells on fibronectin were examined using the *t* test (*, $p < 0.05$).

Figure 4.4

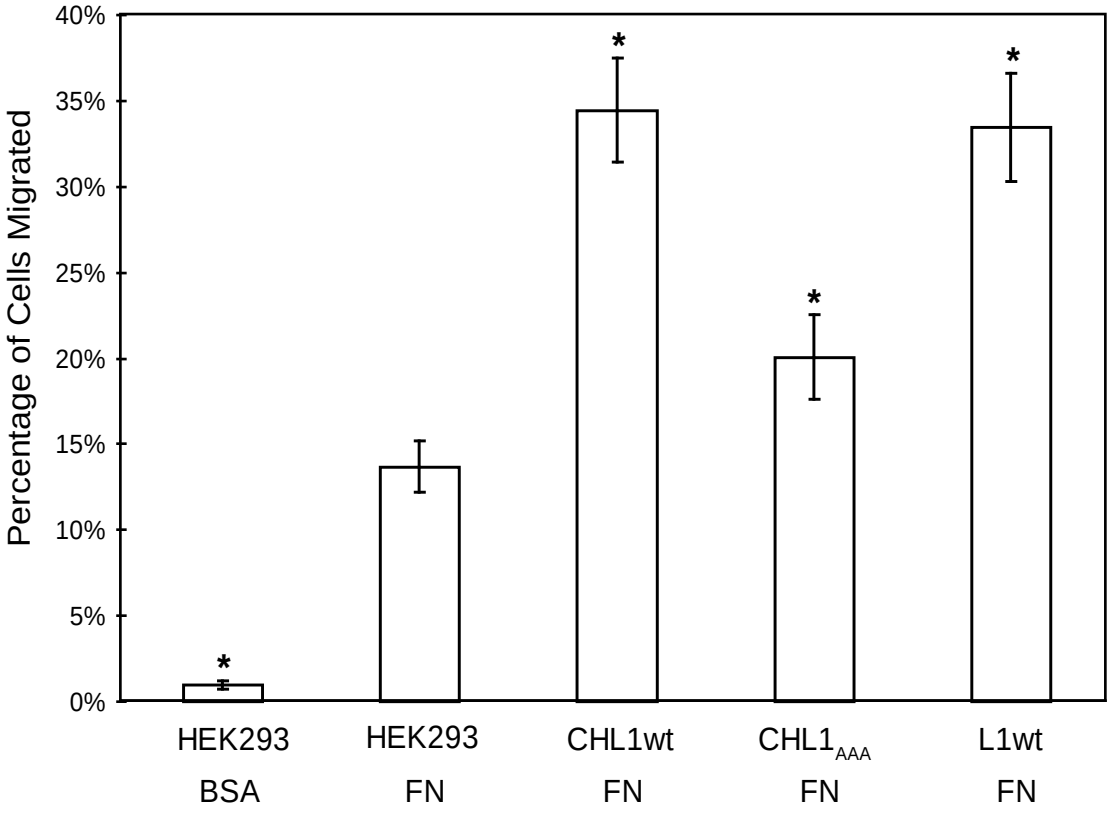
Percentage of Cells Migrated
40%
35%
30%
25%
20%
15%
10%
5%
0%
*
*
*
*
HEK293 BSA
HEK293 FN
CHL1wt FN
CHL1AAA FN
L1wt FN

Figure 4.5: CHL1-Stimulated Neurite Outgrowth and Branching is Dependent on Intracellular ERM Protein Binding

CHL1-minus embryonic cortical neurons (E14.5) were co-transfected with plasmids encoding GFP and pcDNA3 (CHL1-minus), CHL1wt or $CHL1_{AAA}$. After 72 h incubation on a fibronectin substrate, cultures were fixed and GFP-expressing neurons were analyzed.

A. Expression of CHL1 and ERM proteins in CHL1-minus embryonic cortical neurons transfected with CHL1wt or $CHL1_{AAA}$ cDNA after 72 h in culture. Permeabilized neurons were stained with anti-CHL1 antibody/TRITC-conjugated secondary antibody and anti-panERM antibody/Cy5-conjugated secondary antibody, pseudocolored green.

B. Representative DIC images of CHL1-minus embryonic cortical neurons transfected with pcDNA3 ($CHL1^-$), CHL1wt and $CHL1_{AAA}$ after 72 h in culture. CHL1-minus neurons exhibited short neurites and few branches. Expression of CHL1wt in CHL1-minus neurons enhanced neurite outgrowth and branching, while transfection with $CHL1_{AAA}$ did not change morphology of CHL1-minus neurons.

C. Quantification of neurite outgrowth by comparison of longest neurite length and total neurite length. Values were normalized to the mean value of CHL1-minus neurons (65 μm for longest neurite length and 140 μm for total neurite length).

D. Analysis of neurite branching. Branching number represented the total number of branching points exhibited by a neuron. Primary neurites represented the number of branches that extended from the soma. Secondary neurites represented the number of branches that extended from primary neurites. Values were normalized to the mean values of CHL1-minus neurons (Branching number, 3.5; Primary neurites, 2.4; Secondary neurites, 1.1)

For C and D, three independent assays were performed, and shown is a typical experiment with CHL1-minus neurons (n=78) and CHL1-minus neurons transfected with CHL1wt (n=88) or $CHL1_{AAA}$ (n=75). Statistically significant differences in means were compared with CHL1minus neurons using the *t*-test: * ($p<0.05$), ** ($p<0.01$).

Figure 4.5

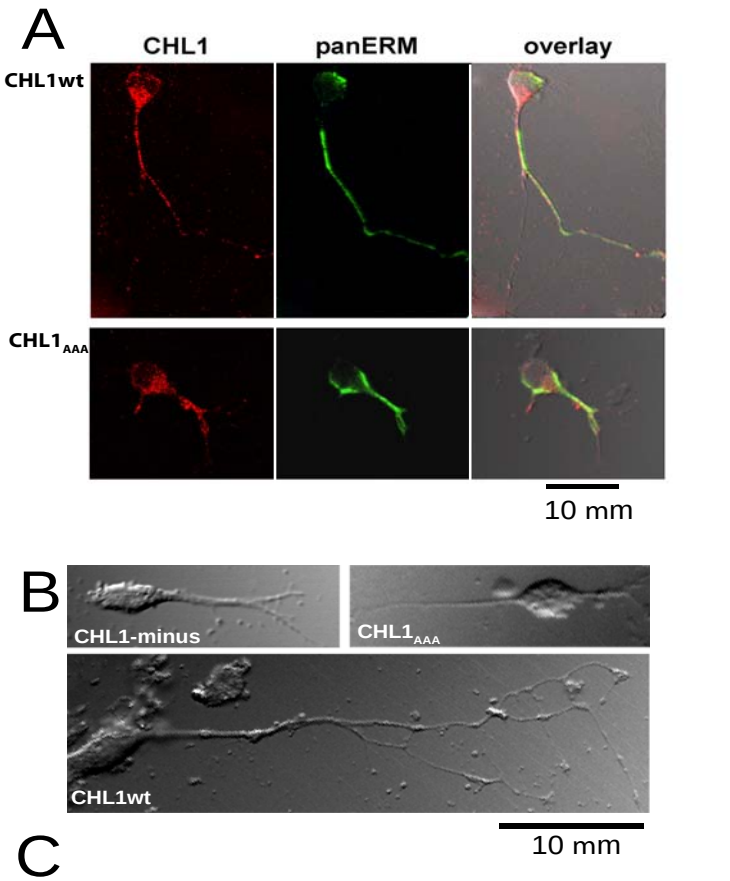
A
CHL1
panERM
overlay
CHL1wt
CHL1AAA
10 mm
B
CHL1-minus
CHL1AAA
CHL1wt
10 mm
C
Neurite Outgrowth (% of control)
180
160
140
120
100
80
60
40
20
0
**
Longest Neurite
Total Neurite Length
CHL1-minus
CHL1wt
CHL1AAA
D
Branching (% of control)
200
180
160
140
120
100
80
60
40
20
0
**
*
**
Branching Number
Primary Neurites
Secondary Neurites
CHL1-minus
CHL1wt
CHL1AAA

Figure 4.6: The ERM Binding Domain of CHL1 is Required for Sema3A-Induced Growth Cone Collapse in Embryonic Cortical Neurons

Dissociated cortical neurons from CHL1-minus embryos (E14.5) were transfected with CHL1wt (a, b), empty vector (CHL1-minus, c, d), or $CHL1_{AAA}$ (e, f) plasmids. After 72 hours, cells were treated with 30nM Fc-AP or Sema3A-AP fusion proteins for 30 minutes. The cultures were fixed and stained with phalloidin to visualize growth cone morphology. The numbers of analyzed growth cones (n) are indicated.

A. Representative examples of growth cones from CHL1-minus, CHL1wt and $CHL1_{AAA}$ neurons. Growth cones expressing CHL1wt (a), empty vector (CHL1-minus, c), or $CHL1_{AAA}$ (e) were not collapsed in response to Fc-AP fusion protein. b) Upon treatment with 30nM Sema3A-AP fusion protein, growth cones of CHL1wt expressing neurons were collapsed. Growth cones of CHL1-minus cortical neurons transfected with empty vector (CHL1-minus, d) or $CHL1_{AAA}$ mutant (f) did not collapse in response to Sema3A-AP fusion protein.

B. Quantitation of percent growth cones collapsed in response to Fc-AP or Sema3A-AP protein treatment. Sema3A significantly (*, $p<0.05$) increased the percentage of collapsed CHL1wt-expressing growth cones compared to Fc-AP. A small, but significant, response to Sema3A remained in CHl1-minus and $CHL1_{AAA}$ neurons compared to Fc-AP control.

Figure 4.6

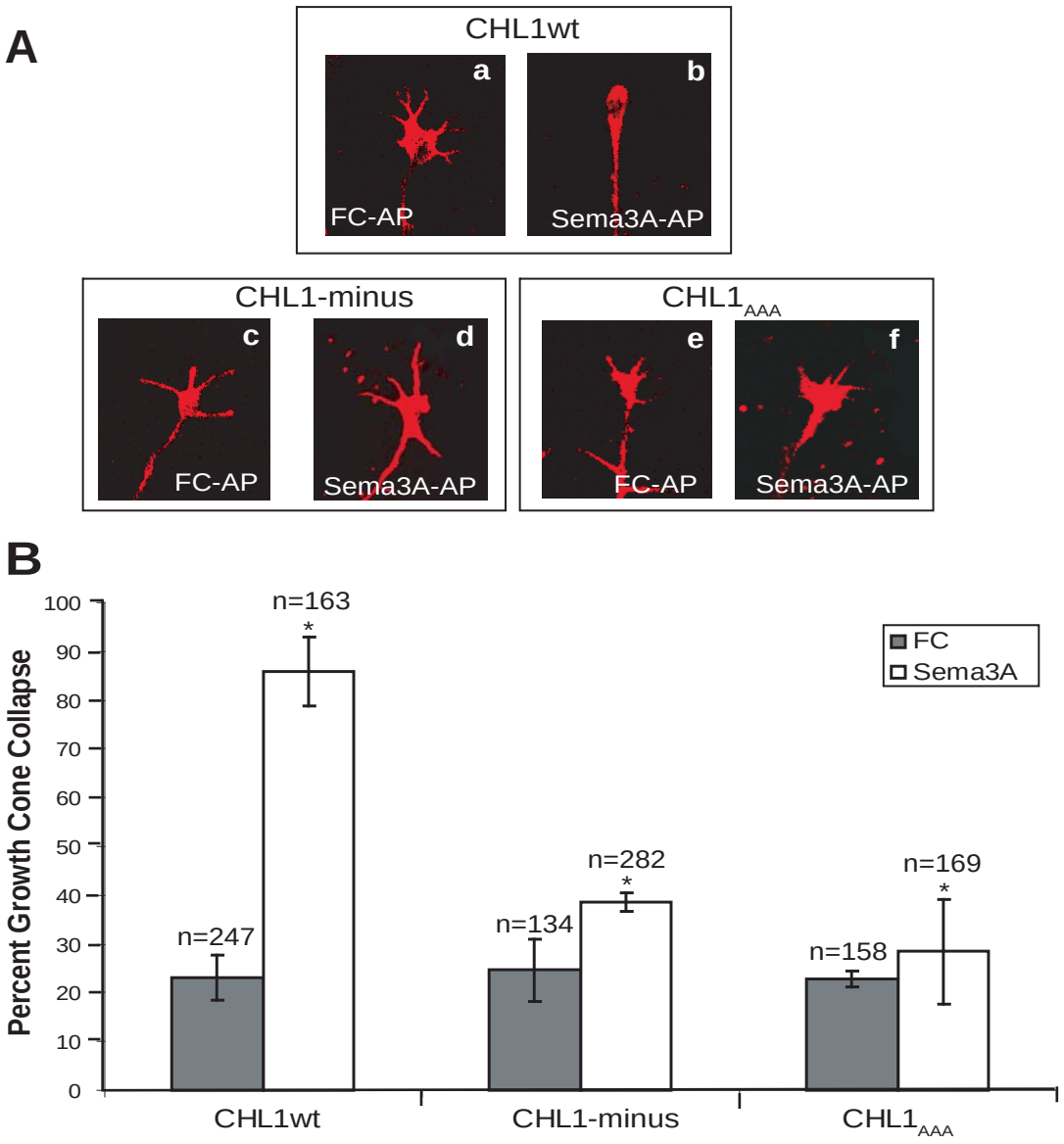
A
CHL1wt
a
b
FC-AP
Sema3A-AP
CHL1-minus
c
d
FC-AP
Sema3A-AP
CHL1AAA
e
f
FC-AP
Sema3A-AP
B
Percent Growth Cone Collapse
100
90
80
70
60
50
40
30
20
10
0
n=163
*
n=247
n=282
*
n=134
n=169
*
n=158
FC
Sema3A
CHL1wt
CHL1-minus
CHL1AAA

Figure 4.7: Semaphorin3A Inhibits CHL1wt-Mediated Neurite Outgrowth and Branching

CHL1-minus embryonic cortical neurons (E14.5) were co-transfected with a plasmid encoding GFP and pcDNA3 (CHL1-minus), CHL1wt or $CHL1_{AAA}$ and plated on fibronectin. After 24 h, cells were treated with 30 nM Sema3A-AP or Fc-AP for 48 h. Cultures were fixed and GFP-expressing neurons were analyzed. In each experiment, the mean values for neurite outgrowth and branching were normalized to the mean value of CHL1-minus neurons. The averages of two independent experiments +/- SEM are shown. 100% values for control CHL1-minus neurons represent 45 µm for longest neurite length, 90 µm for total neurite length and 2.7 for branching number. Numbers of neurons analyzed were for CHL1-minus (Fc), 118; CHL1-minus (Sema3A), 89; for CHL1wt (Fc), 190; CHL1wt (Sema3A), 131; for $CHL1_{AAA}$ (Fc), 174; $CHL1_{AAA}$ (Sema3A),124. Statistically significant differences in means were compared with CHL1-minus or Fc-treated neurons using the t-test, * ($p<0.05$), ** ($p<0.01$).

Figure 4.7

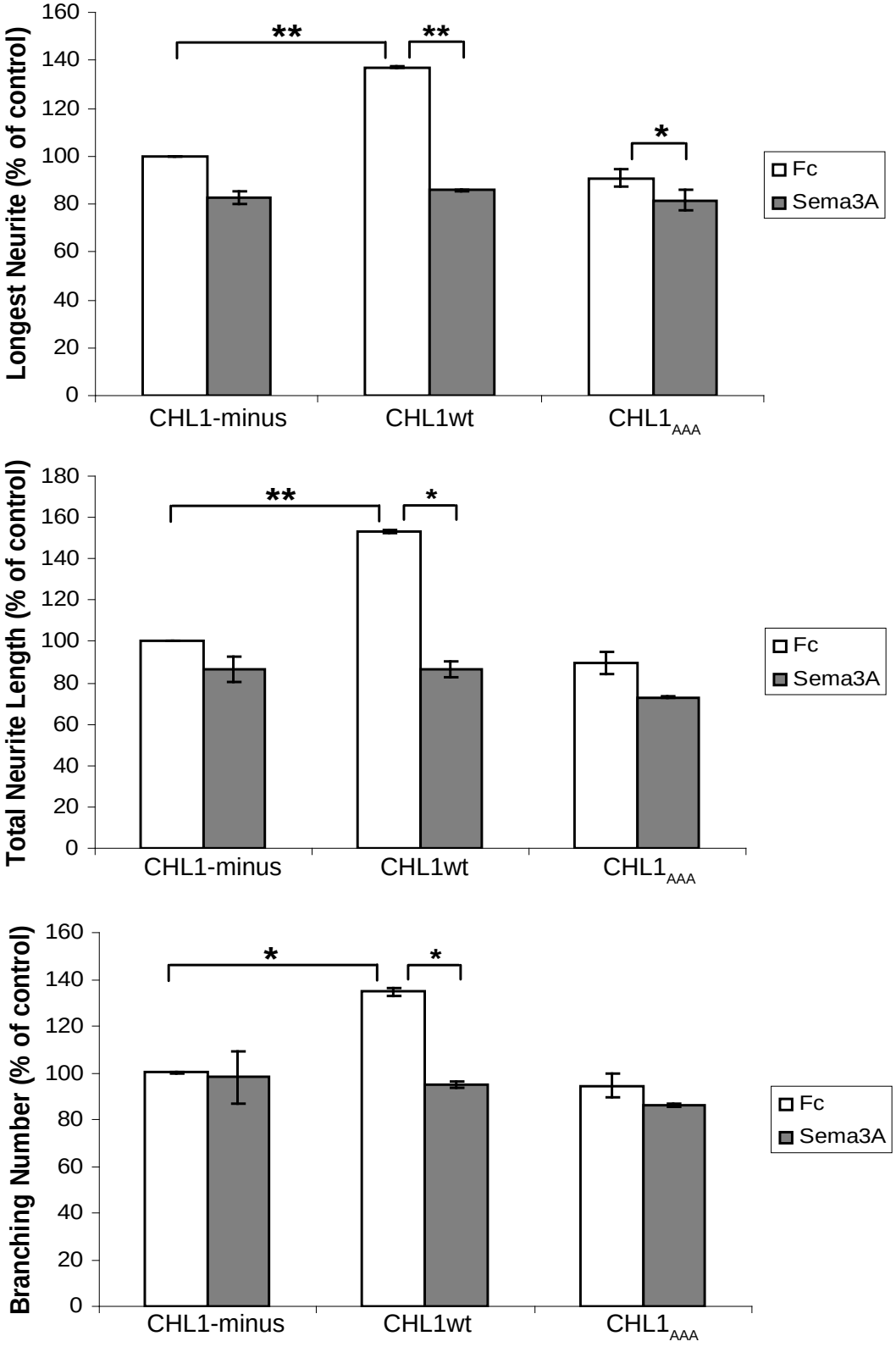
Longest Neurite (% of control)
160
140
120
100
80
60
40
20
0
**
**
*
CHL1-minus
CHL1wt
CHL1AAA
Fc
Sema3A
Total Neurite Length (% of control)
180
160
140
120
100
80
60
40
20
0
**
*
CHL1-minus
CHL1wt
CHL1AAA
Fc
Sema3A
Branching Number (% of control)
160
140
120
100
80
60
40
20
0
*
*
CHL1-minus
CHL1wt
CHL1AAA
Fc
Sema3A

Chapter 5

Close Homolog of L1 is an Enhancer of Integrin-Mediated Cell Migration

Reprinted with Permission from The American Society for Biochemistry and Molecular Biology, Inc.

Buhusi, M., Midkiff, B.R., Gates, A.M., Richter, M., Schachner, M., and Maness, P.F. (2003). Close Homolog of L1 (CHL1) is an enhancer of integrin-mediated cell migration. Journal of Biological Chemistry. **278**, 25024-25031.

This was a collaborative effort. I performed the haptotactic migration assays to demonstrate the signaling intermediates involved in CHL1 enhanced migration and generated figure 5.4.

5.1 Abstract

Close homolog of L1 (CHL1) is a member of the L1 family of cell adhesion molecules expressed by subpopulations of neurons and glia in the central and peripheral nervous system. It promotes neurite outgrowth and neuronal survival *in vitro*. This study describes a novel function for CHL1 in potentiating integrin-dependent cell migration toward extracellular matrix proteins. Expression of CHL1 in HEK293 cells stimulated their haptotactic migration toward collagen I, fibronectin, laminin, and vitronectin substrates in Transwell assays. CHL1-potentiated cell migration to collagen I was dependent on $\alpha_1\beta_1$ and $\alpha_2\beta_1$ integrins, as shown with function blocking antibodies. Potentiated migration relied on the early integrin signaling intermediates, c-Src, phosphatidylinositol 3-kinase, and MAP kinase. Enhancement of migration was disrupted by mutation of a potential integrin interaction motif Asp-Gly-Glu-Ala (DGEA) in the sixth immunoglobulin domain of CHL1, suggesting that CHL1 functionally interacts with β_1 integrins through this domain. CHL1 was shown to associate with β_1 integrins on the cell surface by antibody-induced co-capping. Through a cytoplasmic domain sequence, containing a conserved tyrosine residue (Phe-Ile-Gly-Ala-Tyr), CHL1 recruited the actin cytoskeletal adapter protein ankyrin to the plasma membrane, and this sequence was necessary for promoting integrin-dependent migration to extracellular matrix proteins. These results support a role for CHL1 in integrin-dependent cell migration that may be physiologically important in regulating cell migration in nerve regeneration and cortical development.

5.2 Introduction

In vertebrates, the L1 family of cell adhesion molecules (CAMs) is comprised of four members: L1/NgCAM, close homolog of L1 (CHL1), neurofascin, and NrCAM, all serving multiple functions in the development and function of the nervous system. L1, the prototype of this family of transmembrane glycoproteins, has been shown to participate in cell migration, axon fasciculation, and guidance, as well as synaptogenesis and adult synaptic plasticity (Schmid and Maness, 2001). The importance of L1 function in human brain development is revealed by the association of mutations in the L1 gene with a syndromic form of mental retardation, the L1 syndrome, formerly named CRASH (corpus callosum agenesis, mental retardation, adducted thumbs, spasticity, and hydrocephalus) (Rosenthal et al., 1992; Fransen et al., 1997; Kenwrick et al., 2000). L1 knockout mice display nervous system anomalies similar to those seen in human patients, although there appear to be additional genetic modifiers of the disease (Dahme et al., 1997; Demyanenko et al., 1999; Demyanenko et al., 2001).

L1 family members share a structural plan consisting of an extracellular region comprised of six Ig-like domains, four or five fibronectin type III domains, a single transmembrane segment, and a short, conserved cytoplasmic region (Brummendorf and Lemmon, 2001). The extracellular portion of these proteins is highly glycosylated and allows them to participate in both homophilic and heterophilic interactions with a variety of ligands, including other members of the Ig superfamily. The cytoplasmic domain of L1 family members interacts with components of the actin cytoskeleton (Dickson et al., 2002), protein kinases (Wong et al., 1996b; Wong et al., 1996a;

Kamiguchi and Lemmon, 1997), and complexes associated with endocytosis and protein trafficking in a lipid raft-associated manner (Kamiguchi et al., 1998; Nakai and Kamiguchi, 2002). An important binding partner is ankyrin, a protein that binds to the subcortical actin/spectrin cytoskeleton (Davis and Bennett, 1994; Bennett and Chen, 2001). The interaction of L1 with ankyrin occurs through a conserved FIGQY sequence (Phe-Ile-Gly-Gln-Tyr) within the cytoplasmic domain and is proposed to stabilize axonal membranes and/or intercellular connections (Bennett and Baines, 2001). This idea is supported by the finding that in mice lacking ankyrin B, the axons eventually degenerate (Scotland et al., 1998), although initial axon outgrowth and L1 targeting are relatively normal.

CHL1 is a newly identified member of the L1 family that is expressed in subpopulations of developing neurons in the central and peripheral nervous systems and that persists at low levels in the mature brain in areas of high plasticity (Hillenbrand et al., 1999; Liu et al., 2000). CHL1 is also expressed by Schwann cells, astrocytes, and oligodendrocyte precursors (Holm et al., 1996) and is strikingly up-regulated in Schwann cells and sensory neurons upon nerve crush injury (Zhang et al., 2000). The CALL gene, the human ortholog of the CHL1 gene (Wei et al., 1998), is closely linked to the 3p– syndrome characterized by mental retardation (Angeloni et al., 1999). The human CHL1 gene is mutated in a patient with mental retardation (Frints et al., 2003). An increased risk for schizophrenia associated with a missense polymorphism has also been reported (Sakurai et al., 2002). A recent study (Montag-Sallaz et al., 2002) showed that CHL1-deficient mice display misguided axons within the hippocampus and olfactory tract and anomalies in behavior. These findings

emphasize the importance of CHL1 in the nervous system, although its specific functions are yet unknown.

CHL1 shares the basic structural plan of L1 family members (Holm et al., 1996) and has strong neurite outgrowth promoting capacity (Hillenbrand et al., 1999). The sequence of CHL1 reveals ~60% amino acid identity with L1 in the extracellular region and ~40% identity in the cytoplasmic domain. Yet in contrast to L1, CHL1 has not been shown to self-associate, nor does it bind heterophilically to L1 (Hillenbrand et al., 1999). The extracellular segment of CHL1 contains a potential integrin-binding motif Arg-Gly-Asp (RGD) in the second Ig-like domain, where it may be masked by the predicted horseshoe conformation of the molecule (Freigang et al., 2000; Kunz et al., 2002), rather than within the sixth Ig-like domain as in L1. However, the sixth Ig domain of CHL1 contains another potential integrin interaction motif Asp-Gly-Glu-Ala (DGEA), which has been reported to mediate integrin-collagen interactions in platelets (Staatz et al., 1991). Finally, CHL1 is the only L1 family member with an altered sequence (FIGAY) in the presumed ankyrin-binding domain, and it lacks the RSLE motif, which is characteristic of other family members and is involved in endocytosis.

The structural resemblance and the differences between CHL1 and the other members of the L1 family of CAMs suggest that this molecule might have both similar and distinctive functions within cells. Recently it was shown that L1 promotes integrin-mediated haptotactic migration of cultured cells toward extracellular matrix proteins (Ruppert et al., 1995; Ebeling et al., 1996; Montgomery et al., 1996; Felding-Habermann et al., 1997; Mechtersheimer et al., 2001; Thelen et al., 2002).

Because of potential integrin interaction motifs in CHL1, it was speculated that CHL1 may have a role in integrin-mediated cell migration. Here it is shown that CHL1 promotes haptotactic cell migration toward extracellular matrix proteins, but this function differs from L1 in regard to preference of extracellular matrix substrate and integrin partners. These differences are related to the structural differences between CHL1 and L1 and may be important for differentially regulating cell migration during nerve regeneration and neuronal migration during development.

5.3 Results

CHL1 Potentiates Haptotactic Cell Migration to Extracellular Matrix Proteins Through β_1 Integrins

Extracellular matrix proteins are important in mediating cell migration and neuronal process growth in the developing nervous system (Sobeih and Corfas, 2002) and are implicated in nerve response to injury (Frostick et al., 1998; Previtali et al., 2001). The ability of CHL1 to promote haptotactic migration toward extracellular matrix proteins was studied in Transwell assays in which cells were allowed to migrate from top to bottom chambers through filters coated on the underside with purified matrix molecules (Thelen et al., 2002). The human embryonic kidney cell line, HEK293, was used for these studies, because it expresses defined integrin subunits including α_1, α_2, α_3, α_5, α_v, and β_1, which can serve as extracellular matrix protein receptors (Bodary and McLean, 1990; Simon et al., 1997), and because it does not express detectable levels of cell adhesion molecules of the L1 family

(Needham et al., 2001). HEK293 cells were transfected for transient expression with pcDNA3 plasmids encoding CHL1 or L1, and haptotactic migration was assayed toward purified matrix proteins. Nontransfected HEK293 cells displayed greater migration toward collagen type I, fibronectin, and laminin compared with random migration toward bovine serum albumin but did not migrate significantly toward vitronectin (Fig 5.1). Expression of CHL1 significantly enhanced haptotactic migration toward each of these substrates, as well as to vitronectin (Fig 5.1). In contrast to CHL1, L1 was clearly not capable of enhancing HEK293 cell migration to collagen I, similar to previous findings in rat B35 neuroblastoma cells (Thelen et al., 2002), although L1 was as effective as CHL1 at potentiating cell migration to fibronectin (Fig 5.1). These results showed that CHL1 can promote haptotactic cell migration toward a range of ECM substrates and suggested that CHL1 might functionally interact with integrins.

To determine whether integrins were involved in CHL1-mediated migration, haptotactic migration of HEK293 cells toward collagen I was further evaluated in the presence of function-blocking integrin antibodies. Collagen I was chosen as a substrate, because collagen I, in addition to collagens III and IV, increases at the site of nerve injury and promotes Schwann cell migration (Previtali et al., 2001), and CHL1 is up-regulated in Schwann cells during peripheral nerve regeneration (Hillenbrand et al., 1999; Zhang et al., 2000). Treatment of cells with function-blocking β_1 integrin antibodies (Ni and Wilkins, 1998) strongly inhibited CHL1-mediated HEK293 cell migration toward collagen I, as well as CHL1-independent migration of HEK293 cells (Fig 5.2). Residual migration of CHL1-HEK293 cells in the

presence of anti-β_1 integrin antibodies was low but significantly elevated over that of HEK293 cells ($p < 0.05$), suggesting that CHL1 might function to a small extent through a non-β_1 containing collagen receptor. Because the principal collagen I receptors are known to be $\alpha_1\beta_1$ and $\alpha_2\beta_1$ integrins (van der Flier and Sonnenberg, 2001), function-blocking antibodies against α_1 and α_2 integrins were evaluated next for effects on migration. Antibodies against either α_1 or α_2 integrin strongly inhibited CHL1-mediated migration toward collagen I, whereas α_1 and α_2 integrin antibodies added together were as effective asβ_1 integrin antibodies (Fig 5.2). The α_1 and α_2 integrin antibodies were not as effective as β_1 integrin antibodies in inhibiting the basal migration of HEK293 cells, thus it is likely that these cells use $\alpha_1\beta_1$ and $\alpha_2\beta_1$ integrins in addition to an unidentified β_1 integrin heterodimer for migration to collagen. In summary, these results indicated that CHL1 potentiated the migration of HEK293 cells toward collagen I primarily through $\alpha_1\beta_1$ and $\alpha_2\beta_1$ integrins.

The DGEA Motif in the CHL1 Ig6 Domain Is Required for Potentiating Migration to Collagen I

The mouse CHL1 and human CALL proteins contain a conserved Asp-Gly-Glu-Ala (DGEA) motif in the Ig6 domain of their extracellular regions (Holm et al., 1996; Wei et al., 1998). Interestingly, the DGEA motif is also present in collagen I, where it serves as a recognition site for $\alpha_2\beta_1$ integrin in platelets (Staatz et al., 1991). Mutation of the DGEA sequence in the CHL1 Ig6 domain to Ala-Gly-Glu-Val (AGEV) effectively inhibited CHL1-potentiated migration of HEK293 cells toward collagen I, reducing migration to nearly the level of CHL1-nonexpressing HEK293 cells (Fig

5.3). In the Ig6 domain of L1, an Arg-Gly-Asp (RGD) sequence is required for potentiating migration to fibronectin (Thelen et al., 2002). The Ig2 domain of CHL1 contains an Arg-Gly-Asp (RGD) motif (Holm et al., 1996), and a corresponding sequence (Lys-Gly-Asp) in the human CALL protein is closely conserved, though nonidentical (Wei et al., 1998). This motif might interact with integrins, because RGD is a known adhesion motif that is present in collagen I, fibronectin, and vitronectin, and it is recognized by at least eight integrins (Ruoslahti, 1996). However, mutation of the RGD in the CHL1 Ig2 domain to Lys-Gly-Glu (KGE) did not perturb CHL1-potentiated migration to collagen (Fig 5.3). These results illustrated the importance of the DGEA sequence in the CHL1 Ig6 domain in mediating haptotactic migration toward collagen I through α_1/α_2 β_1 integrins.

CHL1 Enhances Migration through c-Src, PI 3-Kinase, and MAP Kinase

The nonreceptor tyrosine kinase c-Src, PI 3-kinase, and MAP kinase are key signaling intermediates down-stream of cell adhesion molecules such as L1 (Schmid et al., 2000; Juliano, 2002). There is evidence that PI 3-kinase also has a role in integrin receptor recycling (Ng et al., 1999), whereas MAP kinase has well characterized functions in regulating cell migration through regulating new protein synthesis that may be required for synthesis of receptors (Kolch, 2000; Li et al., 2003). It is not known whether CHL1 stimulates signaling pathways, such as those utilized by L1 in potentiating haptotactic migration through integrins. To determine whether Src was required for haptotactic cell migration to collagen I, HEK293 cells and CHL1-HEK293 cells were treated with PP2, a pyrazolopyrimidine inhibitor of Src

family tyrosine kinases. PP2, but not its inactive analog, PP3, is a selective inhibitor of Src family catalytic activity (Hanke et al., 1996). PP2 was a potent inhibitor of CHL1-dependent migration of HEK293 cells to collagen I, whereas PP3 had no effect (Fig 5.4). PP2 also reduced basal migration of nonexpressing HEK293 cells, whereas PP3 did not. To assess the involvement of PI 3-kinase, HEK293 cells and CHL1-HEK293 cells were treated with the PI 3-kinase inhibitor LY294002. LY294002 partially inhibited CHL1-dependent migration of HEK293 cells to collagen, indicating that PI 3-kinase also participated in the CHL1 response (Fig 5.4), but it had no effect on basal migration. To assess the role of MAP kinase in haptotactic migration, the cells were treated with an inhibitor (U0126) of the dual specificity kinase MEK, which normally phosphorylates and activates MAP kinase. The MEK inhibitor selectively suppressed migration of CHL1-expressing cells, indicating that MAP kinase was required for the ability of CHL1 to potentiate haptotactic migration through $\alpha_1/\alpha_2\,\beta_1$ integrins to collagen I (Fig 5.4). Thus, CHL1 appeared to promote integrin-mediated haptotactic migration to collagen I through the signaling intermediates Src and MAP kinase and, to a lesser extent, through PI 3-kinase.

CHL1 Co-caps with β1 Integrins on the Cell Surface

Because these results showed that CHL1 promoted cell migration toward collagen mediated by integrins, we investigated whether CHL1 and β_1 integrins were laterally associated within the plasma membrane on the same cell by co-capping experiments (Wong et al., 2000). Monoclonal antibody MAB2000 specific for β_1 integrins was used to cross-link β_1 integrins on the surface of CHL1-expressing

HEK293 cells. Formation of integrin caps was observed as a cluster of fluorescent spots on the cell surface (Fig 5.5A). CHL1 expression was detected on the same cells by indirect immunofluorescence staining with CHL1 polyclonal antibodies (Fig 5.5B). The overlay image showed CHL1 co-localization within the integrin cap (Fig 5.5C), suggesting that these proteins were associated either directly or indirectly in *cis* within the plasma membrane. CHL1 immunofluorescence staining did not co-localize with all of the β_1 integrin staining, consistent with the interpretation that CHL1 interacted with a subset of β_1 integrins, most likely only the $\alpha_1\beta_1$ and $\alpha_2\beta_1$ subclasses. Integrin caps were formed under these conditions on the majority of cells, and CHL1 co-localized with the integrin caps on all CHL1-expressing cells. In control assays, nonimmune mouse IgG did not induce integrin capping or CHL1 clustering. Interestingly, mutation of the DGEA sequence in the Ig6 domain of CHL1 to AGEV did not perturb its ability to co-cap with β_1 integrins (data not shown), thus indicating that the DGEA motif was neither necessary nor sufficient for the association between CHL1 and β_1 integrins on the cell surface.

The FIGAY Motif in the CHL1 Cytoplasmic Domain Is Required for Ankyrin Recruitment and Potentiating Migration

L1 family members are coupled to the actin cytoskeleton in part through interaction of the intracellular cytoskeletal adapter protein ankyrin with the sequence Phe-Ile-Gly-Gln-Tyr (FIGQY), which is conserved in the cytoplasmic domains of L1, NrCAM, NgCAM, and neurofascin (Davis and Bennett, 1994; Garver et al., 1997) as well as in the single L1 homolog LAD-1 in *Caenorhabditis elegans* (Chen et al.,

2001) and *Drosophila* neuroglian (Hortsch et al., 1998; Hortsch, 2000). Although the structure of CHL1 reveals conservation of most of the functional domains found in other L1 family members (Holm et al., 1996), the cytoplasmic domain of CHL1 bears a nonconservative amino acid substitution in the putative ankyrin interaction motif, resulting in the sequence Phe-Ile-Gly-Ala-Tyr (FIGAY). To examine whether CHL1 was able to bind ankyrin, a cellular ankyrin recruitment assay was carried out as described (Zhang and Bennett, 1998; Needham et al., 2001) using transfected HEK293 cells transiently expressing CHL1 and an ankyrin G fusion protein tagged with green fluorescent protein (ankyrin-GFP). In this assay, the interaction of ankyrin-GFP with CHL1 was detected indirectly through the recruitment of the ankyrin-GFP fluorescent protein from the cytosol to the cell membrane visualized by confocal microscopy. When HEK293 cells were transfected with the ankyrin-GFP plasmid in the absence of CHL1, the fluorescent ankyrin-GFP fusion protein remained cytosolic and was not recruited to the plasma membrane (Fig 5.6A, B), possibly as a result of saturation of binding sites by endogenous ankyrin (Zhang and Bennett, 1998). In contrast, when HEK293 cells were co-transfected with plasmids expressing ankyrin-GFP and CHL1, ankyrin-GFP was redistributed to the plasma membrane, where CHL1 was localized (Fig 5.6C-E). The cells shown in *panels C–H* of (Fig 5.6) were more sparsely plated than those in *panels A* and *B* and were not in contact with other cells throughout most of their cell surfaces. The recruitment of ankyrin to the plasma membrane of HEK293 cells by CHL1 appeared to be independent of cell-cell adhesion, thus differing from L1, which binds ankyrin in a cell contact-dependent manner in *Drosophila* S2 cells (Hortsch et al., 1998). This may be due to differences

in the levels of CHL1 expression or phosphorylation state or to the unique structural features of CHL1. These results showed that CHL1, like the other members of the L1 family, was able to bind ankyrin. No proteins cross-reacting with the anti-mouse CHL1 antibody were detected in this human cell line by Western blot or indirect immunofluorescence analysis (data not shown).

Mutation of the tyrosine residue within the FIGQY motif of the cytoplasmic domain of L1 family members disrupts their ability to recruit ankyrin (Garver et al., 1997; Needham et al., 2001). Mutation of tyrosine 1229 in L1 to histidine occurs in some patients with the L1 mental retardation syndrome (Fransen et al., 1995) and may contribute to the pathogenic mechanism of the disease because of its inability to bind ankyrin (Needham et al., 2001). The tyrosine residue contained within the FIGQY motif of L1 and other family members appears to have a regulatory capability because it undergoes reversible phosphorylation by an unidentified kinase that modulates binding to ankyrin and the microtubule-associated protein doublecortin (Kizhatil et al., 2002). To investigate whether the corresponding residue Tyr^{1186} in the FIGAY sequence of the CHL1 cytoplasmic domain was essential for ankyrin binding, this residue was mutated to alanine, and the resulting CHL1 mutant was evaluated for the ability to recruit ankyrin in the cytofluorescence assay. When co-expressed with ankyrin-GFP, the mutant FIGAA failed to recruit fluorescent ankyrin-GFP to the plasma membrane (Fig 6.5F-H). The CHL1 FIGAA mutant was expressed at a level similar to that of the wild type CHL1 protein and was normally inserted in the plasmalemma of HEK293 cells (Fig 5.6H).

To determine whether ankyrin binding by CHL1 and, in particular, the Tyr^{1186} residue within the FIGAY sequence were important for haptotactic migration to extracellular matrix substrates, wild type CHL1 and the FIGAA mutant were compared for their ability to promote migration of HEK293 cells to collagen I. When the CHL1 FIGAY sequence was mutated to FIGAA, CHL1-potentiated migration was reduced to the level of HEK293 cells not expressing CHL1 (Fig 5.3). Mutation of the CHL1 FIGAY motif to FIGAA did not affect co-capping with β_1 integrins (not shown). These results suggested that CHL1-potentiated cell migration to extracellular matrix proteins may be mediated by physical linkage of its cytoplasmic domain to the actin cytoskeleton through its interaction with ankyrin and that the Tyr^{1186} residue was crucial for this interaction.

5.4 Discussion

This study describes a novel function for CHL1 in potentiating integrin-dependent cell migration toward extracellular matrix proteins. CHL1-potentiated migration of HEK293 cells to collagen I was dependent on $\alpha_1\beta_1$ or $\alpha_2\beta_1$ integrins and was mediated by early integrin signaling intermediates c-Src, PI 3-kinase, and MAP kinase. Co-capping studies demonstrated that CHL1 and β_1 integrins were capable of associating on the cell surface, and a DGEA motif in the Ig6 domain was required for enhancing migration. Through a key tyrosine residue in the FIGAY sequence within the CHL1 cytoplasmic domain, CHL1 was able to recruit ankyrin, an adapter for the spectrin-actin cortical skeleton, suggesting that this capacity was necessary for the promotion of integrin-dependent migration.

Our results describing the functional interaction of CHL1 with β_1 integrins are consistent with a model in which CHL1 associates with β_1 integrins in *cis* on the plasma membrane to promote cell migration on extracellular matrix substrates (Fig 5.7). A direct or indirect association between CHL1 and β_1 integrins is supported by their ability to co-cap on the cell surface upon antibody-induced cross-linking. A potential integrin interaction motif, the DGEA sequence in the Ig6 domain of CHL1, was necessary for potentiating migration to collagen I, but it was not essential for co-capping of CHL1 and β_1 integrin. Other determinants within the CHL1 protein thus may be more important in the association with β_1 integrin, although DGEA or conformational elements of the Ig6 domain may contribute to the interaction. L1 (Felsenfeld et al., 1994; Schmidt et al., 1996; Yip et al., 1998; Silletti et al., 2000; Mechtersheimer et al., 2001; Thelen et al., 2002) and NrCAM (Treubert and Brummendorf, 1998) also cooperate functionally with β_1 integrins, although a physical association has only been reported for L1 (Silletti et al., 2000). Like CHL1, the Ig6 domain in L1 is important for enhancing migration, but in the case of L1, an intrinsic RGD sequence in this domain is the critical motif in promoting migration on fibronectin (Thelen et al., 2002). Although CHL1 contains an RGD domain located in the second Ig domain (Holm et al., 1996), our experiments showed that the mutation of this sequence did not affect the ability of CHL1 to potentiate migration through $\alpha_1\beta_1$ or $\alpha_2\beta_1$ integrins.

CHL1 and L1 are closely related structurally, but they have different effects in regulating haptotactic migration toward extracellular matrix proteins. CHL1 promoted migration of HEK293 cells toward collagen I through the collagen receptors $\alpha_1\beta_1$ and

$\alpha_2\beta_1$ integrins, but L1 did not promote migration to collagen I. Although both cell adhesion molecules stimulated migration to fibronectin, L1-potentiated migration is strongly inhibited by function blocking antibodies against the fibronectin receptor, $\alpha_5\beta_1$ integrin (Thelen et al., 2002), whereas CHL1-potentiated migration to fibronectin was not affected substantially by these antibodies. It is not known whether CHL1 promotes migration toward other matrix substrates such as fibronectin, laminin, or vitronectin through interactions with other integrin subtypes or alternatively through integrin cross-talk (Simon et al., 1997; Blystone et al., 1999; Disatnik and Rando, 1999). An interesting possibility is that different L1 family members may interact with distinct or overlapping subclasses of integrins to potentiate haptotactic migration on diverse extracellular matrix substrates.

CHL1-potentiated migration of HEK293 cells to extracellular matrix proteins depended on c-Src, PI 3-kinase, and MAP kinase. These kinases are components of an early integrin signaling pathway that elicits membrane ruffling and lamellipodia formation and enhances cell migration (Clark et al., 1998; Meng and Lowell, 1998; Miranti et al., 1998). Because L1-potentiated migration also relies on these intermediates (Thelen et al., 2002), they may be sites for integration of signaling by L1 cell adhesion molecules and integrins. Although we do not know whether CHL1 can directly activate these kinases, their catalytic function was necessary for enhancing migration. c-Src may act in this capacity through its ability to down-regulate RhoA GTPase, which has been shown to be necessary for integrin-mediated cell migration (Arthur et al., 2000). Targets of MAP kinase involved in CHL1-stimulated cell migration have not been identified, but a possible candidate is

myosin light chain kinase, which is required for FG carcinoma cell motility on collagen (Klemke et al., 1997). CHL1-stimulated migration also relied in part on the activity of PI 3-kinase, an enzyme that could contribute to cell motility through its ability to influence integrin endocytosis and recycling (Siddhanta et al., 1998; Ng et al., 1999).

The process of cell migration requires dynamic regulation of cell adhesion through coupling of adhesion receptors with the cytoskeleton (Lauffenburger and Horwitz, 1996; Long and Lemmon, 2000). The motif FIGQY in the cytoplasmic domain of all L1 family members, except CHL1, is part of the binding site for ankyrin, a multivalent adapter of the spectrin/actin cortical skeleton (Bennett and Baines, 2001). Although CHL1 possesses a cytoplasmic motif, FIGAY, with a nonconservative substitution, our experiments show that CHL1 recruited ankyrin to the cell membrane and that this motif was essential for potentiated cell migration. This result suggested that ankyrin binding may play a role in the mechanism of cell migration, although other functions of the CHL1 cytoplasmic domain might be perturbed by this mutation, accounting for the abrogation of migration. In any case, ankyrin-binding domains of L1 family members do not have an absolute requirement in regard to sequence specificity. Several studies have shown that the association of L1 family members with ankyrin is regulated by tyrosine phosphorylation of the FIGQY sequence (Garver et al., 1997; Jenkins et al., 2001) and that mutations of the conserved tyrosine perturb the ankyrin-binding function (Zhang and Bennett, 1998; Needham et al., 2001). It is not known whether the tyrosine within the FIGAY sequence of CHL1 is phosphorylated, but its importance is evident from the

perturbation of both ankyrin recruitment and enhancement of haptotactic cell migration toward extracellular matrix proteins when it is mutated to an alanine residue. CHL1 binding to the spectrin-actin skeleton may increase the adhesion between the leading edge of the cell and substrate, which could promote cell migration (Lauffenburger and Horwitz, 1996). Finally, it did not appear that CHL1 required cell-cell contact for ankyrin binding. Although CHL1 is not known to engage in homophilic binding, interaction with the extracellular matrix substrate through *cis* integrin association could provide necessary contact that may regulate ankyrin recruitment.

Taken together these results are consistent with a model (Fig 5.7) in which CHL1 interacts in *cis* with $\alpha_1\beta_1$ and $\alpha_2\beta_1$ integrins on the cell surface to promote intracellular signaling through c-Src, PI 3-kinase, and MAP kinase, which stimulate cell migration on extracellular matrix proteins such as collagen I. The CHL1 Ig6 domain may transiently interact with a binding site on β_1 integrins to stimulate cell signaling, but it is not sufficient for the interaction. Linkage of CHL1 to the actin cytoskeleton through ankyrin binding to the FIGAY sequence is also an important determinant of cell motility and may help stabilize adhesive contacts with the extracellular matrix substrate.

The capacity of CHL1 to potentiate haptotactic migration toward extracellular matrix proteins through integrins in these *in vitro* studies may reflect a physiological role for CHL1 in integrin-dependent cell migration during nerve regeneration. CHL1 may regulate the migration of Schwann cells at sites of nerve injury, because it is strongly up-regulated in Schwann cells during regeneration (Zhang et al., 2000).

Schwann cell migration on regenerating nerves is supported by collagens I, III, IV, and fibronectin, which, along with $\alpha_1\beta_1$ integrin, increase at the injury site (Lefcort et al., 1992; Siironen et al., 1992; Previtali et al., 2001). CHL1 expression is also up-regulated in dorsal root ganglion and thalamic neurons upon injury (Chaisuksunt et al., 2000; Zhang et al., 2000) and is a strong promoter of neurite growth (Hillenbrand et al., 1999), suggesting that it may function analogously to promote axon growth on extracellular matrix substrates. The ability of CHL1 to promote cell migration toward extracellular matrix proteins may also play a role in radial glia-guided migration of cortical neurons in the developing neocortex, where integrin receptors and their ligands are distributed (Schmid and Anton, 2003) and CHL1 is prominently expressed (Liu et al., 2000).

5.5 Methods

Plasmids and Reagents

The following cDNAs were subcloned into pcDNA3 (Stratagene, La Jolla, CA): wild type mouse CHL1, a CHL1 mutant in which the RGD sequence in the Ig2 domain was mutated to KGE, a CHL1 mutant in which the DGEA sequence in the Ig6 domain was mutated to AGEV, a CHL1 mutant in which the cytoplasmic sequence FIGAY was mutated to FIGAA, and human wild type L1 (+RSLE) (from J. Hemperly, BD Technologies, Research Triangle Park, NC). A plasmid encoding ankyrin G fused to green fluorescent protein (ankyrin-GFP) was provided by Vann Bennett (Duke University, Durham, NC). A rabbit polyclonal antibody was made against mouse CHL1-Fc (Holm et al., 1996). Mouse monoclonal antibody Neuro4

against an extracellular epitope of human L1 was a gift of J. Hemperly. The following antibodies were obtained from Chemicon (Temecula, CA): anti-human β_1 integrin monoclonal antibody 2253Z (clone 6s6), an activating monoclonal antibody MAB2000 (clone HB1.1) against human β_1 integrin, anti-human α_1 integrin monoclonal antibody 1973Z (clone FB12), and anti-human α_2 integrin monoclonal antibody 1950Z (clone P1E6). Nonimmune mouse IgG was from Jackson ImmunoResearch Laboratories (West Grove, PA). Human vitronectin, human fibronectin, and murine laminin were from Invitrogen and Peninsula Laboratories (San Carlos, CA). BD Biosciences (Palo Alto, CA) provided type I collagen from rat tail. MEK inhibitor U0126 (Promega, Madison, WI), Src inhibitor PP2 and inactive analog PP3, and PI 3-kinase inhibitor Ly294002 (CalBiochem, San Diego, CA) were dissolved in Me_2SO.

Cell Culture and Haptotactic Migration Assay

HEK293 cell cultures were maintained in Dulbecco's modified Eagle's medium (DMEM) (Mediatech Cellgro), 4.5 mg/ml glucose, 10% heat-inactivated fetal bovine serum, 50 μg/ml gentamicin, and 250 μg/ml kanamycin. Cultures at 80–90% confluence in 60-mm dishes were transfected for transient expression of CHL1 or L1 pcDNA3 plasmids (5 μg) using LipofectAMINE 2000 (Invitrogen) in Opti-MEM I (Invitrogen). After 18–24 h at 37°C, the transfected cells were used for haptotactic migration or ankyrin recruitment assays.

Haptotactic migration of HEK293 cells transiently expressing CHL1 or L1 was assayed as previously reported (Thelen et al., 2002), using modified Boyden chambers with 8-μm pore filters (Transwells 3422, Corning/Costar, Acton, MA) in

serum-free medium (DMEM, 0.4 mM $MnCl_2$, 50 μg/ml gentamicin, 250 μg/ml kanamycin). In the absence of Mn^{2+}, CHL1 potentiated haptotactic migration of HEK293 cells toward collagen I (1.9-fold) to nearly the same extent as in the presence of Mn^{2+} (2.3-fold). The bottom sides of the filters were precoated with extracellular matrix proteins (500 μl of 20 μg/ml) or 2% bovine serum albumin in PBS at 4°C overnight and blocked in 2% bovine serum albumin. The cells were detached with 5 mM Na-EDTA in Hanks' balanced saline solution (HBSS) and plated at 20,000 cells/Transwell. In some experiments, the cells were preincubated in serum-free medium with anti-integrin antibodies (1–4 μg/ml) for 15–30 min at 4°C prior to plating. The cells were allowed to migrate for 3–8h at 37°C in a CO_2 incubator. After migration cultures were fixed in 4% paraformaldehyde, rinsed in PBS, and then treated with blocking solution (10% goat serum, 0.2% fish skin gelatin, PBS) for either 1 h at room temperature or overnight at 4°C.

To score migration, cells from the upper or lower sides of filters were removed, and cells on the opposite side were stained by indirect immunofluorescence with purified CHL1 polyclonal antibodies (20 μg/ml) or L1 monoclonal antibody Neuro4 (5 μg/ml) in blocking solution for 4 h at room temperature, followed by fluorescein isothiocyanate-conjugated secondary antibodies (Jackson ImmunoResearch Laboratories) diluted 1:75 to 1:100 in blocking solution. The cells were counterstained with 10 μM bis-benzimide (Hoechst 33258; Molecular Probes, Eugene, OR). The filters were mounted with Vectashield (Vector Laboratories, Burlingame, CA) on glass slides, and the cells were scored on both top and bottom surfaces of filters under epifluorescence illumination. For each filter, at

least 150 cells were scored from six or more randomly selected fields using a 20x objective. To obtain the total number of cells on each side of a filter, the mean number of cells/field was determined and multiplied by a factor based on the number and size of fields and a filter diameter of 6.5 mm. The percentage of CHL1-immunoreactive cells that transmigrated was calculated as the ratio of CHL1-positive cells on the bottom of filters to total (top and bottom) CHL1-positive cells. The percentage of CHL1-negative bis-benzimide-positive cells that transmigrated was determined similarly. The percentage of cells transmigrated was converted to the total number of cells migrated per Transwell by multiplying the percentage by the number of cells plated. The experiments were performed in duplicate or triplicate, and the results of each condition were averaged. The means and standard errors were determined for each condition. Significant differences between experimental groups were evaluated by Student's *t* test ($p < 0.05$, one-tailed). Transfection efficiency of HEK293 cells was determined as the number of fluorescein isothiocyanate-labeled cells (transfected) divided by the number of bis-benzimide-labeled cells (transfected plus nontransfected) and was 50–70%. There was no deleterious effect of integrin antibodies or inhibitors on cell adhesion, which was evaluated by counting the total number of cells recovered after each assay. Similarly, inhibitors used at concentrations indicated in the signaling experiments (PP2, PP3, Ly294002, and U0126) did not affect the viability or cell recovery.

Co-capping Experiments

HEK293 cells transfected with the pcDNA3-CHL1 plasmid were dissociated in 5 mM EDTA in HBSS, washed with 10% fetal bovine serum in DMEM, and

resuspended in DMEM. The cells (30,000 cells/100 µl) were incubated with anti-integrin β_1 mouse monoclonal antibody MAB2000 (20 µg/ml) at 4°C for 20 min. The cells were washed with ice-cold HBSS, resuspended in DMEM containing 5 µg/ml goat anti-mouse IgG (Fc fragment-specific), and incubated for 20 min at 4°C. After washing in ice-cold HBSS, the cells were resuspended in 10% fetal bovine serum in DMEM, plated onto collagen-coated MatTek plates (MatTek Corp., Ashland, MA), and incubated for 1h at 37°C to allow integrins to cluster. The cells were then fixed in 4% paraformaldehyde in PBS for 15 min, washed, and blocked with 10% donkey serum in PBS for 1 h at room temperature. To label CHL1, the cells were incubated with CHL1 rabbit polyclonal antibody (20 µg/ml in blocking buffer) for 2 h at room temperature, washed with PBS, and then incubated for 1 h at room temperature with fluorescein isothiocyanate-conjugated donkey anti-rabbit IgG and TRITC-conjugated donkey anti-goat IgG diluted 1:100 in blocking buffer. Finally, the cells were rinsed, mounted in Vectashield, and examined using an Olympus FV500 laser confocal microscope at the Microscopy Service Laboratory (Dr. Robert Bagnell, Department of Pathology, University of North Carolina-Chapel Hill) using appropriate filter sets.

Assay for Ankyrin Recruitment

Ankyrin recruitment to CHL1 in the plasma membrane was assayed as previously described for L1 (Needham et al., 2001) with the following modifications. HEK293 cells on poly-D-lysine-coated MatTek dishes were transfected with plasmid pEGFP-N1 expressing a fusion protein between ankyrin G and green fluorescent protein (ankyrin-GFP) (0.05 µg) with or without co-transfection of pcDNA3-CHL1 (0.1 µg) using LipofectAMINE 2000. After 24 h, the cells were fixed with 4%

paraformaldehyde in 0.1M phosphate buffer, pH 7.4, for 15 min, washed, and incubated with blocking buffer (10% normal goat serum in PBS) for 30 min. To label CHL1 on the cell surface, the cells were incubated for 4 h at room temperature with rabbit polyclonal antibody against CHL1 (20 μg/ml in blocking buffer), then washed, and incubated for 2 h with TRITC-conjugated goat anti-rabbit IgG diluted 1:200 in blocking buffer. The cells were washed and mounted in Vectashield. GFP/immunofluorescence images were recorded on an Olympus FV500 laser confocal microscope. The ankyrin-GFP fluorescence was recorded using the 488-nm excitation line of the laser, whereas the TRITC-labeled CHL1 was examined using the 543-nm excitation line of the laser and the appropriate band pass filters. Each experiment was repeated four times.

5.6 References

Angeloni, D., Lindor, N. M., Pack, S., Latif, F., Wei, M. H., and Lerman, M. I. (1999). CALL gene is haploinsufficient in a 3p- syndrome patient. Am J Med Genet *86*, 482-485.

Arthur, W. T., Petch, L. A., and Burridge, K. (2000). Integrin engagement suppresses RhoA activity via a c-Src-dependent mechanism. Curr Biol *10*, 719-722.

Bennett, V., and Baines, A. J. (2001). Spectrin and ankyrin-based pathways: metazoan inventions for integrating cells into tissues. Physiol Rev *81*, 1353-1392.

Bennett, V., and Chen, L. (2001). Ankyrins and cellular targeting of diverse membrane proteins to physiological sites. Curr Opin Cell Biol *13*, 61-67.

Blystone, S. D., Slater, S. E., Williams, M. P., Crow, M. T., and Brown, E. J. (1999). A molecular mechanism of integrin crosstalk: alphavbeta3 suppression of calcium/calmodulin-dependent protein kinase II regulates alpha5beta1 function. J Cell Biol *145*, 889-897.

Bodary, S. C., and McLean, J. W. (1990). The integrin beta 1 subunit associates with the vitronectin receptor alpha v subunit to form a novel vitronectin receptor in a human embryonic kidney cell line. J Biol Chem *265*, 5938-5941.

Brummendorf, T., and Lemmon, V. (2001). Immunoglobulin superfamily receptors: cis-interactions, intracellular adapters and alternative splicing regulate adhesion. Curr Opin Cell Biol *13*, 611-618.

Chaisuksunt, V., Campbell, G., Zhang, Y., Schachner, M., Lieberman, A. R., and Anderson, P. N. (2000). The cell recognition molecule CHL1 is strongly upregulated by injured and regenerating thalamic neurons. J Comp Neurol *425*, 382-392.

Chen, L., Ong, B., and Bennett, V. (2001). LAD-1, the Caenorhabditis elegans L1CAM homologue, participates in embryonic and gonadal morphogenesis and is a substrate for fibroblast growth factor receptor pathway-dependent phosphotyrosine-based signaling. J Cell Biol *154*, 841-855.

Clark, E. A., King, W. G., Brugge, J. S., Symons, M., and Hynes, R. O. (1998). Integrin-mediated signals regulated by members of the rho family of GTPases. J Cell Biol *142*, 573-586.

Dahme, M., Bartsch, U., Martini, R., Anliker, B., Schachner, M., and Mantei, N. (1997). Disruption of the mouse L1 gene leads to malformations of the nervous system. Nature Genetics *17*, 346-349.

Davis, J. Q., and Bennett, V. (1994). Ankyrin binding activity shared by the neurofascin/L1/NrCAM family of cell adhesion molecules. J Biol Chem *269*, 27163-27166.

Demyanenko, G., Tsai, A., and Maness, P. F. (1999). Abnormalities in neuronal process extension, hippocampal development, and the ventricular system of L1 knockout mice. J Neurosci *19*, 4907-4920.

Demyanenko, G. P., Shibata, Y., and Maness, P. F. (2001). Altered distribution of dopaminergic neurons in the brain of L1 null mice. Brain Res Dev Brain Res *126*, 21-30.

Dickson, T. C., Mintz, C. D., Benson, D. L., and Salton, S. R. (2002). Functional binding interaction identified between the axonal CAM L1 and members of the ERM family. J Cell Biol *157*, 1105-1112.

Disatnik, M. H., and Rando, T. A. (1999). Integrin-mediated muscle cell spreading. The role of protein kinase c in outside-in and inside-out signaling and evidence of integrin cross- talk. J Biol Chem *274*, 32486-32492.

Ebeling, O., Duczmal, A., Aigner, S., Geiger, C., Schollhammer, S., Kemshead, J. T., Moller, P., Schwartz-Albiez, R., and Altevogt, P. (1996). L1 adhesion molecule on human lymphocytes and monocytes: expression and involvement in binding to alpha v beta 3 integrin. Eur J Immunol *26*, 2508-2516.

Felding-Habermann, B., Silletti, S., Mei, F., Siu, C. H., Yip, P. M., Brooks, P. C., Cheresh, D. A., O'Toole, T. E., Ginsberg, M. H., and Montgomery, A. M. (1997). A single immunoglobulin-like domain of the human neural cell adhesion molecule L1 supports adhesion by multiple vascular and platelet integrins. J Cell Biol *139*, 1567-1581.

Felsenfeld, D. P., Hynes, M. A., Skoler, K. M., Furley, A. J., and Jessell, T. M. (1994). TAG-1 can mediate homophilic binding, but neurite outgrowth on TAG-1 requires an L1-like molecule and beta 1 integrins. Neuron *12*, 675-690.

Fransen, E., Lemmon, V., Van Camp, G., Vits, L., Coucke, P., and Willems, P. J. (1995). CRASH syndrome: Clinical spectrum of corpus callosum hypoplasia, retardation, adducted thumbs, spastic paralysis and hydrocephalus due to mutation in one single gene, L1. Eur J Hum Genet *3*, 273-284.

Fransen, E., VanCamp, G., Vits, L., and Willems, P. J. (1997). L1-associated diseases: Clinical geneticists divide, molecular geneticists unite. Hum Mol Genet *6*, 1625-1632.

Freigang, J., Proba, K., Leder, L., Diederichs, K., Sonderegger, P., and Welte, W. (2000). The crystal structure of the ligand binding module of axonin-1/TAG-1 suggests a zipper mechanism for neural cell adhesion. Cell *101*, 425-433.

Frints, S. G. M., Marynen, P., Hartmann, D., Fryns, J. P., Steyaert, J., Schachner, M., Rolf, B., Craessaerts, K., Snellinx, A., Hollanders, K.*, et al.* (2003). CALL interrupted in a patient with nonspecific mental retardation: gene dosage-dependent alteration of murine brain development and behavior. Hum Mol Genet *12*, 1463-1474.

Frostick, S. P., Yin, Q., and Kemp, G. J. (1998). Schwann cells, neurotrophic factors, and peripheral nerve regeneration. Microsurgery *18*, 397-405.

Garver, T. D., Ren, Q., Tuvia, S., and Bennett, V. (1997). Tyrosine phosphorylation at a site highly conserved in the L1 family of cell adhesion molecules abolishes ankyrin binding and increases lateral mobility of neurofascin. J Cell Biol *137*, 703-714.

Hanke, J. H., Gardner, J. P., Dow, R. L., Changelian, P. S., Brissette, W. H., Weringer, E. J., Pollok, B. A., and Connelly, P. A. (1996). Discovery of a novel, potent, and Src family-selective tyrosine kinase inhibitor. Study of Lck- and FynT-dependent T cell activation. J Biol Chem *271*, 695-701.

Hillenbrand, R., Molthagen, M., Montag, D., and Schachner, M. (1999). The close homologue of the neural adhesion molecule L1 (CHL1): patterns of expression and promotion of neurite outgrowth by heterophilic interactions. Eur J Neurosci *11*, 813-826.

Holm, J., Hillenbrand, R., Steuber, V., Bartsch, U., Moos, M., Lubbert, H., Montag, D., and Schachner, M. (1996). Structural features of a close homologue of L1 (CHL1) in the mouse: a new member of the L1 family of neural recognition molecules. Eur J Neurosci *8*, 1613-1629.

Hortsch, M. (2000). Structural and functional evolution of the L1 family: are four adhesion molecules better than one? Mol Cell Neurosci *15*, 1-10.

Hortsch, M., Homer, D., Malhotra, J. D., Chang, S., Frankel, J., Jefford, G., and Dubreuil, R. R. (1998). Structural requirements for outside-in and inside-out signaling by Drosophila neuroglian, a member of the L1 family of cell adhesion molecules. J Cell Biol *142*, 251-261.

Jenkins, S. M., Kizhatil, K., Kramarcy, N. R., Sen, A., Sealock, R., and Bennett, V. (2001). FIGQY phosphorylation defines discrete populations of L1 cell adhesion molecules at sites of cell-cell contact and in migrating neurons. J Cell Sci *114*, 3823-3835.

Juliano, R. L. (2002). Signal transduction by cell adhesion receptors and the cytoskeleton: functions of integrins, cadherins, selectins, and immunoglobulin-superfamily members. Annu Rev Pharmacol Toxicol *42*, 283-323.

Kamiguchi, H., and Lemmon, V. (1997). Neural cell adhesion molecule L1: signaling pathways and growth cone motility. J Neurosci Res *49*, 1-8.

Kamiguchi, H., Long, K. E., Pendergast, M., Schaefer, A. W., Rapoport, I., Kirchhausen, T., and Lemmon, V. (1998). The neural cell adhesion molecule L1 interacts with the AP-2 adaptor and is endocytosed via the clathrin-mediated pathway. J Neurosci *18*, 5311-5321.

Kenwrick, S., Watkins, A., and Angelis, E. D. (2000). Neural cell recognition molecule L1: relating biological complexity to human disease mutations. Hum Mol Genet *9*, 879-886.

Kizhatil, K., Wu, Y. X., Sen, A., and Bennett, V. (2002). A new activity of doublecortin in recognition of the phospho-FIGQY tyrosine in the cytoplasmic domain of neurofascin. J Neurosci *22*, 7948-7958.

Klemke, R. L., Cai, S., Giannini, A. L., Gallagher, P. J., de Lanerolle, P., and Cheresh, D. A. (1997). Regulation of cell motility by mitogen-activated protein kinase. J Cell Biol *137*, 481-492.

Kolch, W. (2000). Meaningful relationships: the regulation of the Ras/Raf/MEK/ERK pathway by protein interactions. Biochem J *351 Pt 2*, 289-305.

Kunz, B., Lierheimer, R., Rader, C., Spirig, M., Ziegler, U., and Sonderegger, P. (2002). Axonin-1/TAG-1 mediates cell-cell adhesion by a cis-assisted trans-interaction. J Biol Chem *277*, 4551-4557.

Lauffenburger, D. A., and Horwitz, A. F. (1996). Cell migration: a physically integrated molecular process. Cell *84*, 359-369.

Lefcort, F., Venstrom, K., McDonald, J. A., and Reichardt, L. F. (1992). Regulation of expression of fibronectin and its receptor, alpha 5 beta 1, during development and regeneration of peripheral nerve. Development *116*, 767-782.

Li, Q. J., Yang, S. H., Maeda, Y., Sladek, F. M., Sharrocks, A. D., and Martins-Green, M. (2003). MAP kinase phosphorylation-dependent activation of Elk-1 leads to activation of the co-activator p300. EMBO J *22*, 281-291.

Liu, Q., Dwyer, N. D., and O'Leary, D. D. (2000). Differential expression of COUP-TFI, CHL1, and two novel genes in developing neocortex identified by differential display PCR. J Neurosci *20*, 7682-7690.

Long, K. E., and Lemmon, V. (2000). Dynamic regulation of cell adhesion molecules during axon outgrowth. J Neurobiol *44*, 230-245.

Mechtersheimer, S., Gutwein, P., Agmon-Levin, N., Stoeck, A., Oleszewski, M., Riedle, S., Fogel, M., Lemmon, V., and Altevogt, P. (2001). Ectodomain shedding of L1 adhesion molecule promotes cell migration by autocrine binding to integrins. J Cell Biol *155*, 661-673.

Meng, F., and Lowell, C. A. (1998). A beta 1 integrin signaling pathway involving Src-family kinases, Cbl and PI-3 kinase is required for macrophage spreading and migration. EMBO J *17*, 4391-4403.

Miranti, C. K., Leng, L., Maschberger, P., Brugge, J. S., and Shattil, S. J. (1998). Identification of a novel integrin signaling pathway involving the kinase Syk and the guanine nucleotide exchange factor Vav1. Curr Biol *8*, 1289-1299.

Montag-Sallaz, M., Schachner, M., and Montag, D. (2002). Misguided axonal projections, neural cell adhesion molecule 180 mRNA upregulation, and altered behavior in mice deficient for the close homolog of L1. Mol Cell Biol *22*, 7967-7981.

Montgomery, A. M., Becker, J. C., Siu, C. H., Lemmon, V. P., Cheresh, D. A., Pancook, J. D., Zhao, X., and Reisfeld, R. A. (1996). Human neural cell adhesion molecule L1 and rat homologue NILE are ligands for integrin alpha v beta 3. J Cell Biol *132*, 475-485.

Nakai, Y., and Kamiguchi, H. (2002). Migration of nerve growth cones requires detergent-resistant membranes in a spatially defined and substrate-dependent manner. J Cell Biol *159*, 1097-1108.

Needham, L. K., Thelen, K., and Maness, P. F. (2001). Cytoplasmic domain mutations of the L1 cell adhesion molecule reduce L1- ankyrin interactions. J Neurosci *21*, 1490-1500.

Ng, T., Shima, D., Squire, A., Bastiaens, P. I., Gschmeissner, S., Humphries, M. J., and Parker, P. J. (1999). PKCalpha regulates beta1 integrin-dependent cell motility through association and control of integrin traffic. EMBO J *18*, 3909-3923.

Ni, H., and Wilkins, J. A. (1998). Localisation of a novel adhesion blocking epitope on the human beta 1 integrin chain. Cell Adhes Commun *5*, 257-271.

Previtali, S. C., Feltri, M. L., Archelos, J. J., Quattrini, A., Wrabetz, L., and Hartung, H. (2001). Role of integrins in the peripheral nervous system. Prog Neurobiol *64*, 35-49.

Rosenthal, A., Jouet, M., and Kenwrick, S. (1992). Aberrant splicing of neural cell adhesion molecule L1 mRNA in a family with X-linked hydrocephalus. Nat Genet *2*, 107-112.

Ruoslahti, E. (1996). RGD and other recognition sequences for integrins. Annu Rev Cell Dev Biol *12*, 697-715.

Ruppert, M., Aigner, S., Hubbe, M., Yagita, H., and Altevogt, P. (1995). The L1 adhesion molecule is a cellular ligand for VLA-5. J Cell Biol *131*, 1881-1891.

Sakurai, K., Migita, O., Toru, M., and Arinami, T. (2002). An association between a missense polymorphism in the close homologue of L1 (CHL1, CALL) gene and schizophrenia. Mol Psychiatry *7*, 412-415.

Schmid, R. S., and Anton, E. S. (2003). Role of integrins in the development of the cerebral cortex. Cereb Cortex *13*, 219-224.

Schmid, R. S., and Maness, P. F. (2001). Cell Recognition Molecules and Disorders of Neurodevelopment. In Int. Handbook on Brain and Behaviour in Human Development, A. F. Kalverboer, and A. Gramsbergen, eds. (Groningen, The Netherlands, Kluwer Academic Publishers).

Schmid, R. S., Pruitt, W. M., and Maness, P. F. (2000). A MAP kinase signaling pathway mediates neurite outgrowth on L1 and requires Src-dependent endocytosis. J Neurosci *11*, 4177-4188.

Schmidt, C., Kunemund, V., Wintergerst, E. S., Schmitz, B., and Schachner, M. (1996). CD9 of mouse brain is implicated in neurite outgrowth and cell migration in vitro and is associated with the alpha 6/beta 1 integrin and the neural adhesion molecule L1. J Neurosci Res *43*, 12-31.

Scotland, P., Zhou, D., Benveniste, H., and Bennett, V. (1998). Nervous system defects of AnkyrinB (-/-) mice suggest functional overlap between the cell adhesion molecule L1 and 440-kD AnkyrinB in premyelinated axons. J Cell Biol *143*, 1305-1315.

Siddhanta, U., McIlroy, J., Shah, A., Zhang, Y., and Backer, J. M. (1998). Distinct roles for the p110alpha and hVPS34 phosphatidylinositol 3'- kinases in vesicular trafficking, regulation of the actin cytoskeleton, and mitogenesis. J Cell Biol *143*, 1647-1659.

Siironen, J., Sandberg, M., Vuorinen, V., and Roytta, M. (1992). Expression of type I and III collagens and fibronectin after transection of rat sciatic nerve. Reinnervation compared with denervation. Lab Invest *67*, 80-87.

Silletti, S., Mei, F., Sheppard, D., and Montgomery, A. M. (2000). Plasmin-sensitive dibasic sequences in the third fibronectin-like domain of L1-cell adhesion molecule

(CAM) facilitate homomultimerization and concomitant integrin recruitment. J Cell Biol *149*, 1485-1502.

Simon, K. O., Nutt, E. M., Abraham, D. G., Rodan, G. A., and Duong, L. T. (1997). The alphavbeta3 integrin regulates alpha5beta1-mediated cell migration toward fibronectin. J Biol Chem *272*, 29380-29389.

Sobeih, M. M., and Corfas, G. (2002). Extracellular factors that regulate neuronal migration in the central nervous system. Int J Dev Neurosci *20*, 349-357.

Staatz, W. D., Fok, K. F., Zutter, M. M., Adams, S. P., Rodriguez, B. A., and Santoro, S. A. (1991). Identification of a tetrapeptide recognition sequence for the alpha 2 beta 1 integrin in collagen. J Biol Chem *266*, 7363-7367.

Thelen, K., Kedar, V., Panicker, A. K., Schmid, R. S., Midkiff, B. R., and Maness, P. F. (2002). The neural cell adhesion molecule L1 potentiates integrin-dependent cell migration to extracellular matrix proteins. J Neurosci *22*, 4918-4931.

Treubert, U., and Brummendorf, T. (1998). Functional cooperation of beta1-integrins and members of the Ig superfamily in neurite outgrowth induction. J Neurosci *18*, 1795-1805.

van der Flier, A., and Sonnenberg, A. (2001). Function and interactions of integrins. Cell Tissue Res *305*, 285-298.

Wei, M. H., Karavanova, I., Ivanov, S. V., Popescu, N. C., Keck, C. L., Pack, S., Eisen, J. A., and Lerman, M. I. (1998). In silico-initiated cloning and molecular characterization of a novel human member of the L1 gene family of neural cell adhesion molecules. Hum Genet *103*, 355-364.

Wong, C. W., Wiedle, G., Ballestrem, C., Wehrle-Haller, B., Etteldorf, S., Bruckner, M., Engelhardt, B., Gisler, R. H., and Imhof, B. A. (2000). PECAM-1/CD31 trans-homophilic binding at the intercellular junctions is independent of its cytoplasmic domain; evidence for heterophilic interaction with integrin alphavbeta3 in Cis. Mol Biol Cell *11*, 3109-3121.

Wong, E. V., Schaefer, A. W., Landreth, G., and Lemmon, V. (1996a). Casein kinase II phosphorylates the neural cell adhesion moleculae L1. J Neurochem *66*, 779-786.

Wong, E. V., Schaefer, A. W., Landreth, G., and Lemmon, V. (1996b). Involvement of p90rsk in neurite outgrowth mediated by the cell adhesion molecule L1. J Cell Biol *271*, 18217-18223.

Yip, P. M., Zhao, X., Montgomery, A. M., and Siu, C. H. (1998). The Arg-Gly-Asp motif in the cell adhesion molecule L1 promotes neurite outgrowth via interaction with the alphavbeta3 integrin. Mol Biol Cell *9*, 277-290.

Zhang, X., and Bennett, V. (1998). Restriction of 480/270-kD ankyrin G to axon proximal segments requires multiple ankyrin G-specific domains. J Cell Biol *142*, 1571-1581.

Zhang, Y., Roslan, R., Lang, D., Schachner, M., Lieberman, A. R., and Anderson, P. N. (2000). Expression of CHL1 and L1 by neurons and glia following sciatic nerve and dorsal root injury. Mol Cell Neurosci *16*, 71-86.

Figure 5.1: CHL1 Potentiates Haptotactic Migration of HEK293 Cells to Extracellular Matrix Proteins

Haptotactic cell migration toward extracellular matrix proteins or random migration toward bovine serum albumin was measured in HEK293 cells transiently expressing CHL1, L1, or expressing no L1 family adhesion molecule for 8 h. The samples were assayed in triplicate, and the experiments were repeated at least twice with similar results. *, statistically significant differences in means of transfected (expressing CHL1 or L1) versus nontransfected cells using the t test ($p < 0.05$).

Figure 5.1

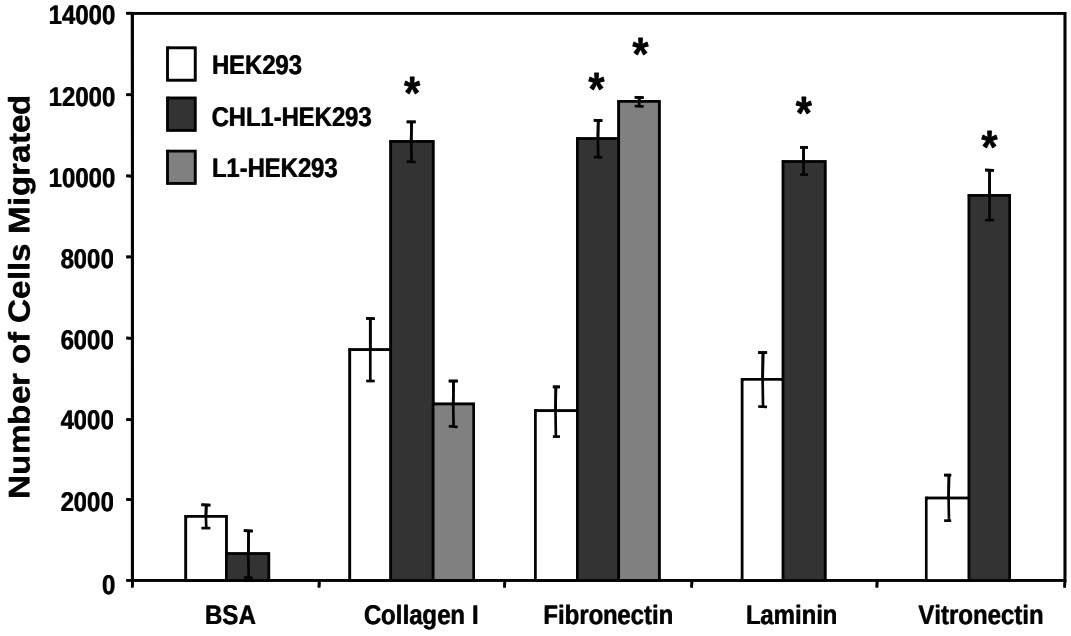
14000
12000
10000
8000
6000
4000
2000
0
Number of Cells Migrated
HEK293
CHL1-HEK293
L1-HEK293
*
*
*
*
*
BSA
Collagen I
Fibronectin
Laminin
Vitronectin

Figure 5.2: CHL1 Potentiates Migration of HEK293 Cells Through β_1 Integrins

Haptotactic migration of CHL1-expressing or nonexpressing HEK293 cells was measured for 3 h toward collagen I. Cells migrating toward collagen I were pretreated with nonimmune mouse IgG (Control; 30 μg/ml), integrin β_1 antibody (Anti-β_1; 30 μg/ml), integrin α_1 antibody (Anti-α_1; 15 μg/ml), integrin α_2 antibody (Anti-α_2; 15 μg/ml), or both antibodies (Anti-α_1 + Anti-α_2; 30 μg/ml). The samples were assayed in triplicate, and the experiments were repeated at least twice with similar results. *, statistically significant differences in means of treated *versus* control samples using the *t* test ($p < 0.05$). *BSA*, bovine serum albumin.

Figure 5.2

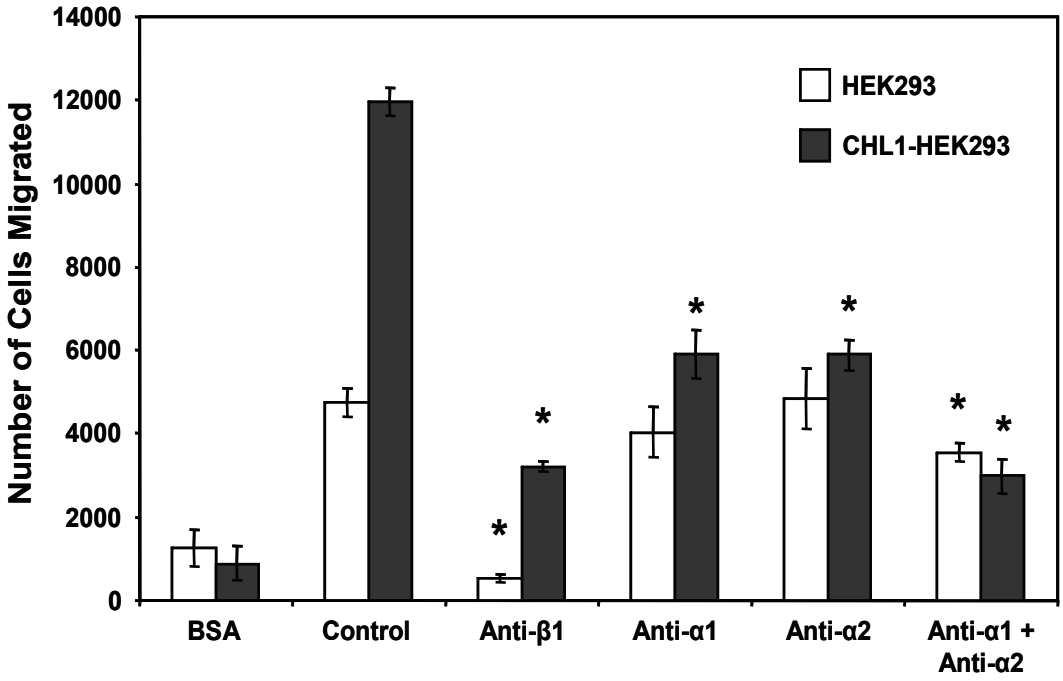
14000
12000
10000
8000
6000
4000
2000
0
Number of Cells Migrated
HEK293
CHL1-HEK293
*
BSA
Control
Anti-β1
Anti-α1
Anti-α2
Anti-α1 +
Anti-α2

Figure 5.3: CHL1 Mutations in Extracellular Ig6 (DGEA) and Cytoplasmic (FIGAY) Domains Suppress CHL1-Potentiated Migration to Collagen

HEK293 cells transiently expressing wild type CHL1, CHL1 with mutations DGEA →AGEV, RGD→KGE, FIGAY→FIGAA, or no CHL1 were assayed for haptotactic migration to collagen I for 3 h. Each sample was assayed in triplicate, and the experiments were repeated at least twice with similar results. *, statistically significant differences in means compared with CHL1 wild type (WT) using the *t* test ($p < 0.05$).

Figure 5.3

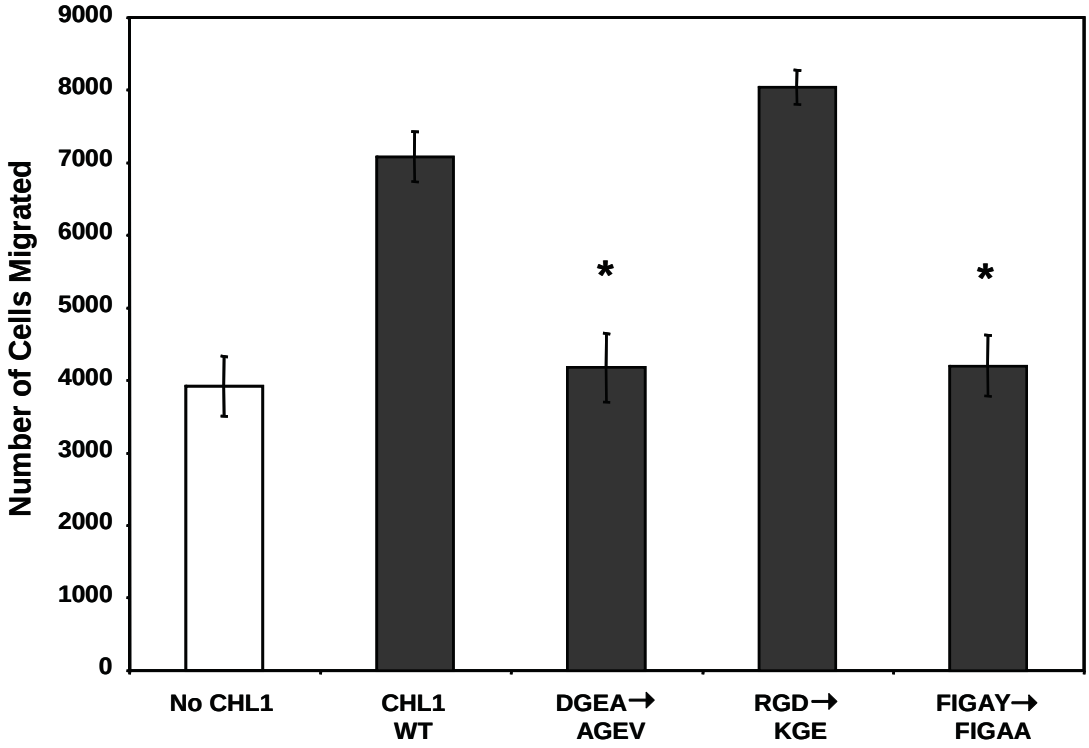
Number of Cells Migrated
9000
8000
7000
6000
5000
4000
3000
2000
1000
0
*
*
No CHL1
CHL1 WT
DGEA→ AGEV
RGD→ KGE
FIGAY→ FIGAA

Figure 5.4: c-Src, PI3 Kinase, and MAP Kinase are Required for CHL1-Potentiated Migration of HEK293 Cells

Migration of CHL1-expressing or nonexpressing HEK293 cells was measured toward collagen I for 3 h. Cells migration was conducted in the presence of 0.05% dimethyl sulfoxide (DMSO, control), Src family inhibitor PP2 (5 μM), PP3 (5 μM), an inactive analog of PP2, PI 3-kinase inhibitor LY294002 (25 μM), or MEK inhibitor U0126 (15 μM). Each sample was assayed in triplicate, and the experiments were repeated at least twice with similar results. *, statistically significant differences in means of treated and untreated (control) cells using the t test ($p < 0.05$).

Figure 5.4

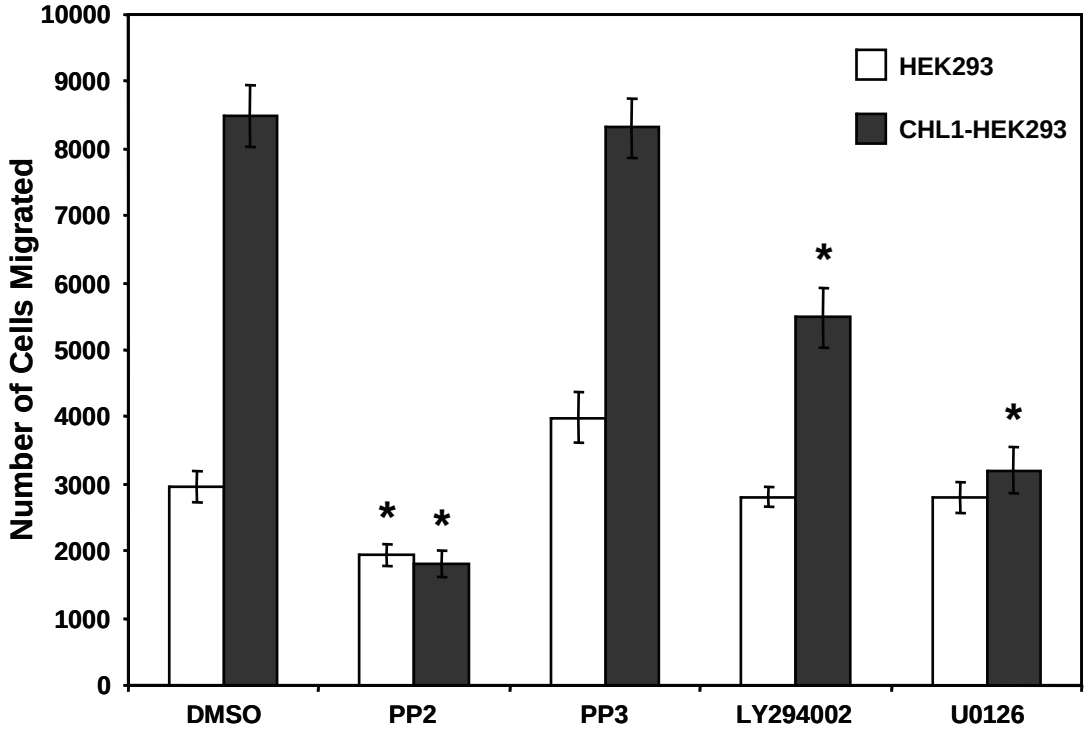
10000
9000
8000
7000
6000
5000
4000
3000
2000
1000
0
Number of Cells Migrated
HEK293
CHL1-HEK293
*
*
*
*
DMSO
PP2
PP3
LY294002
U0126

Figure 5.5: β_1 Integrin and CHL1 Co-cap on the Surface of CHL1-Expressing HEK293 Cells

A. β_1 integrin capping (*red*) was induced by cross-linking with β_1 integrin monoclonal antibody MAB2000 and was detected with a TRITC-labeled secondary antibody.

B. CHL1 protein (green) labeled with CHL1 polyclonal antibodies and fluorescein isothiocyanate-labeled secondary antibody was recruited to the integrin cap.

C. Partial co-localization of β_1 integrin and CHL1 was indicated by the yellow color in the overlay image.

Figure 2.2

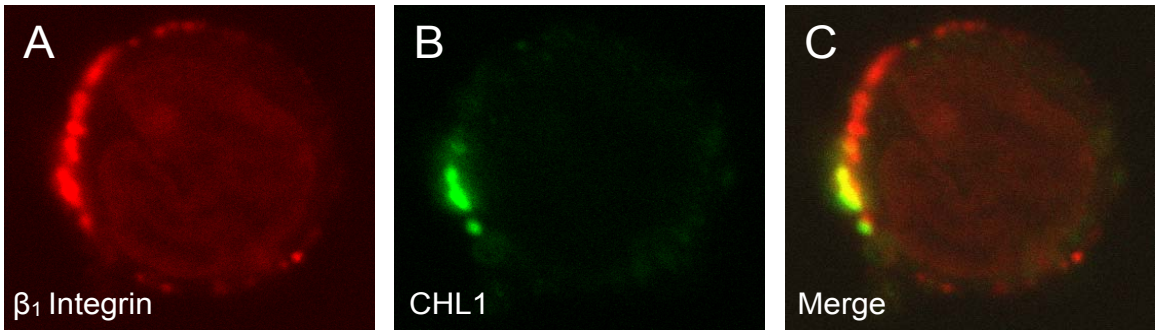

Figure 5.6: CHL1 is Able to Recruit Ankyrin to the Cell Membrane Through the FIGAY Sequence

HEK293 cells were transfected with the ankyrin-GFP expression plasmid alone (*A* and *B*) or together with a second plasmid expressing wild type CHL1 (*C–E*) or FIGAA mutant CHL1 (*F–H*).

A. Differential interference contrast image of HEK293 cells transfected with the ankyrin-GFP construct alone.

B. HEK293 cells shown in *A* expressed ankyrin-GFP with a diffuse cytoplasmic localization.

C. Differential interference contrast image of cells co-transfected with the wild type CHL1 and ankyrin-GFP constructs.

D. Ankyrin-GFP was recruited to the membrane of cells expressing wild type CHL1, shown in *C.*

E. CHL1 was localized on the cell membranes, as shown by immunofluorescence of cells in *C* using CHL1 antibodies and TRITC-conjugated secondary antibody.

F. Differential interference contrast image of cells co-transfected with the CHL1 FIGAA mutant and ankyrin-GFP constructs.

G. Ankyrin-GFP was not recruited to the membrane of cells expressing the mutant CHL1, shown in *F*, and assumes the same diffuse cytoplasmic localization as in cells not expressing CHL1 (*B*).

H. The FIGAA mutant was normally inserted in the plasma membrane.

Figure 5.6

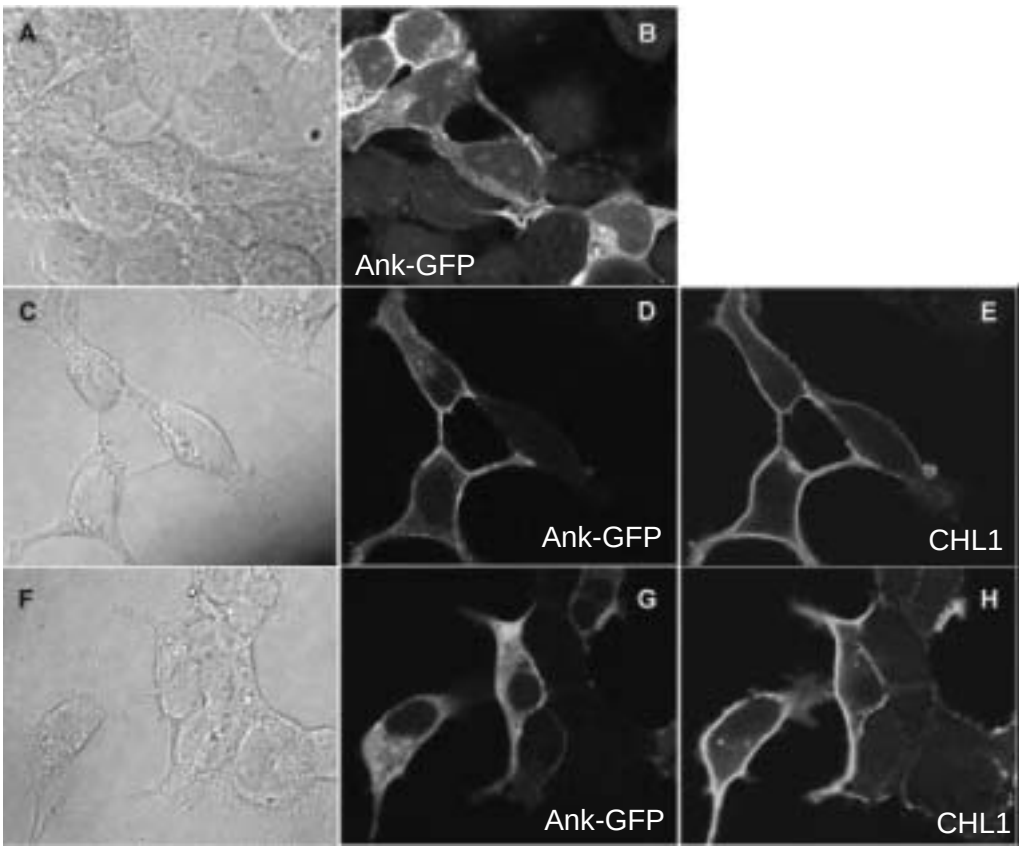

Figure 5.7: Hypothetical Model of the Molecular Interactions Involved in CHL1-Potentiated Migration Through β_1 Integrins

CHL1 interacts with $\alpha_1/\alpha_2\beta_1$ integrins in *cis* on the cell surface and promotes intracellular signaling through c-Src, PI 3-kinase, and MAP kinase, which stimulates cell migration on extracellular matrix (*ECM*) proteins such as collagen I. The CHL1 Ig6 domain, including the DGEA motif, may transiently interact with a binding site on β_1 integrins to stimulate cell signaling, but it is not sufficient for the interaction. Linkage of CHL1 to the actin cytoskeleton through ankyrin binding to the FIGAY sequence is necessary for enhanced cell motility and may stabilize adhesive contacts with the substrate.

Figure 5.7

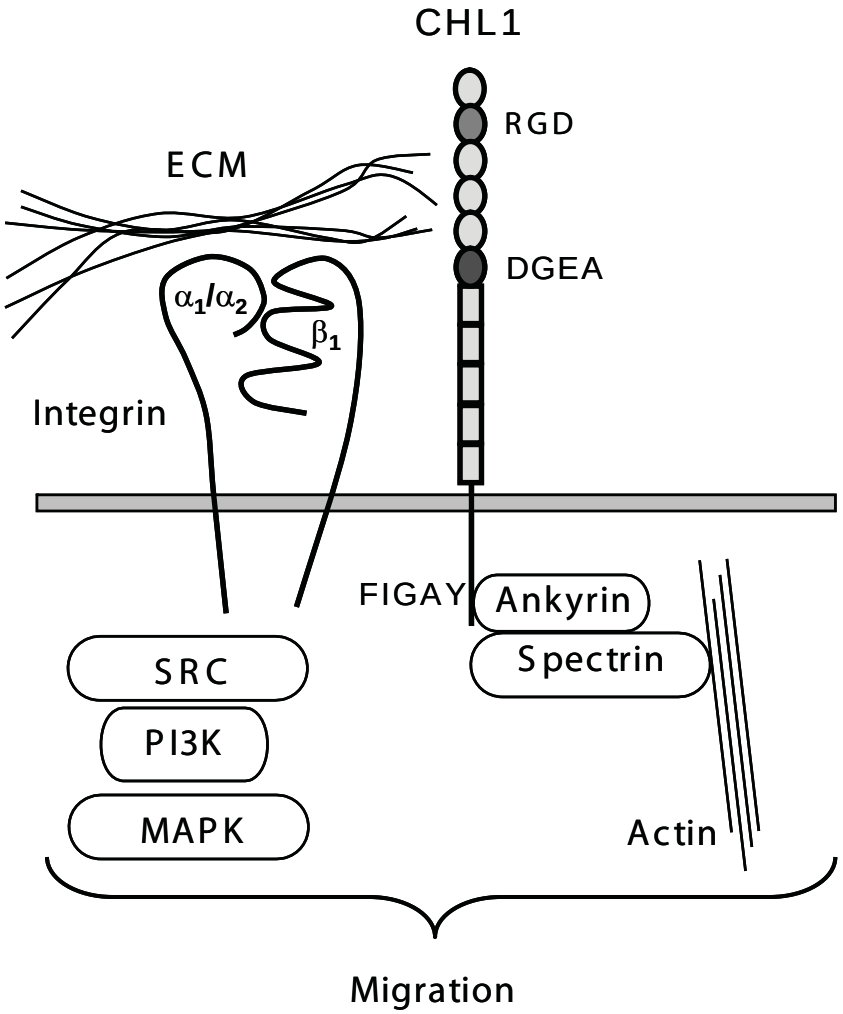
CHL1
RGD
ECM
DGEA
α_1/α_2
β_1
Integrin
FIGAY
Ankyrin
Spectrin
SRC
PI3K
MAPK
Actin
Migration

Chapter 6

Discussion

6.1 CHL1-Neuropilin1 Interaction as a Regulator of Thalamocortical Axon Guidance

This work demonstrates the functional importance of Close Homolog of L1 (CHL1) in thalamocortical axon guidance to the somatosensory cortex. CHL1 is expressed on thalamocortical and corticofugal axons, and regulates thalamocortical axon guidance via extracellular interactions with Npn1 and integrins and intracellular interactions with the actin cytoskeleton. Loss of CHL1 in mice disrupted area-specific targeting of somatosensory thalamic axons, causing them to inappropriately project to the visual cortex. This shift was first observed in the VTe, where axons from the somatosensory thalamus were shifted caudally. CHL1 was also required for preferential guidance of caudal thalamic axons through high Sema3A territories. A similar pattern of aberrant guidance was observed in $Npn1^{Sema-/-}$ mutant embryos, in which axons are nonresponsive to Sema3A, supporting a functional cooperation between CHL1, Npn1, and Sema3A in controlling thalamic axon topography. CHL1 formed a stable complex with Npn1 through a sequence in the extracellular Ig1 domain, which was required for Sema3A-induced growth cone collapse. CHL1 interaction with the cytoskeleton, through the adaptor proteins ezrin, radixin, and moesin (ERM) and ankyrin, was also critical for axon growth and guidance and cell migration. Association of CHL1 with ERM proteins, through a conserved RGGKYSV sequence in the membrane-proximal domain of CHL1, was important for cell migration, neurite outgrowth and branching, and for Sema3A-mediated growth cone collapse. Similarly, ankyrin interacted with the CHL1 cytoplasmic domain through a conserved sequence (Phe-Ile-Gly-Ala-Tyr), which was required for promoting

integrin-dependent migration. CHL1 also functionally interacted with β_1 integrins, leading to activation of a signaling cascade of c-Src, phosphatidylinositol 3-kinase, and ERK MAP kinase, which potentiated migration to extracellular matrix proteins. Taken together, these results identify CHL1 as a new molecular determinant of thalamocortical axon topography, acting in cooperation with Npn1 and cytoskeletal linker proteins to regulate guidance of thalamocortical axons in the VTe and proper targeting to the somatosensory cortex.

6.2 Sema3A-Neuropilin1 Interactions in Thalamocortical Axon Development

Studies have shown that diverse semaphorins, including Sema3A, display transient and regionally-selective patterns of expression throughout embryonic development, corresponding to distinct periods of radial invasion, axon growth, and synaptic targeting (Skaliora et al., 1998). Such patterns of semaphorin expression may control thalamic axon growth through intermediate targets and invasion of distinct cortical areas. Thalamocortical axons emerge from the thalamus at E14 and begin growing through the ganglionic eminence of the VTe, avoiding the neuroepithelium (Skaliora et al., 1998). Expression of Sema4B, 5A, and 5B in the neuroepithelium of the VTe is consistent with the interpretation that axon repulsion by these molecules forces fibers to grow laterally through the ganglionic eminence. I demonstrate here that Sema3A is also expressed in the VTe in a high caudal to low rostral gradient (Chapter 2). The caudal shift of ventral basal (VB) thalamic axons in the telencephalon of CHL1-minus and $Npn1^{Sema-/-}$ mice is consistent with impaired Sema3A repellent guidance. The ability of CHL1 to promote Sema3A-induced

growth cone collapse in thalamic neurons via association with Npn1 supports the interpretation that VB thalamic axons are repelled from the caudally increasing Sema3A gradient along the rostrocaudal axis of the VTe. Moreover, interactions between CHL1 and ERM proteins are necessary for Sema3A-induced growth cone collapse. Depolymerization of actin filaments, attenuated microtubule dynamics and decreased ability to polymerize new F-actin are all consequences of Sema3A-mediated growth cone collapse. Thus, as ERM proteins bind directly to F-actin, a CHL1/ERM/Npn1 complex may connect the plasma membrane to the underlying cytoskeleton to provide the necessary contacts to mediate Sema3A-induced growth cone collapse.

Although it is not entirely clear how caudal thalamic axons navigate through the high Sema3A territory, one possibility is that the repellent activity of Sema3A is overcome by permissive factors that allow growth. For example, axons of ventral telencephalic or cortical neurons are also present in the VTe during this time and have been shown to be important in the pathfinding of thalamic axons (Metin and Godement, 1996; Molnar et al., 1998). These axonal projections could provide the necessary contacts to make an otherwise hostile environment a permissive one for a subset of thalamic axons. Consistent with this interpretation, soluble CHL1 reduced the Sema3A growth cone collapse response of thalamic axons. In support of such a model, *trans* binding of L1 to L1-Npn1 complexes converts Sema3A-mediated repulsion to attraction (Castellani et al., 2004). Therefore, CHL1 on corticofugal axons might act as a binding ligand for CHL1-Npn1 complexes on caudal thalamic

axons, abrogating growth cone collapse and mediating the preferential growth of these axons through posterior territories of the VTe.

Npn1 binds Sema3A, 3C, and, to a lesser extent, Sema3B, 3D, and 3E (Nakamura et al., 2000), thus future thalamocortical mapping and expression studies in Sema3A null mutant mice will be needed to ascertain whether Sema3A is the only ligand responsible for sorting of thalamic axons in the VTe. Limited axon tracing studies in one strain of Sema3A knockout mice (C57Bl/6) showed that some thalamic axon terminals reached layer IV of the somatosensory cortex, but topographic guidance and mistargeting to other cortical areas were not studied (Catalano et al., 1998). My preliminary tracings of Sema3A knockout embryos (n=3) revealed a slight caudal shift of VB axons in the VTe (Wright, unpublished), suggesting that Sema3A is, in part, responsible for guidance of this subset of thalamic axons. However, more work is needed to fully evaluate the contribution of Sema3A and other class 3 semaphorins to thalamocortical axon guidance.

Semaphorins also play an important role in thalamocortical innervation and axonal branching within the cortex. During thalamic axon guidance to the cortex, the ventricular zone and cortical plate express high levels of Sema3A, 4A, 5A, and 5B, while expression in the intermediate zone is very low (Skaliora et al., 1998). Thus, semaphorins could delineate the territories permissive for axon growth in the intermediate zone *en route* to the DTe. Sema3A disappears from the cortical plate between E17-E19 in the rat, coincident with the onset of radial invasion. Expression of Sema4A and 4B is also downregulated in the cortical plate around the same time. As the layers of the cortex develop, Sema3A and 5A may direct the formation of

terminal arbors of thalamocortical axons in layer IV. At early postnatal ages, Sema3A and 5A are expressed in the cortex but confined to deep layers (V-VI). Layer IV is the first layer encountered by thalamic axons that lacks semaphorin expression, thus it could be permissive for axon arborization and synaptic terminal formation. Furthermore, later expression of Sema3A in upper cortical layers (II-III) supports an additional role for Sema3A in inhibiting cortical branching and synapse formation of thalamocortical axons in these regions, forcing them to arborize in layer IV. Several studies have demonstrated that Sema3A is involved in reducing axon branching of cortical (Bagnard et al., 1998; Dent et al., 2004) and hippocampal (Bagri et al., 2003) neurons through actin cytoskeletal rearrangements. It is shown here that suppression of cortical axon branching, due to Sema3A, is dependent upon CHL1-ERM protein interactions. Therefore, it is likely that CHL1 linkage to the actin cytoskeleton through ERM proteins is essential to regulate the organization and dynamics of the cytoskeleton involved in branching of thalamic axons in the neocortex.

6.3 CHL1 in Corticofugal Axon Development

Since CHL1 is expressed on corticofugal axons, some aspects of thalamocortical misrouting in CHL1-minus mice might be secondary to corticothalamic misprojections, based on the handshake hypothesis (Molnar et al., 1998). This idea postulates that corticofugal axons act as reciprocal guides for thalamocortical axons in the VTe. Subplate axons pioneer the pathway of layer VI pyramidal cell axons from the cortex to the thalamus (McConnell et al., 1989) and

are important in patterning thalamocortical connections (Ghosh and Shatz, 1993). CHL1 is expressed by subplate neurons (Liu et al., 2000), but deletion of CHL1 does not appear to affect their generation or laminar positioning (Demyanenko et al., 2004). Corticofugal axons were evident in CHL1-minus mice at E16.5, as observed in segregation experiments (Chapter 2). However, corticothalamic trajectories of layer VI pyramidal cell axons have not been mapped in CHL1-minus mice, and potential misprojection of these axons might influence thalamocortical guidance.

A possible role for CHL1 on corticofugal axons was suggested by the rostral shift of caudal thalamic axons in the VTe. For example, CHL1 on caudal corticofugal axons could act as a binding ligand for CHL1-Npn1 complexes on caudal thalamic axons, contributing to thalamic axon guidance by abrogating growth cone collapse to Sema3A. This silencing may enable caudal thalamic axons to migrate preferentially within caudal territories of the VTe *en route* to the cortex. It will be very exciting to further investigate the requirement of corticothalamic axons on thalamocortical development through the use of cortex-specific CHL1 knockout mice.

6.4 Redundant Functions of CHL1 and L1 in Thalamocortical Development

Overlapping expression patterns and interactions of L1 and CHL1 within the nervous system raise the intriguing possibility of compensatory functions for these L1 family molecules. We have demonstrated a requirement for CHL1 in Sema3A-induced growth cone collapse, which was important for topographic mapping of somatosensory thalamic axons. L1 has been shown to mediate growth cone collapse of postnatal cortical and dorsal root ganglion (DRG) axons in response to

Sema3A (Castellani et al., 2000). While CHL1 and L1 may have similar roles in mediating Sema3A-induced growth cone collapse, differential expression on axonal subtypes at various stages, or interaction with different homophilic and heterophilic binding partners, may account for distinct effects of each molecule. At embryonic stages, thalamocortical axons in L1-minus mice are hyperfasciculated, but normally target the motor, somatosensory, and visual cortex (Ohyama et al., 2004; Wiencken-Barger et al., 2004). Loss of CHL1 does not alter fasciculation, but somatosensory thalamocortical axons are misrouted to the visual cortex, and caudal thalamic axons display guidance errors in the VTe. Thus, L1 and CHL1 may mediate different responses of thalamic axons to Sema3A at this stage in development. For example, L1 may be more important in maintaining heterophilic interactions with the substrate to preserve segregation between thalamic and cortical axons, while CHL1 is responsible for collapse of somatosensory thalamic axons in response to the gradient of Sema3A in the caudal VTe, critical for axon sorting in the intermediate target.

Compensatory functions for L1 and CHL1 in regulating motor thalamic axon guidance were identified by our analysis of $CHL1^{-/-}/L1^{-/y}$ double mutant mice, where motor axons are shifted posteriorly to target the visual cortex. Because thalamic axon guidance to the motor cortex was unaffected in both CHL1-minus and L1-minus mice, the phenotype of $CHL1^{-/-}/L1^{-/y}$ double mutant mice suggests that CHL1 and L1 may compensate for each other in subpopulations of thalamic neurons that target the primary motor cortex. A plausible explanation for the guidance errors in these mice is an impairment in the repellent response to EphA4/ephrinA5 guidance

cues. This response prevents motor axons from entering posterior territories via growth cone collapse (Dufour et al., 2003). Loss of either CHL1 or L1 might not fully disrupt EphA4/ephrinA5 signaling, whereas loss of both adhesion molecules might interrupt the receptor complex, leading to defective growth cone collapse.

6.5 Repulsive Axon Guidance: Economic Molecular Mechanisms

One of the major challenges in developmental neurobiology is understanding the molecular mechanisms that control axon guidance and allow the formation of topographic maps. This study investigated the interaction of CHL1 with two important families of repellent axon guidance cues in thalamocortical development, the semaphorins and ephrins. Interestingly, these same guidance cues are conserved in the formation of other topographic maps. Because the human brain contains about 100 billion neurons (Williams and Herrup, 1988) and the human genome consists of only 20,000-25,000 protein-encoding genes (Pennisi, 2003), it is necessary for organisms to reuse the same molecules to control the development of many different axonal pathways. This economic use of genes requires complex intermolecular interactions underlying sophisticated molecular mechanisms that control the formation of topographic maps.

Semaphorins and neuropilins are regulators of repulsive axon guidance, which are important for pathfinding and fasciculation of olfactory axons, the corticospinal tract, entorhinohippocampal projections, and other major tracts (Kitsukawa et al., 1997; Giger et al., 2000; Cloutier et al., 2002; Gu et al., 2003).

Preferential expression of Sema3A in the ventral olfactory bulb repels Npn1-positive axons, preventing them from entering ventral regions and instead projecting to lateral and medial targets (Henion and Schwarting, 2007). The repulsive role of Sema3A in development of the corticospinal tract has been well documented (Castellani et al., 2000; Gu et al., 2003). A diffusible source of Sema3A in the ventral spinal cord participates in repulsion of L1/Npn1-positive cortical axons, mediating midline crossing to the dorsal columns to form the pyramidal decussation (Castellani et al., 2000). A repulsive guidance mechanism is also prominent in the development of entorhinohippocampal projections, whereby Sema3A acts through Npn1 to restrict axonal projections of entorhinohippocampal neurons to their targets in the stratum lacunosum-moleculare in the ipsilateral hippocampus (Pozas et al., 2001).

This study extends the repulsive role of Sema3A and Npn1 to the thalamocortical pathway. Development of VB thalamic axons relies upon repellent guidance mechanisms of Sema3A and Npn1, mediated by CHL1, for topographic mapping to the somatosensory cortex. Axons from the caudal dorsal thalamus must overcome Sema3A-induced repulsion, possibly via CHL1 interactions with CHL1-Npn1 complexes, to navigate through caudal territories of the VTe. Thus, regulation of axonal responses to Sema3A by CHL1-Npn1 interactions is important for the topographic mapping of thalamocortical axons.

Ephrin/Eph cues also regulate guidance of many major axonal tracts within the central nervous system, including formation of the corticospinal tract and retinocollicular maps (Feldheim et al., 1998; Flanagan and Vanderhaeghen, 1998;

Kullander et al., 2001; Wilkinson, 2001; Dufour et al., 2003; Cang et al., 2005; Torii and Levitt, 2005). EphA4/ephrinB3 forward signaling is required for proper development of the corticospinal tract. EphA4 is endogenously expressed in corticospinal tract fibers, which respond to ephrinB3 stimulation with growth cone collapse to prevent inappropriate midline crossing of corticospinal tract axons (Dottori et al., 1998; Kullander et al., 2001). Ephrin/Eph guidance systems are also involved in retinocollicular mapping (reviewed in Brown et al., 2000). EphrinA/EphA guidance cues mediate repulsive responses important for correct mapping of retinal axons to the anterior-posterior axis of the superior colliculus, and to the dorsal LGN of the thalamus. Inter- and intra-areal thalamocortical topography (Vanderhaeghen et al., 2000; Dufour et al., 2003; Cang et al., 2005), as well as reciprocal corticothalamic projections (Torii and Levitt, 2005), also depend upon repulsive axon guidance mediated by ephrinA/EphA guidance cues.

Here, I demonstrated a posterior shift of motor thalamic axons to the visual cortex in $CHL1^{-/-}/L1^{-/y}$ double mutant mice. Inter-areal guidance of thalamic axons to the motor cortex is dependent upon repellent activity of ephrinA5/EphA4 (Dufour et al., 2003); therefore, it is possible that CHL1 and L1 may functionally cooperate with ephrinA5/EphA4 complexes to prevent motor thalamic axons from entering posterior cortical regions via growth cone collapse.

Taken together, the work presented here highlights the importance of L1 family members as vital elements in repulsive guidance mechanisms that control thalamocortical topography.

6.6 Conclusions

Normal brain function is dependent upon elaborate axon guidance mechanisms and the formation of precise topographic connections. Thalamocortical axons carry sensory and motor information to the cortex via a sophisticated process of axon guidance through various decision points. Much progress has been made in the past decade to identify the molecules that control this complex pathfinding. However, a complete understanding of guidance cues involved in this system and the molecular mechanisms controlling topographic mapping and targeting remain elusive. Here, a novel role for CHL1 has been demonstrated in mediating the cellular responses of Sema3A and Npn1. Compensatory roles for CHL1 and L1 have been demonstrated in mediating repellent responses to EphA4/ephrinA5. In addition, the mechanism by which CHL1 couples to the actin cytoskeleton and the functional consequences of these associations have been defined. These results, for the first time, illustrate the importance of CHL1 as a thalamic axon guidance molecule, important for topographic mapping of thalamocortical axons through its intracellular association with the actin cytoskeleton and extracellular interactions with Npn1 and integrins.

6.7 References

Bagnard, D., Lohrum, M., Uziel, D., Puschel, A. W., and Bolz, J. (1998). Semaphorins act as attractive and repulsive guidance signals during the development of cortical projections. Development *125*, 5043-5053.

Bagri, A., Cheng, H. J., Yaron, A., Pleasure, S. J., and Tessier-Lavigne, M. (2003). Stereotyped pruning of long hippocampal axon branches triggered by retraction inducers of the semaphorin family. Cell *113*, 285-299.

Brown, A., Yates, P. A., Burrola, P., Ortuno, D., Vaidya, A., Jessell, T. M., Pfaff, S. L., O'Leary, D. D., and Lemke, G. (2000). Topographic mapping from the retina to the midbrain is controlled by relative but not absolute levels of EphA receptor signaling. Cell *102*, 77-88.

Cang, J., Kaneko, M., Yamada, J., Woods, G., Stryker, M. P., and Feldheim, D. A. (2005). Ephrin-as guide the formation of functional maps in the visual cortex. Neuron *48*, 577-589.

Castellani, V., Chedotal, A., Schachner, M., Faivre-Sarrailh, C., and Rougon, G. (2000). Analysis of the L1-deficient mouse phenotype reveals cross-talk between Sema3A and L1 signaling pathways in axonal guidance [see comments]. Neuron *27*, 237-249.

Castellani, V., Falk, J., and Rougon, G. (2004). Semaphorin3A-induced receptor endocytosis during axon guidance responses is mediated by L1 CAM. Mol Cell Neurosci *26*, 89-100.

Catalano, S. M., Messersmith, E. K., Goodman, C. S., Shatz, C. J., and Chedotal, A. (1998). Many major CNS axon projections develop normally in the absence of semaphorin III. Mol Cell Neurosci *11*, 173-182.

Cloutier, J. F., Giger, R. J., Koentges, G., Dulac, C., Kolodkin, A. L., and Ginty, D. D. (2002). Neuropilin-2 mediates axonal fasciculation, zonal segregation, but not axonal convergence, of primary accessory olfactory neurons. Neuron *33*, 877-892.

Demyanenko, G. P., Schachner, M., Anton, E., Schmid, R., Feng, G., Sanes, J., and Maness, P. F. (2004). Close homolog of L1 modulates area-specific neuronal positioning and dendrite orientation in the cerebral cortex. Neuron *44*, 423-437.

Dent, E. W., Barnes, A. M., Tang, F., and Kalil, K. (2004). Netrin-1 and semaphorin 3A promote or inhibit cortical axon branching, respectively, by reorganization of the cytoskeleton. J Neurosci *24*, 3002-3012.

Dottori, M., Hartley, L., Galea, M., Paxinos, G., Polizzotto, M., Kilpatrick, T., Bartlett, P. F., Murphy, M., Kontgen, F., and Boyd, A. W. (1998). EphA4 (Sek1) receptor tyrosine kinase is required for the development of the corticospinal tract. Proc Natl Acad Sci U S A *95*, 13248-13253.

Dufour, A., Seibt, J., Passante, L., Depaepe, V., Ciossek, T., Frisen, J., Kullander, K., Flanagan, J. G., Polleux, F., and Vanderhaeghen, P. (2003). Area specificity and topography of thalamocortical projections are controlled by ephrin/Eph genes. Neuron *39*, 453-465.

Feldheim, D. A., Vanderhaeghen, P., Hansen, M. J., Frisen, J., Lu, Q., Barbacid, M., and Flanagan, J. G. (1998). Topographic guidance labels in a sensory projection to the forebrain. Neuron *21*, 1303-1313.

Flanagan, J. G., and Vanderhaeghen, P. (1998). The ephrins and Eph receptors in neural development. Annu Rev Neurosci *21*, 309-345.

Ghosh, A., and Shatz, C. J. (1993). A role for subplate neurons in the patterning of connections from thalamus to neocortex. Development *117*, 1031-1047.

Giger, R. J., Cloutier, J. F., Sahay, A., Prinjha, R. K., Levengood, D. V., Moore, S. E., Pickering, S., Simmons, D., Rastan, S., Walsh, F. S.*, et al.* (2000). Neuropilin-2 is required in vivo for selective axon guidance responses to secreted semaphorins. Neuron *25*, 29-41.

Gu, C., Rodriguez, E. R., Reimert, D. V., Shu, T., Fritzsch, B., Richards, L. J., Kolodkin, A. L., and Ginty, D. D. (2003). Neuropilin-1 conveys semaphorin and VEGF signaling during neural and cardiovascular development. Dev Cell *5*, 45-57.

Henion, T. R., and Schwarting, G. A. (2007). Patterning the developing and regenerating olfactory system. J Cell Physiol *210*, 290-297.

Kitsukawa, T., Shimizu, M., Sanbo, M., Hirata, T., Taniguchi, M., Bekku, Y., Yagi, T., and Fujisawa, H. (1997). Neuropilin-semaphorin III/D-mediated chemorepulsive signals play a crucial role in peripheral nerve projection in mice. Neuron *19*, 995-1005.

Kullander, K., Croll, S. D., Zimmer, M., Pan, L., McClain, J., Hughes, V., Zabski, S., DeChiara, T. M., Klein, R., Yancopoulos, G. D., and Gale, N. W. (2001). Ephrin-B3 is the midline barrier that prevents corticospinal tract axons from recrossing, allowing for unilateral motor control. Genes Dev *15*, 877-888.

Liu, Q., Dwyer, N. D., and O'Leary, D. D. (2000). Differential expression of COUP-TFI, CHL1, and two novel genes in developing neocortex identified by differential display PCR. J Neurosci *20*, 7682-7690.

McConnell, S. K., Ghosh, A., and Shatz, C. J. (1989). Subplate neurons pioneer the first axon pathway from the cerebral cortex. Science *245*, 978-982.

Metin, C., and Godement, P. (1996). The ganglionic eminence may be an intermediate target for corticofugal and thalamocortical axons. J Neurosci *16*, 3219-3235.

Molnar, Z., Adams, R., and Blakemore, C. (1998). Mechanisms underlying the early establishment of thalamocortical connections in the rat. J Neurosci *18*, 5723-5745.

Nakamura, F., Kalb, R. G., and Strittmatter, S. M. (2000). Molecular basis of semaphorin-mediated axon guidance. J Neurobiol *44*, 219-229.

Ohyama, K., Tan-Takeuchi, K., Kutsche, M., Schachner, M., Uyemura, K., and Kawamura, K. (2004). Neural cell adhesion molecule L1 is required for fasciculation and routing of thalamocortical fibres and corticothalamic fibres. Neurosci Res *48*, 471-475.

Pennisi, E. (2003). Human genome. A low number wins the GeneSweep Pool. Science *300*, 1484.

Pozas, E., Pascual, M., Nguyen Ba-Charvet, K. T., Guijarro, P., Sotelo, C., Chedotal, A., Del Rio, J. A., and Soriano, E. (2001). Age-dependent effects of secreted Semaphorins 3A, 3F, and 3E on developing hippocampal axons: in vitro effects and phenotype of Semaphorin 3A (-/-) mice. Mol Cell Neurosci *18*, 26-43.

Skaliora, I., Singer, W., Betz, H., and Puschel, A. W. (1998). Differential patterns of semaphorin expression in the developing rat brain. Eur J Neurosci *10*, 1215-1229.

Torii, M., and Levitt, P. (2005). Dissociation of corticothalamic and thalamocortical axon targeting by an EphA7-mediated mechanism. Neuron *48*, 563-575.

Vanderhaeghen, P., Lu, Q., Prakash, N., Frisen, J., Walsh, C. A., Frostig, R. D., and Flanagan, J. G. (2000). A mapping label required for normal scale of body representation in the cortex. Nat Neurosci *3*, 358-365.

Wiencken-Barger, A. E., Mavity-Hudson, J., Bartsch, U., Schachner, M., and Casagrande, V. A. (2004). The role of L1 in axon pathfinding and fasciculation. Cereb Cortex *14*, 121-131.

Wilkinson, D. G. (2001). Multiple roles of EPH receptors and ephrins in neural development. Nat Rev Neurosci *2*, 155-164.

Williams, R. W., and Herrup, K. (1988). The control of neuron number. Annu Rev Neurosci *11*, 423-453.